Philipps Universität Marburg

Neuroendokrine Regulation der Energie und Glukosehomöostase

- Vom zentralen WNT- Signalweg über hypothalamische Inflammation und Leptinsensitivität -

---

Dissertation
zur
Erlangung des Doktorgrades
der Naturwissenschaften
(Dr. rer. nat.)

dem Fachbereich Biologie
der Philipps-Universität Marburg
vorgelegt von

JONAS BENZLER

aus
Gießen
Marburg/Lahn
August 2013

Vom Fachbereich Biologie der Philipps-Universität Marburg als

Dissertation am 28.10.2013 angenommen.

Erstgutachter: Dr. Alexander Tups
Zweitgutachter: Prof. Dr. Gerhard Heldmaier

Tag der mündlichen Prüfung am: 15.11.2013

Inhaltsverzeichnis

1. Abkürzungsverzeichnis

AAV:	**A**deno-**a**ssoziierte **V**iren
AP-1:	**a**citvated **p**rotein-**1**
APC:	**A**denomatosis **p**olyposis **c**oli
AdipoR:	**Adipo**nektin**r**ezeptor
AgRP:	**Ag**outi-**r**elated **p**eptide
AMPK:	**A**denosin**m**ono**p**hosphat-aktivierte **K**inase
APPL:	**A**daptor protein containing **p**leckstrin homology domain **p**hosphotyrosine binding domain, and **l**eucine zipper motif
ARC:	Nucleus **arc**uatus
BBB:	Blut-Hirn-Schranke; **b**lood **b**rain **b**arrier
BMI:	**B**ody-**m**ass-**i**ndex; Körpermasse-index
CART:	**C**ocaine- and **a**mphetamine **r**egulated **t**ranscript
DEXA:	**D**ual **e**nergy **x**-ray **a**bsorbtiometry
DKK:	**D**ic**kk**opf
DVL:	**D**ishe**vel**led
ELISA:	**E**nzyme **l**inked **i**mmunosorbent **a**ssay
Fz:	**F**ri**z**zled
FzR:	**F**ri**z**zled**r**ezeptor
GSK:	**G**lykogen- **S**ynthase- **K**inase
HFD:	hochkalorische Diät; **h**igh **f**at **d**iet
icv:	**i**ntra**c**erebro**v**entrikular;
IKK:	**I**nhibitor von NF-**κ**B- **K**inase
IκBα:	**I**nhibitor von NF-**κB**
Il:	**I**nter**l**eukin
Ip:	**i**ntra**p**eritoneal
IR:	**I**nsulin**r**ezeptor
IRS:	**I**nsulin**r**ezeptor**s**ubstrat
JAK:	**Ja**nus**k**inase
JNK:	c-**J**un-**N**-terminale **K**inase
LEF:	**l**ymphoid **e**nhancer **f**actor
Lep $^{ob/ob}$:	leptindefiziente Mauslinie
LepR:	**Lep**tin**r**ezeptor
LHA:	laterale hypothalamische Region: **l**ateral **h**ypothalamic **a**rea
LRP:	**l**ow-density lipoprotein **r**eceptor-related **p**rotein
MAPK:	**m**itogen-**a**ctivated **p**rotein **k**inase

MBH:	**M**edio**b**asaler **H**ypothalamus
MyD88:	**my**eloid-**d**ifferentiation factor **88**
mRNA:	**m**essenger **r**ibo **n**ucleic **a**cid
NPY:	**N**euro**p**eptid **Y**
AKT:	auch als Proteinkinase B bekannt
PI3K:	**P**hospho**i**nositol-3-**K**inase
POMC:	**P**ro**o**pio**m**elano**c**ortin
PVN:	**P**ara**v**entrikulärer **N**ucleus
SOCS:	**S**uppressor **o**f **c**ytokine **s**ignalling
STAT:	**S**ignal **t**ransducers and **a**ctivators of **t**ranscription
TNFα:	**T**umor **n**ecrosis **f**actor-**a**lpha
TCF:	**T**-**c**ell **f**actor
TLR:	**T**oll-**l**ike-**R**ezeptor
VMH:	**V**entro**m**edialer **H**ypothalamus
ZNS:	**Z**entrales **N**erven**s**ystem
WHO:	Weltgesundheitsorganisation: **W**orld **H**ealth **O**rganization

2. Eigene Beiträge zu den veröffentlichten Teilen der Arbeit

Laut §8, Absatz 3 der Promotionsordnung der Philipps-Universität Marburg (Fassung vom 12.4.2000) müssen bei den Teilen der Dissertation, die aus gemeinsamer Forschungsarbeit entstanden sind, „die individuellen Leistungen des Doktoranden deutlich abgrenzbar und bewertbar sein." Dies betrifft die Kapitel 4.1 - 4.5 sowie die zusätzlichen wissenschaftlichen Arbeiten (Kapitel 5.1 – 5.3). Die Beiträge werden im Folgenden detailliert erläutert.

Kapitel 4.1:

Leptin rapidly improves glucose homeostasis in obese mice by increasing hypothalamic insulin sensitivity

- Durchführung von 25 % der immunohistochemischen Untersuchungen.

Dieses Kapitel wurde im Dezember 2010 bei „**Journal of Neuroscience**" publiziert.

*Christiane Koch, Rachael A. Augustine, Juliane Steger, Goutham K. Ganjam, **Jonas Benzler**, Corinna Pracht, Chrishanthi Lowe Michael W. Schwartz, Peter R. Shepherd, Greg M. Anderson, David R. Grattan, and Alexander Tups*

PMID: 21123564

Kapitel 4.2:

Hypothalamic WNT signalling is impaired during obesity and reinstated by leptin treatment in male mice

- Durchführung aller Versuche in den Abbildungen 1-3.
- Auswertung und statistische Analyse von allen Daten der angegebenen Versuche.
- Anfertigung aller Abbildungen in Zusammenarbeit mit Sigrid Stöhr.
- Anfertigung des Manuskriptes in Zusammenarbeit mit Dr. Alexander Tups und Prof David R. Grattan.

Dieses Kapitel wurde im August 2013 zur Veröffentlichung bei „**Endocrinology**" eingereicht und befindet sich derzeit unter Begutachtung.

***Jonas Benzler**, Zane B. Andrews, Corinna Pracht, Sigrid Stöhr, Peter R. Shepherd, David R Grattan and Alexander Tups*

Kapitel 4.3:

Hypothalamic glycogen synthase kinase 3β has a central role in the regulation of food intake and glucose metabolism

- Durchführung aller Versuche in Abbildungen 1, 2 und 5, sowie die *in-situ* Hybridisierungen in den Abbildungen 3f und 4g.
- Auswertung und statistische Analyse von allen Daten der angegebenen Versuche.
- Anfertigung der Abbildungen in Zusammenarbeit mit Sigrid Stöhr.
- Anfertigung des Manuskriptes in Zusammenarbeit mit Dr. Alexander Tups, Prof. David R. Grattan und Prof. Peter R. Shepherd.

Dieses Kapitel wurde im Juli 2012 bei „**Biochemical Journal**“ publiziert.

***Jonas Benzler**, Goutham K. Ganjam, Manon Krüger, Olaf Pinkenburg, Maria Kutschke, Sigrid Stöhr, Juliane Steger, Christiane E. Koch, Rebecca Ölkrug, Michael W. Schwartz, Peter R. Shepherd, David R. Grattan and Alexander Tups*

PMID: 22849606

Kapitel 4.4:

Acute inhibition of central c-Jun N-terminal kinase restores hypothalamic insulin signalling and alleviates glucose intolerance in diabetic mice

- Durchführung aller Experimente.
- Auswertung und statistische Analyse von allen Daten.
- Anfertigung aller Abbildungen in Zusammenarbeit mit Sigrid Stöhr.
- Anfertigung des Manuskriptes in Zusammenarbeit mit Dr. Alexander Tups.

Dieses Kapitel wurde im April 2013 bei „**Journal of Neuroendocrinology**“ veröffentlicht.

***J. Benzler**, G. K. Ganjam, K. Legler, S. Stöhr, M. Krüger, J. Steger and A. Tups*

PMID: 23301857

Kapitel 4.5:

Central inhibition of NF-κB signalling improves glucose homeostasis in mice

- Durchführung aller Experimente bis auf Abbildung 1a.
- Auswertung und statistische Analyse von allen Daten mit Beratung von Dr. Rebecca Ölkrug.
- Anfertigung aller Abbildungen in Zusammenarbeit mit Sigrid Stöhr.
- Anfertigung des Manuskriptes in Zusammenarbeit mit Dr. Alexander Tups

Dieses Kapitel wird voraussichtlich im September 2013 zur Veröffentlichung bei „**Diabetes**“ eingereicht.

***Jonas Benzler**, Goutham K. Ganjam, Christiane E. Koch, Dominik Pretz, Rebecca Oelkrug, Christiane E. Koch, Karen Legler, Sigrid Stöhr, Carsten Culmsee, Lynda M. Williams and Alexander Tups.*

Kapitel 5.1:

Central Adiponectin Acutely Improves Glucose Tolerance in Male Mice

- Durchführung und Auswertung der Experimente in Abb. 5

Dieses Kapitel wurde im August 2013 zur Veröffentlichung bei „**Endocrinology**“ eingereicht und befindet sich derzeit unter Begutachtung.

*Christiane E. Koch, Chrishanthi Lowe, Karen Legler, **Jonas Benzler**, Juliane Steger, David R. Grattan, Lynda M. Williams and Alexander Tups*

Kapitel 5.2:

Overexpression of suppressor of cytokine signaling 3 in the arcuate nucleus of juvenile Phodopus sungorus alters seasonal body weight changes

- Durchführung aller *in-situ* Hybridisierungen.

Dieses Kapitel wurde im Juli 2013 bei „**Journal of Comparative Physiology B**“ publiziert.

*Ganjam GK, **Benzler J**, Pinkenburg O, Stöhr S, Steger J, Krüger M, Culmsee C, Tups A. PMID: 23860586*

Kapitel 5.3:

The time course and mechanisms contributing to ghrelin resistance after high fat diet exposure

- Durchführung und Auswertung des Experiments in Abb. 4c.

Dieses Kapitel wird im August 2013 zur Veröffentlichung bei „**Diabetes**“ eingereicht.

*Briggs Dl, Lockie SH, **Benzler J**, Wu Q, Hoy AJ, Myra BL, Stark R, Coleman HA, Parkington HC, Tups A, Andrews ZB*

3. Zusammenfassung

3.1 Einleitung

In der modernen Wohlstandsgesellschaft hat sich Adipositas zu einem der größten Gesundheitsprobleme entwickelt. Laut Weltgesundheitsorganisation (WHO) gelten Menschen mit einem Body-Mass-Index (BMI) über 30 kg Körpergewicht pro Körpergröße zum Quadrat als adipös [1]. Umgangssprachlich auch als Fettsucht bekannt, ist Adipositas eine über das normale Maß hinausgehende Vermehrung des Körperfetts mit verheerenden Folgen für den Energie- und Glukosemetabolismus. Adipositas wird als einer der Hauptrisikofaktoren für die Entstehung von Diabetes mellitus Typ II angesehen [2]. Diabetes mellitus Typ II, im Volksmund auch Zuckerkrankheit genannt, ist eine Stoffwechselkrankheit, die mit einer massiven Störung des Glukosehaushalts einhergeht. Charakteristisch für Diabetes mellitus Typ II ist ein erhöhter Blutzuckerspiegel der zu Schädigungen der Blutgefäße führen kann. Bei der endgültigen Manifestation von Diabetes mellitus Typ II werden schließlich die pankreatischen β-Zellen durch die chronische Überbelastung zerstört und es kommt, wie bei Diabetes mellitus Typ I, zum Insulinmangel. Hieraus können schwerwiegende Folgeerkrankungen resultieren. Zu diesen zählen Schädigungen der mikrovaskulären Gefäße, die wiederum Auswirkungen auf Augen (Retinopathie), Nieren (Nephropathie) und Nerven (Neuropathie) haben können [1]. Makrovaskuläre Schädigungen können kardiovaskuläre Krankheiten wie Durchblutungsstörungen bis hin zur Amputation, Herzinfarkt und Schlaganfall verursachen [1]. Um diesen Folgeerscheinungen entgegenzuwirken, ist eine intakte Glukosehomöostase essentiell. In den letzten drei Jahrzehnten hat sich die Anzahl der an Adipositas erkrankten Menschen fast verdoppelt [1], wobei gleichzeitig die Diabetes mellitus Typ II - Rate in der Erwachsenengesellschaft sogar um das Siebenfache angestiegen ist [3]. Früher traten diese metabolischen Störungen überwiegend bei Erwachsenen auf, jedoch sind mittlerweile auch vermehrt Kinder und Jugendliche betroffen. Weltweit wurden 2010 bereits über 40 Millionen übergewichtige Kinder unter 5 Jahren verzeichnet, wobei mangelnde Bewegung und übermäßiger Konsum fettreicher Nahrung maßgeblich zur Ausprägung des adipösen Phänotyps beitragen [1]. Einhergehend mit Adipositas stieg auch das Risiko für Diabetes mellitus Typ II in dieser Altersgruppe stark an. In den letzten 20 Jahren hat sich die Anzahl der betroffenen Kinder und Jugendlichen in den USA bereits verzehnfacht und es wird eine ähnliche Entwicklung für Deutschland prognostiziert. Die mit diesen Störungen verbundenen Kosten sind in Deutschland für etwa 10 % der derzeitigen Gesamtausgaben des Gesundheitssystems verantwortlich [3]. Daher ist es unabdingbar die molekularen Mechanismen des Energie- und Glukosehaushaltes besser zu verstehen, um Zusammenhänge mit der Entstehung von Diabetes mellitus Typ II und dessen Prävention entschlüsseln zu können.

3.1.1 Die zentrale Regulation der Energie- und Glukosehomöostase

Als Hauptenergielieferant des Organismus haben Kohlenhydrate zusammen mit Fetten und Proteinen den quantitativ höchsten Anteil an der täglich aufgenommenen Nahrung. Im Körper werden Kohlenhydrate enzymatisch verdaut, wobei unter anderem Glukose entsteht. Um eine konstante Energieversorgung des Organismus zu gewährleisten ist die Aufrechterhaltung eines kontrollierten Blutglukosespiegels (Glukosehomöostase) essentiell. Die Glukosehomöostase ist ein physiologisch ausgewogener Mechanismus, der hauptsächlich von drei parallel ablaufenden Prozessen gesteuert wird. Zu diesen zählen die Insulinsekretion der Pankreas, die Glukosespeicherung der Leber, sowie die Glukoseaufnahme des peripheren Gewebes (Muskel und Fett). Zusätzlich zu der aus der Nahrung gewonnenen Glukose können Fettgewebe (Glukoneogenese) sowie Leber und Muskel (Glykogenolyse) Glukose synthetisieren. Hauptsächlich wird die Glukosehomöostase durch das Peptidhormon Insulin reguliert, das von den β-Zellen der pankreatischen Langerhans-Inseln produziert und sezerniert wird. Es ermöglicht die Aufnahme von Glukose aus dem Blut in die verschiedenen Gewebe und induziert die Glykogenbildung in der Leber, wodurch der Blutglukosespiegel gesenkt wird. Der Gegenspieler von Insulin ist das Hormon Glukagon. Ist der Blutzuckerspiegel zu niedrig, wird seine Ausschüttung aus den Langerhans-Inseln induziert, was zum Abbau von Glykogen zu Glukose in der Leber führt und der Blutglukosespiegel steigt.

Das Gehirn galt lange Zeig als insulininsensitiv und man nahm an, dass der Glukosehaushalt ausschließlich in der Peripherie gesteuert wird. Mittlerweile wurde jedoch mehrfach beschrieben, dass Insulin über den Blutkreislauf zum Gehirn gelangt, wo es in spezifischen hypothalamischen Kernregionen die Energie- und Glukosehomöostase reguliert [4-9]. Hierbei ist der mediobasale Hypothalamus (MBH, Abb. 1) mit seinen assoziierten Nuclei als Hauptregulationszentrum der zentralen Energie- und Glukosehomöostase anzusehen [10]. Periphere Signale erreichen über den Blutkreislauf den Hypothalamus, binden dort an ihre Rezeptoren und vermitteln so den peripheren Energiestatus an das zentrale Nervensystem (ZNS) [10]. Hierbei ist der *Nucleus arcuatus* (ARC) die erste neuronale Verbindungsstelle, indem sich verschiedene neuropeptid-produzierende Neurone befinden, die eine wichtige Rolle in der Energiehomöostase spielen. Hierzu zählen die anorexigen (appetithemmend) wirkenden „Proopiomelanocortin/Cocaine- and amphetamine regulated Transcript“ (POMC/CART) -Neurone, sowie die orexigen (appetiterzeugend) wirkenden „Neuropeptide Y/Agouti-related peptide“ (NPY/AgRP) -Neurone, die maßgeblich and der Steuerung der Energie- und Glukosehomöostase beteiligt sind [11]. Diese sogenannten Neurone erster Ordnung innervieren anteriore Regionen wie den paraventrikulären Nucleus (PVN), die lateral hypothalamische Region (lateral hypothalamic area, LHA) oder den ventromedialen Nucleus (VMH), wo sie Synapsen mit Neuronen zweiter Ordnung bilden und die Energiehomöostase regulieren.

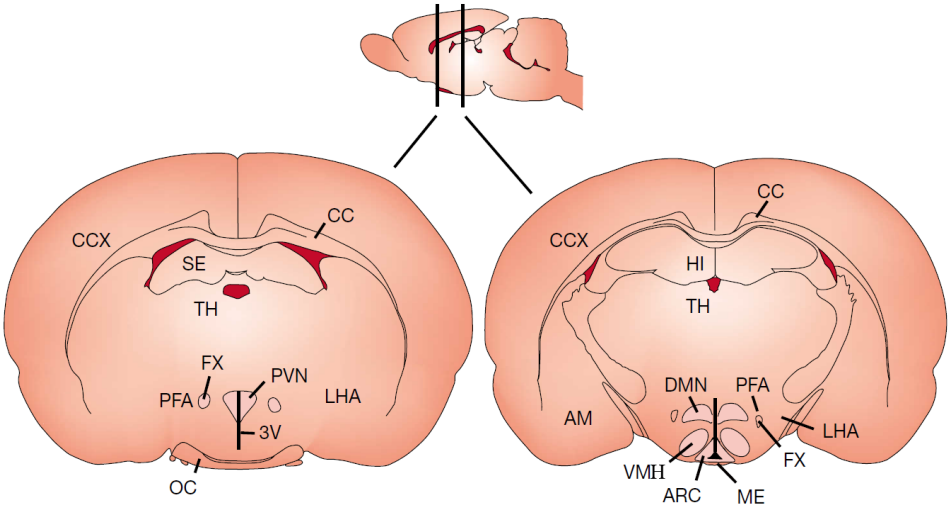

Abb. 1: Anatomie eines Rattengehirns und die Hauptregionen der Energiehomöostase im Hypothalamus: Eine Sagittalansicht des Rattengehirns (oben) zeigt die Position des Hypothalamus (Abgrenzung durch die zwei vertikale Balken), das Zentrum der Energie- und Glukosehomöostase. Unten ist eine Frontalansicht des anterioren (links) und posterioren (rechts) Bereichs des Hypothalamus abgebildet. Neurone, die auf periphere Signale reagieren, befinden sich im ARC und innervieren anteriore Regionen wie den PVN und die LHA. Zusätzlich spielt auch der, dem ARC anliegende, VMH eine wichtige Rolle in der Energiehomöostase. ARC: Nucleus arcuatus; PVN: paraventrikulärer Nucleus; LHA: lateral hypothalamische Region; VMH: ventromedialer Hypothalamus; OC: optisches Chiasma; 3V: dritter Ventrikel. Verändert nach Schwartz MW, 2000 [10].

Die anorexigenen Hormone Leptin und Insulin, die proportional zum Körperfettgehalt sezerniert werden [10;12], sowie das vom Magen produzierte, orexigene Hormon Ghrelin spielen bei dieser hypothalamischen Regulation der Energie- und Glukosehomöostase eine entscheidende Rolle. Insulin und Leptin inhibieren die NPY/AgRP- Neurone im ARC und stimulieren gleichzeitig die POMC Neurone über komplexe intrazelluläre Signalwege, wohingegen Ghrelin die NPY/AgRP- Neurone aktiviert, wodurch die neuroendokrine Regulation der Glukosehomöostase gesteuert wird [11].

Die Rolle von Insulin und Leptin

Die Hauptaufgabe von Insulin liegt in der Aufrechterhaltung der Glukosehomöostase, indem es die Rate der Glukoseaufnahme in den insulinsensitiven Geweben wie Muskel und Fettgewebe, relativ zum Blutglukosespiegel, erhöht. Sobald Insulin die Blut-Hirn-Schranke (BBB) passiert, bindet es an seinen Tyrosinkinasenrezeptor, der unter anderem im ARC des Hypothalamus lokalisiert ist und aktiviert den nachgeschalteten Insulinrezeptorsubstrat (IRS)/ Phosphoinositol-3-Kinase (PI3K) - Signalweg (Abb. 2). Dieser Signalweg gilt als hauptverantwortlich für die Regulation der Glukosehomöostase. Eine Störung dieser Kaskade geht mit einer verminderten Glukosetoleranz einher [12]. Bei normoglykämischen Individuen bewirkt die Insulinrezeptor-Bindung eine Rekrutierung und Aktivierung des nachgeschalteten, zytosolischen IRS [5]. Diese sind durch verschiedene Threonin- und Serin- Phosphorylierungsstellen gekennzeichnet, wodurch die Insulinsignaltransduktion sowohl

positiv als auch negativ beeinflusst werden kann [13;14]. Die Hauptfunktion der IRS- Proteine liegt in der Aktivierung der PI3K, die als Schlüsselenzym der Insulinsignaltransduktion zu betrachten ist [5]. Sie besteht aus einem heterodimeren Komplex mit einer regulatorischen- (p85α, p85β, p55γ) und einer katalytischen (p110α, β, γ, δ)- Untereinheit [15]. Die Aktivierung der PI3K vermittelt die Phosphorylierung der, auch als AKT bekannten, Proteinkinase B an den Stellen Threonin 308 und Serin 473. Hierbei ist die Phosphorylierung an Stelle Threonin 308 für die vollständige Phosphorylierung von AKT essentiell, hat allerdings ohne die folgende Serin- Phosphorylierung bisher keine bekannte biologische Funktion. Die Phosphorylierung von AKT (Serin 473) wird somit üblicherweise als Marker für die PI3K- Aktivität herangezogen und ist gleichzeitig der Auslöser der mannigfaltigen Wirkung von Insulin auf die Energie- und Glukosehomöostase [5].

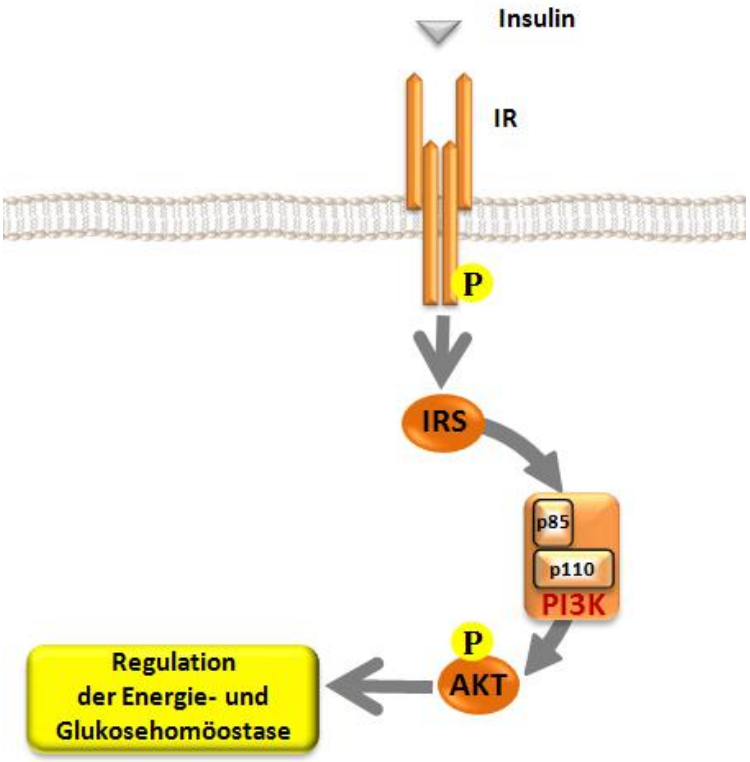

Abb. 2: Der IRS/PI3K- Signalweg. Ein Insulinsignal bewirkt die Autophosphorylierung des IR, wodurch das IRS rekrutiert und die PI3K aktiviert wird. Die PI3K phosphoryliert AKT, wodurch die Regulation der Energie- und Glukosehomöostase vermittelt wird. IRS: Insulinrezeptorsubstrat; IR: Insulinrezeptor; PI3K: Phosphoinositol-3-Kinase.

Der Name Leptin (griechisch: schlank) ist auf die anorexigene Wirkung des Hormons zurückzuführen und wurde daher auch umgangssprachlich als das „Schlankheitshormon“ oder „Sättigungshormon“ bezeichnet. 1994 konnten Friedman und seine Kollegen das mutierte *obese* Gen in sogenannten leptindefizienten Mäusen ($Lep^{ob/ob}$- Mäusen) identifizieren. Diese Mäuse sind durch einen adipösen und glukoseintoleranten Phänotypen charakterisiert, welcher mit einer übermäßigen Nahrungsaufnahme und einem reduzierten Stoffwechsel einhergeht [16]. Da Adipositas als einer der

Hauptrisikofaktoren für die Entstehung von Diabetes mellitus Typ II angesehen wird [2], rückte Leptin in den Fokus der Diabetesforschung. Leptin wird von weißen Adipozyten sekretiert, wobei die Konzentration von zirkulierendem Leptin proportional zum Körperfettgehalt vorliegt [17]. Dadurch liefert Leptin Informationen über den Energiestatus des Körpers und hilft einer möglichen Gewichtszunahme entgegenzuwirken. Der Hauptwirkungsort von Leptin auf den Energie- und Glukosemetabolismus liegt im MBH. Unter anderem hier wird die lange Form des Leptinrezeptors (LepR) exprimiert, welcher in der Lage ist die Leptin-Signalkaskade adäquat zu aktivieren [18-20]. Zirkulierendes Leptin erreicht die BBB und kann diese vermutlich über die kurze Form des LepR passieren [21;22]. Der Transport verläuft bei niedrigen Leptinspiegeln linear, wodurch das ZNS adäquat über den peripheren Energiezustand informiert werden kann [23]. Durch Bindung von Leptin an seinen Rezeptor (siehe dazu Abb. 3), welcher durch eine extrazelluläre Transmembran-Bindedomäne und eine zytoplasmatische Signaldomäne gekennzeichnet [24] ist, wird die Januskinase 2 (JAK2) aktiviert [25]. Diese Aktivierung ist notwendig, da der LepR über keine endogene Kinase-Aktivität verfügt und ermöglicht die Phosphorylierung des LepR. Infolgedessen kommt es zur Bindung des „Signal Transducer and Activator of Transcription-3“ (STAT3) an den Rezeptor und somit zur Phosphorylierung von STAT3 an der Stelle Tyrosin 705. Nach der Phosphorylierung lösen sich die phospho-STAT3 (Tyrosin 705)- Monomere vom Rezeptor, dimerisieren und translozieren in den Nucleus, wo sie die Transkription von Zielgenen regulieren und dadurch die Nahrungsaufnahme und den Energiehaushalt steuern [26]. Durch die Transkription des natürlichen Inhibitors der Leptintransduktion, den „Suppressor of cytokine signalling“ (SOCS3), entsteht eine negative Rückkopplung dieses Signalweges, wodurch dieser nach erfolgreicher Transduktion gestoppt werden kann [27].

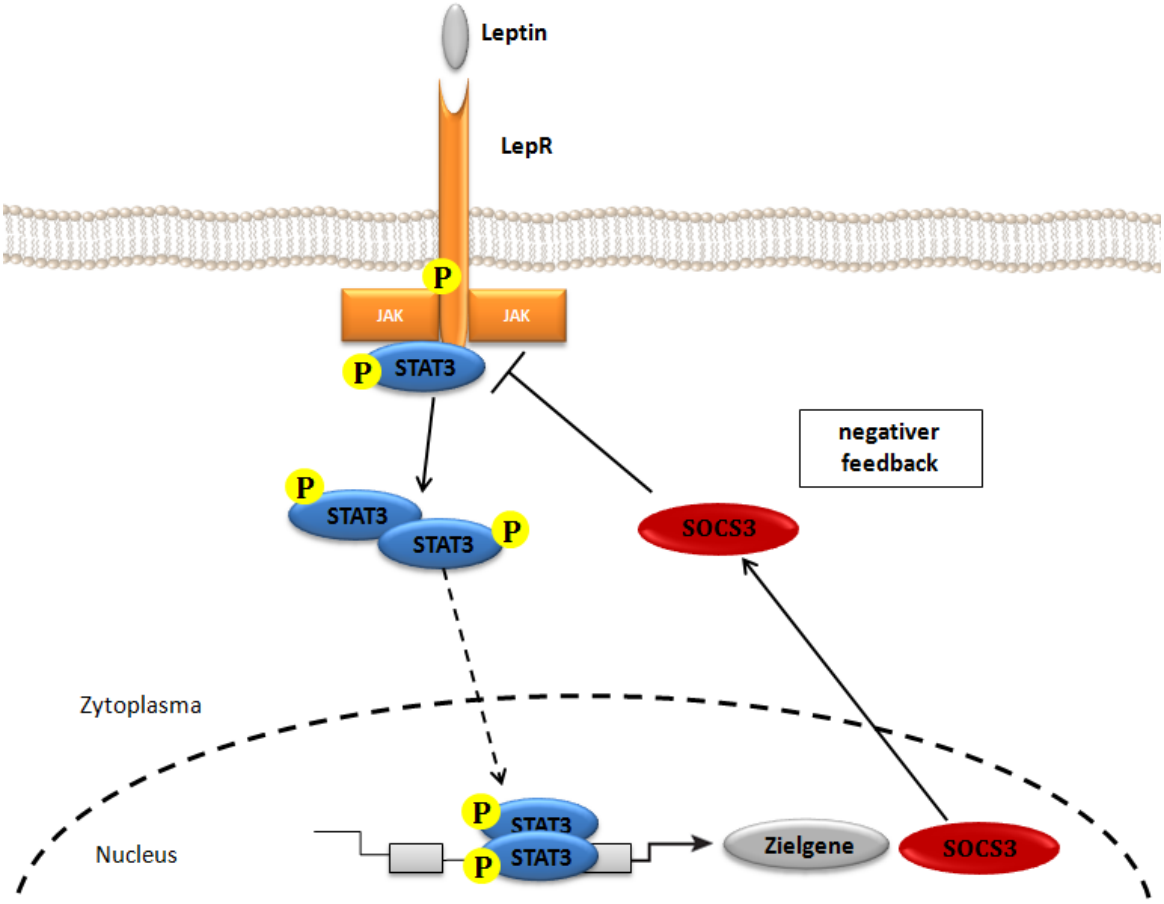

Abb. 3: Der JAK-STAT- Signalweg. Ein Leptinsignal führt zur Aktivierung der JAK, die wiederum den LepR und STAT3 phosphoryliert. Phospho-STAT3 translociert als Dimer in den Nucleus, wo es die Transkription der Zielgene aktiviert. Hierzu zählt auch SOCS3, wodurch eine negativer feedback entsteht. JAK: Januskinase; LepR: Leptinrezeptor; STAT3: Signal Transducer and Activator of Transcription; SOCS3: Suppressor of cytokine signaling.

3.1.2 Diabetes mellitus Typ II: Wissenschaftlicher Stand der Ursachenforschung

Wie bereits erwähnt, wird Adipositas als einer der Hauptrisikofaktoren für die Entstehung von Diabetes mellitus Typ II angesehen [2]. Neben einer diätinduzierten Adipositas, die durch hyperkalorische Ernährung und Bewegungsmangel hervorgerufen wird, können auch genetische Defekte, wie z.B. der Verlust von Leptin oder des LepR, für die Entstehung verantwortlich sein [28;29]. Im Gegensatz zur diätinduzierten Adipositas treten diese jedoch eher selten auf. Mit Zunahme des Körpergewichtes kommt es gleichzeitig zum Anstieg von Insulin, da dieses proportional zum Körperfettgehalt sezerniert wird [12]. Im Verlaufe der Gewichtszunahme und dem damit ansteigenden Körperfettgehalt kommt es, trotz des erhöhten Serumspiegels von Insulin, zu einer verringerten Sensitivität gegenüber diesem Hormon [30;31] und es manifestiert sich eine sogenannte Insulinresistenz. Dies hat zur Folge, dass die insulin-induzierte PI3K-Aktivität reduziert ist, was zu einer Störung der Glukosehomöostase führt [12]. Die möglichen Ursachen für die entstehende Insulinresistenz sind bis heute nur unvollständig verstanden. Neben dem mittlerweile gut charakterisierten Einfluss von Leptin auf die Regulation der Nahrungsaufnahme und des Energieverbrauchs durch den JAK2/STAT3- Signalweg, deuten neuere Publikationen darauf hin, dass Leptin auch die PI3K aktivieren kann [32;33] und somit möglicherweise für eine funktionelle Weiterleitung des Insulinsignals im ZNS notwendig ist. Da Übergewicht ebenfalls mit einer Leptinresistenz assoziiert ist, könnte die gestörte Leptinsignaltransduktion den Zusammenhang von Adipositas und Diabetes mellitus Typ II erklären [31]. Im Zuge der diätbedingten Gewichtszunahme steigen die zirkulierenden Leptinspiegel proportional zum Körperfettgehalt an [31] und es kommt zur Hyperleptinämie [17;34]. Ungeachtet der erhöhten Serum- Leptinspiegel wird jedoch die anorexigene Wirkung von Leptin stark beeinträchtigt. Die zugrundeliegenden molekularen Mechanismen dieser, auch als Leptinresistenz bezeichneten, Signalstörung sind jedoch nur unvollständig verstanden. Bei Übergewicht und der damit assoziierten Hyperleptinämie ist der Transport von Leptin über die BBB allerdings nicht mehr linear, sondern verläuft nahezu gesättigt [23], wodurch das ZNS Fehlinformationen über den metabolischen Zustand der Peripherie erhält und einer Gewichtszunahme nicht weiter entgegenwirken kann. Da Leptin möglicherweise auch die PI3K aktivieren kann [32;33], hätte diese zentrale Leptinresistenz einen außerordentlichen Einfluss auf den IRS/PI3K- Signalweg und somit auf die Steuerung der Glukosehomöostase. Eine Hypothese, die dadurch unterstützt wird, dass sowohl leptindefiziente als auch leptinresistente Individuen neben einem adipösen Phänotypen eine ausgeprägte Glukoseintoleranz und eine verminderte Insulinsensitivität im MBH aufweisen [16;35]. Allerdings ging aus den bisherigen Studien nicht hervor, ob der adipöse Phänotyp oder das Fehlen des hypothalamischen Leptinsignals für die Glukoseintoleranz verantwortlich ist. Die chronische Behandlung von $Lep^{ob/ob}$- Mäusen mit Leptin verbessert zwar die Glukosetoleranz, ist aber auch mit einer deutlichen Reduktion des Körpergewichts verbunden [16;36].

Der akute Einfluss von Leptin auf die den Glukosemetabolismus und den zentralen IRS/PI3K- Signalweg

Um zwischen dem Einfluss des Körperfettes und dem Verlust des Leptinsignals unterscheiden zu können wurde der akute Effekt von Leptin auf die Glukosehomöostase sowie die molekulare Interaktionen zwischen Leptin und dem IRS/PI3K- Signalweg in einer Studie von Dr. Christiane E. Koch (Kapitel 4.1) untersucht. Eine akute Leptinbehandlung ermöglichte es den Einfluss von Leptin auf den Glukosehaushalt in $Lep^{ob/ob}$- Mäusen zu untersuchen, ohne dass das Körpergewicht oder der Körperfettgehalt der Mäuse beeinträchtigt wird. Diese Mäuse zeichnen sich, trotz Adipositas und Glukoseintoleranz, durch eine hohe Leptinsensitivität aus und unterscheiden sie sich von Mäusen, die eine diätinduzierte (Fütterung einer hochkalorischen Diät) Adipositas aufweisen, da diese mit einer Leptinresistenz assoziiert ist. Es konnte gezeigt werden, dass der genetische Verlust des Leptinsignals den Glukosemetabolismus maßgeblich beeinträchtigt und zu einer Glukoseintoleranz führt. Hierbei wiesen normalgewichtige $Lep^{ob/ob}$- Mäuse einen vergleichbaren glukoseintoleranten Phänotypen wie *ad libitum* gefütterte $Lep^{ob/ob}$- Mäuse auf (Kapitel 4.1 Abb. 1b und c). Die akute Wiederherstellung des Leptinsignals, mittels intraperitonealer (ip) - oder zentraler- Applikation von Leptin, verbesserte die Glukosetoleranz der Mäuse. Jedoch war die Wiederherstellung des Leptinsignals in adipösen $Lep^{ob/ob}$- Mäusen nicht ausreichend, um die Glukosetoleranz zu normalisieren, wohingegen dies bei den normalgewichtigen $Lep^{ob/ob}$- Mäusen möglich war (Kapitel 4.1 Abb. 1b und c). Diese Ergebnisse legen nahe, dass auch der Körperfettanteil an der Entstehung von Diabetes mellitus Typ II beteiligt ist (siehe dazu Kapitel 3.1.4). Eine vorherige Inhibition des zentralen IRS/PI3K- Signalweges, mittels intracerebroventricularer (icv) Injektion spezifischer PI3K-Inhibitoren (PIK75 und TGX221), unterdrückte jedoch den positiven Einfluss von Leptin auf die Glukosehomöostase (Kapitel 4.1 Abb. 2d). Diese Ergebnisse deuteten darauf hin, dass Leptin zentral über diesen Signalweg in die Regulation der Glukosehomöostase eingreift und von einem intakten zentralen IRS/PI3K- Signalweg abhängig ist. Darüber hinaus modulierte Leptin das Phosphorylierungsmuster von IRS-1 im MBH. Eine Leptininjektion verringerte dabei die Anzahl der phospho-IRS-1 (Serin 612) immunoreaktiven Zellen im ARC von $Lep^{ob/ob}$- Mäusen (Kapitel 4.1 Abb. 4a). Diese Phosphorylierungsstelle ist als eine negative Phosphorylierung der IRS Proteine beschrieben und mit Insulinresistenz assoziiert [37]. Es scheint, dass diese Verringerung der IRS- Phosphorylierung durch Leptin die Insulinsensitivität erhöht und dadurch zu einer verbesserten Glukosetoleranz von leptindefizienten Mäusen führt. Durch das Fehlen einer intakten Leptinsignaltransduktion wird die Insulinsensitivität reduziert und es kommt zur Beeinträchtigung des IRS/PI3K- Signalweges und des Glukosehaushalts. Diese Daten zeigen deutlich, dass Leptin maßgeblich für die hypothalamische Insulinsignaltransduktion und die Regulation der Glukosehomöostase notwendig ist und somit die, bei Adipositas auftretende, Leptinresistenz der entscheidende Faktor bei der Entstehung von Diabetes mellitus Typ II sein könnte (Abb. 4). Jedoch

blieb offen, wie Leptin in die IRS/PI3K- Signalkaskade eingreift, wodurch sich die erste Fragestellung der vorliegenden Arbeit ergab:

Durch welche molekularen Mechanismen moduliert Leptin den IRS/PI3K- Signalweg? Sind die beobachteten Effekt auf eine direkte Interaktion von Leptin zurückzuführen oder sind noch andere Signalwege involviert?

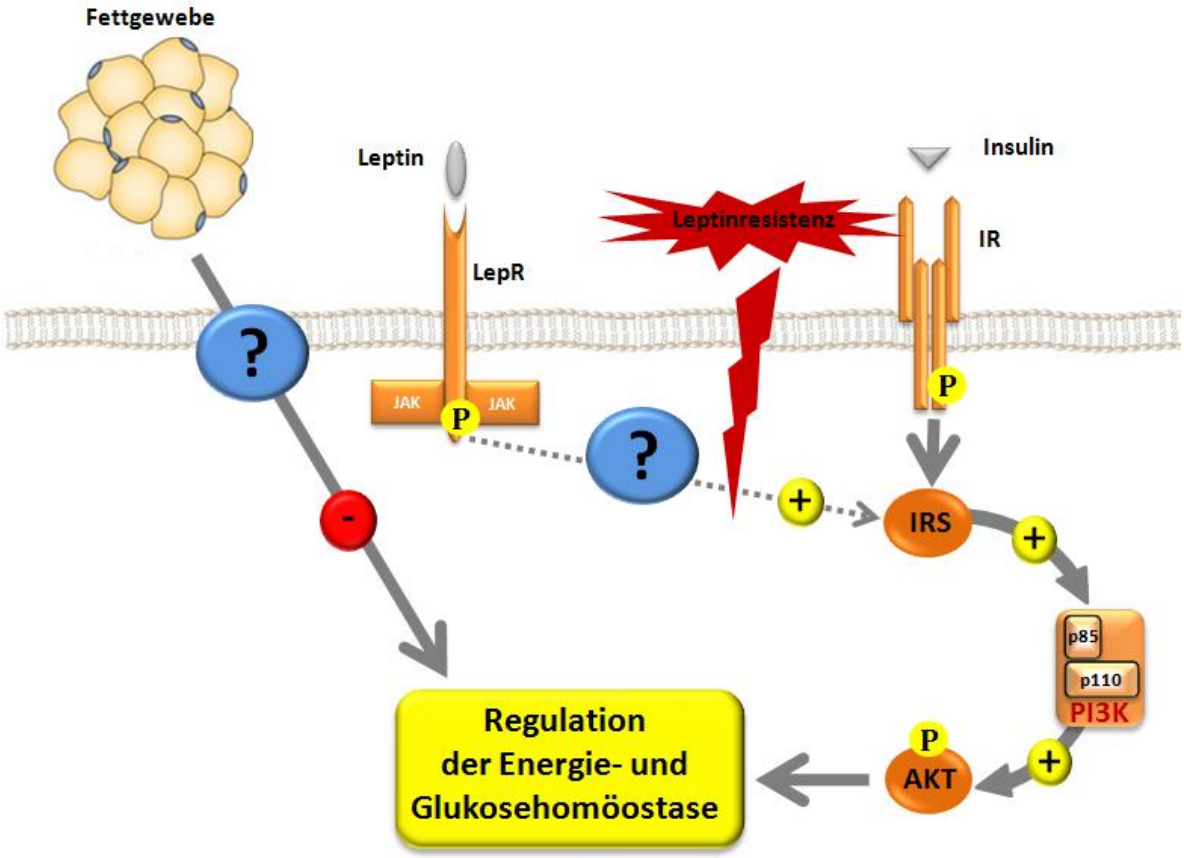

Abb. 4: Schematische Darstellung der zentralen Interaktionen von Leptin und Insulin. In normoglykämischen Mäusen stabilisiert Leptin das IRS durch einen noch unbekannten Mechanismus. Somit kann Insulin die PI3K über IRS aktivieren, was zur Phosphorylierung von AKT und zur Regulation der Glukosehomöostase führt. Durch den Verlust des Leptinsignals bzw. das Auftreten einer zentralen Leptinresistenz wird die Insulinsensitivität reduziert. Insulin kann hierdurch die Aktivierung der PI3K und Phosphorylierung von AKT nicht mehr adäquat induzieren, was es zu einer gestörten Glukosetoleranz führt. Zusätzlich beeinträchtigt das Fettgewebe die Aufrechterhaltung der Glukosehomöostase durch noch unbekannte Mechanismen. Gelbe Symbole: positive Wirkung; dunkelrote Symbole: negative Wirkung; IRS: Insulinrezeptorsubstrat; LepR: Leptinrezeptor; PI3K: Phosphoinositol-3-Kinase; IR: Insulinrezeptor; JAK: Januskinase.

Von Leptin ist bekannt, dass es neben dem JAK-STAT- und IRS/PI3K- Signalweg auch noch andere Signalwege beeinflussen kann. So konnte z.B. *in-vitro* gezeigt werden, dass Leptin mit dem WNT/β Catenin- Signalweg interagiert [38;39]. Interessanterweise sind genetische Polymorphismen dieses Signalweges mit einem erhöhten Risiko an Diabetes mellitus Typ II zu erkranken assoziiert. Hierbei sind insbesondere das *TCF-7*- und das *LRP-6*- Gen zu nennen

[40-42]. Um der ersten Frage der vorliegenden Dissertation nachzugehen, war die Charakterisierung dieses Signalweges im MBH und die Untersuchung von möglichen Interaktionen zwischen Leptin mit diesem Signalweg das erste Hauptziel dieser Arbeit (siehe dazu Kapitel 4.2) und wird im nächsten Kapitel näher erläutert.

3.1.3 Der WNT/β Catenin- Signalweg

Der WNT/β Catenin (WNT)- Signalweg ist ein im gesamten Tierreich vorkommender und hoch konservierter Signalweg. Er steuert eine Vielzahl von grundlegenden zellulären Prozessen wie z.B. die Proliferation und die Stammzelldifferenzierung [43]. Infolgedessen besitzt dieser Signalweg zum einen eine elementare Funktion in der Embryogenese und zum anderen aber auch in der Tumorgenese und anderen assoziierten Krankheiten [44-46]. Der Name des WNT- Signalweges leitet sich aus den Begriffen *Wg* für *wingless* und Int-1 ab. Ersteres stammt aus Experimenten mit der Taufliege *Drosophila melanogaster*, bei welchen eine Mutation im *Wg*- Gen zu einer flügellosen Variante führte. Int-1 hingegen ist eine Bezeichnung für das *Int-1*-Gen, welches mittlerweile auch WNT-1 genannt wird und zu den WNT- Liganden zählt [47]. An der Signaltransduktion des WNT-Signalweges sind zahlreiche Proteine beteiligt. Sowohl im humanen als auch im murinen System unterscheidet man 19 verschiedene WNT- Liganden, die sogenannten WNT´s. Bis heute ist nicht viel über die Sekretion und Modifikation dieser morphogenen und hydrophoben Signalmoleküle bekannt. Eine N-terminale Signalsequenz sowie eine hoch konservierte Verteilung von 23 Zysteinen ist jedoch charakteristisch [48]. Darüber hinaus werden sie posttranslational glykolisiert und lipidmodifiziert. Mögliche Veränderungen der Aktivität durch diese Modulationen sind allerdings noch weitgehend unbekannt und variieren zwischen den verschiedenen WNT- Liganden [49].

Neben den extrazellulären Liganden besteht der WNT- Signalweg aus dem G-Protein gekoppelten, 7-transmembran- Rezeptor Frizzled (Fz) und dessen Co-Rezeptor, dem „low-density lipoprotein receptor-related protein“ -6 (LRP-6). In Abwesenheit der Liganden bildet das Schlüsselenzym, die Glykogen-Synthase-Kinase-3β (GSK-3β), einen Komplex mit dem Gerüstprotein Axin, Adenomatosis polyposis coli (APC) und Dishevelled (DVL). Diese Komplexbildung führt zur Phosphorylierung von β-Catenin durch GSK-3β, welche die proteasomale Degradierung von β-Catenin zur Folge hat. Zusätzlich kann der WNT- Signalweg durch extrazelluläre Antagonisten wie z.B. Dickkopf-1 (DKK-1) inhibiert werden. Bindet jedoch ein WNT- Signalprotein an den Fz-Rezeptor, so kommt es zur einer Heterodimerisierung zwischen jenem und dem Co-Rezeptor LRP-6. Dies hat zur Folge, dass DVL zum Co-Rezeptor rekrutiert wird, wodurch der Destruktionskomplex aufgelöst und die GSK-3β, durch Phosphorylierung an Serin 9, inhibiert wird (Abb. 5). Infolgedessen kommt es zur Stabilisierung und Anreicherung von β-Catenin im Zytoplasma und letztendlich auch im Zellkern. Hier aktiviert β-Catenin die Transkriptionsfaktoren „T-cell factor“ -7 (TCF-7) und „Lymphoid enhancer factor“ (LEF), wodurch Zielgene, wie z.B. Axin-2 und Cylin-D1, transkribiert werden. [50]. Neben dieser Signaltransduktion, auch als „kanonischer-WNT –Signalweg“ bekannt, gibt es einen weiteren, β-Catenin- unabhängigen Aktivierungsmechanismus, dem sogenannten nicht-kanonischen WNT-Signalweg, auf den jedoch in der vorliegenden Arbeit nicht näher eingegangen wird.

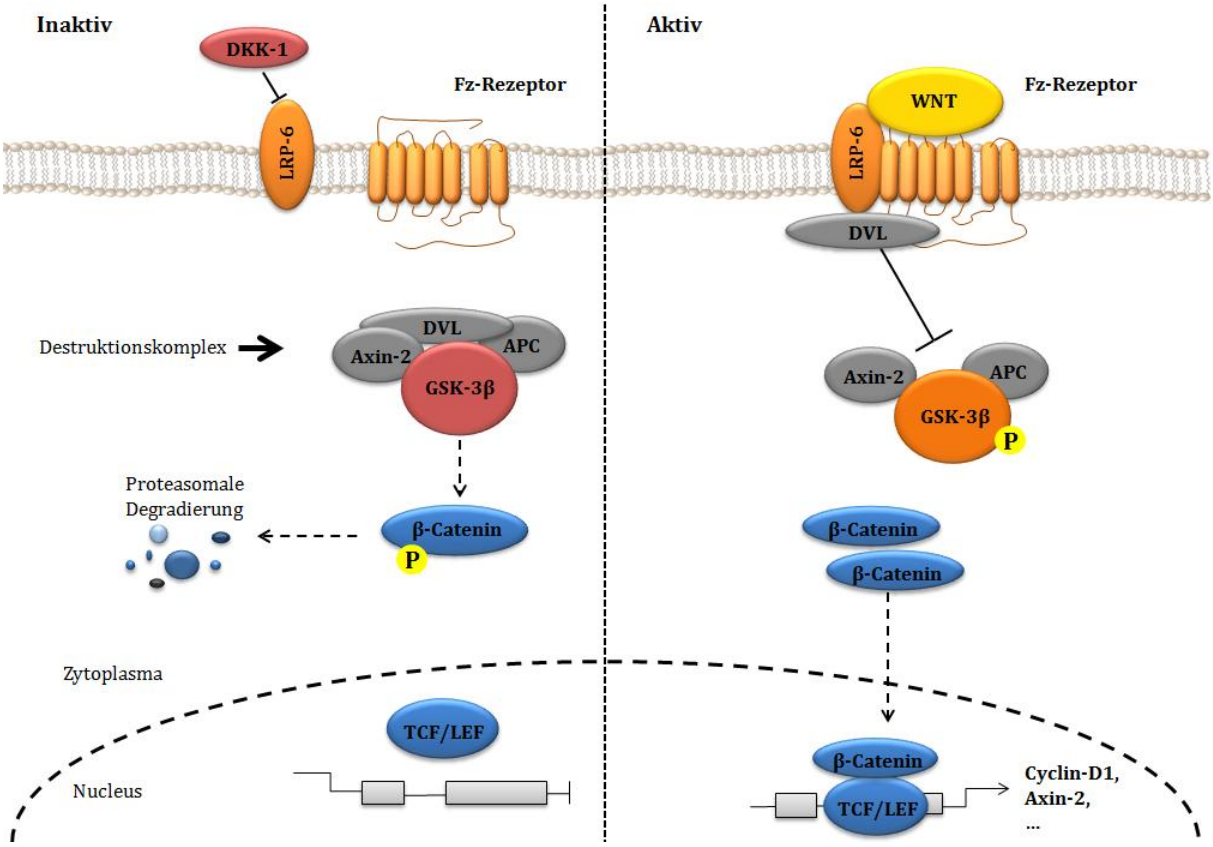

Abb. 5: Der WNT- Signalweg. Bei Abwesenheit der WNT- Liganden (links) oder Anwesenheit des Antagonisten DKK-1 bilden Axin-2, DVL, APC und die GSK-3β einen Komplex. Hierbei phosphoryliert die aktive GSK-3β das zytoplasmatische β-Catenin, wodurch dieses abgebaut wird. Die Anwesenheit eines Liganden (rechts) bewirkt eine Heterodimerisierung des Fz- Rezeptors mit dem Co-Rezeptor LRP-6, wodurch DVL zum Rezeptor rekrutiert wird. Hierdurch wird die GSK-3β phosphoryliert und damit inaktiviert. Somit transloziert β-Catenin in den Nucleus und bindet an Transkriptionsfaktoren TCF-7 und LEF, wodurch die Zielgene transkribiert werden. DKK-1: Dickkopf; DVL: Dishevelled; APC: Adenomatosis polyposis coli; GSK-3β: Glykogen-Synthase Kinase -3β; Fz: Frizzled; LRP: low-density lipoprotein receptor-related protein; TCF: T-cell factor; LEF: Lymphoid enhancer factor.

Der WNT –Signalweg und die Assoziation mit Diabetes mellitus Typ II

Im Jahre 2006 veröffentlichten drei unabhängige Studien fast zeitgleich, dass genetische Polymorphismen im *TCF-7*- Gen mit einem stark erhöhten Risiko an Diabetes mellitus Typ II zu erkranken einhergehen [40-42]. Kurz darauf wurde bekannt, dass auch eine Mutation im *LRP-6*- Gen die Wahrscheinlichkeit an dieser metabolischen Störung zu erkranken deutlich erhöht [51]. Neben diesen Prädispositionen sind auch genetisch unabhängige Interaktionen des WNT- Signalweges mit dem Glukosemetabolismus bekannt. Hierbei nimmt das Schlüsselenzym, die GSK-3β, eine bedeutende Rolle ein. Sie ist eine konstitutiv aktive Serin/Threonin Kinase und wurde ursprünglich als ein Enzym definiert, das die Glykogensynthese als Antwort auf ein Insulinsignal reguliert. Darüber hinaus ist bekannt, dass die GSK-3β eine noch unbekannte Funktion im Insulin- Signalweg einnimmt. Nach Insulinstimulation und Aktivierung der PI3K wird die GSK-3β durch die Proteinkinase B an Serin 9 phosphoryliert und somit inhibiert [52-56]**.** Es konnte gezeigt werden, dass eine Inhibition der GSK-3β

in der Peripherie die Glukosehomöostase in glukoseintoleranten Tieren deutlich verbessert [57-59], jedoch ist weder ein Mechanismus noch das dafür verantwortliche Gewebe bekannt. Des Weiteren wurde in *in-vitro* Studien gezeigt, dass Leptin mit diesem Signalweg interagiert [38;39]. Da Leptin maßgeblich an der Steuerung der Glukosehomöostase beteiligt ist [36;60], könnte dieser Signalweg auch im Glukosemetabolismus involviert sein. Unser Kooperationspartner Professor Peter R. Shepherd (Auckland, Neuseeland) konnte zeigen, dass Glukose den WNT- Signalweg in Makrophagen aktiviert [61], wodurch die Vermutung nahe liegt, dass dieser Signalweg eine sensorische Funktion für Glukose einnehmen könnte. Bis heute existieren jedoch weder Erkenntnisse über die Präsenz noch über eventuelle Funktionen dieses Signalweges im Hypothalamus von adulten Mäusen. Um der ersten Frage der vorliegenden Dissertation nachzugehen wurde daher das Expressionsmuster der WNT-Signalkomponenten im MBH analysiert und der Einfluss von Leptin auf diesen Signalweg untersucht (siehe dazu Kapitel 4.2). Darüber hinaus ergab sich die zweite Fragestellung der vorliegenden Arbeit, die in Kapitel 4.3 untersucht wurde:

Welche Rolle nimmt die zentrale GSK-3β in der Regulation des Glukose- und Energiemetabolismus ein?

Neueste Forschungsergebnisse deuten zusätzlich darauf hin, dass die GSK-3β auch als Regulator von inflammatorischen Prozessen dient [62], welche mit Adipositas und der Entstehung von Diabetes mellitus Typ II assoziiert sind [63-65]. Es konnte gezeigt werden, dass eine Inhibition der GSK-3β eine pro-inflammatorische Antwort in eine anti-inflammatorische Antwort umwandeln kann [66]. Darüber hinaus wurden bereits anti-inflammatorische Effekte von GSK-3β- Inhibitoren beschrieben [67], die zugrunde liegenden Mechanismen konnten jedoch noch nicht entschlüsselt werden.

3.1.4 Die hypothalamische Inflammation

In den letzten Jahren etablierte sich die hypothalamische Inflammation als ein neues Forschungsgebiet. Unter dem Begriff Inflammation versteht man im Allgemeinen eine Antwort des Organismus auf gesundheitsschädliche Stimuli. Diese können physikalisch, chemisch oder biologisch sein. In Bezug auf Adipositas versteht man in diesem Zusammenhang ein erhöhtes Aufkommen zirkulierender pro-inflammatorischer Zytokine (= regulatorische Peptide, die an der Steuerung der Immunantwort beteiligt sind), welche mit einer verminderten Insulin- und Leptinsignaltransduktion im MBH assoziiert sind [63-65]. Diese sogenannte „metabolische"- oder auch „low-grade"- Inflammation ist durch einen niedrigen, jedoch chronischen Zytokinspiegel charakterisiert. Dadurch unterscheidet sie sich von einer akuten Immunantwort, wie sie zum Beispiel bei einer bakteriellen Infektion ausgelöst wird.

Wie bereits erwähnt steht auch der erhöhte Körperfettanteil im Verdacht an der Entstehung von Diabetes mellitus Typ II beteiligt zu sein (Kapitel 4.1 Abb. 1b und c). Während der Entwicklung von Adipositas infiltrieren Makrophagen des Immunsystems vor allem das viszerale Fettgewebe, was unter anderem zu einer erhöhten Sekretion der Zytokine „Tumor necrosis factor-alpha" (TNFα) und Interleukin-6 (Il-6) führt [68]. Beide Zytokine sind in der Lage die BBB zu passieren [69;70], binden dort an spezifische Zytokinrezeptoren und könnten inflammatorische Signalwege aktivieren. Hierzu zählen der c-Jun N-terminale Kinase (JNK) - sowie der „Inhibitor von NF-κB- Kinase (IKKβ) / NF-κB"- Signalweg [68]. Darüber hinaus stehen hochkalorische Diäten im Verdacht eine direkte inflammatorische Antwort, unabhängig von Adipositas, auszulösen [63-65]. Hierbei wird die Immunantwort über Toll-like-Rezeptoren (TLR) vermittelt, die in fast allen Zellen des ZNS exprimiert werden [71]. Die in der Nahrung enthaltenen gesättigten Fettsäuren können die BBB passieren [72], binden dort an TLR [73] und aktivieren möglicherweise die oben genannten Signaltransduktionen [68].

Der JNK- Signalweg

Die JNK ist eine Serin/Threonin Kinase und gehört zur Superfamilie der „mitogen-activated protein kinase" (MAPK). Bisher sind drei verschiedene Isoformen (JNK-1- 3) bekannt, wobei JNK-1 und JNK-2 in allen Geweben und Zellen vorzufinden sind [74], hingegen die Expression von JNK-3 fast ausschließlich auf das Herz und das ZNS beschränkt ist [75]. Eine Aktivierung kann über TLR [68] als auch über die Zytokine TNFα und Il-6 und deren Rezeptoren erfolgen [76]. Eine Liganden-Rezeptor-Bindung bewirkt hierbei, dass Adaptermoleküle, beispielsweise der „myeloid-differentiation factor 88" (MyD88), rekrutiert werden, wodurch es im weiteren Verlauf zur Phosphorylierung (Threonin 183 und Thyrosin 185) und damit zur Aktivierung der JNK kommt [77]. Letztendlich wird der

Transkriptionsfaktor „acitvated protein-1“ (AP-1) aktiviert, transloziert in den Zellkern und vermittelt die Transkription spezifischer Zielgene [68;78].

In peripherem Gewebe wurde festgestellt, dass die aktive JNK mit dem IRS/PI3K- Signalweg interagiert. Dabei phosphoryliert sie das IRS-1 und reduziert die Insulinsensitivität, wodurch die Weiterleitung des Insulinsignals vermindert ist [75;79-82]. Ein totaler Verlust der JNK-1, herbeigeführt durch einen genetischen knockout, schützt hingegen vor diätinduzierter Adipositas und Insulinresistenz [75], wobei die Antwort auf das hauptverantwortliche Organ oder Gewebe in dieser Studie offen blieb. Jahre später konnte jedoch gezeigt werden, dass eine erhöhte JNK-Aktivität im Hypothalamus mit Adipositas assoziiert ist [83] und, dass ein rein neuronaler knockout von JNK-1 vor diätinduzierter Adipositas schützt [84;85]. Da diese Studien keine Untersuchungen über die zentralen molekularen Mechanismen lieferten, ergab sich die dritte Fragestellung der vorliegenden Arbeit (siehe dazu Kapitel 4.4):

Welche hypothalamischen Nuclei sind durch Adipositas mit einer erhöhten JNK-Aktivität assoziiert und gibt es Interaktionen zwischen der JNK und dem hypothalamischen Insulin- Signalweg?

Der IKKβ / NF-κB- Signalweg

Neben dem JNK- Signalweg spielt auch der IKKβ / NF-κB- Signalweg eine zentrale Rolle bei der Immunantwort [86]. Im inaktiven Zustand ist der Transkriptionsfaktor NF-κB an den Inhibitor von NF-κB (IκBα) gebunden und verbleibt im Zytoplasma [87]. Eine Aktivierung des Signalweges erfolgt über den TLR oder die Zytokinrezeptoren [68] und bewirkt eine Rekrutierung des Adapterproteins MyD88, was zu einer Phosphorylierung und damit zu einer Aktivierung der Serin-Kinase IKKβ führt. Diese phosphoryliert IκBα an den Stellen Serin 32 und Serin 36, wodurch es inhibiert und schließlich abgebaut wird. Dadurch gelangt NF-κB in den Nucleus und induziert die Transkription der Zielgene, die in viele zelluläre Prozesse, wie Inflammation, Proliferation und Apoptose, involviert sind [87].

In den letzten Jahren konnte gezeigt werden, dass der zentrale IKKβ / NF-κB- Signalweg eine große Rolle bei metabolischen Erkrankungen spielt und, dass eine Aktivierung dieses Signalweges mit einer zentralen Leptin- als auch Insulinresistenz assoziiert ist [83;88-90]. Die exakten molekularen Mechanismen und die Beteiligung der spezifischen Nuclei sind allerdings unklar. Darüber hinaus wurde noch keine Zusammenhänge zwischen diesem zentralen Signalweg und dem Energiemetabolismus untersucht, wodurch sich die vierte Fragestellung dieser Arbeit ergab (siehe dazu Kapitel 4.5):

Welche Rolle spielt der zentrale IKKβ / NF-κB- Signalweg in der Regulation der Energie- und Glukosehomöostase?

3.2 Zielsetzung

Die grundlegenden molekularen Mechanismen der hypothalamischen Signalverarbeitung, in Bezug auf die Steuerung der Energie- und Glukosehomöostase, sind mittlerweile weitestgehend beschrieben. Die mögliche Beteiligung weiterer Signalwege, sowie die Modifikation der involvierten Signalwege bei der Entstehung von Diabetes mellitus Typ II sind jedoch noch nicht vollständig verstanden. Ziel dieser Doktorarbeit war das Erlangen von neuen Erkenntnissen über regulatorische Prozesse, die zur Entstehung von Adipositas und Diabetes mellitus Typ II führen. Folgende Fragestellungen lagen dieser Doktorarbeit zu Grunde:

Der WNT/β Catenin- Signalweg

1. Existiert ein funktionaler WNT/β Catenin- Signalweg im MBH und gibt es zentrale Interaktionen von Leptin mit diesem Signalweg?

2. Welche Rolle nimmt die zentrale GSK-3β in der Regulation des Glukose- und Energiemetabolismus ein?

Die metabolische Inflammation

1. Welche hypothalamischen Nuclei sind durch Adipositas mit einer erhöhten JNK- Aktivität assoziiert und gibt es Interaktionen zwischen der JNK und dem hypothalamischen Insulin-Signalweg?

2. Welche Rolle spielt der zentrale IKKβ / NF-κB- Signalweg in der Regulation der Energie- und Glukosehomöostase?

3.3 Methoden

Die in dieser Doktorarbeit verwendeten Methoden werden im Folgenden kurz erläutert.

- Die Genexpression der ausgewählten Gene wurde mittels ***in-situ* Hybridisierung** bestimmt und quantifiziert. Hierfür wurde zunächst das gewünschte DNA-Fragment mittels Polymerase-Kettenreaktion amplifiziert und anschließend aus einem Agarosegel extrahiert. Durch die Ligation in den pGEM®-T Easy Vektor (Promega, Mannheim) und die Transformation in *E.Coli* DH5α Zellen, wurde das DNA-Fragment vervielfältigt und nachfolgend sequenziert. Zur Herstellung der radioaktiv (S^{35}) komplementären RNA-Sonden, mittels *in-vitro* Transkription, wurde entweder die SP6- oder T7- RNA-Polymerase (Invitrogen) verwendet. Anschließend wurden die koronale Gehirnschnitte mit den markierten RNA-Sonden inkubiert und später mit Hilfe des Computerprogramms Image-Pro® Plus ausgewertet.

- Mittels **Immunohistochemie** wurde die Aktivität der zentralen Signalwege im MBH lokalisiert und ausgezählt. Dafür wurden koronale Hirnschnitte mit den jeweiligen spezifischen Antikörpern inkubiert. Diese waren gegen ein Epitop des Zielproteins gerichtet, wobei dieses entweder alle vorhandenen Zielproteine oder nur spezifisch phosphorylierte Zielproteine detektierte. In der vorliegenden Arbeit wurden die Anzahl von phospho-AKT (Serin 473), phospho-IRS (Serin 612 oder Serin 307), phospho-LRP-6 (Serin 1490), phospho-JNK (Threonin 183 und Thyrosin 185), phospho-GSK-3β (Serin 9), phospho-AMPK (Threonin 172), phospho-STAT3 (Thyrosin 705) und gesamt IκBα in den verschiedenen hypothalamischen Nuclei ermittelt.

- Um die Protein-Konzentrationen semiquantitative zu bestimmen wurden **Westernblot** Analysen mit dem jeweiligen Gewebe oder Zellen durchgeführt. Hierbei wurden die Proteine im elektrischen Feld, entsprechend ihrer Größe, in einem Polyacrylamid-Gel aufgetrennt und anschließend auf eine Nitrozellulosemembran übertragen. Danach erfolgte die Detektion des gewünschten Proteins mittels spezifischer Antikörper. Die Auswertung wurde mit Hilfe des Computerprogrammes ImageJ durchgeführt.

- Die Bestimmung der Serumkonzentration von Insulin erfolgte mittels **Enzyme Linked Immunosorbent Assay (ELISA)**. Hierfür wurden die gefasteten Tiere dekapitiert, ausgeblutet und das gewonnene Serum für den ELISA verwendet.

- Für die **icv Applikationen** wurde den Mäuse, mit Hilfe eines stereotaktischen Apparates, eine Kanüle in den lateralen zerebralen Ventrikel implantiert. Hierfür wurden die Mäuse mit Isofluran betäubt.

- Um die Glukosetoleranz der Tiere zu messen, wurden **intraperitoneale Glukosetoleranztests** durchgeführt. Hierfür wurde den gefasteten Tieren eine 12,5% Glukoselösung ip injiziert (1,0 – 1,5g Glukose/kg Körpergewicht) und die Blutglukosekonzentrationen zu definierten Zeitpunkten mittels handelsüblichen Glukosometern (Roche) bestimmt. Die Blutentnahme erfolgte hierbei aus der Gesichtsvene der Mäuse.

  Um die Glukoseproduktion der Leber zu ermitteln, wurde ein Pyruvattoleranztest durchgeführt. Pyruvat ist ein Substrat der Glukoneogenese und eine erhöhte Umwandlung von Pyruvat zu Glukose reflektiert somit die Glukoseproduktion der Leber. Hierfür wurde anstelle von Glukose ip Pyruvat (1,5g Pyruvat/kg Körpergewicht) injiziert und die Messung, wie oben beschrieben, durchgeführt.

- Die Körperzusammensetzung der Tiere wurde mittels **DEXA-Messungen** (dual energy X-ray absorptiometry) unter leichter Isofluran-Narkose bestimmt (Lunar PIXImus Densitometer, GE Medical Systems). Bei dieser nicht-invasiven Methode werden die Versuchstiere mit zwei unterschiedlichen Wellenlängen durchleuchtet. Durch das unterschiedliche Absoprtionsverhalten von Knochen, Fett und fettfreier Masse kann die Körperzusammensetzung der Tiere ermittelt werden.

- Die **Überexpression** der ausgewählten Gene wurde mittels Adeno-assoziierten Viren (AAV) gewährleistet. Um die Expression auf Neurone zu beschränken wurde das virale Konstrukt unter die Kontrolle des Synapsin-1 Promotors gestellt. Unter Isofluranbetäubung wurde den Tieren mit Hilfe des stereotaktischen Apparates je $4*10^{10}$ Vektorgenome bilateral in den ARC injiziert.

- Um die Stoffwechselrate sowie den Respiratorischen Quotienten der Tiere zu ermitteln, wurde die **indirekte Kalorimetrie** verwendet. Hierbei wurde die O_2-Aufnahme und die CO_2-Abgabe der Tier *in-vivo* gemessen und daraus indirekt der Energieumsatz errechnet.

3.4 Ergebnisse und Diskussion

3.4.1 Der hypothalamische WNT- Signalweg

Charakterisierung des hypothalamischen WNT- Signalweges und der Einfluss von Leptin

Neuere Forschungsergebnisse zeigen, dass der WNT- Signalweg, bekannt aus der Embryogenese und Tumorgenese [44;45], auch eine Rolle in der Pathogenese von Diabetes mellitus Typ II spielen könnte. Genetische Polymorphismen im *TCF-7*- oder *LRP*-6- Gen sind mit einem erhöhten Risiko an dieser metabolischen Störung zu erkranken assoziiert [40;41;51]. Darüber hinaus konnte gezeigt werden, dass Glukose diesen Signalweg aktivieren kann [61] und, dass Leptin mit diesem Signalweg interagiert [38;39]. Da wir (Kapitel 4.1) und andere zeigen konnten, dass Leptin maßgeblich an der zentralen Steuerung der Glukosehomöostase beteiligt ist [36;60] könnte Leptin über diesen Signalweg in den Glukosemetabolismus eingreifen. Jedoch existierten weder Erkenntnisse über die Präsenz noch über eventuelle Funktionen dieses Signalweges im Hypothalamus. Daher wurde zunächst das Expressionsmuster der WNT- Signalkomponenten im MBH analysiert und mögliche Interaktionen von Leptin mit diesem Signalweg untersucht.

Das Expressionsmuster des WNT- Signalweges im MBH von adulten Mäusen.

Die messenger RNA (mRNA)-Analyse der Signalkomponenten ergab, dass alle untersuchten Gene im ARC von wildtyp Mäusen exprimiert werden (Kapitel 4.2 Abb.1). Darüber hinaus zeigte sich, dass die Expression von verschiedenen Liganden (WNT-7a und WNT-4) als auch von Zielgenen (Axin-2 und Cyclin-D1) dieses Signalweges im ARC von $Lep^{ob/ob}$- Mäusen reduziert war (Kapitel 4.2 Abb. 2a, b und c). Ein ähnlicher Befund wurde auf der Ebene des Co-Rezeptors LRP-6 erfasst. Eine Phosphorylierung von LRP-6 an Serin 1490 ist für eine Fz-Rezeptor-Aktvierung erforderlich und somit essentiell für einen intakten WNT- Signalweg [91]. Die Anzahl der phospho-LRP-6 (Serin 1490) immunoreaktiven Zellen war jedoch im ARC von $Lep^{ob/ob}$- Mäusen im Vergleich zu wildtyp Mäusen stark verringert (Kapitel 4.2 Abb. 3a). Diese Ergebnisse deuteten auf eine verringerte Aktivität des WNT- Signalweges im ARC von $Lep^{ob/ob}$- Mäusen auf allen hierarchischen Ebenen (auf Liganden-, auf Rezeptor- und auch auf Ebene der Zielgene) hin.

Ist der Mangel von endogenem Leptin für die verringerte Aktivität des WNT- Signalweges im ARC verantwortlich?

Da der ARC als Hauptregulationszentrum der zentralen Energie- und Glukosehomöostase anzusehen ist [10], verstärkte sich die Annahme, dass der WNT- Signalweg auch in die Regulation des Glukosemetabolismus involviert sein könnte. Leptin ist maßgeblich an der zentralen Steuerung der Glukosehomöostase beteiligt [36;60] und das Fehlen von Leptin war eine mögliche Ursache für die verminderte Aktivität dieses Signalweges im ARC von $Lep^{ob/ob}$ -Mäusen. Zusätzlich konnten bereits Interaktionen mit dem Schlüsselenzym des WNT- Signalweges, die GSK-3β, *in-vitro* gezeigt werden [38;39]. Daher wurde der Effekt von Leptin auf den hypothalamischen WNT- Signalweg in $Lep^{ob/ob}$-Mäusen untersucht. Die Wiederherstellung des Leptinsignals, mittels ip Leptin Applikation, erhöhte hierbei die Expression der Zielgene Axin-2 und Cyclin-D1 (Kapitel 4.2 Abb. 2b und c) sowie die Anzahl der phospho-LRP-6 immunoreaktiven Zellen (Kapitel 4.2 Abb. 3a) im ARC. Diese Ergebnisse zeigen deutlich, dass eine Interaktion zwischen Leptin und dem WNT- Signalweg vorliegt und bestätigen darüber hinaus die Funktionalität dieses Signalweges im Hypothalamus. Durch welche exakten molekularen Mechanismen die Interaktion von Leptin mit diesem Signalweg vermittelt wird bleibt allerdings offen. Denkbar wäre z.B. eine Involvierung der JAK2 des Leptin- Signalweges.

Ist die Interaktion zwischen Leptin und dem WNT- Signalweg physiologisch relevant?

Neben den WNT- Liganden existieren auch WNT- Antagonisten wie z.B. DKK-1. Eine icv Injektion dieses Antagonisten verminderte, im Gegensatz zu Leptin, die Anzahl der phospho-LRP-6 immunoreaktiven Zellen im ARC von normoglykämischen Mäusen (Kapitel 4.2 Abb. 3b). Um zu überprüfen, ob die positiven Eigenschaften von Leptin auf die Glukosetoleranz mit dem WNT-Signalweg in Verbindung stehen, wurde DKK-1 icv vor einer ip Injektion von Leptin appliziert. Überraschenderweise unterdrückte diese Behandlung die positiven Eigenschaften von Leptin auf die Glukosetoleranz von $Lep^{ob/ob}$- Mäusen, während die alleinige Injektion von Leptin die Glukosetoleranz deutlich verbesserte (Kapitel 4.2 Abb. 3c). Diese Daten lassen vermuten, dass Leptin, in Bezug auf die Verbesserung der Glukosetoleranz, zumindest von funktionalen LRP-6 Rezeptoren abhängig ist. Ob Leptin noch mit anderen WNT- Signalkomponenten zusammenspielt blieb an dieser Stelle ungeklärt. Wie in Kapitel 3.1 beschrieben, sind unter anderem die, im ARC befindlichen, NPY- Neurone maßgeblich an der Steuerung der Energie- und Glukosehomöostase beteiligt [11]. Die katabolen Eigenschaften von Leptin sind hierbei von einer Inhibition der orexigenen NPY- Neurone abhängig [10], wodurch die Produktion von Glukose in der Leber unterdrückt werden kann [92]. Da Leptin die Expression der WNT- Zielgene erhöht und auf der Ebene des Co-Rezeptors LRP-6 agiert wurde untersucht, ob Leptin auch in diesen Neuronen mit dem WNT- Signalweg interagiert. Hierbei wurde das Schlüsselenzym des WNT- Signalweges (die GSK-3β) analysiert, dessen Phosphorylierung an Serin 9 eine Inhibition und damit eine Aktivierung des Signalweges nach sich zieht [52;53;55]. Eine Behandlung mit Leptin erhöhte die Anzahl an phospho-GSK-3β (Serin 9) immunoreaktiven Zellen,

wobei 70% dieser Zellen ebenfalls NPY- Neurone waren (Kapitel 4.2 Abb. 4c). Diese Daten legen die Vermutung nahe, dass Leptin die NPY- Neurone durch eine Aktivierung des WNT- Signalweges inhibiert und hierdurch die positiven Eigenschaften von Leptin auf die Glukosetoleranz vermittelt werden. Ob Interaktionen von Leptin mit dem WNT- Signalweg auch in POMC- Neuronen vorkommen, werden zukünftige Studien zeigen.

Die Daten zeigen deutlich, dass ein funktionaler WNT- Signalweg im Hypothalamus von adulten Mäusen vorliegt. Die Aktivität des WNT- Signalwegs war jedoch im ARC von glukoseintoleranten, adipösen $Lep^{ob/ob}$- Mäusen stark vermindert und kann im Verlust des endogenen Leptinsignals begründet werden. Eine Behandlung mit Leptin konnte diese verminderte Aktivität, durch die Inhibition der GSK-3β, wiederherstellen (Abb. 6). Darüber hinaus scheinen die positiven Eigenschaften von Leptin auf die Glukosetoleranz von einem intakten WNT- Signalweg abhängig zu sein. Daher wurde in der nächsten Studie das Schlüsselenzym dieses Signalweges, die GSK-3β, näher untersucht.

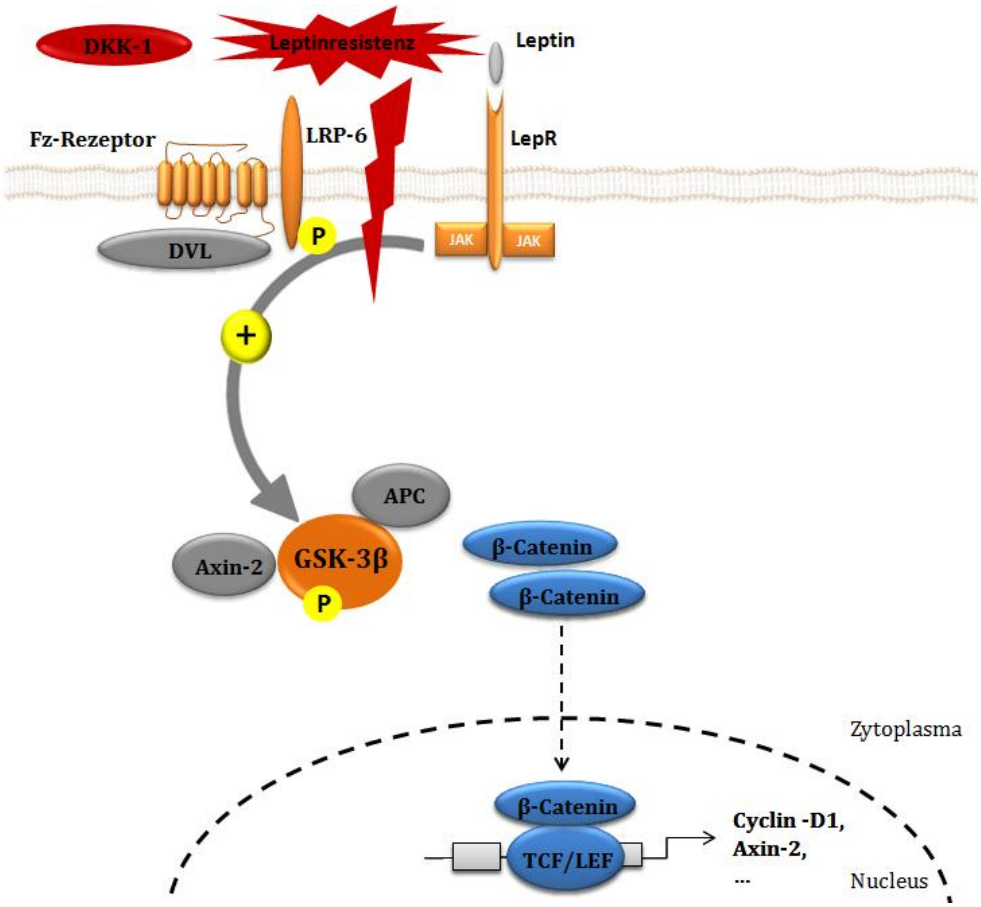

Abb. 6: Interaktionen von Leptin mit dem zentralen WNT-Signalweg im ARC. Leptin phosphoryliert und aktiviert den Co-Rezeptor LRP-6, wodurch DVL zum Rezeptor rekrutiert wird. Hierdurch wird die GSK-3β phosphoryliert und damit inaktiviert. Somit transloziert β-Catenin in den Nucleus und bindet an die Transkriptionsfaktoren TCF-7 und LEF, wodurch die Zielgene transkribiert werden. Der Verlust des Leptinsignals oder die Anwesenheit des WNT- Antagonisten DKK-1 führt hingegen zu einer verminderten Transkription der Zielgene. Gelbe Symbole: positive Wirkung; dunkelrote Symbole: negative Wirkung; ARC: Nucleus arcuatus LRP: low-density lipoprotein receptor-related protein; DVL: Dishevelled; TCF-7: T-cell factor -7; LEF: Lymphoid enhancer factor; GSK: Glykogen- Synthase- Kinase; DKK: Dickkopf; Fz: Frizzled; JAK: Januskinase; LepR: Leptinrezeptor; APC: Adenomatosis polyposis coli.

Die zentrale GSK-3β in der Regulation der Energie- und Glukosehomöostase

Bis heute sind die zentralen Zusammenhänge zwischen der GSK-3β und der hypothalamischen Regulation des Glukosehaushaltes ungeklärt. Aus peripheren Studien geht allerding hervor, dass die GSK-3β durch Insulinstimulation und der damit einhergehenden Aktivierung der PI3K durch die Proteinkinase B an Serin 9 phosphoryliert und dadurch inhibiert wird [52-56]. Darüber hinaus verbessert die periphere Inhibition der GSK-3β die Glukosehomöostase in glukoseintoleranten Tieren [57-59], jedoch ist weder ein Mechanismus noch das dafür verantwortliche Gewebe bekannt. In Kapitel 4.2 konnte gezeigt werden, dass die positiven Eigenschaften von Leptin auf die Glukosetoleranz von einem intakten WNT- Signalweg abhängig sind und, dass Leptin in der Lage ist die GSK-3β in Neuronen des ARC zu inhibieren. Aufgrund dieser Daten wurde vermutet, dass die GSK-3β auch an der zentralen Regulation der Energie- und Glukosehomöostase beteiligt sein könnte. Zunächst wurde mittels Immunohistochemie untersucht, ob die Aktivität dieses Enzyms im ARC durch genetisch-induzierte- ($Lep^{ob/ob}$- Mäuse) oder diätinduzierte- Adipositas erhöht war. Im Vergleich zu den jeweiligen Kontrollen war die Anzahl der phospho- GSK-3β (Serin 9) immunoreaktiven Zellen im ARC erniedrigt. Dieses Ergebnis war für beide Mausmodelle gleichermaßen zutreffend (Kapitel 4.3 Abb. 1a und b) und deutete auf eine erhöhte GSK-3β Aktivität im ARC durch Adipositas hin.

Welche Rolle nimmt die zentrale GSK-3β in der Regulation des Glukosemetabolismus ein?

Die akute Inhibition der zentralen GSK-3β, mittels icv Injektion eines pharmakologischen GSK-3β Inhibitors, verbesserte die Glukosetoleranz von $Lep^{ob/ob}$- Mäusen (Kapitel 4.3 Abb. 1c) und lässt auf eine bedeutende Funktion der GSK-3β in der Glukosehomöostase schließen. Der zentrale Insulin-Signalweg (IRS/PI3K) ist essentiell für die Regulation der Glukosehomöostase [4;6;7;93-95]. Die immunohistochemische Analyse ergab, dass die zentrale Inhibition der GSK-3β die Anzahl der phospho-IRS-1 (Serin 612) positiven Zellen im ARC verringerte. Gleichzeitig erhöhte diese Behandlung die Anzahl der phospho-AKT (Serin 473) immunoreaktiven Zellen in diesem Nucleus (Kapitel 4.3 Abb. 2a und b). Die Phosphorylierung von IRS-1 an Serin 612 ist mit einem negativen Einfluss auf die PI3K verbunden, die Phosphorylierung von AKT an Serin 473 hingegen wird als Marker für eine PI3K Aktivierung angesehen [95]. Die Ergebnisse zeigen daher, dass die positiven Effekte der zentralen GSK-3β Inhibition auf die Glukosetoleranz mit einer Verbesserung des hypothalamischen IRS/PI3K- Signalweges assoziiert waren. Darüber hinaus deuten die Ergebnisse darauf hin, dass diese Effekte von einem intakten IRS/PI3K- Signalweg abhängig sind. Hierbei unterdrückte eine zentrale Applikation von spezifischen PI3K Inhibitoren (PIK75 and TGX221) die positiven Effekte der zentralen GSK-3β Inhibition auf die Glukosetoleranz von $Lep^{ob/ob}$- Mäusen (Kapitel 4.3 Abb. 2c).

Werden die positiven Effekte von Leptin auf den Glukosemetabolismus durch eine Inhibition der zentralen GSK-3β vermittelt?

Interessanterweise ähneln sich die Effekte einer zentralen Leptin Injektion (vergleiche hierzu Kapitel 4.1 Abb. 2d und 4a) mit den hier gezeigten Effekten der GSK-3β Inhibition. Beide, zentral applizierten, Moleküle verbesserten die Glukosetoleranz von $Lep^{ob/ob}$- Mäusen, verringerten die Anzahl der phospho-IRS-1 (Serin 612) immunoreaktiven Zellen im ARC und waren von einem intakten zentralen IRS/PI3K- Signalweg abhängig. Zusätzlich konnte in Kapitel 4.2 gezeigt werden, dass Leptin in der Lage ist die GSK-3β im ARC zu inhibieren und, dass die positiven Effekte von Leptin auf die Glukosetoleranz von einem intakten WNT- Signalweg abhängig sind. Diese Ergebnisse führten zu der Annahme, dass die positiven Eigenschaften von Leptin auf die Glukosehomöostase über eine Inhibition der GSK-3β vermittelt werden. Des Weiteren verringerte die zentrale Applikation des GSK-3β Inhibitors die Futteraufnahme von $Lep^{ob/ob}$- Mäusen innerhalb von 24 Stunden um 15% (Kapitel 4.3 Abb. 2d) wie es auch von Leptin bekannt ist [16], wodurch die Hypothese weiter bekräftigt wurde.

Generell lässt sich festhalten, dass eine erhöhte GSK-3β Aktivität im ARC von $Lep^{ob/ob}$- Mäusen mit einer Glukoseintoleranz und Hyperphagie dieser Tiere assoziiert ist. Eine mögliche Ursache für die erhöhte GSK-3β Aktivität könnte, neben dem Fehlen von Leptin, die gesteigerte mRNA Expression des WNT- Signalweg- Antagonisten, DKK-1, im ARC von $Lep^{ob/ob}$- Mäusen sein (Kapitel 4.3 Abb. 2e). Von diesem Antagonisten ist bekannt, dass er die GSK-3β in Neuronen aktiviert [96]. Darüber hinaus unterdrückte DKK-1 die positiven Eigenschaften von Leptin auf die Glukosetoleranz von $Lep^{ob/ob}$- Mäusen (siehe Kapitel 4.2 Abb. 3c). Eine akute icv Injektion von DKK-1 in normoglykämische Mäuse ergab eine deutliche Verschlechterung der Glukosetoleranz (Kapitel 4.3 Abb. 2f), die mit dem glukoseintoleranten Phänotyp von $Lep^{ob/ob}$- Mäusen vergleichbar war. Diese Daten bestätigen die Hypothese, dass die zentrale Regulation der Glukosehomöostase von einem intakten WNT- Signalweg abhängig ist und, dass die positiven Eigenschaften von Leptin auf die Glukosehomöostase über eine Inhibition der GSK-3β vermittelt werden.

Welchen Einfluss hat eine erhöhte GSK-3β Aktivität im ARC auf die Energie- und Glukosehomöostase?

Eine zentrale Inhibition der GSK-3β verbesserte die Glukosehomöostase von leptindefizienten Mäusen, jedoch konnte nicht geklärt werden, welche neuroanatomischen Nuclei für die beobachteten Effekte verantwortlich sind. Durch die icv Injektionen in den dritten Ventrikel gelangen die injizierten Substanzen unter anderem zum Hypothalamus. Neben dem ARC können jedoch auch weitere hypothalamische Nuclei, wie z.B. der VMH oder der PVN, von den icv Injektionen betroffen sein. Da diese Nuclei ebenfalls in die Regulation der zentralen Energie- und Glukosehomöostase involviert sind

[10], ist nicht eindeutig, ob noch andere hypothalamischen Kernregionen für die beobachteten Effekte verantwortlich waren. Um den Einfluss der GSK-3β in Neuronen des ARC zu untersuchen, wurde ein virales Konstrukt generiert und die GSK-3β mit Hilfe eines Adenoassoziierten Virus 2 (AAV2) überexprimiert. Um die Überexpression auf Neurone zu beschränken, wurde der virale Vektor unter die Kontrolle eines Synapsin-1 Promotors gestellt (Kapitel 4.3 Abb. 3a-e). Durch intraparenchymale Injektionen wurden je $4*10^{10}$ Vektorgenome bilateral in den ARC von normoglykämischen Mäusen injiziert und mittels *in-situ* Hybridisierung verifiziert (Kapitel 4.3 Abb. 3f). Der virale Kontrollvektor enthielt dabei „enhanced green fluorescent protein“ (EGFP). Auf Standardfutter induzierte die Überexpression von GSK-3β im ARC nur einen leichten Anstieg des Körpergewichtes (Kapitel 4.3 Abb. 4a), jedoch ergab sich bereits an Tag 58 eine signifikante Verschlechterung der Glukosetoleranz (Kapitel 4.3 Abb.4b). Nach 78 Tagen wurden beide Gruppen mit einer hochkalorischen Diät (HFD) gefüttert. Innerhalb von nur zwei Tagen erhöhte sich das Körpergewicht der AAV2-GSK-3β Mäuse signifikant im Vergleich zu den AAV2-EGFP Mäusen. In den folgenden 18 Tagen erreichten die AAV2-GSK-3β Mäuse ein 17% höheres Körpergewicht als die Kontrollmäuse (Kapitel 4.3 Abb. 4a). Der anschließende ip Glukosetoleranztest (GTT) zeigte eine deutliche Verschlechterung der Glukosetoleranz der AAV2-GSK-3β Mäuse im Vergleich zur Kontrollgruppe (Kapitel 4.3 Abb. 4b). Darüber hinaus ergab die „dual energy X-ray absorptiometry“ (DEXA) -Analyse eine deutliche Reduktion der relativen fettfreien Masse und eine Zunahme des Fettgewebes in den AAV2-GSK-3β Mäuse auf der HFD, hingegen keine Unterschiede auf der Standard-Diät zu verzeichnen waren (Kapitel 4.3 Abb. 4c). Eine Erklärung für die Körpergewichtsunterschiede lieferte die erhöhte kumulative Futteraufnahme der AAV2-GSK-3β Mäuse im Vergleich den entsprechenden Kontrollen (Kapitel 4.3 Abb. 4d), während keine Unterschiede im Energieverbrauch der Gruppen auftraten (Kapitel 4.3 Abb. 4e). Der Respiratorische Quotient (RQ), als ein Indikator der Substratverwertung, war jedoch in AAV2-GSK-3β Mäusen auf beiden Diäten reduziert (Kapitel 4.3 Abb. 4f). Dieses Ergebnis lässt, zusätzlich zur erhöhten Futteraufnahme auf der HFD, eine gesteigerte Verwertung von Fetten bei den AAV2-GSK-3β Mäusen vermuten, die zu einer vermehrten Energieaufnahme führte. Die gezeigten Ergebnisse liefern klare Anzeichen, dass eine erhöhte Aktivität der GSK-3β im ARC mit einer gestörten Regulation der Energie- und Glukosehomöostase einhergeht. Die Diskrepanz, dass die neuronale Überexpression der GSK-3β im ARC keine oder nur sehr leichte Effekte auf der Standard-Diät nach sich zog, ist möglicherweise durch die hochkonservierte Funktion der GSK-3β zu erklären. Da dieses Enzym an einer Vielzahl von zellulären Prozessen beteiligt ist, wäre es denkbar, dass verschiedene Kompensationsmechanismen aktiviert werden, um der Enzymaktivität entgegenzuwirken. Die Fütterung einer HFD geht allerdings auch mit einer Aktivierung pro-inflammatorischer Signalwege im MBH einher, unter anderem der JNK- Signalweg [63]. Die hypothalamische Aktivität dieser Kinase ist mit Adipositas assoziiert [83], und es konnte gezeigt werden, dass sie die GSK-3β *in-vitro* aktiviert [97], wodurch mögliche Kompensationsmechanismen außer Kraft gesetzt werden könnten.

Die erhöhte SOCS3 Expression der AAV2-GSK-3β Mäuse im ARC im Vergleich zu den Kontrollmäusen auf der HFD (Kapitel 4.3 Abb. 4g), lässt vermuten, dass die Überexpression der GSK-3β auch in die Expression von SOCS3 involviert ist, welches die Leptin- und Insulinsignalkaskaden beeinträchtigt [27;98]. Darüber hinaus konnte gezeigt werden, dass die aktive GSK-3β pro-inflammatorische Antworten induzieren kann [66]. Diese Befunde lassen auf eine erhöhte Inflammation und eine verstärkte Leptinresistenz durch die Überexpression von GSK-3β schließen. Da die Leptinresistenz möglicherweise der Schlüssel zum Verständnis und der Prävention von der Entstehung von Diabetes mellitus Typ II ist, könnte eine Inhibition der zentralen GSK-3β demnach einen großen Stellenwert in der Behandlung dieser metabolischen Störung einnehmen.

Durch welche Mechanismen beeinflusst die zentrale GSK-3β den peripheren Glukosemetabolismus?

Trotz der Beeinträchtigung der Energie- und Glukosehomöostase durch die zentrale GSK-3β Überexpression während einer HFD, konnten nur eine leichte Veränderung der Serum-Insulinkonzentration festgestellt werden (Kapitel 4.3 Abb. 4h). Eine erhöhte Insulinsekretion ist mit einer verringerten Sensitivität gegenüber diesem Hormon assoziiert [30;31]. Die hypothalamische Insulin- und Leptinsignaltransduktion ist jedoch auch mit einer Inhibition der Glukoseproduktion der Leber assoziiert [6;7], welche über den *Nervus vagus* vermittelt wird [99]. Um zu überprüfen, ob die zentrale GSK-3β Aktivität an der Glukoseproduktion der Leber beteiligt ist, wurde ein Pyruvattoleranztest (PTT) durchgeführt. Pyruvat ist ein Substrat der Glukoneogenese und eine erhöhte Umwandlung von Pyruvat zu Glukose reflektiert somit die Glukoseproduktion der Leber. Die zentrale Inhibition der GSK-3β, mittels icv Injektion eines GSK-3β Inhibitors, führte zu einer verminderten Umwandlung von Pyruvat zu Glukose in $Lep^{ob/ob}$- Mäusen (Kapitel 4.3 Abb. 5a). Darüber hinaus ergab die gleiche Behandlung, dass die Proteinmenge der Phosphoenolpyruvat- Carboxykinase in der Leber von $Lep^{ob/ob}$- Mäusen im Vergleich zu den Kontrollen erniedrigt war (Kapitel 4.3 Abb. 5b) und wird durch Daten aus *in-vitro* Untersuchungen unterstützt [100]. Dieses Enzym ist der geschwindigkeitsbestimmende Faktor der Glukoneogenese und daher geht eine Reduktion dieses Enzyms mit einer verminderten Umwandlung von Pyruvat zu Glukose einher. Die erlangten Ergebnisse bekräftigen die Hypothese, dass eine erhöhte zentrale GSK-3β Aktivität an einem erhöhten Blutzuckerspiegel beteiligt ist und auf eine erhöhte Glukoseproduktion der Leber zurückgeführt werden kann. Ein Phänomen, dass auch durch eine Inhibition der hypothalamischen PI3K auftritt [6] und bei diabetischen Tieren und Menschen zu beobachten ist [101;102].

Die periphere Applikation von GSK-3β Inhibitoren wurde, in Bezug auf Diabetes mellitus Typ II, bereits in verschiedenen Tiermodellen erfolgreich getestet [103-106], jedoch waren die molekularen Mechanismen oder das verantwortliche Organ bisher unbekannt. Durch die hier gezeigten Untersuchungen können diese positiven Befunde nun besser verstanden werden.

In diesem Kapitel lässt sich nun in einem Modell festhalten (siehe dazu Abb. 7), dass Leptin die GSK-3β in Neuronen des ARC, durch eine Aktivierung des Co-Rezeptors LRP-6, inhibiert. Eine zentrale Inhibition dieses Enzyms geht mit einer Stabilisierung des IRS-1 und einer Aktivierung der Proteinkinase B (AKT) einher. Von dieser ist bekannt, dass sie wiederum eine inhibitorische Wirkung auf die GSK-3β besitzt [54], wodurch eine positive Rückkopplungsschleife entsteht. Dieser aktive zentrale IRS/PI3K- Signalweg verbessert die Glukosetoleranz und verringert die Nahrungsaufnahme von $Lep^{ob/ob}$- Mäusen. Eine erhöhte GSK-3β Aktivität im ARC hingegen ist mit Adipositas assoziiert, erhöht die Nahrungsaufnahme und führt zu Regulationsstörungen der Energie- und Glukosehomöostase, welche vermutlich auf eine verringerte Leptinsensitivität zurückzuführen sind. Somit unterstreichen diese Ergebnisse den übergeordneten Einfluss des ZNS in der Regulation des Energie- und Glukosemetabolismus.

Die Ursachen für eine erhöhte Aktivität der hypothalamischen GSK-3β bei Adipositas sind allerdings unklar. Unsere Ergebnisse deuten darauf hin, dass Leptin seine katabolen Eigenschaften durch dieses Enzym vermittelt. Daher wäre es denkbar, dass bei Adipositas und der damit assoziierten Leptinresistenz [107], Leptin nicht länger in der Lage ist die GSK-3β zu inhibieren, wodurch sich die negativen Eigenschaften der Leptinresistenz äußern. Eine andere Möglichkeit wäre die, bei Adipositas auftretende, zentrale Inflammation [83]. Hierbei wurde z.B. von der JNK gezeigt, dass sie in der Lage ist die GSK-3β *in-vitro* zu aktivieren [97], was demnach die Ursache der Leptinresistenz sein könnte, wodurch die Störung des Energie- und Glukosemetabolismus hervorgerufen wird.

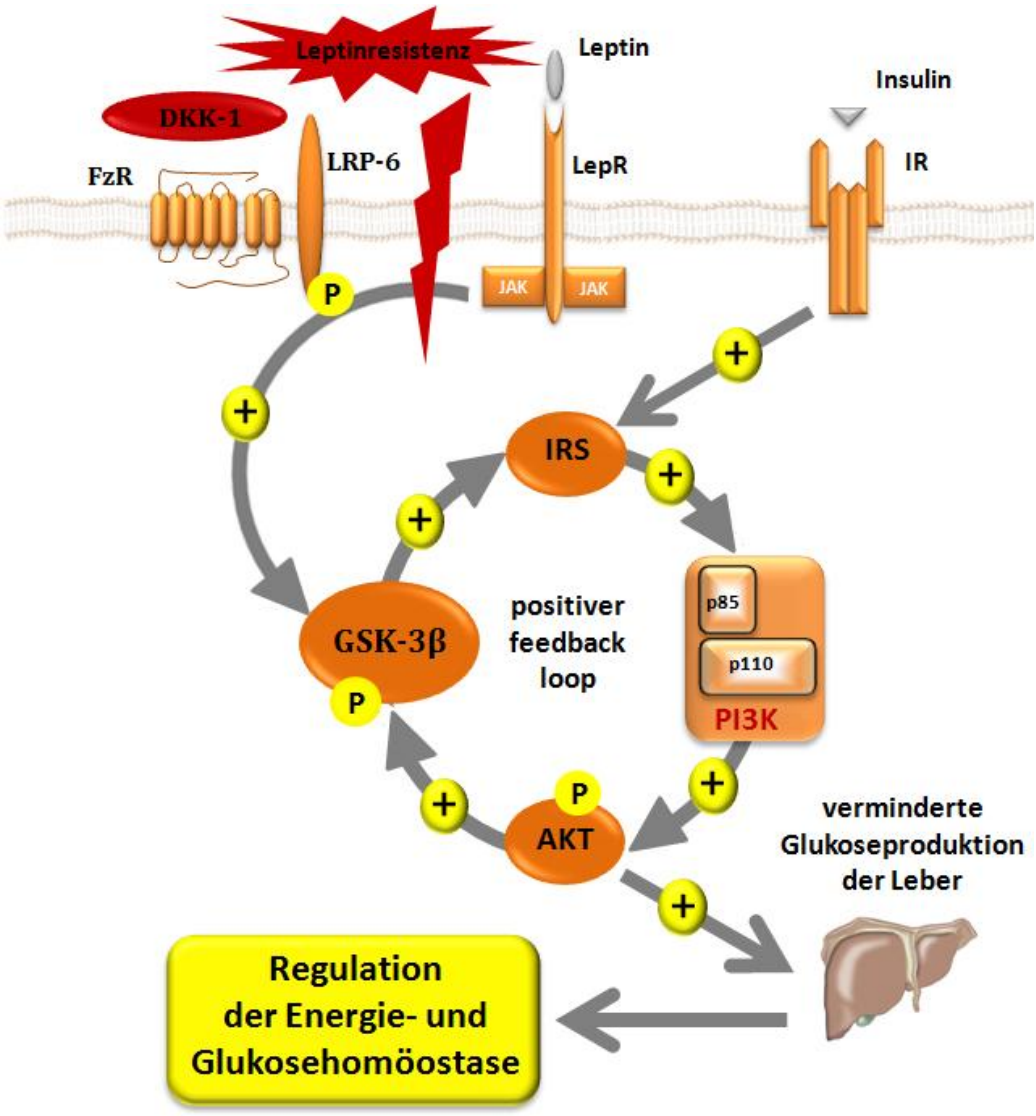

Abb. 7: Leptin, Insulin und der WNT- Signalweg im ARC. In normoglykämischen und leptinsensitiven Tieren phosphoryliert Leptin den Co-Rezeptor LRP-6, wodurch die GSK-3β inaktiviert wird. Somit ist Insulin in der Lage den IRS/PI3K- Signalweg zu aktivieren und die Glukoseproduktion der Leber zu reduzieren, wodurch die Glukosehomöostase gesteuert wird. Eine erhöhte Phosphorylierung von AKT führt wiederum zu einer weiteren Inhibition der GSK-3β [54], wodurch ein positiver feedback entsteht. Durch eine Leptinresistenz oder die Anwesenheit WNT- Antagonisten DKK-1 ist Leptin nicht länger in der Lage LRP-6 zu phosphorylieren, was in einer aktiven GSK-3β resultiert. Diese wiederum inaktiviert IRS und es manifestiert sich eine Glukoseintoleranz. Gelbe Symbole: positive Wirkung: dunkelrote Symbole: negative Wirkung. LRP: low-density lipoprotein receptor-related protein; GSK-3β: Glykogen-Synthase-Kinase-3β; IRS: Insulinrezeptorsubstrat; PI3K: Phosphoinositol-3-Kinase; DKK: Dickkopf; FzR: Frizzledrezeptor; LepR: Leptinrezeptor; IR: Insulinrezeptor.

3.4.2 Der Einfluss der hypothalamische Inflammation auf die Energie- und Glukosehomöostase

Der hypothalamische JNK- Signalweg in der Regulation des Glukosemetabolismus

Im Jahre 2005 konnte erstmals gezeigt werden, dass eine erhöhte JNK-Aktivität im Hypothalamus mit Adipositas assoziiert ist [83]. In den nächsten Jahren etablierte sich ein Modell der hypothalamischen Inflammation, welches mit einer verminderten Insulin- und Leptinsignaltransduktion im MBH in Verbindung gebracht wird [63-65]. Hierbei scheint, neben dem IKKβ / NF-κB- Signalweg, der JNK-Signalweg eine äußerst tragende Rolle zu spielen [63;83;84;90]. Es konnte gezeigt werden, dass ein neuronaler knockout von JNK-1 vor diätinduzierter Adipositas schützt [84;85], wodurch wiederum die übergeordnete Rolle des ZNS in der Regulation des Energie- und Glukosemetabolismus herausgestellt wurde. Die beschriebenen Studien lieferten aber keine Untersuchungen über die zentralen molekularen Mechanismen, ob und wie JNK mit dem Insulin- Signalweg interagiert und welche hypothalamischen Nuclei von einer erhöhten JNK-Aktivität betroffen sind. Daher wurde die neuroanatomische JNK-Aktivität untersucht und der Einfluss der zentralen JNK auf die Regulation der peripheren Glukosehomöostase analysiert.

Welche hypothalamischen Nuclei sind durch Adipositas von einer erhöhten JNK Aktivität betroffen?

Die Anzahl von phospho-JNK (Threonin 183 und Thyrosin 185) immunoreaktiven Zellen im ARC und VMH war in zwei verschiedenen Modellen von glukoseintoleranten Mäusen stark erhöht, wobei die untersuchten Phosphorylierungsstellen mit einer erhöhten Aktivität der Kinase assoziiert sind (Kapitel 4.4 Abb. 1). Zum einen wurden $Lep^{ob/ob}$- Mäuse untersucht, die durch das Fehlen von Leptin und eine hohe Leptinsensitivität gekennzeichnet sind. Zum anderen wurden Mäuse analysiert, die eine diätinduzierte Adipositas aufwiesen (Leptinresistenz und hohe Serum- Leptinspiegel). Die erhobenen Daten lassen vermuten, dass die JNK-Aktivität im ARC und VMH, welche ebenfalls in die Regulation der zentralen Energie- und Glukosehomöostase involviert sind [10], erhöht war. Hierbei waren die beobachteten Effekte unabhängig von endogenen Leptinspiegeln, wodurch ausgeschlossen werden konnte, dass Leptin in die Aktivierung der JNK involviert ist. Daher konnte der adipöse Phänotyp und die damit einhergehende Zunahme des Fettgewebes als Ursache für die erhöhte JNK-Aktivität angesehen werden.

Ist die zentrale JNK an der Störung der Glukosehomöostase durch Adipositas beteiligt?

Aus der Peripherie ist bekannt, dass die JNK IRS-1 phosphoryliert und somit die Weiterleitung des Insulinsignals vermindert [75;79-82]. Diese Ergebnisse konnten in einer hypothalamischen Zelllinie, durch Behandlung mit einem pharmakologischen JNK- Inhibitor (SP600125), verifiziert werden. Hierbei ergab die JNK- Inhibition eine deutliche Reduktion der phospho-IRS-1 (Serin 612) - Proteinmenge (Kapitel 4.4 Abb. 2). Somit wurde die Hypothese bekräftigt, dass eine zentrale Inhibition der JNK den hypothalamischen IRS/PI3K- Signalweg und somit möglicherweise die Glukosetoleranz verbessern könnte. In der Tat, eine akute icv Injektion des JNK- Inhibitors (2 nmol oder 5 nmol) steigerte dosisabhängig die Glukosetoleranz von $Lep^{ob/ob}$- Mäusen im Vergleich zu den Kontrollmäusen (Kapitel 4.4 Abb. 3a und b). Darüber hinaus verbesserte die höhere Dosis (5 nmol) ebenfalls die Glukosetoleranz von Mäusen, die eine diätinduzierte Adipositas aufwiesen (Kapitel 4.4 Abb. 3c). Jedoch waren immer noch signifikante Unterschiede zwischen den behandelten adipösen Mäusen und der normalgewichtigen Kontrollgruppe, die mit keiner hochkalorischen Diät gefüttert wurden, zu verzeichnen. Ob die verwendete Konzentration des JNK- Inhibitors nicht ausreichend war, oder ob andere pro-inflammatorische Signalwege, wie z.B. der IKKβ / NF-κB- Signalweg, ebenso eine große Rolle spielen, bleibt ungewiss. Die erlangten Daten werden durch die Ergebnisse der neuronalen JNK-1 knockout Studie unterstützt [84;85] und lieferten sogar deutlich größere Effekte auf die Glukosetoleranz. Ursachen hierfür könnten bei dem hier verwendete JNK- Inhibitor liegen. Im Gegensatz zur der knockout Studie von JNK-1 inhibierte der hier verwendete JNK- Inhibitor alle 3 JNK- Isoformen gleichermaßen, wodurch die Vermutung nahe liegt, dass die anderen zwei Isoformen ebenfalls in die zentrale Regulation der Glukosehomöostase involviert sind.

Welche molekularen Mechanismen sind für die beobachteten Effekte verantwortlich?

Die akuten Effekte der JNK- Inhibition auf die Glukosetoleranz (innerhalb von 30 Minuten) können nicht durch transkriptionale Veränderungen der JNK- Zielgene hervorgerufen werden. Viel plausibler sind an dieser Stelle posttranslationale Modifikationen oder auch Veränderungen der neuronalen Aktivität, wie sie z.B. durch eine sympathische Innervation gewährleistet werden könnte [108]. Es konnte gezeigt werden, dass sehr hohe Konzentrationen (46 µmol / Tag) des verwendeten JNK-Inhibitors den Insulin- Signalweg in Homogenaten von Rattenhypothalami verbesserte [83]. Ob diese Veränderungen auch in den, für die zentralen Regulation der Glukosehomöostase, wichtigen Nuclei stattfinden wurde jedoch nicht untersucht. Die Analyse ergab, dass eine akute Inhibition des zentralen JNK- Signalweges mit einer verringerten Anzahl der phospho-IRS-1 (Serin 612) immunoreaktiven Zellen im ARC und VMH von $Lep^{ob/ob}$- Mäusen einhergeht (Kapitel 4.4 Abb. 4a) und bestätigt die Daten aus der hypothalamischen Ziellinie (Kapitel 4.4 Abb. 2). Darüber hinaus konnte gezeigt werden, dass die gleiche Behandlung die Anzahl der phospho-AKT (Serin 473) immunoreaktiven Zellen in beiden Nuclei im Vergleich zu den Kontrollmäusen erhöhte (Kapitel 4.4 Abb. 4b), was auf eine verstärkte Aktivierung des IRS/PI3K- Signalweg schließen lässt und dadurch die positiven Effekte der

zentralen JNK- Inhibition auf den Glukosehaushalt erklären. Ob die JNK direkt in diesen Signalweg eingreift oder ob noch andere Faktoren in diese Regulation involviert sind, werden zukünftige Studien zeigen.

Interessanterweise waren diese Ergebnisse im ARC mit der Inhibition der GSK-3β, in Bezug auf die verstärkte Aktivierung des IRS/PI3K- Signalweges, vergleichbar (siehe Kapitel 4.3 Abb. 2a und b). Daher wurde der Effekt auf die GSK-3β nach zentraler JNK- Inhibition untersucht. Die Analyse ergab dass die Anzahl der phospho-GSK-3β (Serin 9) immunoreaktiven Zellen im ARC und VMH von $Lep^{ob/ob}$- Mäusen durch die Applikation des JNK- Inhibitors deutlich reduziert war (Kapitel 4.4 Abb. 4c). Da auch *in-vitro* gezeigt werden konnte, dass die JNK in der Lage ist die GSK-3β zu aktivieren [97], deuten die Ergebnisse darauf hin, dass die beobachteten Effekte der zentralen JNK- Inhibition auf eine zentrale Inhibition der GSK-3β zurückzuführen sind. Ob diese Inhibition eine direkte oder indirekte Konsequenz der JNK- Inhibition ist bleibt allerdings offen. Bekräftigend kommt hinzu, dass eine zentrale Inhibition der JNK die Futteraufnahme von Ratten reduziert [83], wie es auch durch die zentrale Inhibition der GSK-3β in $Lep^{ob/ob}$- Mäusen gezeigt werden konnte (siehe Kapitel 4.3 Abb. 2d).

Zusammenfassend lässt sich festhalten, dass die JNK-Aktivität im ARC und VMH, zwei wichtige Nuclei für die Regulation der Glukosehomöostase, in zwei verschiedenen Modellen von Adipositas erhöht war. Diese erhöhte JNK-Aktivität scheint dabei unabhängig von endogenem Leptin ($Lep^{ob/ob}$-Mäuse) oder einer Hyperleptinämie (durch Fütterung einer HFD) zu sein. Eine akute Inhibition des zentralen JNK- Signalweges verbesserte die Glukoseintoleranz von beiden untersuchten Mausmodellen und war mit einer Verbesserung des zentralen Insulin- Signalweges assoziiert. Die Daten legen nahe, dass diese positiven Effekte auf eine zentrale Inhibition der GSK-3β zurückzuführen sind (siehe dazu Abb. 8). Da die zentrale Applikation des JNK- Inhibitors jedoch keine Normalisierung der Glukosetoleranz der HFD Mäuse ergab, lässt sich nicht ausschließen, dass auch andere inflammatorische Signalwege, wie z.B. der IKKβ / NF-κB- Signalweg, in diese metabolische Störung involviert sind.

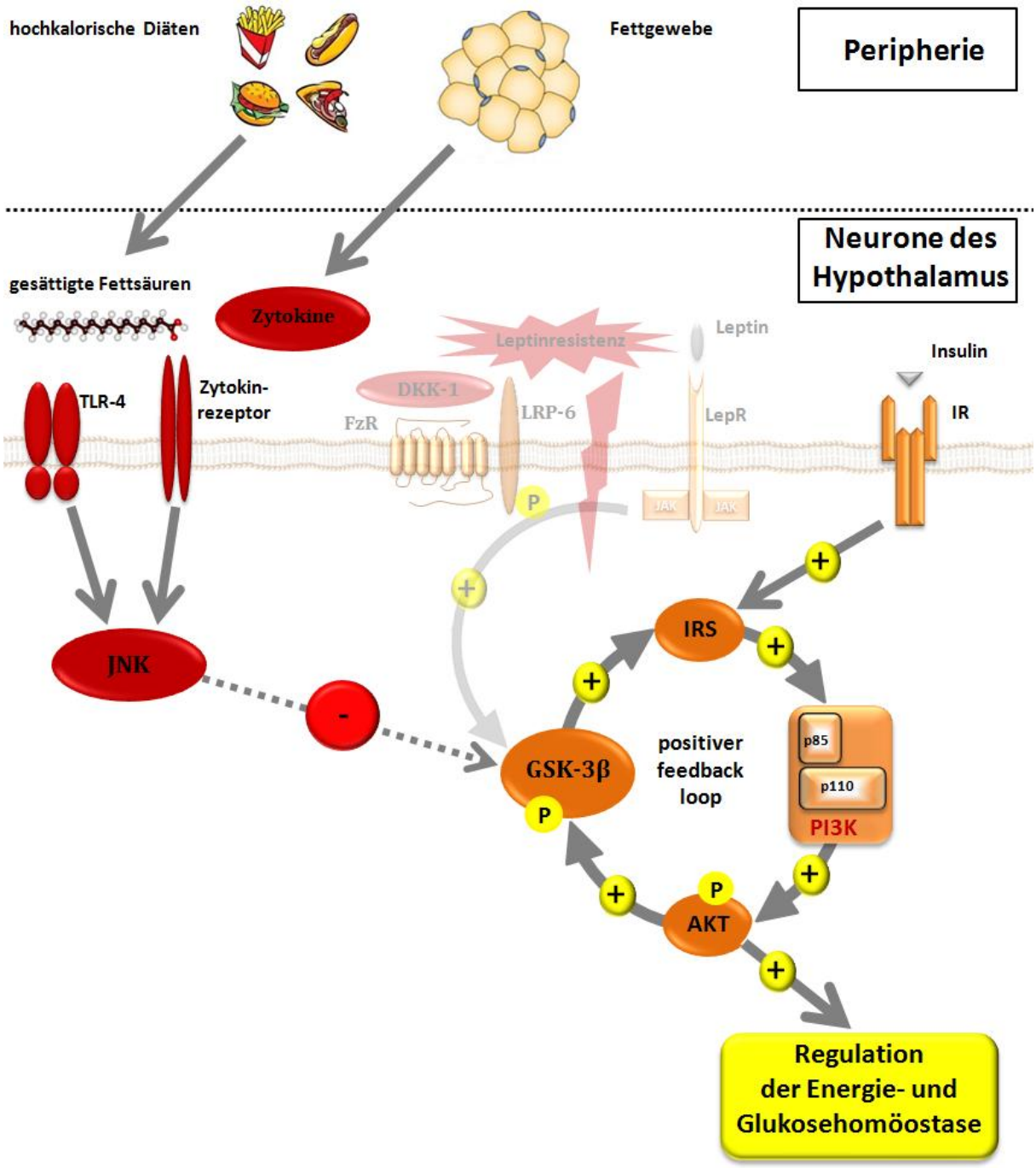

Abb. 8: Modell der hypothalamische JNK in der Regulation des Glukosemetabolismus. Zum einen aktivieren gesättigte Fettsäuren, wie sie in vielen hochkalorischen Diäten vorzufinden sind, den TLR-4 Rezeptor. Zum anderen kommt es, bedingt durch Adipositas, zu einer erhöhten Sekretion von Zytokinen aus dem Fettgewebe. Beide Ereignisse führen zu einer vermehrten Aktivierung der jeweiligen Rezeptoren im ZNS, wodurch die JNK aktiviert wird, was eine Aktivierung der GSK-3β zur Folge hat. Diese wiederum inaktiviert IRS und es manifestiert sich eine Glukoseintoleranz. Gelbe Symbole: positive Wirkung; dunkelrote Symbole: negative Wirkung; Gestrichelte Pfeile: indirekter oder unbekannter Mechanismus; TLR-4: Toll-like-Rezeptor-4; ZNS: Zentrales Nervensystem; JNK: c-Jun N-terminale Kinase; GSK-3β: Glykogen-Synthase-Kinase-3β; IRS: Insulinrezeptorsubstrat; PI3K: Phosphoinositol-3-Kinase; LRP: low-density lipoprotein receptor-related protein; DKK: Dickkopf; FzR: Frizzledrezeptor; LepR: Leptinrezeptor; IR: Insulinrezeptor; IRS: Insulinrezeptorsubstrat.

Der zentrale IKKβ / NF-κB- Signalweg in der Regulation der Energie- und Glukosehomöostase

Neben dem JNK- Signalweg spielt der IKKβ / NF-κB- Signalweg ebenfalls eine große Rolle in der Immunantwort [86]. Eine Erhöhung der hypothalamischen Aktivität dieses Signalweges ist sowohl mit einer diätinduzierten Adipositas [83] als auch mit dem Fehlen von Leptin assoziiert [109] und wird mit einer zentralen Leptin- und Insulinresistenz in Verbindung gebracht [83;88-90]. In den letzten Jahren konnte darüber hinaus die GSK-3β als Regulator von inflammatorischen Prozessen identifiziert werden [62]. Neben den zirkulierenden Zytokinen scheint auch die aktive GSK-3β eine Immunantwort über den IKKβ / NF-κB- Signalweg auslösen zu können [110-113], wohingegen eine Inhibition der GSK-3β eine inflammatorische Antwort unterdrückt [66;67;114]. In Kapitel 4.3 konnte gezeigt werden, dass eine neuronale Überexpression von GSK-3β im ARC zu einer Regulationsstörung der Energie- und Glukosehomöostase führte, die somit möglicherweise auch auf eine Erhöhung des IKKβ / NF-κB- Signalweges zurückzuführen ist. Daher wurde der Einfluss des zentralen IKKβ / NF-κB-Signalweges auf die Energie- und Glukosehomöostase von wildtyp- und $Lep^{ob/ob}$- Mäusen analysiert.

Welche Auswirkungen hat eine zentrale Inhibition des IKKβ / NF-κB- Signalwege auf den Glukosemetabolismus von glukoseintoleranten Mäusen?

In einem ersten Versuchsansatz wurde der IKKβ / NF-κB- Signalweg, durch eine orale Verabreichung von Butein, in glukoseintoleranten $Lep^{ob/ob}$- Mäusen, inhibiert. Das Flavonoid Butein zählt zu den sekundären Pflanzeninhaltsstoffen und wird aus dem Lackbaum (*Rhus verniciflua*) gewonnen. Es ist in der traditionellen chinesischen Medizin weit verbreitet und inhibiert den IKKβ / NF-κB- Signalweg, durch eine direkte Inhibition der hauptverantwortlichen Kinase IKKβ [109]. Die akute orale Applikation einer 8 mg/kg Körpergewicht verabreichten Buteinlösung verbesserte die Glukosetoleranz von $Lep^{ob/ob}$- Mäusen im Vergleich zu den Kontrollmäusen. Die Verabreichung von niedrigeren Konzentrationen konnte zwar die Glukosetoleranz nicht signifikant verbessern, induzierte jedoch eine dosisabhängige Steigerung der Glukosetoleranz (Kapitel 4.5 Abb. 1a). Da die Verbesserung auch durch eine akute icv Injektion von Butein hervorgerufen wurde, zeigte sich, dass die beobachteten Effekte auf die Glukosetoleranz über einen zentralen Mechanismus vermittelt wurden (Kapitel 4.5 Abb. 1b). Die akute icv Injektion von Butein (innerhalb von 30 Minuten), legt nahe, dass die Verbesserung der Glukosetoleranz nicht von einer Transkription von NF-κB Zielgenen abhängig ist. Auch hier waren posttranskriptionale Modifikationen, wie z.B. Phosphorylierungen beteiligter Proteine oder Veränderungen auf neuronaler Ebene viel wahrscheinlicher. Wie schon in den vorherigen Studien wurde der IRS/PI3K- Signalweg analysiert. Eine akute icv Injektion von Butein erhöhte die Anzahl der phospho-AKT (Serin 473) immunoreaktiven Zellen im ARC von $Lep^{ob/ob}$-Mäusen im Vergleich zu den Kontrollmäusen (Kapitel 4.5 Abb. 1c). Dieser Befund gibt Grund zu der Annahme, dass Butein die Glukosetoleranz durch eine verstärkte Aktivierung des IRS/PI3K-

Signalweges verbessert und wird durch eine Studie von Gao et. al. unterstützt, bei welcher IKKβ die Weiterleitung des Insulinsignals durch eine direkte negative Phosphorylierung des IRS-1 minderte [115]. Darüber hinaus verbesserte die icv Applikation von Butein die Glukosetoleranz von Mäusen, die eine diätinduzierte Adipositas aufwiesen, wodurch die beobachteten Effekte nicht auf den Genotyp der $Lep^{ob/ob}$- Mäuse begrenzt waren (Kapitel 4.5 Abb. 1d). Von Butein wurde jedoch auch gezeigt, dass es mit anderen Proteinen interagieren kann. Daher ist nicht eindeutig, ob die Verbesserung der Glukosetoleranz alleine auf der Inhibition der IKKβ beruht. So konnte z.B. gezeigt werden, dass Butein Sirtiun-1 aktiviert [116]. Von diesem ist bekannt, dass es einen großen Einfluss auf den Energie und Glukosemetabolismus im Hypothalamus besitzt [117].

Wirkt eine chronische Inhibition des IKKβ / NF-κB- Signalweges im ARC einer diätinduzierten Adipositas entgegen?

Die icv Injektionen von Butein hatten keine Aussage, ob neben dem ARC noch weitere neuroanatomischen Nuclei für die beobachteten Effekte verantwortlich sind. Hypothalamische Nuclei wie z.B. der VMH oder der PVN könnten, durch ihre Nähe zum dritten Ventrikel, ebenfalls von der Butein Applikation betroffen sein. Um den exakten und dauerhaften Einfluss des NF-κB- Signalweges auf die Energie und Glukosehomöostase in Neuronen des ARC zu entschlüsseln, wurde ein virales Konstrukt generiert. Hierfür wurde das inhibitorische Protein von NF-κB, IκBα, mit Hilfe eines AAV2 überexprimiert. Zusätzlich wurden die Aminosäuren Serin 32 und Serin 36 von IκBα gegen Alanin ausgetauscht, wodurch das sogenannte IκBα- Mutant (mt) nicht mehr durch IKKβ phosphoryliert und damit abgebaut werden konnte. Hierdurch wurde sichergestellt, dass NF-κB im Zytoplasma verblieb und keine inflammatorische Antwort durch diesen Signalweg induziert werden konnte. Wie auch in Kapitel 4.3 wurde die Überexpression durch den Einsatz des Synapsin-1 Promotors auf Neurone beschränkt. Auch hier wurden je $4*10^{10}$ Vektorgenome von entweder AAV2-IκBα-mt oder AAV2-EGFP bilateral in den ARC von wildtyp- Mäusen injiziert und am Ende der Studie mittels *in-situ* Hybridisierung verifiziert (Kapitel 4.5 suppl. Fig. Abb. 1c). Die neuronale Überexpression von IκBα-mt im ARC verminderte die Gewichtszunahme der Mäuse auf der HFD im Vergleich zu den HFD-Kontrollmäusen. Nach 17 Tagen auf der HFD erreichten die AAV2-IκBα-mt Mäuse einen Gewichtsunterschied von 10%, der bis zum Ende der Studie (Tag 50) erhalten blieb (Kapitel 4.5 Abb. 2a). Diese Daten werden von eine Studie von Zhang et al. unterstützt, in welcher ein neuronaler knockout von IKKβ ebenfalls vor diätinduzierter Adipositas schützte und die Glukosetoleranz verbesserte [90]. Wir konnten zeigen, dass sich die verminderte Gewichtszunahme in einem reduzierten Anteil der Fettmasse im Vergleich zu den Kontrollmäusen äußerte (Kapitel 4.5 Abb. 2b). Zusätzlich verringerte die neuronale Überexpression von IκBα-mt im ARC die basalen Blutglukosewerte (Kapitel 4.5 Abb. 3a) und verbesserte die Glukosetoleranz (Kapitel 4.5 Abb. 3b) im Vergleich zu den Kontrollmäusen. Die Erhöhung der Insulinsensitivität der AAV2-IκBα-mt Mäuse im Vergleich zu den AAV2-EGFP Mäusen ist jedoch, da die relative Aufnahme von Glukose in die

Zellen unverändert blieb, auf die unterschiedlichen basalen Blutglukosespiegel zurückzuführen (Kapitel 4.5 Abb. 3c). Um die Ursache des reduzierten Körpergewichtes der AAV2-IκBα-mt Mäuse zu entschlüsseln wurden metabolische Messungen mittels indirekter Kalorimetrie durchgeführt. Die Sauerstoffaufnahme und der Energieverbrauch der AAV2-IκBα-mt Mäuse war im Vergleich zu den AAV2-EGFP Mäusen erhöht, der RQ und die Futteraufnahme war jedoch vergleichbar (Kapitel 4.5 Abb. 4). Die beobachtete Körpergewichtsreduktion war demzufolge nicht auf eine Veränderung der Substratverwertung oder Futteraufnahme zurückzuführen, sondern basierte auf eine Erhöhung der basalen Stoffwechselrate. Da keine Unterschiede im maximalen Sauerstoffverbrauch detektiert werden konnte, war auszuschließen, dass die beobachteten Effekte auf den Energiemetabolismus durch eine erhöhte physische Aktivität der Tiere hervorgerufen wurden (Abb. 4g).

Wird die Leptinsensitivität durch den IKKβ / NF-κB- Signalwege beeinflusst?

Die neuronale Überexpression von IκBα-mt im ARC führte in der gleichen Region zu einer verminderten Expression der SOCS3- mRNA im Vergleich zu den AAV2-EGFP Mäusen auf der HFD (Kapitel 4.5 Abb. 5). Dies führte zu der Annahme, dass der IKKβ / NF-κB- Signalwege im ARC an der Regulation der Leptinsensitivität beteiligt ist und, dass eine Inhibition dieses Signalweges die Leptinsensitivität steigert. Unterstützt wird diese Hypothese von einer *in-vitro* Studie, in der gezeigt werden konnte, dass SOCS3 ein Zielgen des IKKβ / NF-κB- Signalweges ist [90]. Darüber hinaus ist bekannt, dass Leptin die Sauerstoffaufnahme und den Energieverbrauch erhöht [118], was in dieser Studie ebenfalls gezeigt werden konnte. Diese Daten untermauern die Hypothese, dass der IKKβ / NF-κB- Signalweg in die Entstehung der zentralen Leptinresistenz involviert ist und, dass die beobachteten Effekte der Überexpression von IκBα-mt auf die Energie- und Glukosehomöostase durch eine erhöhte Leptinsensitivität vermittelt wurden.
Interessanterweise führte die neuronale Überexpression von GSK-3β im ARC zu einer Erhöhung der SOCS3- mRNA Expression (vergleiche Kapitel 4.3). Zusätzlich konnte *in-vitro* gezeigt werden, dass die GSK-3β den IKKβ / NF-κB- Signalweg aktiviert [110-113]. Daher wird vermutet, dass die GSK-3β ein zentralen Regulator der hypothalamischen Inflammation und somit auch der zentralen Leptinsensitivität darstellt.

Grundsätzlich lässt sich hier festhalten, dass das Flavonoid Butein die Glukosetoleranz verbessert. Diese ist unabhängig davon, ob die Glukoseintoleranz durch das Fehlen von Leptin oder durch eine diätinduzierte Adipositas hervorgerufen wurde und ist auf eine Sensitivierung des hypothalamischen Insulin- Signalweges zurückzuführen. Die neuronale Überexpression von IκBα-mt im ARC verminderte die Zunahme des Körpergewichtes und der Körperfettmasse und verbesserte den Glukosemetabolismus von Mäusen auf einer HFD. Darüber hinaus erhöhte die Inhibition des IKKβ / NF-κB- Signalweges im ARC die Sauerstoffaufnahme, den Energieverbrauch und die basale metabolische Rate, was durch die erhöhte Leptinsensitivität erklärt werden kann (siehe dazu Abb. 9).

Interessanterweise inhibieren Salicylate, wie sie z.B. auch in Aspirin enthalten sind, den IKKβ / NF-κB- Signalweg [119-121] und verbessern den Glukosemetabolismus von Diabetes mellitus Typ II-Patienten [122-124]. Zum einen fehlen jedoch noch Langzeitstudien und zum anderen werden für diese systemischen Behandlungen hohe Konzentrationen benötigt, die das Risiko für Nebenwirkungen deutlich erhöhen. Daher ist es unabdingbar, die Rolle des Gehirns bei der Entstehung von Diabetes mellitus Typ II weiter zu entschlüsseln, um eventuell gewebs- oder organspezifische Behandlungen zu ermöglichen

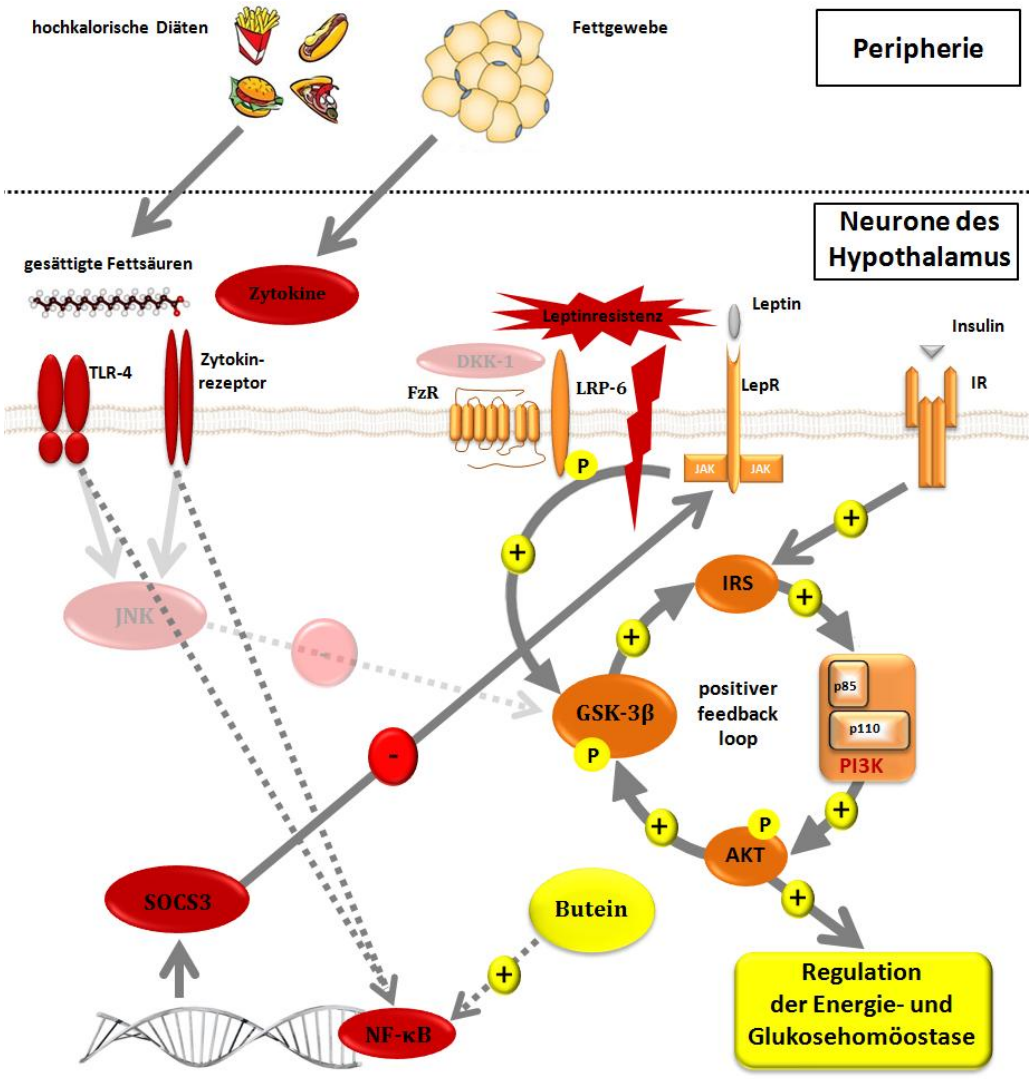

Abb. 9: Modell des IKKβ / NF-κB- Signalweges in der Regulation der Energie und Glukosehomöostase im ARC. Das erhöhte Aufkommen von zirkulierenden Zytokinen und gesättigten Fettsäuren durch Adipositas führt zu der Aktivierung der jeweiligen Rezeptoren im ZNS. Dadurch kommt es zur Aktivierung des Transkriptionsfaktors NF-κB, wodurch die Transkription von weiteren Zytokinen und SOCS3 induziert wird. SOCS3 wiederum inhibiert den Leptin- Signalweg, wodurch die Inaktivierung der zentralen GSK-3β ausbleibt und der hypothalamische Insulin- Signalweg beeinträchtigt wird. Eine Inhibition des IKKβ / NF-κB durch das Flavonoid Butein wirkt dieser Störung entgegen, was eine Verbesserung der Glukosehomöostase nach sich zieht. Gelbe Symbole: positive Wirkung; dunkelrote Symbole: negative Wirkung; Gestrichelte Pfeile: indirekter oder unbekannter Mechanismus; TLR-4: Toll-like-Rezeptor-4; ZNS: Zentrales Nervensystem; GSK-3β: Glykogen-Synthase-Kinase-3β; IRS: Insulinrezeptorsubstrat; PI3K: Phosphoinositol-3-Kinase; LRP: low-density lipoprotein receptor-related protein; DKK: Dickkopf; FzR: Frizzledrezeptor; LepR: Leptinrezeptor; IR: Insulinrezeptor; IRS: Insulinrezeptorsubstrat; SOCS: Suppressor of cytokine signaling.

3.5 Fazit

Die Regulation der Energie- und Glukosehomöostase erfolgt über ein komplexes neuronales Netzwerk aus verschiedenen, miteinander interagierenden Signalwegen. Diese Arbeit zeigt, dass noch weitere Signaltransduktionskaskaden an diesem neuroendokrinen System beteiligt sind und, dass die, mit Adipositas und Diabetes mellitus Typ II assoziierten, Veränderungen auf eine Vielzahl von metabolischen Modifikationen zurückzuführen sind.

Der genetische Verlust des Leptinsignals beeinträchtigt maßgeblich, unabhängig vom Körpergewicht, den Glukosemetabolismus und führt zu einer Glukoseintoleranz. Die Wiederherstellung des Leptinsignals in adipösen $Lep^{ob/ob}$- Mäusen war jedoch nicht ausreichend, um die Glukosetoleranz zu normalisieren, wohingegen dies bei normalgewichtigen $Lep^{ob/ob}$- Mäusen möglich war. Diese Ergebnisse deuten darauf hin, dass auch der Körperfettanteil an der Entstehung von Diabetes mellitus Typ II beteiligt ist. Darüber hinaus konnte gezeigt werden, dass Leptin das hypothalamische Phosphorylierungsmuster von IRS moduliert und ermöglicht bzw. verbessert somit die Insulinsignalweiterleitung über die PI3K. All diese Daten belegen, dass eine zentrale Leptin-Signalkaskade essentiell für die Aufrechterhaltung des Glukosemetabolismus ist und somit der Schlüssel zur Prävention von Adipositas und Diabetes mellitus Typ II darstellen könnte. Jedoch war nur unvollständig verstanden durch welche molekularen Mechanismen Leptin in den IRS/PI3K-Signalwege eingreift und ob noch andere Signaltransduktionen an dieser Interaktion beteiligt sind.

Existiert ein funktionaler WNT/β Catenin- Signalweg im MBH und gibt es zentrale Interaktionen von Leptin mit diesem Signalweg?

Alle untersuchten Gene des WNT- Signalweges wurden im ARC von adulten Mäusen exprimiert, wobei die Expression von WNT- Liganden und Zielgenen im ARC von adipösen $Lep^{ob/ob}$- Mäusen stark reduziert war. Die Wiederherstellung des Leptinsignals erhöhte die Expression der Zielgene und aktivierte den Co-Rezeptor LRP-6, wodurch die verminderte Aktivität dieses Signalweges im ARC auf das Fehlen von Leptin zurückzuführen war. Darüber hinaus bestätigt dieser Befund die Funktionalität des hypothalamischen WNT- Signalweges. Des Weiteren unterdrückte die Inhibition des zentralen WNT- Signalweges die positiven Eigenschaften von Leptin auf die Glukosetoleranz. Dieses Ergebnis legt nahe, dass die katabolen Effekte von Leptin von einem intakten WNT-Signalweg abhängig sind.

Welche Rolle nimmt die zentrale GSK-3β in der Regulation des Glukose- und Energiemetabolismus ein?

Eine gesteigerte GSK-3β Aktivität im ARC war mit Adipositas assoziiert, erhöhte die Nahrungsaufnahme und führte zu Störungen der Energie- und Glukosehomöostase. Die Daten legen nahe, dass die beobachteten Effekte ein Resultat der verminderten Leptinsensitivität sind. Im Gegensatz dazu ging eine zentrale Inhibition dieses Enzyms mit einer verstärkten Aktivierung des hypothalamischen IRS/PI3K- Signalweges einher, wodurch die Glukosetoleranz von $Lep^{ob/ob}$- Mäusen deutlich verbessert und die Nahrungsaufnahme verringert wurde. Darüber hinaus konnte gezeigt werden, dass Leptin in der Lage ist dieses Enzym in Neuronen des ARC zu inhibieren. Daher wird vermutet, dass die katabolen Eigenschaften von Leptin über diese Kinase vermittelt werden und, dass die hypothalamische GSK-3β als ein zentraler Regulator der Energie- und Glukosehomöostase angesehen werden kann.

Welche hypothalamischen Nuclei sind durch Adipositas mit einer erhöhten JNK-Aktivität assoziiert und gibt es Interaktionen zwischen der JNK und dem hypothalamischen Insulin- Signalweg?

Adipositas verursachte eine erhöhte JNK-Aktivität im ARC und VMH in zwei verschiedenen Mausmodellen. Die erhöhte JNK-Aktivität scheint dabei unabhängig von endogenem Leptin ($Lep^{ob/ob}$-Mäuse) oder einer Hyperleptinämie (durch Fütterung einer HFD) zu sein. Eine akute Inhibition des zentralen JNK- Signalweges verbesserte die Glukoseintoleranz der adipösen Mausmodelle und war mit einer verstärkten Aktivierung des zentralen Insulin- Signalweges verbunden. Die Daten legen nahe, dass diese Verbesserungen auf eine zentrale Inaktivierung der GSK-3β zurückzuführen sind.

Welche Rolle spielt der zentrale IKKβ / NF-κB- Signalweg in der Regulation der Energie- und Glukosehomöostase?

Eine erhöhte Aktivität des hypothalamischen IKKβ / NF-κB- Signalweges ist mit Adipositas assoziiert und wird möglicherweise durch die pro-inflammatorischen Eigenschaften der GSK-3β vermittelt. Die zentrale Inhibition des IKKβ / NF-κB- Signalweges, durch das Flavonoid Butein, verbesserte die Glukosetoleranz unabhängig von Leptin und war auf eine Sensitivierung des hypothalamischen Insulin- Signalweges zurückzuführen. Die chronische Inhibition des IKKβ / NF-κB- Signalweges im ARC, mittels Überexpression von IκBα-mt, verminderte die Zunahme des Körpergewichtes und der Körperfettmasse, und verbesserte den Glukosemetabolismus von Mäusen auf einer HFD. Darüber hinaus erhöhte diese Behandlung die Sauerstoffaufnahme, den Energieverbrauch und die basale metabolische Rate, was mit einer erhöhten Leptinsensitivität verbunden war. Da die Leptinsensitivität der Schlüssel zum Verständnis von der Entstehung von Diabetes mellitus Typ II sein könnte, stellt eine Inhibition des zentralen IKKβ / NF-κB- Signalweges ein sehr großes therapeutisches Potential in

der Behandlung dieser metabolischen Störung dar. Aus diesem Grund könnte die nutritive Behandlung mit dem Flavonoid Butein einen großen Stellenwert in der Behandlung von Diabetes mellitus Typ II einnehmen.

In dieser Arbeit konnte gezeigt werden, dass die Energie- und Glukosehomöostase durch eine Vielzahl von zentralen Interaktionen und Modifikationen verschiedener Hormone und Enzyme aufrechterhalten wird und bestätigt somit die übergeordnete Rolle des ZNS in der Regulation des Glukosemetabolismus. Eine chronische Störung dieses neuroendokrinen Systems durch Adipositas, und der damit einhergehenden hypothalamischen Inflammation, führt zu einer Dysregulation des Energie- und Glukosehaushaltes und letztendlich zur Manifestation von Diabetes mellitus Typ II. Daher untermauert diese Arbeit die hypothalamische Inflammationstheorie in Bezug auf diese metabolische Störung. Hierbei ist vor allem die hypothalamische GSK-3β zu nennen, welche die metabolischen Eigenschaften von Leptin und Insulin vermittelt. Durch eine hyperkalorische Ernährung, und der damit aufkommenden hypothalamischen Inflammation, wird dieses Enzym negativ beeinflusst, wodurch die katabolen Effekte von Leptin auf den Glukosemetabolismus verloren gehen. Darüber hinaus steht die GSK-3β im Verdacht die Expression von SOCS3, durch eine Aktivierung des IKKβ / NF-κB- Signalweges, zu induzieren, wodurch die verminderte Leptinsensitivität weiter verschärft wird. Somit kann dieses Enzym als zentraler Regulator des Energie- und Glukosemetabolismus angesehen werden und wodurch neue Interventionsmöglichkeiten in der Behandlung von Adipositas und Diabetes mellitus Typ II entstehen könnten. Die gezeigten und vermuteten Interaktionen der Signalwege sind in Abb. 10 dargestellt.

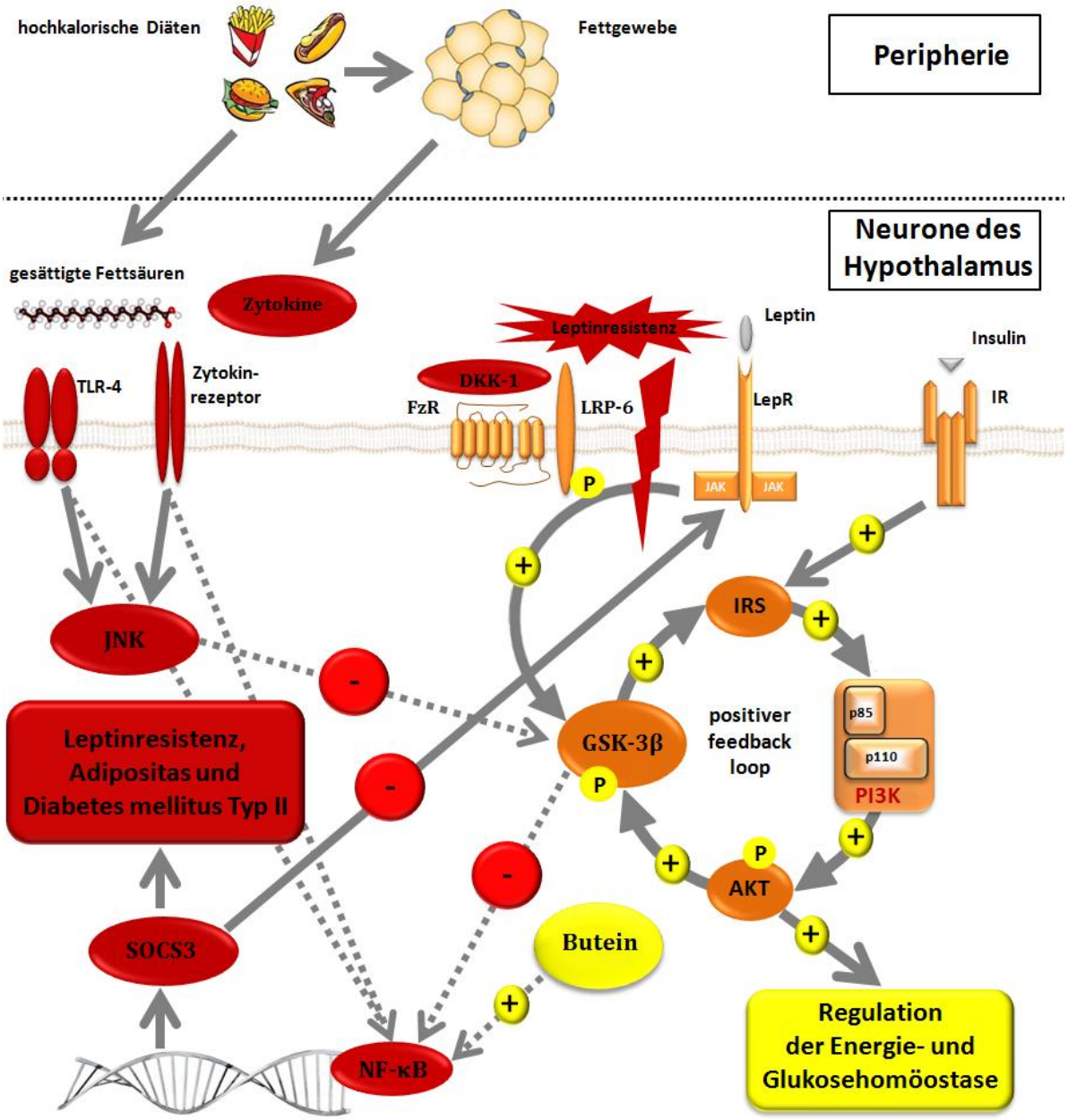

Abb. 10: Modell der komplexen Regulation der Energie und Glukosehomöostase im ARC. Die Aufrechterhaltung der Energie- und Glukosehomöostase wird zentral durch die Hormone Leptin und Insulin gesteuert. Durch eine hyperkalorische Ernährung wird dieses endokrine System gestört und es manifestiert sich Adipositas und schließlich Diabetes mellitus Typ II. Im Laufe einer fettreichen Diät aktivieren gesättigte Fettsäuren und zirkulierende Zytokine pro-inflammatorische Signalkaskaden im Hypothalamus, was eine Aktivierung des JNK- und IKKβ / NF-κB- Signalweges nach sich zieht. Infolgedessen aktiviert die JNK die GSK-3β, wodurch IRS phosphoryliert und der IRS/PI3K- Signalweg vermindert wird. Darüber hinaus blockiert die erhöhte GSK-3β Aktivität die katabolen Effekte von Leptin auf den Glukosemetabolismus. Eine erhöhte Aktivität dieses Enzyms geht, genau wie eine hyperkalorische Ernährung, mit der Aktivierung des Transkriptionfaktors NF-κB einher. Dieser vermittelt die Expression von SOCS3, wodurch die Leptinsensitivität weiter vermindert wird und einer Inhibition der GSK-3β durch Leptin entgegenwirkt. Durch diese mehrfache Beeinträchtigung der Leptin- und Insulinsignalweiterleitung kann die Glukosehomöostase nicht länger aufrechterhalten werden und es manifestiert sich Glukoseintoleranz. Anti-inflammatorische Substanzen wie z.B. Butein können dieser pro-inflammatorischen Antwort entgegenwirken und die Aufrechterhaltung der Leptinsensitivität und somit der Glukosehomöostase gewährleisten. Gelbe Symbole: positive Wirkung; dunkelrote Symbole: negative Wirkung; Gestrichelte Pfeile: indirekter oder unbekannter Mechanismus. GSK-3β: Glykogen-Synthase Kinase -3β; IRS: Insulinrezeptorsubstrat; JNK. c-Jun N-terminale Kinase; LepR: Leptinrezeptor; IR: Insulinrezeptor: AdipoR: Adiponektinrezeptor; TLR: Toll-like-Rezeptor; FzR: Frizzled Rezeptor; JAK: Januskinase; DKK: Dickkopf; LRP: low-density lipoprotein receptor-related protein; SOCS: Suppressor of cytokine signaling

3.6 Ausblick

In dieser Arbeit konnten offene Fragen über die zentrale Regulation der Energie- und Glukosehomöostase entschlüsselt werden. Darüber hinaus liefert diese Arbeit neue Interventionspunkte in der Behandlung von Adipositas und Diabetes mellitus Typ II. Das Rätsel über die Interaktion von Adipositas und Diabetes mellitus Typ II ist jedoch noch nicht vollständig gelöst. Bisher ist unklar, welche exakten Initialschritte die Energie- und Glukosehomöostase aus dem Gleichgewicht bringen. Eine zentrale Inhibition der GSK-3β könnte die Leptinwirkung und die damit einhergehenden positiven Eigenschaften von Leptin auf den Energie und Glukosemetabolismus wieder herstellen und liefert somit neue therapeutische Interventionsmöglichkeiten bei der Entstehung von Adipositas und Diabetes mellitus Typ II. In der Tat kann eine chronische Inhibition der zentralen GSK-3β die Glukosetoleranz von leptindefizienten Mäusen verbessern, die 10 Tage mit einer hochkalorischen Diät gefüttert wurden (Abb. 11, unveröffentlichte Daten). Die positiven Effekte auf den Glukosemetabolismus in diesem sehr extremen Modell von Adipositas und Glukoseintoleranz verdeutlichen das Potential der zentralen GSK-3β Inhibition in Bezug auf Diabetes mellitus Typ II.

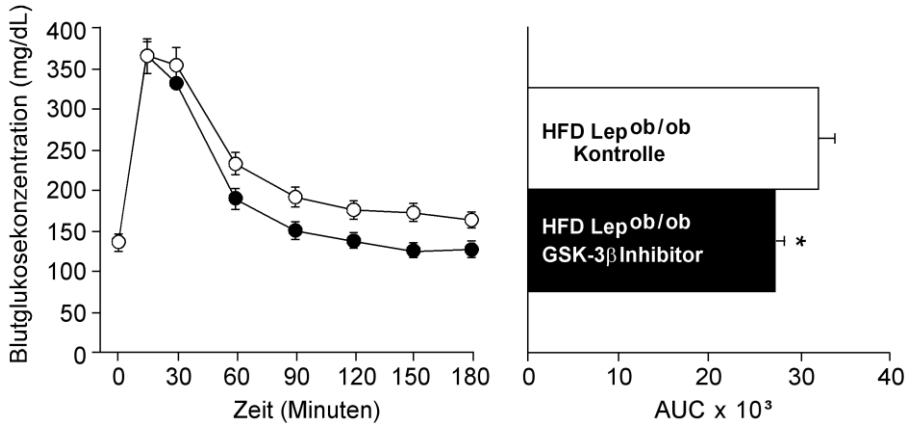

Abb. 11: Die Verbesserung der Glukosehomöostase durch eine dauerhafte Inhibition der zentralen GSK-3β. Die chronische Inhibition der zentralen GSK-3β wurde durch die Implantation von osmotischen Pumpen in den lateralen Ventrikel gewährleistet, wodurch der GSK-3β Inhibitor (oder Kontrolle) kontinuierlich in das ZNS verabreicht wurde (1nmol / 24 h). Die leptindefizienten Mäuse wurden nach der Operation für 10 Tage mit einer hochkalorischen Diät gefüttert. Anschließend wurde der Glukosetoleranztest durchgeführt. n= 6 Tiere / Gruppe. **P*=0.048. GSK-3β: Glykogen-Synthase Kinase-3β; $Lep^{ob/ob}$- Mäuse: leptindefiziente Mäuse; HFD: hochkalorische Diät; AUC: Area under the curve; ZNS: zentrales Nervensystem.

Es ist jedoch dringend erforderlich den Grund der erhöhten GSK-3β Aktivität zu entschlüsseln. Es konnte hier gezeigt werden, dass sowohl eine akute als auch eine chronische Unterdrückung einer pro-inflammatorischen Antwort die Energie- und Glukosehomöostase positiv beeinflusst. Da die GSK-3β als pro-inflammatorischer Regulator angesehen wird, vermuten wir, dass die zirkulierenden Zytokine und gesättigten Fettsäuren für diese Dysregulation der GSK-3β verantwortlich sind. Die aktuelle Forschung von Antidiabetika beschäftigt sich bereits eindringlich mit anti-inflammatorischen Substanzen und liefert vielversprechende Ergebnisse in Bezug auf Diabetes mellitus Typ II. Auch das

körpereigene Hormon Adiponektin besitzt solche anti-inflammatorischen Eigenschaften und eine zentrale Applikation verbesserte die Glukosetoleranz von Mäusen (siehe Kapitel 5.1). Mit Zunahme des Körpergewichtes sinken jedoch die Konzentrationen von zirkulierendem Adiponektin, wodurch die positiven Wirkungen verloren gehen. Daher könnte die Einnahme von anti-inflammatorische Substanzen oder Medikamenten, wie das hier gezeigte Flavonoid Butein, ein großes Potential in Bezug auf die Behandlung von Diabetes mellitus Typ II besitzen. Bis jetzt sind vor allem systemische Applikationen von anti-inflammatorischen Substanzen analysiert worden. Die, bei Diabetes mellitus Typ II notwendige, chronische Gabe hoher Konzentrationen bringt aber meist Komplikationen und Nebenwirkungen mit sich. Um Medikamente zu entwickeln, die eventuell eine gezielte Behandlung der verantwortlichen Gewebe oder Organe möglich macht, ist es notwendig, die exakten molekularen Mechanismen der zentralen Regulation der Energie- und Glukosehomöostase weiter zu entschlüsseln.

3.7 Literaturverzeichnis

1 World health organization.: 2013. http://www.who.int/en

2 Feve B, Bastard JP, Vidal H: [Relationship between obesity, inflammation and insulin resistance: new concepts]. C R Biol 2006;329:587-597.

3 Diabetes deutschland. http://www.diabetes-deutschland.de

4 Bruning JC, Gautam D, Burks DJ, Gillette J, Schubert M, Orban PC, Klein R, Krone W, Muller-Wieland D, Kahn CR: Role of brain insulin receptor in control of body weight and reproduction. Science 2000;289:2122-2125.

5 Niswender KD, Morrison CD, Clegg DJ, Olson R, Baskin DG, Myers MG, Jr., Seeley RJ, Schwartz MW: Insulin activation of phosphatidylinositol 3-kinase in the hypothalamic arcuate nucleus: a key mediator of insulin-induced anorexia. Diabetes 2003;52:227-231.

6 Obici S, Zhang BB, Karkanias G, Rossetti L: Hypothalamic insulin signaling is required for inhibition of glucose production. Nat Med 2002;8:1376-1382.

7 Obici S, Feng Z, Karkanias G, Baskin DG, Rossetti L: Decreasing hypothalamic insulin receptors causes hyperphagia and insulin resistance in rats. Nat Neurosci 2002;5:566-572.

8 Okamoto H, Nakae J, Kitamura T, Park BC, Dragatsis I, Accili D: Transgenic rescue of insulin receptor-deficient mice. Journal of Clinical Investigation 2004;114:214-223.

9 Okamoto H, Obici S, Accili D, Rossetti L: Restoration of liver insulin signaling in Insr knockout mice fails to normalize hepatic insulin action. Journal of Clinical Investigation 2005;115:1314-1322.

10 Schwartz MW, Woods SC, Porte D, Jr., Seeley RJ, Baskin DG: Central nervous system control of food intake. Nature 2000;404:661-671.

11 Morton GJ, Schwartz MW: The NPY/AgRP neuron and energy homeostasis. Int J Obes Relat Metab Disord 2001;25 Suppl 5:S56-S62.

12 Niswender KD, Schwartz MW: Insulin and leptin revisited: adiposity signals with overlapping physiological and intracellular signaling capabilities. Front Neuroendocrinol 2003;24:1-10.

13 Gual P, Le Marchand-Brustel Y, Tanti JF: Positive and negative regulation of insulin signaling through IRS-1 phosphorylation. Biochimie 2005;87:99-109.

14 Hanke S, Mann M: The phosphotyrosine interactome of the insulin receptor family and its substrates IRS-1 and IRS-2. Mol Cell Proteomics 2009;8:519-534.

15 Geering B, Cutillas PR, Vanhaesebroeck B: Regulation of class IA PI3Ks: is there a role for monomeric PI3K subunits? Biochem Soc Trans 2007;35:199-203.

16 Zhang YY, Proenca R, Maffei M, Barone M, Leopold L, Friedman JM: Positional Cloning of the Mouse Obese Gene and Its Human Homolog. Nature 1994;372:425-432.

17 Frederich RC, Hamann A, Anderson S, Lollmann B, Lowell BB, Flier JS: Leptin levels reflect body lipid content in mice: evidence for diet-induced resistance to leptin action. Nat Med 1995;1:1311-1314.

18 Banks AS, Davis SM, Bates SH, Myers MG, Jr.: Activation of downstream signals by the long form of the leptin receptor. J Biol Chem 2000;275:14563-14572.

19 Bjorbaek C, Uotani S, da SB, Flier JS: Divergent signaling capacities of the long and short isoforms of the leptin receptor. J Biol Chem 1997;272:32686-32695.

20 Mercer JG, Hoggard N, Williams LM, Lawrence CB, Hannah LT, Trayhurn P: Localization of leptin receptor mRNA and the long form splice variant (Ob-Rb) in mouse hypothalamus and adjacent brain regions by in situ hybridization. FEBS Lett 1996;387:113-116.

21 Kastin AJ, Pan W, Maness LM, Koletsky RJ, Ernsberger P: Decreased transport of leptin across the blood-brain barrier in rats lacking the short form of the leptin receptor. Peptides 1999;20:1449-1453.

22 Bjorbaek C, Elmquist JK, Michl P, Ahima RS, van BA, McCall AL, Flier JS: Expression of leptin receptor isoforms in rat brain microvessels. Endocrinology 1998;139:3485-3491.

23 Banks WA, Kastin AJ, Huang W, Jaspan JB, Maness LM: Leptin enters the brain by a saturable system independent of insulin. Peptides 1996;17:305-311.

24 Tartaglia LA: The leptin receptor. J Biol Chem 1997;272:6093-6096.

25 Myers MG, Jr.: Leptin receptor signaling and the regulation of mammalian physiology. Recent Prog Horm Res 2004;59:287-304.

26 Bjorbaek C, Kahn BB: Leptin signaling in the central nervous system and the periphery. Recent Prog Horm Res 2004;59:305-331.

27 Bjorbaek C, Elmquist JK, Frantz JD, Shoelson SE, Flier JS: Identification of SOCS-3 as a potential mediator of central leptin resistance. Mol Cell 1998;1:619-625.

28 Farooqi IS: Monogenic human obesity. Front Horm Res 2008;36:1-11.

29 Farooqi IS, O'Rahilly S: Mutations in ligands and receptors of the leptin-melanocortin pathway that lead to obesity. Nat Clin Pract Endocrinol Metab 2008;4:569-577.

30 Griffin ME, Marcucci MJ, Cline GW, Bell K, Barucci N, Lee D, Goodyear LJ, Kraegen EW, White MF, Shulman GI: Free fatty acid-induced insulin resistance is associated with activation of protein kinase C theta and alterations in the insulin signaling cascade. Diabetes 1999;48:1270-1274.

31 Schwartz MW, Niswender KD: Adiposity signaling and biological defense against weight gain: absence of protection or central hormone resistance? J Clin Endocrinol Metab 2004;89:5889-5897.

32 Niswender KD, Morton GJ, Stearns WH, Rhodes CJ, Myers MG, Jr., Schwartz MW: Intracellular signalling. Key enzyme in leptin-induced anorexia. Nature 2001;413:794-795.

33 Zhao AZ, Huan JN, Gupta S, Pal R, Sahu A: A phosphatidylinositol 3-kinase phosphodiesterase 3B-cyclic AMP pathway in hypothalamic action of leptin on feeding. Nat Neurosci 2002;5:727-728.

34 Lin S, Thomas TC, Storlien LH, Huang XF: Development of high fat diet-induced obesity and leptin resistance in C57Bl/6J mice. Int J Obes Relat Metab Disord 2000;24:639-646.

35 Segal KR, Landt M, Klein S: Relationship between insulin sensitivity and plasma leptin concentration in lean and obese men. Diabetes 1996;45:988-991.

36 German JP, Wisse BE, Thaler JP, Matsen ME, Taborsky GJ, Schwartz MW, Morton GJ: Insulin Resistance Induced by Uncontrolled Diabetes Is Mediated by Leptin Deficiency. Diabetes 2010;59:A410.

37 Harrington LS, Findlay GM, Gray A, Tolkacheva T, Wigfield S, Rebholz H, Barnett J, Leslie NR, Cheng S, Shepherd PR, Gout I, Downes CP, Lamb RF: The TSC1-2 tumor suppressor controls insulin-PI3K signaling via regulation of IRS proteins. J Cell Biol 2004;166:213-223.

38 Li Z, Shen J, Wu WK, Yu X, Liang J, Qiu G, Liu J: Leptin induces cyclin D1 expression and proliferation of human nucleus pulposus cells via JAK/STAT, PI3K/Akt and MEK/ERK pathways. PLoS One 2012;7:e53176.

39 Valerio A, Ghisi V, Dossena M, Tonello C, Giordano A, Frontini A, Ferrario M, Pizzi M, Spano P, Carruba MO, Nisoli E: Leptin increases axonal growth cone size in developing mouse cortical neurons by convergent signals inactivating glycogen synthase kinase-3beta. J Biol Chem 2006;281:12950-12958.

40 Florez JC, Jablonski KA, Bayley N, Pollin TI, de Bakker PI, Shuldiner AR, Knowler WC, Nathan DM, Altshuler D: TCF7L2 polymorphisms and progression to diabetes in the Diabetes Prevention Program. N Engl J Med 2006;355:241-250.

41 Grant SF, Thorleifsson G, Reynisdottir I, Benediktsson R, Manolescu A, Sainz J, Helgason A, Stefansson H, Emilsson V, Helgadottir A, Styrkarsdottir U, Magnusson KP, Walters GB, Palsdottir E, Jonsdottir T, Gudmundsdottir T, Gylfason A, Saemundsdottir J, Wilensky RL, Reilly MP, Rader DJ, Bagger Y, Christiansen C, Gudnason V, Sigurdsson G, Thorsteinsdottir U, Gulcher JR, Kong A, Stefansson K: Variant of transcription factor 7-like 2 (TCF7L2) gene confers risk of type 2 diabetes. Nat Genet 2006;38:320-323.

42 Kiessling A, Ehrhart-Bornstein M: Transcription factor 7-like 2 (TCFL2) - a novel factor involved in pathogenesis of type 2 diabetes. Comment on: Grant et al., Nature Genetics 2006, Published online 15 January 2006. Horm Metab Res 2006;38:137-138.

43 Hoppler S, Kavanagh CL: Wnt signalling: variety at the core. J Cell Sci 2007;120:385-393.

44 Moon RT, Brown JD, Torres M: WNTs modulate cell fate and behavior during vertebrate development. Trends Genet 1997;13:157-162.

45 Peifer M, Polakis P: Wnt signaling in oncogenesis and embryogenesis--a look outside the nucleus. Science 2000;287:1606-1609.

46 Logan CY, Nusse R: The Wnt signaling pathway in development and disease. Annu Rev Cell Dev Biol 2004;20:781-810.

47 Nusse R, Varmus HE: Many tumors induced by the mouse mammary tumor virus contain a provirus integrated in the same region of the host genome. Cell 1982;31:99-109.

48 Miller JR: The Wnts. Genome Biol 2002;3:REVIEWS3001.

49 Harterink M, Korswagen HC: Dissecting the Wnt secretion pathway: key questions on the modification and intracellular trafficking of Wnt proteins. Acta Physiol (Oxf) 2012;204:8-16.

50 MacDonald BT, Tamai K, He X: Wnt/beta-catenin signaling: components, mechanisms, and diseases. Dev Cell 2009;17:9-26.

51 Mani A, Radhakrishnan J, Wang H, Mani A, Mani MA, Nelson-Williams C, Carew KS, Mane S, Najmabadi H, Wu D, Lifton RP: LRP6 mutation in a family with early coronary disease and metabolic risk factors. Science 2007;315:1278-1282.

52 Sutherland C, Leighton IA, Cohen P: Inactivation of glycogen synthase kinase-3 beta by phosphorylation: new kinase connections in insulin and growth-factor signalling. Biochem J 1993;296 (Pt 1):15-19.

53 Stambolic V, Woodgett JR: Mitogen inactivation of glycogen synthase kinase-3 beta in intact cells via serine 9 phosphorylation. Biochem J 1994;303 (Pt 3):701-704.

54 Cross DA, Alessi DR, Cohen P, Andjelkovich M, Hemmings BA: Inhibition of glycogen synthase kinase-3 by insulin mediated by protein kinase B. Nature 1995;378:785-789.

55 Dajani R, Fraser E, Roe SM, Young N, Good V, Dale TC, Pearl LH: Crystal structure of glycogen synthase kinase 3 beta: structural basis for phosphate-primed substrate specificity and autoinhibition. Cell 2001;105:721-732.

56 Woodgett JR: Judging a protein by more than its name: GSK-3. Sci STKE 2001;2001:re12.

57 Cline GW, Johnson K, Regittnig W, Perret P, Tozzo E, Xiao L, Damico C, Shulman GI: Effects of a novel glycogen synthase kinase-3 inhibitor on insulin-stimulated glucose metabolism in Zucker diabetic fatty (fa/fa) rats. Diabetes 2002;51:2903-2910.

58 Kaidanovich-Beilin O, Eldar-Finkelman H: Long-term treatment with novel glycogen synthase kinase-3 inhibitor improves glucose homeostasis in ob/ob mice: molecular characterization in liver and muscle. J Pharmacol Exp Ther 2006;316:17-24.

59 Rao R, Hao CM, Redha R, Wasserman DH, McGuinness OP, Breyer MD: Glycogen synthase kinase 3 inhibition improves insulin-stimulated glucose metabolism but not hypertension in high-fat-fed C57BL/6J mice. Diabetologia 2007;50:452-460.

60 Hedbacker K, Birsoy K, Wysocki RW, Asilmaz E, Ahima RS, Farooqi IS, Friedman JM: Antidiabetic Effects of IGFBP2, a Leptin-Regulated Gene. Cell Metabolism 2010;11:11-22.

61 Anagnostou SH, Shepherd PR: Glucose induces an autocrine activation of the Wnt/beta-catenin pathway in macrophage cell lines. Biochemical Journal 2008;416:211-218.

62 Beurel E: Regulation by glycogen synthase kinase-3 of inflammation and T cells in CNS diseases. Front Mol Neurosci 2011;4:18.

63 Posey KA, Clegg DJ, Printz RL, Byun J, Morton GJ, Vivekanandan-Giri A, Pennathur S, Baskin DG, Heinecke JW, Woods SC, Schwartz MW, Niswender KD: Hypothalamic proinflammatory lipid accumulation, inflammation, and insulin resistance in rats fed a high-fat diet. Am J Physiol Endocrinol Metab 2009;296:E1003-E1012.

64 Thaler JP, Schwartz MW: Minireview: Inflammation and obesity pathogenesis: the hypothalamus heats up. Endocrinology 2010;151:4109-4115.

65 Thaler JP, Yi CX, Schur EA, Guyenet SJ, Hwang BH, Dietrich MO, Zhao X, Sarruf DA, Izgur V, Maravilla KR, Nguyen HT, Fischer JD, Matsen ME, Wisse BE, Morton GJ, Horvath TL, Baskin DG, Tschop MH, Schwartz MW: Obesity is associated with hypothalamic injury in rodents and humans. J Clin Invest 2012;122:153-162.

66 Jope RS, Yuskaitis CJ, Beurel E: Glycogen synthase kinase-3 (GSK3): inflammation, diseases, and therapeutics. Neurochem Res 2007;32:577-595.

67 Ramirez SH, Fan S, Zhang M, Papugani A, Reichenbach N, Dykstra H, Mercer AJ, Tuma RF, Persidsky Y: Inhibition of glycogen synthase kinase 3beta (GSK3beta) decreases inflammatory responses in brain endothelial cells. Am J Pathol 2010;176:881-892.

68 Cai D, Liu T: Hypothalamic inflammation: a double-edged sword to nutritional diseases. Ann N Y Acad Sci 2011;1243:E1-39.

69 Banks WA, Kastin AJ, Gutierrez EG: Penetration of interleukin-6 across the murine blood-brain barrier. Neurosci Lett 1994;179:53-56.

70 Osburg B, Peiser C, Domling D, Schomburg L, Ko YT, Voigt K, Bickel U: Effect of endotoxin on expression of TNF receptors and transport of TNF-alpha at the blood-brain barrier of the rat. Am J Physiol Endocrinol Metab 2002;283:E899-E908.

71 Thaler JP, Choi SJ, Schwartz MW, Wisse BE: Hypothalamic inflammation and energy homeostasis: resolving the paradox. Front Neuroendocrinol 2010;31:79-84.

72 Mitchell RW, Hatch GM: Fatty acid transport into the brain: of fatty acid fables and lipid tails. Prostaglandins Leukot Essent Fatty Acids 2011;85:293-302.

73 Milanski M, Degasperi G, Coope A, Morari J, Denis R, Cintra DE, Tsukumo DM, Anhe G, Amaral ME, Takahashi HK, Curi R, Oliveira HC, Carvalheira JB, Bordin S, Saad MJ, Velloso LA: Saturated fatty acids produce an inflammatory response predominantly through the activation of TLR4 signaling in hypothalamus: implications for the pathogenesis of obesity. J Neurosci 2009;29:359-370.

74 Davis RJ: Signal transduction by the JNK group of MAP kinases. Cell 2000;103:239-252.

75 Hirosumi J, Tuncman G, Chang L, Gorgun CZ, Uysal KT, Maeda K, Karin M, Hotamisligil GS: A central role for JNK in obesity and insulin resistance. Nature 2002;420:333-336.

76 Dong C, Davis RJ, Flavell RA: MAP kinases in the immune response. Annu Rev Immunol 2002;20:55-72.

77 Kyriakis JM, Avruch J: Mammalian mitogen-activated protein kinase signal transduction pathways activated by stress and inflammation. Physiol Rev 2001;81:807-869.

78 Konner AC, Bruning JC: Toll-like receptors: linking inflammation to metabolism. Trends Endocrinol Metab 2011;22:16-23.

79 Aguirre V, Uchida T, Yenush L, Davis R, White MF: The c-Jun NH(2)-terminal kinase promotes insulin resistance during association with insulin receptor substrate-1 and phosphorylation of Ser(307). J Biol Chem 2000;275:9047-9054.

80 Aguirre V, Werner ED, Giraud J, Lee YH, Shoelson SE, White MF: Phosphorylation of Ser307 in insulin receptor substrate-1 blocks interactions with the insulin receptor and inhibits insulin action. J Biol Chem 2002;277:1531-1537.

81 Lee YH, Giraud J, Davis RJ, White MF: c-Jun N-terminal kinase (JNK) mediates feedback inhibition of the insulin signaling cascade. J Biol Chem 2003;278:2896-2902.

82 Nguyen MT, Satoh H, Favelyukis S, Babendure JL, Imamura T, Sbodio JI, Zalevsky J, Dahiyat BI, Chi NW, Olefsky JM: JNK and tumor necrosis factor-alpha mediate free fatty acid-induced insulin resistance in 3T3-L1 adipocytes. J Biol Chem 2005;280:35361-35371.

83 De Souza CT, Araujo EP, Bordin S, Ashimine R, Zollner RL, Boschero AC, Saad MJ, Velloso LA: Consumption of a fat-rich diet activates a proinflammatory response and induces insulin resistance in the hypothalamus. Endocrinology 2005;146:4192-4199.

84 Belgardt BF, Mauer J, Wunderlich FT, Ernst MB, Pal M, Spohn G, Bronneke HS, Brodesser S, Hampel B, Schauss AC, Bruning JC: Hypothalamic and pituitary c-Jun N-terminal kinase 1 signaling coordinately regulates glucose metabolism. Proc Natl Acad Sci U S A 2010;107:6028-6033.

85 Sabio G, Cavanagh-Kyros J, Barrett T, Jung DY, Ko HJ, Ong H, Morel C, Mora A, Reilly J, Kim JK, Davis RJ: Role of the hypothalamic-pituitary-thyroid axis in metabolic regulation by JNK1. Genes Dev 2010;24:256-264.

86 Baeuerle PA, Baltimore D: NF-kappa B: ten years after. Cell 1996;87:13-20.

87 Vaughan S, Jat PS: Deciphering the role of nuclear factor-kappaB in cellular senescence. Aging (Albany NY) 2011;3:913-919.

88 Cai D: NFkappaB-mediated metabolic inflammation in peripheral tissues versus central nervous system. Cell Cycle 2009;8:2542-2548.

89 Kleinridders A, Schenten D, Konner AC, Belgardt BF, Mauer J, Okamura T, Wunderlich FT, Medzhitov R, Bruning JC: MyD88 signaling in the CNS is required for development of fatty acid-induced leptin resistance and diet-induced obesity. Cell Metab 2009;10:249-259.

90 Zhang X, Zhang G, Zhang H, Karin M, Bai H, Cai D: Hypothalamic IKKbeta/NF-kappaB and ER stress link overnutrition to energy imbalance and obesity. Cell 2008;135:61-73.

91 Tamai K, Semenov M, Kato Y, Spokony R, Liu C, Katsuyama Y, Hess F, Saint-Jeannet JP, He X: LDL-receptor-related proteins in Wnt signal transduction. Nature 2000;407:530-535.

92 van den Hoek AM, Voshol PJ, Karnekamp BN, Buijs RM, Romijn JA, Havekes LM, Pijl H: Intracerebroventricular neuropeptide Y infusion precludes inhibition of glucose and VLDL production by insulin. Diabetes 2004;53:2529-2534.

93 Gelling RW, Morton GJ, Morrison CD, Niswender KD, Myers MG, Jr., Rhodes CJ, Schwartz MW: Insulin action in the brain contributes to glucose lowering during insulin treatment of diabetes. Cell Metab 2006;3:67-73.

94 Koch L, Wunderlich FT, Seibler J, Konner AC, Hampel B, Irlenbusch S, Brabant G, Kahn CR, Schwenk F, Bruning JC: Central insulin action regulates peripheral glucose and fat metabolism in mice. J Clin Invest 2008;118:2132-2147.

95 Koch C, Augustine RA, Steger J, Ganjam GK, Benzler J, Pracht C, Lowe C, Schwartz MW, Shepherd PR, Anderson GM, Grattan DR, Tups A: Leptin rapidly improves glucose homeostasis in obese mice by increasing hypothalamic insulin sensitivity. J Neurosci 2010;30:16180-16187.

96 Scali C, Caraci F, Gianfriddo M, Diodato E, Roncarati R, Pollio G, Gaviraghi G, Copani A, Nicoletti F, Terstappen GC, Caricasole A: Inhibition of Wnt signaling, modulation of Tau phosphorylation and induction of neuronal cell death by DKK1. Neurobiol Dis 2006;24:254-265.

97 Hu D, Fang W, Han A, Gallagher L, Davis RJ, Xiong B, Yang W: c-Jun N-terminal kinase 1 interacts with and negatively regulates Wnt/beta-catenin signaling through GSK3beta pathway. Carcinogenesis 2008;29:2317-2324.

98 Tups A, Ellis C, Moar KM, Logie TJ, Adam CL, Mercer JG, Klingenspor M: Photoperiodic regulation of leptin sensitivity in the Siberian hamster, Phodopus sungorus, is reflected in arcuate nucleus SOCS-3 (suppressor of cytokine signaling) gene expression. Endocrinology 2004;145:1185-1193.

99 German J, Kim F, Schwartz GJ, Havel PJ, Rhodes CJ, Schwartz MW, Morton GJ: Hypothalamic leptin signaling regulates hepatic insulin sensitivity via a neurocircuit involving the vagus nerve. Endocrinology 2009;150:4502-4511.

100 Lochhead PA, Coghlan M, Rice SQ, Sutherland C: Inhibition of GSK-3 selectively reduces glucose-6-phosphatase and phosphatase and phosphoenolypyruvate carboxykinase gene expression. Diabetes 2001;50:937-946.

101 Consoli A, Nurjhan N, Capani F, Gerich J: Predominant role of gluconeogenesis in increased hepatic glucose production in NIDDM. Diabetes 1989;38:550-557.

102 Gerich JE, Nurjhan N: Gluconeogenesis in type 2 diabetes. Adv Exp Med Biol 1993;334:253-258.

103 Eldar-Finkelman H, Ilouz R: Challenges and opportunities with glycogen synthase kinase-3 inhibitors for insulin resistance and Type 2 diabetes treatment. Expert Opin Investig Drugs 2003;12:1511-1519.

104 Frame S, Zheleva D: Targeting glycogen synthase kinase-3 in insulin signalling. Expert Opin Ther Targets 2006;10:429-444.

105 Henriksen EJ, Dokken BB: Role of glycogen synthase kinase-3 in insulin resistance and type 2 diabetes. Curr Drug Targets 2006;7:1435-1441.

106 Woodgett JR: Physiological roles of glycogen synthase kinase-3: potential as a therapeutic target for diabetes and other disorders. Curr Drug Targets Immune Endocr Metabol Disord 2003;3:281-290.

107 Niswender KD, Baskin DG, Schwartz MW: Insulin and its evolving partnership with leptin in the hypothalamic control of energy homeostasis. Trends Endocrinol Metab 2004;15:362-369.

108 Klieverik LP, Janssen SF, van RA, Foppen E, Bisschop PH, Serlie MJ, Boelen A, Ackermans MT, Sauerwein HP, Fliers E, Kalsbeek A: Thyroid hormone modulates glucose production via a sympathetic pathway from the hypothalamic paraventricular nucleus to the liver. Proc Natl Acad Sci U S A 2009;106:5966-5971.

109 Pandey MK, Sandur SK, Sung B, Sethi G, Kunnumakkara AB, Aggarwal BB: Butein, a tetrahydroxychalcone, inhibits nuclear factor (NF)-kappaB and NF-kappaB-regulated gene expression through direct inhibition of IkappaBalpha kinase beta on cysteine 179 residue. J Biol Chem 2007;282:17340-17350.

110 Gong R, Rifai A, Ge Y, Chen S, Dworkin LD: Hepatocyte growth factor suppresses proinflammatory NFkappaB activation through GSK3beta inactivation in renal tubular epithelial cells. J Biol Chem 2008;283:7401-7410.

111 Gong R, Ge Y, Chen S, Liang E, Esparza A, Sabo E, Yango A, Gohh R, Rifai A, Dworkin LD: Glycogen synthase kinase 3beta: a novel marker and modulator of inflammatory injury in chronic renal allograft disease. Am J Transplant 2008;8:1852-1863.

112 Hoeflich KP, Luo J, Rubie EA, Tsao MS, Jin O, Woodgett JR: Requirement for glycogen synthase kinase-3beta in cell survival and NF-kappaB activation. Nature 2000;406:86-90.

113 Yuskaitis CJ, Jope RS: Glycogen synthase kinase-3 regulates microglial migration, inflammation, and inflammation-induced neurotoxicity. Cell Signal 2009;21:264-273.

114 Dugo L, Collin M, Allen DA, Patel NS, Bauer I, Mervaala EM, Louhelainen M, Foster SJ, Yaqoob MM, Thiemermann C: GSK-3beta inhibitors attenuate the organ injury/dysfunction caused by endotoxemia in the rat. Crit Care Med 2005;33:1903-1912.

115 Gao Z, Hwang D, Bataille F, Lefevre M, York D, Quon MJ, Ye J: Serine phosphorylation of insulin receptor substrate 1 by inhibitor kappa B kinase complex. J Biol Chem 2002;277:48115-48121.

116 Howitz KT, Bitterman KJ, Cohen HY, Lamming DW, Lavu S, Wood JG, Zipkin RE, Chung P, Kisielewski A, Zhang LL, Scherer B, Sinclair DA: Small molecule activators of sirtuins extend Saccharomyces cerevisiae lifespan. Nature 2003;425:191-196.

117 Ramadori G, Fujikawa T, Anderson J, Berglund ED, Frazao R, Michan S, Vianna CR, Sinclair DA, Elias CF, Coppari R: SIRT1 deacetylase in SF1 neurons protects against metabolic imbalance. Cell Metab 2011;14:301-312.

118 Hwa JJ, Fawzi AB, Graziano MP, Ghibaudi L, Williams P, Van HM, Davis H, Rudinski M, Sybertz E, Strader CD: Leptin increases energy expenditure and selectively promotes fat metabolism in ob/ob mice. Am J Physiol 1997;272:R1204-R1209.

119 Frantz B, O'Neill EA: The effect of sodium salicylate and aspirin on NF-kappa B. Science 1995;270:2017-2019.

120 Grilli M, Pizzi M, Memo M, Spano P: Neuroprotection by aspirin and sodium salicylate through blockade of NF-kappaB activation. Science 1996;274:1383-1385.

121 Pierce JW, Read MA, Ding H, Luscinskas FW, Collins T: Salicylates inhibit I kappa B-alpha phosphorylation, endothelial-leukocyte adhesion molecule expression, and neutrophil transmigration. J Immunol 1996;156:3961-3969.

122 Goldfine AB, Silver R, Aldhahi W, Cai D, Tatro E, Lee J, Shoelson SE: Use of salsalate to target inflammation in the treatment of insulin resistance and type 2 diabetes. Clin Transl Sci 2008;1:36-43.

123 Goldfine AB, Fonseca V, Jablonski KA, Pyle L, Staten MA, Shoelson SE: The effects of salsalate on glycemic control in patients with type 2 diabetes: a randomized trial. Ann Intern Med 2010;152:346-357.

124 Goldfine AB, Fonseca V, Jablonski KA, Chen YD, Tipton L, Staten MA, Shoelson SE: Salicylate (salsalate) in patients with type 2 diabetes: a randomized trial. Ann Intern Med 2013;159:1-12.

16180 • The Journal of Neuroscience, December 1, 2010 • 30(48):16180–16187

Behavioral/Systems/Cognitive

Leptin Rapidly Improves Glucose Homeostasis in Obese Mice by Increasing Hypothalamic Insulin Sensitivity

Christiane Koch,[1] Rachael A. Augustine,[2] Juliane Steger,[1] Goutham K. Ganjam,[1] Jonas Benzler,[1] Corinna Pracht,[1] Chrishanthi Lowe,[1] Michael W. Schwartz,[4] Peter R. Shepherd,[3] Greg M. Anderson,[2] David R. Grattan,[2] and Alexander Tups[1]

[1]Department of Animal Physiology, Faculty of Biology, Philipps University Marburg, D-35043 Marburg, Germany, [2]Centre for Neuroendocrinology and Department of Anatomy and Structural Biology, University of Otago, Dunedin 9054, New Zealand, [3]Maurice Wilkins Centre for Molecular Biodiscovery and Department of Molecular Medicine and Pathology, University of Auckland, 92019 Auckland, New Zealand, and [4]Division of Metabolism, Endocrinology and Nutrition, University of Washington, Seattle, Washington 98195

Obesity is associated with resistance to the actions of both leptin and insulin via mechanisms that remain incompletely understood. To investigate whether leptin resistance per se contributes to insulin resistance and impaired glucose homeostasis, we investigated the effect of acute leptin administration on glucose homeostasis in normal as well as leptin- or leptin receptor-deficient mice. In hyperglycemic, leptin-deficient $Lep^{ob/ob}$ mice, leptin acutely and potently improved glucose metabolism, before any change of body fat mass, via a mechanism involving the p110α and β isoforms of phosphatidylinositol-3-kinase (PI3K). Unlike insulin, however, the anti-diabetic effect of leptin occurred independently of phospho-AKT, a major downstream target of PI3K, and instead involved enhanced sensitivity of the hypothalamus to insulin action upstream of PI3K, through modulation of IRS1 (insulin receptor substrate 1) phosphorylation. These data suggest that leptin resistance, as occurs in obesity, reduces the hypothalamic response to insulin and thereby impairs peripheral glucose homeostasis, contributing to the development of type 2 diabetes.

Introduction

In addition to its essential role in the control of body weight, the adipose tissue-derived hormone, leptin, contributes to the maintenance of glucose homeostasis (Pelleymounter et al., 1995; Muzzin et al., 1996; Schwartz et al., 1996; Farooqi et al., 1999; Yu et al., 2008). In fact, recent data suggest that leptin is more potent at regulating glucose levels in blood than it is at suppressing appetite (Hedbacker et al., 2010). As the effect of leptin on glucose homeostasis is likely to be mediated centrally via activation of specific neuronal subpopulations in the hypothalamus (Kievit et al., 2006; German et al., 2009; Hill et al., 2009; Hedbacker et al., 2010), in the present study, we aimed to investigate the central mechanisms mediating the anti-diabetic properties of leptin. Leptin action on glucose homeostasis is dependent on signal transduction via phosphatidylinositol-3-kinase (PI3K) activity (Mauvais-Jarvis et al., 2002; Niswender et al., 2003; Morton et al., 2005; Hill et al., 2009), a pathway also used by the insulin receptor. We have recently shown that unlike insulin, leptin does not induce phosphorylation of AKT, a key downstream mediator of insulin-stimulated PI3K activity, in the hypothalamus (Tups et al., 2010). Since insulin action in the CNS is also implicated in the regulation of peripheral glucose homeostasis (Brüning et al., 2000; Okamoto et al., 2004, 2005), we hypothesized that leptin might exert its glucose-lowering effects in part through an interaction with insulin signaling in the hypothalamus. Using a range of leptin- and leptin receptor-deficient mice, we demonstrate here that leptin rapidly and markedly enhances hypothalamic sensitivity to insulin. These data provide new insight into mechanisms underlying impaired glucose homeostasis in obesity.

Received June 22, 2010; revised Sept. 24, 2010; accepted Sept. 28, 2010.

This study was funded by the German Ministry of Education and Research (Ref. No: 0315087, to A.T.) and the Health Research Council of New Zealand (to G.M.A. and D.R.G.).

Correspondence should be addressed to Dr. Alexander Tups, Department of Animal Physiology, Faculty of Biology, Philipps University Marburg, Karl-von-Frisch Strasse 8, D-35043 Marburg, Germany. E-mail: alexander.tups@staff.uni-marburg.de.

DOI:10.1523/JNEUROSCI.3202-10.2010

 0270-6474/10/3016180-08$15.00/0

Materials and Methods

Animals

In all experiments only male animals were analyzed. Mice were either purchased from Janvier or drawn from the breeding colonies of the University of Marburg (Marburg, Germany) or the University of Otago, (Dunedin, New Zealand). Sprague Dawley rats were purchased from the Animal Facility, University of Otago. Neuron-specific Lepr knock-out mice ($Lepr^{fl/fl}$ × CaMKIIα-*Cre*) were generated at the University of Otago as described previously (Quennell et al., 2009). All animals were 8–13 weeks old and housed individually under standard conditions with a light/dark cycle of 12 h. The ambient temperature for mice was 26°C, for rats 23°C. Apart from the dark phase before the experiments, all animals had access to standard rodent diet and water *ad libitum*.

Stereotaxic implantation of intracerebroventricular cannulae

Mouse. Under isoflurane anesthesia (CP-Pharma) and carprofen analgesia (5 mg/kg; Rimadyl, Pfizer) a stainless steel guide cannula (internal cannula 2.8 mm with 1 mm projection 33 gauge, C315I-5/Spc, Plastics One) was stereotaxically implanted into the lateral cerebral ventricle of 7-week-old $Lep^{ob/ob}$ mice (0.9 lateral and 0.1 posterior to bregma, 2.2 ventral to the surface of the skull). The cannula was fixed with dental

cement on one small steel screw (screw 00-96x1/96). Cannula placement was tested with an angiotensin II (Sigma-Aldrich) injection [5 ng in 2 μl of artificial CSF (aCSF)] 5 d after surgery. Mice were observed after injection and were only chosen for the experiment if they drank immediately.

Rat. Under isoflurane anesthesia (CP-Pharma) and carprofen analgesia (5 mg/kg; Rimadyl, Pfizer), a stainless steel guide cannula (internal cannula 4 mm with 1 mm projection 28 gauge, C313I/Spc, Plastics One) was stereotaxically implanted into the lateral cerebral ventricle of 7-week-old male rats (1.3 lateral to bregma; 3.0 ventral to the surface of the skull). The cannula was fixed with dental cement on three steel screws (0-80x3/32; Plastics One), which were placed around the cannula. Five days after surgery, correct cannula placement was verified by injecting angiotensin II (20 ng in 2 μl of aCSF). Rats that drank <5 ml water in 30 min were excluded from the experimental treatment.

Food restriction experiment

During the first 8 d of the experiment a group of $Lep^{ob/ob}$ mice was pair-fed to $Lep^{ob/+}$ mice whereas one group of $Lep^{ob/ob}$ mice was fed *ad libitum* ($n = 10$ animals/group). Despite being pair-fed $Lep^{ob/ob}$ mice still had a significantly higher body weight compared with $Lep^{ob/+}$ mice after 8 d. The amount of food given to the animals was subsequently reduced to 2–3 g/d to match the body weight of $Lep^{ob/+}$ mice. When the body weight trajectories of the $Lep^{ob/ob}$ and the $Lep^{ob/+}$ mice were similar (8 weeks of age), the food-restricted group of $Lep^{ob/ob}$ mice was subdivided into two weight-matched groups ($n = 4–6$ animals/group), one of which received an intraperitoneal vehicle (PBS) injection and one an intraperitoneal leptin injection (1.25 mg/kg in PBS). The intraperitoneal glucose tolerance test (ipGTT) was performed in the morning, whereas on the same day in the afternoon the body composition was analyzed under isoflurane anesthesia (CP-Pharma) via DEXA-scan (Lunar PIXImus Densitometer; GE Medical Systems).

Glucose tolerance tests in leptin- or leptin receptor-deficient mice

Three different obese mouse strains ($Lepr^{db/db}$; $Lepr^{fl/fl}$ × CaMKIIα-*Cre* and $Lep^{ob/ob}$) and their controls ($Lepr^{db/+}$, $Lepr^{fl/fl}$, and $Lep^{ob/+}$) were subjected to an ipGTT. All animals were 8 weeks old except $Lepr^{fl/fl}$ × CaMKIIα-*Cre* and the respective control $Lepr^{fl/fl}$, which were at 13 weeks of age, and were food deprived for 16 h before the experiment. The individual strains received an intraperitoneal injection of either vehicle (PBS) or leptin (1.25 mg/kg, i.p., in PBS) 15 min before glucose application (1 g glucose/kg, i.p.; $n = 4–6$ animals/group). To determine the blood glucose the vena facialis was punctuated and the glucose concentration was detected by using a commercially available glucometer (Roche; Accu-Check Performa). $Lep^{ob/ob}$ mice were divided into three groups, the first one received the leptin injection as stated above 15 min before the glucose tolerance test (GTT), the second was injected 90 min before the GTT and the third group received two injections 540 and 60 min before the GTT.

Glucose tolerance test after intracerebroventricular injection of leptin and isoform-specific PI3K inhibitors

$Lep^{ob/ob}$ mice (8 weeks of age) that were deprived for 16 h food before the experiment, received an intracerebroventricular injection of isoform-specific PI3K inhibitors (PIK-75/TGX-221 0.1 nM in 5% DMSO/aCSF) or 5% DMSO/aCSF followed by an intracerebroventricular injection of leptin (4 μg in aCSF) or aCSF 45 min later ($n = 5–6$ animals/group). One hour after leptin application, an intraperitoneal GTT (1 g glucose/kg) was performed. Blood was collected from the vena facialis and analyzed as described above.

Insulin-induced phosphorylation of AKT (Ser473)

Three different mouse strains ($Lepr^{db/db}$; $Lepr^{fl/fl}$ × CaMKIIα-*Cre*; $Lep^{ob/ob}$) and their respective controls ($Lepr^{db/+}$, $Lepr^{fl/fl}$, $Lep^{ob/ob}$, $Lep^{ob/+}$) were fasted for 24 h and perfused in the middle of the light phase. Mice lacking forebrain or global leptin receptor and their appropriate controls were divided into two groups. Accordingly one of the two groups received an injection of insulin (1 mg/kg, i.p.; $n = 3–6$ animals/group), the other one vehicle (PBS; $n = 3–4$) 15 min before transcardial perfusion with 4% paraformaldehyde/phosphate buffer under pentobarbital anesthesia (Narcoren; Merial GmbH). In a different experiment, $Lep^{ob/ob}$ mice and heterozygous controls ($Lep^{ob/+}$) were each divided into four groups that received two injections 15 min apart. The first group received two vehicle injections, the second vehicle followed by insulin, the third leptin followed by vehicle and the fourth leptin followed by insulin. The animals were transcardially perfused 15 min after the second injection (vehicle/vehicle $n = 2$ animals/group; all other groups $n = 4$ animals/group).

Effect of leptin on phosphorylation of phospho-IRS(Ser307 and Ser612)

Nine-week-old male $Lep^{ob/ob}$ mice were fasted for 16 h and divided into two groups ($n = 5–6$ animals/group). The first group received an intracerebroventricular leptin injection (4 μg in aCSF) and the other 5% DMSO/aCSF. Fifteen minutes later mice were perfused with 4% paraformaldehyde/phosphate buffer under pentobarbital anesthesia (Narcoren; Merial GmbH) and brains were analyzed by immunohistochemistry.

Characterization of hypothalamic insulin signaling after antagonism of leptin signaling

After 24 h food restriction, 8-week-old Sprague Dawley rats ($n = 3–4$ animals/group) received an intracerebroventricular injection of aCSF or a competitive rat leptin antagonist (200 μg in aCSF; L39A/D40A/F41A Protein Laboratories Rehovot) (Solomon et al., 2006) directly followed by an intracerebroventricular injection of insulin (10 mU) or leptin (4 μg in aCSF; R&D Systems). Fifteen minutes later rats were transcardially perfused with 4% paraformaldehyde/phosphate buffer under pentobarbital anesthesia (Narcoren; Merial GmbH).

Immunohistochemistry

For immunohistochemistry, animals were anesthetized with pentobarbital (Narcoren; Merial GmbH) and perfused with 0.9% saline containing heparin followed by 4% paraformaldehyde in 0.1 M phosphate buffer, pH 7.4. Brains were removed and stored in the same solution for 1 d followed by dehydration in 30% sucrose/0.1 M phosphate buffer. When brains had sunk, they were frozen in isopentane, cooled on dry ice for 1 min, and sectioned coronally at 35 μm throughout the hypothalamus on a freezing microtome. Brain slides were collected in four series and stored in cryoprotectant at 4°C. Free-floating sections were incubated in 0.3% H_2O_2 diluted in PB for 15 min to quench endogenous peroxide followed by incubation in blocking solution (1% normal goat serum, 5% BSA, 0.5% Triton X-100 in phosphate buffer) for 60 min. Sections were incubated with the primary antibody overnight at 4°C (anti-phospho-AKT Ser473, IHC-specific; catalog #9277, or anti-phospho-IRS1 Ser612; cat. no 3203, or anti-phospho-IRS1 Ser 307 catalog #2381; Cell Signaling Technology) diluted in blocking-solution (both 1:500). On the day after, sections were incubated with a biotinylated secondary goat anti-rabbit antibody for 1 h (1:1000, in blocking solution containing 1% normal goat serum, 3% BSA, 0.5% Triton X-100), and then treated with ABC (Vector Laboratories) solution for 1 h. Between the steps, all sections were washed in phosphate buffer (containing 0.5% Triton X-100 before secondary antibody). Finally, the signal was developed by nickel-diaminobenzidine solution (Vector Laboratories), giving a gray/black precipitate. Section images were captured by using a digital camera mounted on a microscope.

Statistics

Data were analyzed by one- or two-way ANOVA followed by a Holm–Sidak comparison test, as appropriate, using SigmaStat statistical software (Jandel). Where data failed equal variance or normality tests they were analyzed by one-way ANOVA on ranks followed by Dunn's multiple-comparison test. Results are presented as means ± SEM, and differences were considered significant if $p < 0.05$.

Results

To separate the role of hypothalamic leptin action on glycemia from its effects on body fat mass, we food-restricted obese (and diabetic) leptin-deficient $Lep^{ob/ob}$ mice such that their body weight trajectory matched that of lean $Lep^{ob/+}$ controls (Fig. 1*a*).

16182 • J. Neurosci., December 1, 2010 • 30(48):16180–16187 Koch et al. • Crosstalk of Leptin and Insulin in the Brain

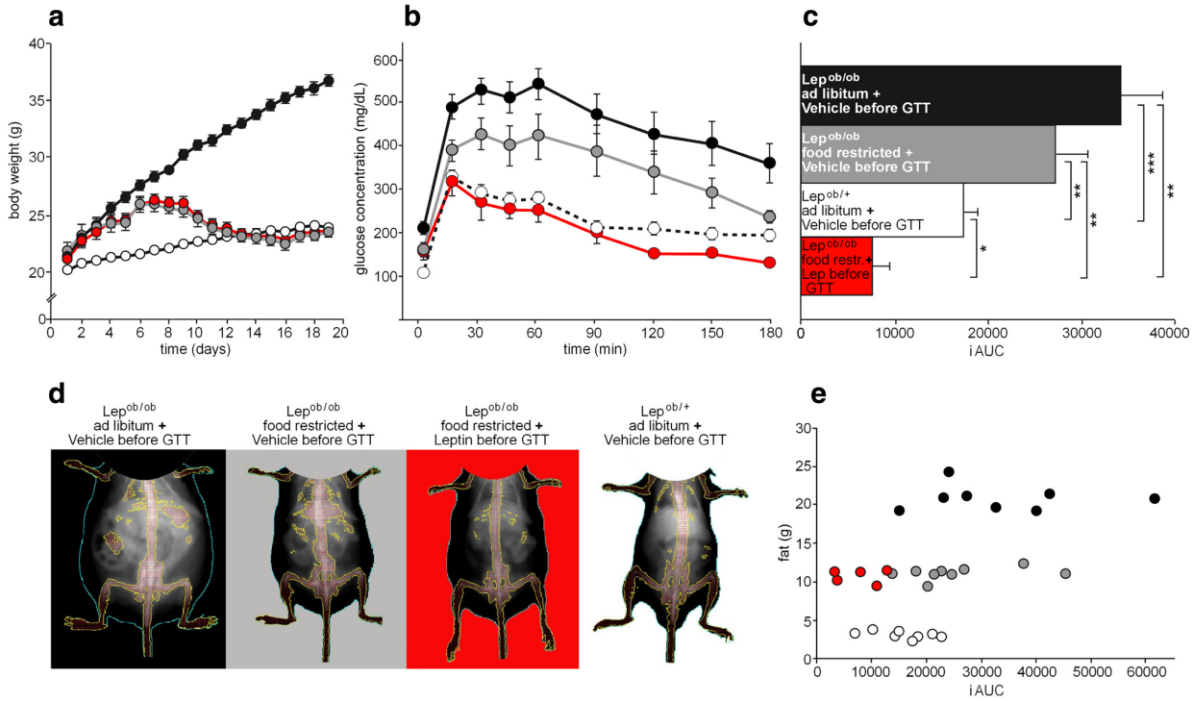

Figure 1. Body weight, glucose concentration, and associated AUC and body composition of Lep $^{ob/ob}$ mice after food restriction. ***a***, Body weight trajectory of Lep $^{ob/ob}$ mice (black; $n = 10$) and control Lep $^{ob/+}$ mice (white; $n = 10$). Two subgroups of Lep $^{ob/ob}$ mice (red and gray; $n = 4–6$ animals/group) were pair-fed during the first 8 d of the experiment followed by a further reduction of available food to 2–3 g/d to match the body weight of the controls. Data show means ± SEM. ***b***, ***c***, ipGTT (***b***) and integrated AUC (***c***) of food-restricted Lep $^{ob/ob}$ mice pretreated with PBS or leptin (1.25 mg/kg) 15 min before glucose application (1 g/kg). White, *Ad libitum*-fed vehicle (PBS)-treated Lep $^{ob/+}$ mice; red, food-restricted leptin-treated Lep $^{ob/ob}$ mice; gray, food-restricted vehicle (PBS)-treated Lep $^{ob/ob}$ mice; black, *ad libitum*-fed vehicle (PBS)-treated Lep $^{ob/ob}$ mice. Data show means ± SEM. $*p < 0.05$, $**p < 0.01$, $***p < 0.001$. ***d***, Representative DEXA-Scan images of one animal in each treatment group. The image was taken immediately after the ipGTT was performed. ***e***, Correlation of AUC and body fat mass of *ad libitum*-fed Lep $^{ob/+}$ mice, *ad libitum*-fed Lep $^{ob/ob}$ mice, and slim pair-fed/food-restricted Lep $^{ob/ob}$ mice, which received a vehicle or leptin injection. Note the lack of correlation between fat content in GTT AUC in individual treatment groups.

Despite the fact that food-restricted Lep $^{ob/ob}$ mice had the same body weight and fasting glucose levels as their heterozygous littermates (Fig. 1*a*), they remained glucose intolerant as determined by an intraperitoneal GTT after 20 d of food restriction ($p = 0.007$; Fig. 1*b*,*c*) and exhibited 11% reduced bone mineral density (0.041 g/cm ^{3}) compared with their heterozygous littermates (0.046 g/cm ^{3}; $p < 0.001$). It is important to acknowledge that food-restricted Lep $^{ob/ob}$ mice continued to have a higher fat content, as measured by dual energy x-ray absortiometry (DEXA; $p < 0.001$; Fig. 1*d*). Within these groups, however, there was no correlation between body fat and glucose homeostasis as measured by the GTT (Fig. 1*e*). While food restriction did not effectively improve glucose metabolism, plasma glucose levels were completely normalized in these mice following intraperitoneal injection of leptin ($p < 0.018$ compared with food restricted controls; Fig. 1*b*,*c*).

Having established that leptin administration improves glucose tolerance in food-restricted Lep $^{ob/ob}$ mice, we next investigated whether this beneficial effect is intact in Lep $^{ob/ob}$ mice allowed to feed *ad libitum*. As expected, vehicle-treated Lep $^{ob/ob}$ mice exhibited severe hyperglycemia and impaired glucose tolerance compared with Lep $^{ob/+}$ mice (Fig. 2*a*,*b*) ($p < 0.05$). As was observed in food-restricted animals, intraperitoneal leptin administration normalized glucose tolerance in Lep $^{ob/ob}$ mice ($p = 0.016$ vs heterozygous controls; Fig. 2*a*). This effect was maximal when leptin was acutely administered as little as 15 min before the glucose challenge, and was not further enhanced by extending leptin pretreatment for up to 9 h before the GTT (data not shown). Since the response to leptin did not vary between time points, a leptin injection 60 min before GTT was chosen for subsequent experiments to minimize stress due to injection handling. By comparison, in euglycemic, nondiabetic heterozygous control animals, exogenous leptin had no effect on glucose tolerance (Fig. 2*b*).

To determine whether the effects of intraperitoneal leptin on glucose homeostasis were mediated centrally or peripherally, we investigated whether leptin receptor deletion specifically in forebrain neurons [*Lepr* $^{fl/fl}$ × CaMKIIα-*Cre* (Quennell et al., 2009)] disrupted leptin's glucose-lowering effect. As seen in Lep $^{ob/ob}$ mice glucose tolerance was markedly impaired in these animals compared with controls lacking Cre-recombinase (Fig. 2*c*) ($p = 0.0134$). The degree of impaired glucose tolerance in these animals was very similar to that seen in Lepr $^{db/db}$ mice, which lack a functional leptin receptor in the whole body. Unlike the effect seen in Lep $^{ob/ob}$ mice, acute peripheral leptin injection 60 min before the GTT did not improve glucose tolerance in either strain (Fig. 2*c*). These data confirm that the effect of leptin on glucose homeostasis is specifically mediated through leptin receptors expressed in the forebrain.

It has been proposed that leptin action on glucose homeostasis involves the PI3K pathway (Mauvais-Jarvis et al., 2002; Niswender et al., 2003; Morton et al., 2005; Hill et al., 2009). As, in previous work, we had not observed leptin-induced activation of AKT in the hypothalamus (Tups et al., 2010), we sought to test whether hypothalamic PI3K signaling was involved in the leptin-

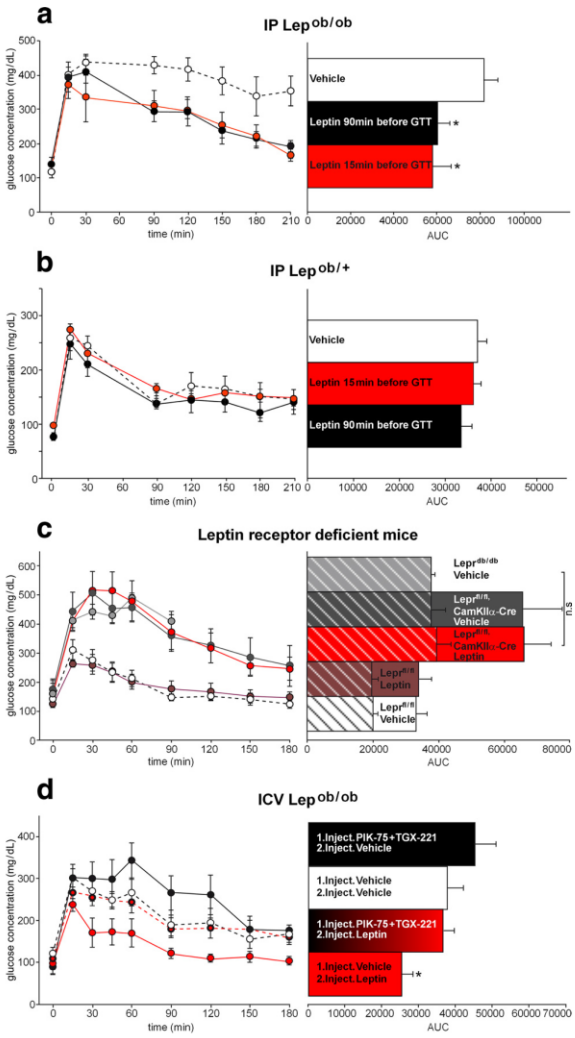

Figure 2. Glucose concentrations (left) and associated AUC (right) during ipGTT in a range of leptin- and leptin receptor-deficient mice. ***a***, Leptin very acutely improves glucose tolerance in obese, *ad libitum*-fed Lep$^{ob/ob}$ mice (1.25 mg/kg, i.p.). AUC was significantly decreased by leptin pretreatment compared with PBS-pretreated Lep$^{ob/ob}$ mice, independent of the injection time. White, Vehicle (PBS); black: intraperitoneal leptin injection 90 min before glucose application; red, intraperitoneal leptin injection 15 min before glucose application. Vehicle, $n = 4$ animals; leptin, $n = 5$ animals/group; Data show means ± SEM. *$p < 0.05$. ***b***, Heterozygous controls to experiment presented in ***a***. Leptin had no effect on normal glucose tolerance in Lep$^{ob/+}$ mice. White, Vehicle (PBS); black, intraperitoneal leptin injection 90 min before glucose application; red, intraperitoneal leptin injection 15 min before glucose application. Vehicle, $n = 6$ animals; leptin, $n = 5$ animals/group; Data show means ± SEM. ***c***, Leptin (1.25 mg/kg, i.p.) did not ameliorate the glucose tolerance and AUC of mice lacking leptin receptor in the forebrain. White, *Lepr*$^{fl/fl}$ mice (lean, $n = 6$) received a vehicle (PBS) injection; brown, *Lepr*$^{fl/fl}$ mice ($n = 5$) received a leptin injection; dark gray, *Lepr*$^{fl/fl}$ × CaMKIIα-*Cre* mice (obese, $n = 6$) received a vehicle (PBS) injection; red, *Lepr*$^{fl/fl}$ × CaMKIIα-*Cre* mice ($n = 5$) received a leptin injection; light gray, Lepr$^{db/db}$ mice (obese, $n = 5$) received a vehicle (PBS) injection. Since the GTT for the Lepr$^{db/db}$ mice was terminated after 90 min, two AUCs are presented. Shaded bars show the AUC of all treatment groups over 90 min, while plain bars show AUC of all treatment groups (except Lepr$^{db/db}$ mice) over 180 min. Data show means ± SEM. n.s., Nonsignificant. ***d***, Central application of leptin 60 min before ipGTT (1 g/kg) ameliorated the glucose tolerance similar to intraperitoneal injection of the hormone. The effect was completely blocked by intracerebroventricular pretreatment with isoform selective PI3K inhibitors PIK-75 (specific for p110α) and TGX-221 specific for (p110β). Inhibitors (0.1 nM each) were given 45 min before intracerebroventricular leptin injection (4 μg). White, Vehicle (aCSF/5% DMSO)/vehicle (aCSF), $n = 5$ animals; red, vehicle (aCSF/5% DMSO)/leptin, $n = 5$ animals; black, PIK-75+TGX 221/aCSF, $n = 6$ animals; black/red, PIK-75 +TGX 221/leptin, $n = 6$ animals. Data show means ± SEM. *$p < 0.05$.

induced normalization of glucose homeostasis in Lep$^{ob/ob}$ mice. To do this, we examined glucose tolerance in the presence of combined inhibition of the p110α- and p110β-isoforms of PI3K (Tups et al., 2010). Selective inhibitors of these two proteins (0.1 nM each) were administered into the lateral ventricle (intracerebroventricularly) of Lep$^{ob/ob}$ mice 45 min before intracerebroventricular injection of leptin (4 μg) or vehicle. Sixty minutes later, a GTT was performed. As expected glucose tolerance was markedly impaired in vehicle-treated Lep$^{ob/ob}$ mice. Consistent with the data showing that central actions of leptin mediate the effect on glucose homeostasis, an acute intracerebroventricular injection of leptin significantly improved glucose tolerance in Lep$^{ob/ob}$ mice, as effectively as peripheral injection in earlier experiments ($p = 0.047$; Fig. 2*d*). The PI3K inhibitors had no effect in vehicle-treated animals but markedly reduced the effect of leptin on peripheral glucose tolerance ($p = 0.025$; Fig. 2*d*).

To investigate the mechanisms activating PI3K, we measured phosphorylation of AKT in hypothalamic neurons following administration of leptin, or insulin, or a combination of the two hormones. AKT is a key target of PI3K activity and phosphorylation results in activation of this molecule. Phospho-AKT (Ser473) was measured by immunohistochemistry using a phospho-specific antibody in the mouse brain. Mice were killed 15 min after an intraperitoneal insulin injection, and cells immunoreactive for phospho-AKT (Ser473) were counted in the arcuate nucleus (ARC) (Tups et al., 2010). In lean heterozygous Lep$^{ob/+}$ mice, acute intraperitoneal injection of insulin resulted in a marked increase in phospho-AKT (Ser473)-immunoreactive cells in the ARC ($p = 0.024$; Fig. 3*a*,*b*). In contrast, acute peripheral leptin injection only marginally induced phospho-AKT (Ser473), and the combined administration of leptin followed 15 min later by insulin was no more effective than insulin alone. In obese Lep$^{ob/ob}$ mice, however, there was a significant 60% reduction in the number of insulin-induced phospho-AKT (Ser473)-immunoreactive cells in the ARC compared with the lean littermates. Similar to lean animals, leptin treatment alone had no effect on phospho-AKT (Ser473) expression in Lep$^{ob/ob}$ mice. Pretreatment with leptin, however, markedly enhanced the response to an insulin injection 15 min later (vehicle vs insulin nonsignificant; vehicle vs leptin+insulin: $p = 0.009$; Fig. 3*a*) such that it was similar to that seen in lean controls. We repeated these studies in mice lacking a functional leptin receptor, either specifically in forebrain neurons (*Lepr*$^{fl/fl}$ × CaMKIIα-*Cre*) or globally (Lepr$^{db/db}$). In both of these strains of mice, the number of cells in the ARC which showed insulin-induced phosphorylation of AKT (Ser473) was reduced to ~30% of that observed in control mice ($p < 0.05$; Fig. 3*c*,*d*).

Up to this stage, all data has been generated using mice with genetic disruptions of leptin or leptin signal transduction, raising the question of whether this phenomenon might be specific to this extreme form of leptin deficiency or leptin resistance. Hence, in parallel studies, we sought to investigate the interaction between leptin and insulin signaling in a more physiological model. To do this, we acutely suppressed leptin signaling in lean, nondiabetic Sprague Dawley rats using a competitive leptin receptor antagonist (Solomon et al., 2006) that has been shown to block leptin-induced phospho-STAT3 in the brain (Zhang et al., 2007). A specific leptin receptor antagonist (200 μg) or vehicle was injected intracerebroventricularly immediately followed by insulin or vehicle intracerebroventricularly, and animals were transcardially perfused with 4% paraformaldehyde 15 min later. As seen in mice studies, intracerebroventricular insulin resulted in a significant increase of phospho-AKT (Ser473) in the ARC. Acute

16184 • J. Neurosci., December 1, 2010 • 30(48):16180–16187 Koch et al. • Crosstalk of Leptin and Insulin in the Brain

treatment with the leptin antagonist, however, completely prevented this effect of insulin ($p = 0.015$; Fig. 3*e*).

The data above strongly suggested that leptin acts acutely in the brain to enhance sensitivity to central insulin signaling through the PI3K pathway. However, the mechanism by which leptin acts to acutely sensitize insulin signaling in the hypothalamus is unknown at present. Since our work has suggested that leptin, by itself, does not significantly activate AKT, we suspect that it must be acting upstream in the PI3K pathway. Insulin is thought to induce tyrosine phosphorylation of either insulin receptor substrate (IRS) 1 or 2 in the brain (Folli et al., 1994; Yamada et al., 1997; Kubota et al., 2004; Lin et al., 2004; Choudhury et al., 2005; Taguchi et al., 2007). The ability of IRS proteins to signal, however, is regulated by the degree to which IRS is serine phosphorylated on a number of different sites (Harrington et al., 2004). To test the hypothesis that leptin might directly affect serine phosphorylation of IRS1, Lep$^{ob/ob}$ mice were treated with intracerebroventricular leptin or vehicle 15 min before an intraperitoneal glucose injection (to mimic the conditions during an intraperitoneal GTT). Fifteen minutes after glucose treatment, the mice were transcardially perfused with paraformaldehyde and immunohistochemistry was performed for phospho-IRS1 (Ser307 and Ser612, in separate sections) on cryosections throughout the ARC. Leptin significantly reduced the number of phospho-IRS1 (Ser612)-immunoreactive cells by ~50% compared with the control (glucose-only) group ($p < 0.001$) (Fig. 4*a*, left). Interestingly, for phospho-IRS1 (Ser307) leptin had the opposite effect and increased the number of immunoreactive cells by ~40% ($p < 0.001$) (Fig. 4*a*, right).

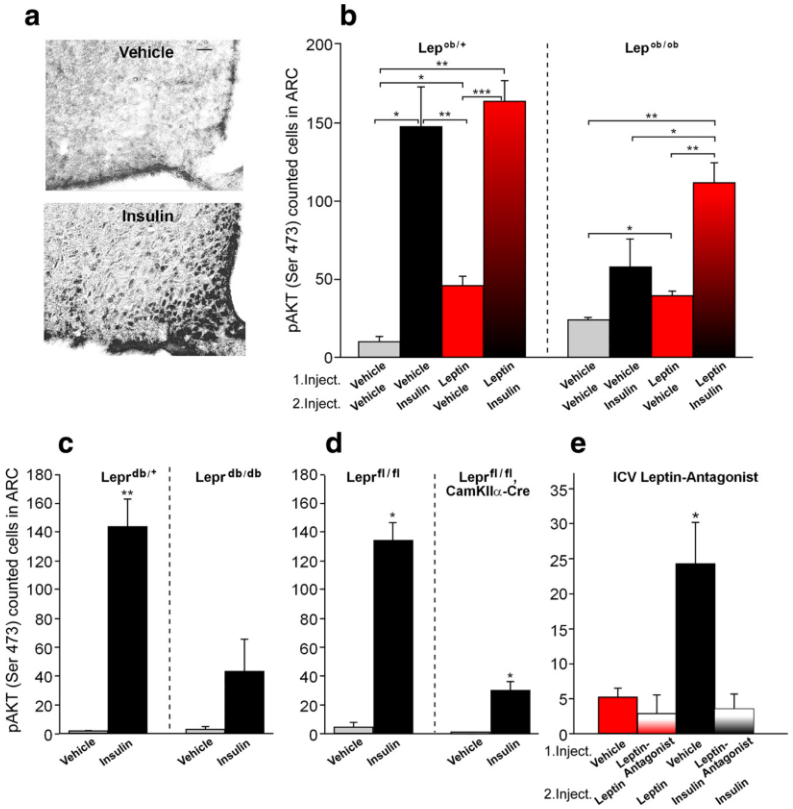

Figure 3. Crosstalk of insulin and leptin on phosphorylation of AKT(Ser 473) in the ARC. ***a***, Representative images showing phospho-AKT(Ser473) immunoreactivity in the ARC of Lep$^{ob/+}$ mice. Mice received either two vehicle (PBS) injections (top), or a vehicle followed by an insulin injection (1 mg/kg, bottom). Scale bar, 30 μm. ***b***, Insulin signaling is impaired in the ARC of Lep$^{ob/ob}$ mice and can be restored by leptin replacement. Lep$^{ob/ob}$ and Lep$^{ob/+}$ mice received two intraperitoneal injections 15 min apart with either vehicle/vehicle, vehicle/insulin, leptin/vehicle, or leptin/insulin. In Lep$^{ob/+}$ mice, insulin (1 mg/kg) markedly increased the number of phospho-AKT (Ser 473)-immunoreactive cells in the ARC, whereas leptin (2 mg/kg) had only a minor effect. Leptin did not further enhance the action of insulin. In Lep$^{ob/ob}$ mice, insulin signaling was impaired as reflected in a decrease in insulin-induced phospho-AKT expression. Leptin pretreatment, however, could partially restore insulin signaling in the leptin/insulin group. Vehicle, $n = 2$ animals/group; insulin, leptin, and leptin/insulin, $n = 4$ animals/group. Data show means ± SEM. $^*p < 0.05$, $^{**}p < 0.01$, $^{***}p < 0.001$. ***c***, Leptin receptor-deficient mice exhibit impaired insulin signaling in the ARC. Lepr$^{db/db}$ mice and their controls (Lepr$^{db/+}$) received an intraperitoneal insulin injection (1 mg/kg) 15 min before transcardial perfusion. phospho-AKT(Ser473)-immunoreactive cells were counted in the ARC. Gray bars depict the vehicle (PBS)-treated whereas the black bars depict the insulin (1 mg/kg)-treated groups of the respective genotype ($n = 3$–6). Data show means ± SEM. ***d***, Mice with a neuron-specific deletion of the leptin receptor (*Lepr$^{fl/fl}$* × CaMKIIα-*Cre*) also exhibit impaired insulin signaling in the hypothalamus. The experimental paradigm was identical to Figure 3*c*, and the respective controls were Lepr$^{fl/fl}$ mice. Vehicle $n = 3$ animals/group; insulin $n = 5$ animals/group. Data show means ± SEM. $^*p < 0.05$, $^{**}p < 0.01$. ***e***, A leptin receptor antagonist blocks insulin-induced pAKT in healthy, nondiabetic Sprague Dawley rats. The leptin antagonist was injected (200 μg) immediately before insulin (10 mU) was injected. One group received a vehicle injection (aCSF) followed by leptin (4 μg), one the antagonist, followed by leptin (4 μg), and one vehicle (aCSF) followed by insulin (10 mU). The insulin-induced phosphorylation of AKT (Ser473) was blocked by an intracerebroventricular injection of the leptin antagonist (200 μg) directly before insulin injection. All injections were intracerebroventricular. Red, aCSF/leptin, $n = 3$ animals; red/white, leptin antagonist/leptin, $n = 3$ animals; black, aCSF/insulin, $n = 4$ animals; black/white, leptin antagonist/insulin, $n = 4$ animals. $^*p < 0.05$.

Discussion

Leptin has been implicated in regulating glucose homeostasis in a wide range of studies. It has been known for a long time that leptin deficiency results in the development of severe type 2 diabetes, both in humans and experimental animals (Zhang et al., 1994; Segal et al., 1996). Leptin treatment reverses these symptoms, associated with weight loss. Recent studies, however, have demonstrated that leptin can improve glucose metabolism independent of its effects on energy homeostasis (German et al., 2010; Hedbacker et al., 2010). Although it has been reported that leptin might exert its anti-diabetic properties by preferentially enhancing insulin signaling in the liver (German et al., 2010), whether leptin also modulates hypothalamic insulin signaling is only poorly understood. A wide range of studies have demonstrated that insulin signaling in the brain plays a major role in maintaining peripheral glucose homeostasis (Brüning et al., 2000; Gelling et al., 2006; Koch et al., 2008; Obici et al., 2002a,b). Here, we corroborate the notion that central insulin signaling is a major factor controlling peripheral glucose homeostasis. Moreover, we present evidence that insulin action in the hypothalamus is dependent on intact leptin signaling in the brain.

In our first experiment, we demonstrated that leptin, itself, is a major contributor to an enhanced glucose tolerance, and that this action is very acute and does not require a leptin-induced

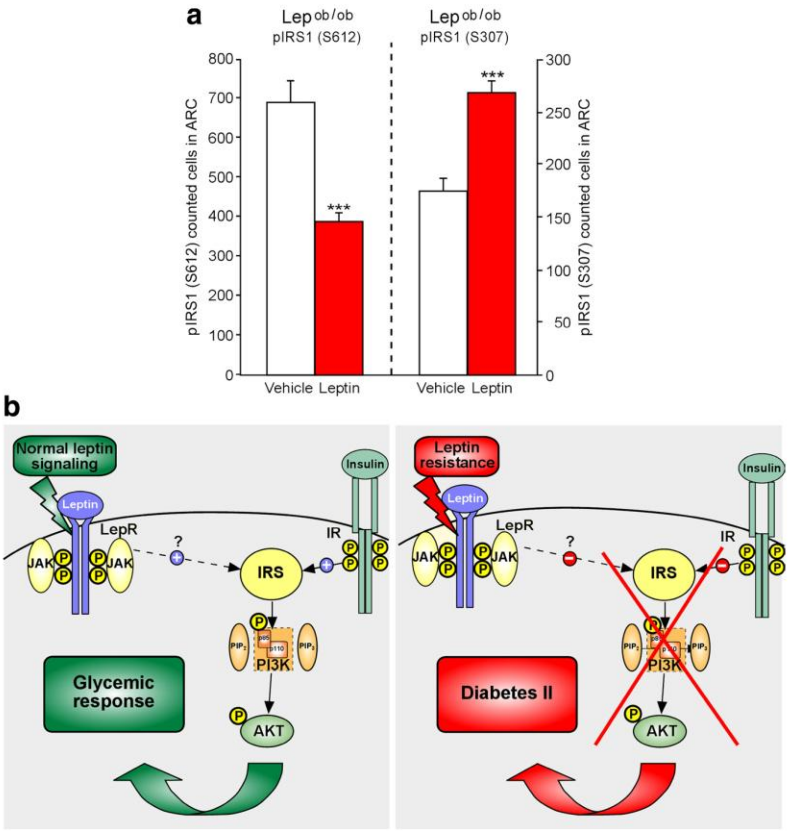

Figure 4. IRS phosphorylation in the hypothalamus: a potential mechanism for leptin's action on glycemia? ***a***, Analysis of phospho-IRS1(Ser612) (left) and for phospho-IRS1(Ser307) (right) by immunohistochemistry in the ARC of Lep$^{ob/ob}$ mice (n = 5–6 animals/group). phospho-IRS1-immunoreactive cells within the medial part of the ARC were counted in four region-matched representative sections of each animal. Fifteen minutes after either vehicle (aCSF) or leptin (4 μg) intracerebroventricular injection, animals were transcardially perfused. Data show means ± SEM. ***$p < 0.001$. ***b***, Model proposing the central mechanism of sensitization of insulin signaling by leptin. In nonobese, leptin-sensitive animals, leptin might activate IRS1 to promote insulin action through the IRS1-PI3K pathway to regulate glucose homeostasis (left). During obesity, with the onset of leptin resistance, leptin might lose its ability to activate IRS1, resulting in a modification of this molecule to a lower affinity to insulin signal transduction (right). This will result in chronically impaired insulin signaling and the development of type 2 diabetes. LepR, Leptin receptor; IR, insulin receptor; JAK, Janus kinase.

reduction of body weight and loss of body fat mass. Pair-feeding and subsequent food restriction of Lep$^{ob/ob}$ mice to reduce body weight to the level of lean Lep$^{ob/+}$ mice only revealed a trend toward an improvement in glucose tolerance. There was no correlation between body fat content and glucose tolerance [area under the curve (AUC)] in these individuals. Only after adding an acute leptin injection was glucose tolerance significantly improved, resulting in even better clearance than in vehicle-treated Lep$^{ob/+}$ controls. Thus, lack of leptin, rather than the associated obesity, was the primary cause of impaired glucose homeostasis in Lep$^{ob/ob}$ mice. These data are consistent with the hypothesis that leptin resistance is a primary cause of type 2 diabetes. However, the possibility that some additional adverse effects are caused by excessive adipose tissue cannot be eliminated, since there was some trend toward an improvement in glucose tolerance simply after pair-feeding/ food restriction in Lep$^{ob/ob}$ mice. Corticosteronemia, glucagon and circulating catecholamines could potentially contribute to observed outcomes and warrant future investigation.

The effect of leptin on glucose metabolism was exclusively mediated centrally, because leptin was equally effective whether administered centrally or peripherally, and there was no beneficial effect of leptin in mice lacking a functional leptin receptor specifically in forebrain neurons. Surprisingly, leptin was able to act very acutely (within 15 min) to improve glucose tolerance. This suggests that the effect is not mediated through enhanced transcription of leptin target genes, but rather through more rapid effects such as phosphorylation events or acute changes in the neuronal firing rate. Crosstalk of both hormones particularly in pro-opiomelanocortin neurons of the hypothalamus has been suggested. Both insulin and leptin induced a transient nuclear export of FoxO1 from these neurons (Fukuda et al., 2008) and affected neuronal firing in a PI3K-dependent manner (Hill et al., 2008). A recent report suggests that this crosstalk may be mediated through segregated actions of leptin and insulin on distinct cells within the POMC network, rather than on the same cells (Williams et al., 2010).

In the present study, inhibition of the p110α and β isoforms of PI3K totally blunted the glycemic action of leptin, suggesting that leptin-induced enhancement of glucose homeostasis is dependent on PI3K signaling in the brain. In our previous work in rats (Tups et al., 2010), we demonstrated that leptin did not directly activate phospho-AKT, the primary target of PI3K-activity in the hypothalamus. Hence, we hypothesized that the suppression of leptin action that occurred following inhibition of PI3K might be based on disruption of insulin signaling. Consistent with this interpretation, in Lep$^{ob/+}$ mice we observed that the ability of insulin to activate phospho-AKT was much higher than that of leptin, but that this effect of insulin was markedly reduced in all of the models with impaired leptin signaling; the Lep$^{ob/ob}$, the Lepr$^{db/db}$ and the *Lepr*$^{fl/fl}$ × CaMKIIα-*Cre* mouse. In the Lep$^{ob/ob}$ mouse, which is leptin-deficient but remains responsive to leptin, leptin treatment acutely restored insulin sensitivity, suggesting a potent crosstalk of the two hormones. The sensitization of insulin signaling by leptin was not limited to mouse models with extreme metabolic and neuroendocrine derangements, such as genetic modification. Acute antagonism of central leptin action in healthy nondiabetic rats totally impaired the number of insulin-induced phospho-AKT-immunoreactive cells in the arcuate nucleus, confirming the essential role of leptin in maintaining insulin sensitivity in the hypothalamus.

Unlike our previous work in rats, in the present study in mice, leptin was able to induce a small increase in phospho-AKT in the arcuate nucleus. Because PI3K inhibition completely prevented the leptin-induced enhancement of glucose homeostasis, it is possible that this effect of leptin is mediated by a direct action on PI3K. It seems more likely, however, that the marked improvement in glucose homeostasis observed after leptin treatment was

due to the leptin-induced sensitization of insulin signaling in the hypothalamus. As a possible mechanism for this effect, we hypothesized that leptin stimulated insulin signaling through PI3K, through an action upstream of PI3K at the level of IRS1. We observed that leptin reduced the number of phospho-IRS1(Ser612)-immunoreactive cells in the arcuate nucleus and had the opposite effect for phospho-IRS1(Ser307). Whether serine phosphorylation of IRS1 negatively or positively regulates insulin signaling *in vivo* is only poorly understood. In most studies, serine phosphorylation at multiple sites is associated with insulin resistance (Harrington et al., 2004). Hence, leptin-induced reduction in Ser612 phosphorylation of IRS1 may promote sensitivity to insulin signaling. However, the effect of leptin on serine phophorylation of IRS1 was not uniform at all sites examined. We also observed a leptin-induced increase in Ser307 phosphorylation. Very recently, Ser307 phosphorylation of IRS1 was shown to be essential for maintaining insulin sensitivity in mice, with insulin resistance occurring in mice in which Ser307 was replaced with alanine (Copps et al., 2010). Leptin-induced Ser307 phosphorylation of IRS1, therefore, may also sensitize insulin action in the hypothalamus. These data are consistent with the hypothesis that leptin may directly regulate insulin sensitivity in the hypothalamus, at least in part, through specific modulation of serine phosphorylation on IRS1 at multiple sites (Fig. 4*b*).

Our data support the concept that central insulin signaling is a major factor controlling peripheral glucose homeostasis. Previous studies have demonstrated that hypothalamic insulin signal transduction is required for the inhibition of hepatic glucose production (Obici et al., 2002a,b) and that hypothalamic actions of leptin appear to improve peripheral insulin sensitivity via a mechanism involving the vagus nerve (German et al., 2009). Furthermore, it was reported that hepatic glucose production is controlled by central nutrient sensing mechanisms (Pocai et al., 2005). The results presented above provide a key link between these important observations. We have shown that leptin is essential for insulin action in the hypothalamus, allowing central insulin to maintain blood glucose homeostasis. The profound correlation of obesity with type 2 diabetes can therefore be explained by the onset of hypothalamic leptin resistance associated with obesity. This results in a loss of insulin sensitivity and consequent impaired glucose homeostasis.

References

Brüning JC, Gautam D, Burks DJ, Gillette J, Schubert M, Orban PC, Klein R, Krone W, Müller-Wieland D, Kahn CR (2000) Role of brain insulin receptor in control of body weight and reproduction. Science 289:2122–2125.

Choudhury AI, Heffron H, Smith MA, Al-Qassab H, Xu AW, Selman C, Simmgen M, Clements M, Claret M, Maccoll G, Bedford DC, Hisadome K, Diakonov I, Moosajee V, Bell JD, Speakman JR, Batterham RL, Barsh GS, Ashford ML, Withers DJ (2005) The role of insulin receptor substrate 2 in hypothalamic and beta cell function. J Clin Invest 115:940–950.

Copps KD, Hancer NJ, Opare-Ado L, Qiu W, Walsh C, White MF (2010) Irs1 serine 307 promotes insulin sensitivity in mice. Cell Metab 11:84–92.

Farooqi IS, Jebb SA, Langmack G, Lawrence E, Cheetham CH, Prentice AM, Hughes IA, McCamish MA, O'Rahilly S (1999) Effects of recombinant leptin therapy in a child with congenital leptin deficiency. N Engl J Med 341:879–884.

Folli F, Bonfanti L, Renard E, Kahn CR, Merighi A (1994) Insulin receptor substrate-1 (IRS-1) distribution in the rat central nervous system. J Neurosci 14:6412–6422.

Fukuda M, Jones JE, Olson D, Hill J, Lee CE, Gautron L, Choi M, Zigman JM, Lowell BB, Elmquist JK (2008) Monitoring FoxO1 localization in chemically identified neurons. J Neurosci 28:13640–13648.

Gelling RW, Morton GJ, Morrison CD, Niswender KD, Myers MG Jr, Rhodes CJ, Schwartz MW (2006) Insulin action in the brain contributes to glucose lowering during insulin treatment of diabetes. Cell Metab 3:67–73.

German J, Kim F, Schwartz GJ, Havel PJ, Rhodes CJ, Schwartz MW, Morton GJ (2009) Hypothalamic leptin signaling regulates hepatic insulin sensitivity via a neurocircuit involving the vagus nerve. Endocrinology 150:4502–4511.

German JP, Wisse BE, Thaler JP, Oh-IS, Sarruf DA, Ogimoto K, Kaiyala KJ, Fischer JD, Matsen ME, Taborsky GJ Jr, Schwartz MW, Morton GJ (2010) Leptin deficiency causes insulin resistance induced by uncontrolled diabetes. Diabetes 59:1626–1634.

Harrington LS, Findlay GM, Gray A, Tolkacheva T, Wigfield S, Rebholz H, Barnett J, Leslie NR, Cheng S, Shepherd PR, Gout I, Downes CP, Lamb RF (2004) The TSC1–2 tumor suppressor controls insulin-PI3K signaling via regulation of IRS proteins. J Cell Biol 166:213–223.

Hedbacker K, Birsoy K, Wysocki RW, Asilmaz E, Ahima RS, Farooqi IS, Friedman JM (2010) Antidiabetic effects of IGFBP2, a leptin-regulated gene. Cell Metab 11:11–22.

Hill JW, Williams KW, Ye C, Luo J, Balthasar N, Coppari R, Cowley MA, Cantley LC, Lowell BB, Elmquist JK (2008) Acute effects of leptin require PI3K signaling in hypothalamic proopiomelanocortin neurons in mice. J Clin Invest 118:1796–1805.

Hill JW, Xu Y, Preitner F, Fukuda M, Cho YR, Luo J, Balthasar N, Coppari R, Cantley LC, Kahn BB, Zhao JJ, Elmquist JK (2009) Phosphatidyl inositol 3-kinase signaling in hypothalamic proopiomelanocortin neurons contributes to the regulation of glucose homeostasis. Endocrinology 150:4874–4882.

Kievit P, Howard JK, Badman MK, Balthasar N, Coppari R, Mori H, Lee CE, Elmquist JK, Yoshimura A, Flier JS (2006) Enhanced leptin sensitivity and improved glucose homeostasis in mice lacking suppressor of cytokine signaling-3 in POMC-expressing cells. Cell Metab 4:123–132.

Koch L, Wunderlich FT, Seibler J, Könner AC, Hampel B, Irlenbusch S, Brabant G, Kahn CR, Schwenk F, Brüning JC (2008) Central insulin action regulates peripheral glucose and fat metabolism in mice. J Clin Invest 118:2132–2147.

Kubota N, Terauchi Y, Tobe K, Yano W, Suzuki R, Ueki K, Takamoto I, Satoh H, Maki T, Kubota T, Moroi M, Okada-Iwabu M, Ezaki O, Nagai R, Ueta Y, Kadowaki T, Noda T (2004) Insulin receptor substrate 2 plays a crucial role in beta cells and the hypothalamus. J Clin Invest 114:917–927.

Lin X, Taguchi A, Park S, Kushner JA, Li F, Li Y, White MF (2004) Dysregulation of insulin receptor substrate 2 in beta cells and brain causes obesity and diabetes. J Clin Invest 114:908–916.

Mauvais-Jarvis F, Ueki K, Fruman DA, Hirshman MF, Sakamoto K, Goodyear LJ, Iannacone M, Accili D, Cantley LC, Kahn CR (2002) Reduced expression of the murine p85alpha subunit of phosphoinositide 3-kinase improves insulin signaling and ameliorates diabetes. J Clin Invest 109:141–149.

Morton GJ, Gelling RW, Niswender KD, Morrison CD, Rhodes CJ, Schwartz MW (2005) Leptin regulates insulin sensitivity via phosphatidylinositol-3-OH kinase signaling in mediobasal hypothalamic neurons. Cell Metab 2:411–420.

Muzzin P, Eisensmith RC, Copeland KC, Woo SL (1996) Correction of obesity and diabetes in genetically obese mice by leptin gene therapy. Proc Natl Acad Sci U S A 93:14804–14808.

Niswender KD, Morrison CD, Clegg DJ, Olson R, Baskin DG, Myers MG Jr, Seeley RJ, Schwartz MW (2003) Insulin activation of phosphatidylinositol 3-kinase in the hypothalamic arcuate nucleus: a key mediator of insulin-induced anorexia. Diabetes 52:227–231.

Obici S, Feng Z, Karkanias G, Baskin DG, Rossetti L (2002a) Decreasing hypothalamic insulin receptors causes hyperphagia and insulin resistance in rats. Nat Neurosci 5:566–572.

Obici S, Zhang BB, Karkanias G, Rossetti L (2002b) Hypothalamic insulin signaling is required for inhibition of glucose production. Nat Med 8:1376–1382.

Okamoto H, Nakae J, Kitamura T, Park BC, Dragatsis I, Accili D (2004) Transgenic rescue of insulin receptor-deficient mice. J Clin Invest 114:214–223.

Okamoto H, Obici S, Accili D, Rossetti L (2005) Restoration of liver insulin signaling in Insr knockout mice fails to normalize hepatic insulin action. J Clin Invest 115:1314–1322.

Pelleymounter MA, Cullen MJ, Baker MB, Hecht R, Winters D, Boone T, Collins F (1995) Effects of the obese gene product on body weight regulation in ob/ob mice. Science 269:540–543.

Pocai A, Obici S, Schwartz GJ, Rossetti L (2005) A brain-liver circuit regulates glucose homeostasis. Cell Metab 1:53–61.

Quennell JH, Mulligan AC, Tups A, Liu X, Phipps SJ, Kemp CJ, Herbison AE, Grattan DR, Anderson GM (2009) Leptin indirectly regulates gonadotropin-releasing hormone neuronal function. Endocrinology 150:2805–2812.

Schwartz MW, Baskin DG, Bukowski TR, Kuijper JL, Foster D, Lasser G, Prunkard DE, Porte D Jr, Woods SC, Seeley RJ, Weigle DS (1996) Specificity of leptin action on elevated blood glucose levels and hypothalamic neuropeptide Y gene expression in ob/ob mice. Diabetes 45:531–535.

Segal KR, Landt M, Klein S (1996) Relationship between insulin sensitivity and plasma leptin concentration in lean and obese men. Diabetes 45:988–991.

Solomon G, Niv-Spector L, Gonen-Berger D, Callebaut I, Djiane J, Gertler A (2006) Preparation of leptin antagonists by site-directed mutagenesis of human, ovine, rat, and mouse leptin's site III. Ann NY Acad Sci 1091:531–539.

Taguchi A, Wartschow LM, White MF (2007) Brain IRS2 signaling coordinates life span and nutrient homeostasis. Science 317:369–372.

Tups A, Anderson GM, Rizwan M, Augustine RA, Chaussade C, Shepherd PR, Grattan DR (2010) Both p110α and p110β isoforms of phosphatidylinositol 3-OH-kinase are required for insulin signalling in the hypothalamus. J Neuroendocrinol 22:534–542.

Williams KW, Margatho LO, Lee CE, Choi M, Lee S, Scott MM, Elias CF, Elmquist JK (2010) Segregation of acute leptin and insulin effects in distinct populations of arcuate proopiomelanocortin neurons. J Neurosci 30:2472–2479.

Yamada M, Ohnishi H, Sano S, Nakatani A, Ikeuchi T, Hatanaka H (1997) Insulin receptor substrate (IRS)-1 and IRS-2 are tyrosine-phosphorylated and associated with phosphatidylinositol 3-kinase in response to brain-derived neurotrophic factor in cultured cerebral cortical neurons. J Biol Chem 272:30334–30339.

Yu X, Park BH, Wang MY, Wang ZV, Unger RH (2008) Making insulin-deficient type 1 diabetic rodents thrive without insulin. Proc Natl Acad Sci U S A 105:14070–14075.

Zhang J, Matheny MK, Tümer N, Mitchell MK, Scarpace PJ (2007) Leptin antagonist reveals that the normalization of caloric intake and the thermic effect of food after high-fat feeding are leptin dependent. Am J Physiol Regul Integr Comp Physiol 292:R868–R874.

Zhang Y, Proenca R, Maffei M, Barone M, Leopold L, Friedman JM (1994) Positional cloning of the mouse obese gene and its human homologue. Nature 372:425–432.

Hypothalamic WNT signalling is impaired during obesity and reinstated by leptin treatment in male mice

Jonas Benzler*, Zane B. Andrews[#], Corinna Pracht*, Sigrid Stöhr*, Peter R. Shepherd[ϕ], David R Grattan[†] and Alexander Tups*

*Department of Animal Physiology, Faculty of Biology, Philipps University Marburg, Marburg, Germany

[#]Department of Physiology, Monash University, Melbourne, Australia

[ϕ] Maurice Wilkins Centre for Molecular Biodiscovery and Department of Molecular Medicine and Pathology, University of Auckland, Auckland, New Zealand

[†] Centre for Neuroendocrinology and Department of Anatomy, University of Otago, Dunedin, New Zealand and

Proofs and correspondence to:
Dr. Alexander Tups
Department of Animal Physiology, Faculty of Biology, Philipps University Marburg, Karl-von-Frisch Str. 8 D-35043 Marburg, Germany
e-mail: alexander.tups@staff.uni-marburg.de

Keywords: LRP-6, diabetes type II, glycogen synthase kinase 3, NPY, hypothalamus

Acknowledgments
This study was funded by the German Ministry of Education and Research (Ref. No: 0315087, to AT).

Disclosure Summary: The authors have nothing to disclose.

Abstract

The WNT- pathway has been well characterized in embryogenesis and tumorigenesis. In humans, specific polymorphisms in the transcription factor TCF-7 and the WNT co-receptor LRP-6, both prominent components of this pathway, correlate with a higher incidence of type-2 diabetes, suggesting the WNT pathway might be involved in the control of adult glucose homeostasis. We previously demonstrated that GSK-3β, the key enzyme of the WNT pathway, is increased in the hypothalamus during obesity and exacerbates high-fat diet-induced weight gain as well as glucose intolerance. These data suggest that WNT action in the hypothalamus might be required for normal glucose homeostasis. Here we characterized whether WNT-signalling in general is altered in the hypothalamus of adult obese mice relative to controls. First we identified expression of multiple components of this pathway in the murine arcuate nucleus (ARC) by *in-situ* hybridization. In this region mRNA of ligands and target genes of the WNT pathway were down-regulated in obese and glucose intolerant leptin-deficient mice. Similarly, the number of cells immunoreactive for the phosphorylated (active) form of the WNT-coreceptor LRP-6 were also decreased in leptin-deficient mice. Leptin treatment normalized expression of the WNT-target genes Axin-2 and Cylin-D1 and increased the number of phospho-LRP-6 immunoreactive cells reaching levels of lean controls. Leptin also increased the levels of phosphorylated (inactive) GSK-3β in the arcuate nucleus, and this effect was colocalized to neuropeptide-Y (NPY) neurons, suggesting that inactivation of GSK-3β may contribute to the neuroendocrine control of energy homeostasis. Taken together our findings identify hypothalamic WNT-signalling as an important novel pathway that integrates peripheral information of the body's energy status encoded by leptin.

Introduction

Type II diabetes is increasing at an alarming rate [1]. During the last decade, emerging evidence suggests that the brain represents a main insulin target tissue [2;3]. However, the molecular mechanisms and the absolute impact of the brain in the pathogenesis of type II diabetes remain incompletely understood. Striking recent observations suggest that the WNT-pathway, typically associated with its essential function in embryogenesis and tumorigenesis [4;5], may also be involved in the pathogenesis of type II diabetes. Human polymorphisms in genes involved in this signalling pathway (particularly the transcription factor T-cell specific transcription factor 7, or TCF-7) were associated with an increased risk to develop type II diabetes [6-8]. Recently, we demonstrated that glucose activates the WNT-pathway in an autocrine fashion in macrophage cell lines [9], suggesting that this pathway might function as a glucose sensory system.

The WNT-pathway consists of extracellular ligands (WNTs) that bind to cell surface receptors of the Frizzled (Fz) family and associated co-receptors, the low-density lipoprotein receptor-related proteins (LRP, e.g. LRP-6). In addition to multiple WNT ligands, there are also a number of endogenously secreted antagonists, including Dickkopf (DKK) proteins and secreted Fz proteins. In the absence of WNT ligands, cytoplasmic β-catenin is phosphorylated by the key enzyme glycogen-synthase-kinase-3 beta (GSK-3β), targeting it for proteasomal degradation. GSK-3β is held in a complex including Axin, Dishevelled (DSL), and Adenomatous polyposis coli (APC). Ligands binding to both the Fz receptors and LRP co-receptors lead to breakdown of this complex and inactivation of GSK-3β, allowing stabilization of β-catenin within the cytoplasm and translocation to the nucleus. Within the nucleus, β-catenin acts together with TCF-7 (also known as TCF-4) to activate the gene expression that is characteristic of the canonical WNT-signalling pathway [10].

The key enzyme GSK-3 is known to be involved in insulin signal transduction, as it is phosphorylated and thereby inhibited by protein kinase B (AKT) [11-13]. Furthermore, inhibition of GSK-3 improves whole body glucose homeostasis [14;15]. We recently demonstrated that hypothalamic GSK-3β activity is elevated during obesity and that neuron-specific over-expression of GSK-3β in the mediobasal hypothalamus exacerbated hyperphagia, obesity and impaired glucose tolerance [16]. In contrast, acute inhibition of this enzyme within the CNS improved whole body glucose homeostasis, decreased food intake and we demonstrated that GSK-3β facilitates the interaction between insulin- and leptin –signaling pathways in the hypothalamus [16]. Inhibition of GSK-3β led to improved hypothalamic insulin signalling via activation of PI3K (phosphoinositide 3-kinase), a key intracellular mediator of both leptin and insulin action [17]. The crosstalk between these hormones is critical for the central regulation of glucose homeostasis, but the precise nature of the interaction remained unclear.

Based on the association of the WNT pathway with type 2 diabetes, and our observation of a central role of the key WNT-responsive enzyme GSK-3β in mediation of central actions of leptin and insulin, in the current study we tested the hypothesis that WNT signalling is active in the hypothalamus of adult mice and is activated by the key body weight regulatory hormone leptin. Therefore, we initially

characterised the gene expression pattern of most components of this pathway in the hypothalamus of wildtype mice, and then investigated whether key genes are differentially expressed between wildtype and leptin-deficient obese mice in the arcuate nucleus (ARC), the key region involved in neuronal control of metabolism. We furthermore analyzed whether leptin is involved in expression of mRNA for major WNT target genes, and whether leptin regulates the WNT-coreceptor LRP6 on a post-translational level. To assess the potential importance of WNT signalling in regulating energy homeostasis via acting specifically in the hypothalamus, we additionally tested whether leptin selectively alters WNT activity in leptin responsive neurons of the hypothalamus, expressing Neuropeptide Y (NPY).

Materials and methods

Animals

All procedures involving animals were licensed under German animal ethics legislation and received approval by the federal public authority for animal ethics. Experiments that were performed in Australia were conducted in accordance with the Monash University Animal Ethics Committee guidelines. All experiments used male mice that were purchased from Janvier (Le Genest-Saint-Isle, France). All mice (wildtype and $Lep^{ob/ob}$ mice) were on the C57BL/6JRj genetic background. Additionally, we used Neruopeptide Y (NPY) -GFP mice (B6.FVB-Tg (Npy-hrGFP)1Lowl/J) which were drawn from the breeding colonies of the Monash University (Melbourne, Australia). Animals were two months old and housed individually under standard conditions with a light/dark cycle of 12 hours. The ambient temperature for mice was 23°C. Apart from the dark phase before the experiments, all animals had access to standard chow diet. For central administration of drugs**,** cannulae were stereotaxically implanted into the left lateral ventricle as described previously [17].

Expression of genes that are involved or targets of WNT-signalling in the brain detected by *in-situ* hybridization

To determine the central expression pattern of genes, that are involved in or are targets of the WNT-pathway, we performed *in-situ* hybridization on brains from $Lep^{+/+}$ mice. For differential expression of mice with and without impaired glucose tolerance, we performed a separate experiment employing one group of $Lep^{+/+}$ and one group of $Lep^{ob/ob}$ mice. Riboprobes complementary to the genes were generated from cloned cDNA from the hypothalamus of *Mus musculus*. cDNA synthesis was performed by using a cDNA synthesis kit (Invitrogen, Carlsbad, CA), according to the manufacturer's instructions. Primers used for amplification of the fragments were designed using Primer Select (suppl. table 1; Lasergene, DNA-Star Software). DNA fragments were ligated into pGEM-T-Easy (Promega, Madison), transformed into DH5-α *Escherichia coli* and sequenced. For cRNA synthesis of antisense riboprobes by *in vitro* transcription, SP6-polymerase or T7-polymerase (Invitrogen) was used. To generate the sense control for all riboprobes, cRNA synthesis was performed by the converse polymerase. As previously described [18], forebrain sections (16 µm) were collected throughout the extent of the arcuate nucleus (ARC) onto a set of twelve slides, with twelve sections mounted on each slide. Accordingly, slides spanned the hypothalamic region approximating from -2.7 to -0.4 mm relative to Bregma according to the atlas of the mouse brain [19]. *In-situ* hybridization and analysis was performed as described previously [18]. A detailed description of primer selection for the genes that were analyzed and their sequences are provided in suppl. table 1.

To test whether leptin activates expression of WNT-genes, we performed *in-situ* hybridization for mRNA of these genes on coronal brain cryo-sections of mice that were injected with leptin. Therefore, leptin-deficient $Lep^{ob/ob}$ mice and $Lep^{+/+}$ mice received either a leptin (2mg/kg) or a vehicle (PBS) ip

injection 2 hours before decapitation and *in-situ* hybridization was performed as described above (n=6/group).

Immunohistochemistry

We analyzed whether leptin acts on the Fz co-receptor LRP-6 in the hypothalamic ARC. Therefore, leptin-deficient $Lep^{ob/ob}$ mice and $Lep^{+/+}$ mice received either a leptin (2mg/kg) or a vehicle (PBS) ip injection 15 minutes before transcardial perfusion and immunohistochemistry was performed (n=5-6/group), using an anti-phospho-LRP-6 Ser1490 antibody (cat. no. 2568, Cell Signalling Technology). To analyze whether DKK-1 antagonizes the WNT pathway at the level of phospho-LRP-6, wild-type mice received an intracerebroventricular (icv) injection of either DKK-1 (1µg in 1µl artificial cerebral spinal fluid (aCSF)) or vehicle (aCSF), 15 minutes before transcardial perfusion and immunohistochemistry was performed using the same antibody as described above (n= 9/group).
To further establish whether leptin interacts with the WNT pathway in neurons, we investigated the effect of leptin on phosphorylation of GSK-3β (Ser9) in NPY-GFP mice. Phosphorylation of GSK-3β at Ser9 is critical to inactivate the enzyme [11-13]. Therefore, 8 weeks old mice (n=5/group) were fasted for 16h and received a single icv injection of either leptin (2 µg/ in 1 µl aCSF) or aCSF 45 minutes before transcardial perfusion and immunohistochemistry was performed using an anti-phosphoGSK-3β (Ser9, cat no. 9323, Cell Signalling Technology) antibody as described [17;20]. For visualisation, the second antibody Alexa Fluor® 594 (Invitrogen) was used and analyzed by fluorescence light microscopy (Axio Imager.M2, Zeiss).

Glucose tolerance test

In this experiment, we tested whether the prominent glucose lowering effects of leptin are mediated via the WNT pathway. Therefore we inhibited WNT-signalling, using the WNT antagonist DKK-1 prior to the assessment of leptin's effect on glucose tolerance. $Lep^{ob/ob}$ mice were fasted for 16h and divided into three groups. The first group were icv injected with the WNT antagonist DKK-1 (1µg in 1µl aCSF, R&D Systems, 5897-DK/CF), followed by ip leptin thirty minutes later (2 mg/kg body weight in PBS). The second group was injected with vehicle icv (aCSF) followed by leptin, whereas the third group received two vehicle injections [(icv: aCSF; ip: PBS) n= 7 each group]. The glucose tolerance test (GTT, 1mg glucose/kg body weight) was performed 30 minutes after the second injection and glucose levels were measured in blood collected from the *Vena facialis* as described previously [17].

Statistics

The data were analysed by one-way ANOVA followed by a Holm–Sidak comparison test, as appropriate, using SigmaStat statistical software (Jandel). Where the data failed equal variance or normality tests, they were analysed by one-way ANOVA on ranks followed by Dunn's multiple

comparison test. The results are presented as means±S.E.M. and differences were considered significant if $P<0.05$.

Results

Genes involved in the WNT-pathway are expressed in the mediobasal hypothalamus

To morphologically characterize the WNT-pathway in the brain, we first analyzed the mRNA expression pattern of genes that encode selected ligands (WNT-4, WNT-7a), receptor and co-receptor (Frizzled-5, LRP-6), other downstream components of the pathway (Axin-1, Dishevelled, GSK-3β, β-catenin, and TCF-7) or target genes (Axin-2 and Cyclin-D1). An initial screen was carried out on wild-type $Lep^{+/+}$ mice. The hybridization signal for almost all investigated genes was not confined to the hypothalamus, and could be observed in extra-hypothalamic regions with the highest density in the hippocampus, cortex and thalamus. However, most genes were strongly expressed in the mediobasal hypothalamus and many showed particular prominence in the arcuate nucleus (ARC, Fig. 1). The control sense probes generated low intensity nonspecific signals (one example, Axin-1, is shown in Fig. 1).

In our recent study, we demonstrated that the antagonist Dickkopf-1 was increased in $Lep^{ob/ob}$ mice compared with wild type mice, suggesting that WNT signalling is downregulated in these mice [16]. Therefore, we further characterized the expression of selected ligands and target genes in the ARC. A comparison of gene expression between $Lep^{+/+}$ mice and leptin-deficient $Lep^{ob/ob}$ mice revealed that expression of the ligands WNT-7a and WNT-4 was significantly down regulated by about 60% and 70% in the ARC of $Lep^{ob/ob}$ mice compared with wild-types (Fig. 2 a, b, P= 0.004, P= 0.038). Moreover, target gene expression of Axin-2 and Cyclin-D1-mRNA was downregulated by about 60% and 25% respectively in the ARC of $Lep^{ob/ob}$ mice in comparison with the controls (Fig. 2 c and d, P= 0.002, P= 0.043).

To test whether the lack of leptin is responsible for the differential downregulation of WNT target genes in $Lep^{ob/ob}$ mice, we investigated the effect of leptin replacement on the expression of these genes in the ARC. Leptin treatment completely restored Axin-2 and Cyclin-D1 mRNA levels, such that no difference relative to wildtype mice was detected (Fig. 2c and d, n=5-6/group).

Effects of leptin on the activity of the WNT-coreceptor LRP-6

Having established that components of the WNT pathway are expressed in the ARC, and that leptin activates WNT target-gene expression, as a possible mechanism we tested whether leptin activates the co-receptor LRP-6, which is an essential modulator of WNT activity at the receptor level. LRP-6 is activated by phosphorylation at Ser1490 [21] and therefore, we used immunohistochemistry to investigate whether leptin increases the number of phospho-LRP-6 (Ser1490) immunoreactive cells in the ARC. Leptin-deficient $Lep^{ob/ob}$ mice exhibited a significant 50% reduction of phospho-LRP-6 (Ser1490) immunoreactive cells in the ARC compared with lean controls (Fig. 3a; P= 0.009). Leptin fully restored phospho-LRP-6 (Ser 1490) immunoreactivity to the wildtype controls (Fig. 3a; vehicle $Lep^{ob/ob}$ mice vs. ip leptin $Lep^{ob/ob}$ mice, P= 0.013). In line with these findings, antagonizing WNT

signalling via icv injection of DKK-1 reduced the number of phospho-LRP-6 (Ser1490) immunoreactive cells by about 25% in the ARC of lean wildtype relative to vehicle injected mice (Fig. 3b; *P*= 0.019, n= 10 animals/group). Since we had previously identified a potent impairment of glucose homeostasis followed by icv DKK-1 injection, we tested whether this ligand also antagonized the ability of leptin to decrease blood glucose [16]. While leptin robustly improved glucose homeostasis in $Lep^{ob/ob}$ mice (*P*= 0.047) after vehicle pre-treatment, this effect was totally abolished in mice that were icv injected with DKK-1 prior to the leptin challenge (Fig. 3c, n= 7/group).

Leptin inhibits GSK-3β in NPY neurons

Hypothalamic leptin- and insulin signalling converge in individual neurons, controling transcription of important neuropeptides that regulate energy homeostasis, such as Neuropeptide Y (NPY) [22]. The catabolic action of leptin involves inhibition of orexigenic NPY neurons [23], which is required to suppress hepatic glucose production [24]. Having established that leptin increases WNT target gene expression and acts on the Fz co-receptor LRP-6 in the ARC, we further investigated whether leptin specifically inhibits GSK-3β in NPY neurons. Therefore, we first identified the proportion of NPY neurons that contain phospho-GSK-3β and are responsive to leptin treatment. Leptin treatment did not affect NPY staining, as shown in Fig. 4a. However, leptin treatment enhanced the number of phospho-GSK-3β (Ser9) positive cells in the ARC by 30% (Fig. 4b, *P*< 0.01), and increased the number of immunoreactive NPY-GFP neurons co-expressing phospho-GSK-3β (Ser9) by 50% in these mice (Fig.4 c, *P*< 0.01).

Discussion

The WNT-pathway plays a well established role in embryogenesis and tumorigenesis. Recently, however, it was demonstrated that glucose activated the WNT-pathway in an autocrine fashion *in vitro* [9]. Furthermore, polymorphisms within the gene encoding TCF-7 contribute to an increased risk of developing type II diabetes in humans [6-8]. These findings, together with our recent observation that the key enzyme of the WNT pathway, GSK-3β, plays an essential role in the neuronal control of food intake and glucose metabolism [16], strongly suggested that hypothalamic WNT-signalling may have a key role in the neuroendocrine control of metabolism.

The surprising finding that all investigated genes involved in the WNT-pathway are expressed in the ARC of the hypothalamus of the adult mouse brain (Fig. 1) indicates that this pathway might be associated with the hypothalamic control of body weight and glucose metabolism. The ligands WNT-7a [25] and WNT-4 [26], which activate the WNT-pathway were down-regulated in the ARC of $Lep^{ob/ob}$ mice (Fig. 2a and b). This is consistent with our previous finding that the known receptor antagonist (DKK-1) was increased in this area [16], suggesting impaired receptor activation of this pathway in the ARC of $Lep^{ob/ob}$ mice. The finding that gene expression of the WNT targets Axin-2 [27] and Cyclin-D1 [28] was also regulated in the same manner strongly suggests that the activity of the WNT pathway is functionally impaired in the hypothalamus of obese mice (Fig. 2c and d). This novel concept is further corroborated by reduced phospho-LRP-6 immunoreactivity in the ARC of $Lep^{ob/ob}$ mice, which suggests reduced endogenous WNT receptor activity (Fig. 3a).

The adipokine leptin can improve glucose metabolism, independent of its effects on energy homeostasis [17;29;30]. We have recently established that these effects of leptin occur very rapidly, suggesting that they involve posttranslational modifications in hypothalamic signalling pathways [17]. Leptin sensitized insulin action in the hypothalamus upstream of PI3K via altering phosphorylation of IRS-1 at Ser307 and Ser612 [17]. Recently, we surprisingly found parallel affects by pharmacological inhibition of GSK-3β [16]. Since leptin inactivates GSK-3β *in vitro* [31;32], a direct action of this hormone on canonical WNT signalling in the adult hypothalamus appears likely. This idea is supported by the finding that leptin treatment normalizes reduced gene expression of the WNT target genes (Axin-2 and Cyclin D1, Fig. 2c and d) in the ARC of leptin deficient mice and inactivates GSK-3β, as indicated by increased phospho-Ser9 GSK-3β immunoreactivity in the ARC (Fig. 4b). Since leptin was capable of normalising the reduced phospho-LRP-6 immunoreactivity seen in the ARC in $Lep^{ob/ob}$ mice (Fig. 3a), it is plausible that leptin selectively activates the WNT pathway via modulation of WNT receptor activity. Phosphorylation at Ser1490 of the co-receptor LRP-is required for Fz receptor activation [21] and therefore for intact WNT-signalling. Whether leptin directly activates the WNT co-receptor e.g. via intrinsic janus-kinase 2 activity or whether this effect occurs via yet unknown indirect mechanisms remains to be identified in future studies.

The hypothesis that the WNT pathway is functional in the adult mouse hypothalamus is supported by the finding that the WNT antagonist DKK-1, contrary to leptin, reduces the number of phospho-LRP-6 immunoreactive cells in the ARC of wildtype mice (Fig. 3b). Intriguingly, DKK-1 icv injection 30 minutes before leptin, totally abolished the glucose lowering properties of the hormone (Fig. 3c). This suggests that the glucose lowering effects of leptin largely depend on neuronal signalling via the WNT pathway and in particular on the level of phosho-LRP-6. It is plausible that the catabolic action of leptin is also transduced by hypothalamic WNT signalling, since we previously observed that GSK-3β overexpresssion in the ARC increased food intake, body weight and was associated with leptin resistance [16]. Consistent with increased food intake and body weight, phospho-GSK-3β (Ser9) immunoreactivity was abundant in NPY neurons of the mediobasal hypothalamus (Fig. 4c) suggesting that this key WNT signalling kinase is involved in regulating activity of these prominent orexigenic neurons. Interestingly, more than 70% of leptin-induced phospho-GSK-3β (Ser9) cells were identified as NPY neurons. The catabolic action of leptin involves inhibition of orexigenic NPY neurons [23], hence it seems possible that leptin inhibits the NPY neurons via involvement of the WNT pathway, particularly GSK-3β. Whether the remaining 30% of leptin-induced phospho-GSK-3β (Ser9) cells in the MBH are POMC neurons remains to be identified in future studies.

Central insulin and leptin signalling plays a very important role in regulating peripheral glucose metabolism [3;17;33-36]. We previously showed that the central glucose lowering properties of leptin appear to be indirect. Rather than a direct action on the IRS/PI3K pathway, leptin sensitizes insulin action through this pathway [17]. We demonstrated that GSK-3β has an essential control in the neuronal control of glucose homeostasis via sensitisation of this pathway [16]. This together with the current study suggests that hypothalamic GSK-3β signalling through the WNT pathway not only has a pivotal role in the neuroendocrine control of glucose homeostasis, it also represents a critical signalling pathway utilized by leptin, and this may be a key mechanism providing convergence in the actions of leptin and insulin. The fact that leptin increased phospho-LRP-6 immunoreactivity and inhibited GSK-3β in NPY neurons, suggests that the sensitization effect of leptin on insulin signalling is mediated via the WNT pathway. This hypothesis is supported by the data published in [16] which revealed that inhibition of GSK-3β sensitizes insulin signalling via the IRS/PI3K pathway. Furthermore phospho-AKT has been robustly shown to phosphorylate and inactivate GSK-3β [11-13], which suggests a possible feedback-loop in hypothalamic neurons by which glucose homeostasis is maintained. A model summarizing the potential interaction of leptin and insulin signalling with the WNT-pathway is presented in Fig. 5.

Taken together, our data strongly support a central role of WNT signalling in the neuronal control of metabolism. This is supported by the fact that WNT signalling is differentially regulated by endogenous leptin deficiency and leptin replacement therapy on various hierarchical levels. This includes the ligands WNT-4 and WNT-7a, the co-receptor LRP-6, the key enzyme GSK-3β [16] and the target genes Axin-2 and Cyclin-D1. Aberrant WNT-signalling has also been associated with the

pathogenesis of diabetic retinopathy [37], coronary artery disease [38], osteoporosis [38], cancer and Alzheimer's disease [39]. The proposed role of leptin in the brain in regulating WNT-signalling might unravel an important link between type II diabetes and the pathogenesis of these other severe diseases.

Reference List

1 Chan JC, Malik V, Jia W, Kadowaki T, Yajnik CS, Yoon KH, Hu FB: Diabetes in Asia: epidemiology, risk factors, and pathophysiology. JAMA 2009;301:2129-2140.

2 Marks JL, Porte D, Jr., Stahl WL, Baskin DG: Localization of insulin receptor mRNA in rat brain by in situ hybridization. Endocrinology 1990;127:3234-3236.

3 Bruning JC, Gautam D, Burks DJ, Gillette J, Schubert M, Orban PC, Klein R, Krone W, Muller-Wieland D, Kahn CR: Role of brain insulin receptor in control of body weight and reproduction. Science 2000;289:2122-2125.

4 Moon RT, Brown JD, Torres M: WNTs modulate cell fate and behavior during vertebrate development. Trends Genet 1997;13:157-162.

5 Peifer M, Polakis P: Wnt signaling in oncogenesis and embryogenesis--a look outside the nucleus. Science 2000;287:1606-1609.

6 Florez JC, Jablonski KA, Bayley N, Pollin TI, de Bakker PI, Shuldiner AR, Knowler WC, Nathan DM, Altshuler D: TCF7L2 polymorphisms and progression to diabetes in the Diabetes Prevention Program. N Engl J Med 2006;355:241-250.

7 Grant SF, Thorleifsson G, Reynisdottir I, Benediktsson R, Manolescu A, Sainz J, Helgason A, Stefansson H, Emilsson V, Helgadottir A, Styrkarsdottir U, Magnusson KP, Walters GB, Palsdottir E, Jonsdottir T, Gudmundsdottir T, Gylfason A, Saemundsdottir J, Wilensky RL, Reilly MP, Rader DJ, Bagger Y, Christiansen C, Gudnason V, Sigurdsson G, Thorsteinsdottir U, Gulcher JR, Kong A, Stefansson K: Variant of transcription factor 7-like 2 (TCF7L2) gene confers risk of type 2 diabetes. Nat Genet 2006;38:320-323.

8 Kiessling A, Ehrhart-Bornstein M: Transcription factor 7-like 2 (TCFL2) - a novel factor involved in pathogenesis of type 2 diabetes. Comment on: Grant et al., Nature Genetics 2006, Published online 15 January 2006. Horm Metab Res 2006;38:137-138.

9 Anagnostou SH, Shepherd PR: Glucose induces an autocrine activation of the Wnt/beta-catenin pathway in macrophage cell lines. Biochemical Journal 2008;416:211-218.

10 MacDonald BT, Tamai K, He X: Wnt/beta-catenin signaling: components, mechanisms, and diseases. Dev Cell 2009;17:9-26.

11 Cross DA, Alessi DR, Cohen P, Andjelkovich M, Hemmings BA: Inhibition of glycogen synthase kinase-3 by insulin mediated by protein kinase B. Nature 1995;378:785-789.

12 Stambolic V, Woodgett JR: Mitogen inactivation of glycogen synthase kinase-3 beta in intact cells via serine 9 phosphorylation. Biochem J 1994;303 (Pt 3):701-704.

13 Sutherland C, Leighton IA, Cohen P: Inactivation of glycogen synthase kinase-3 beta by phosphorylation: new kinase connections in insulin and growth-factor signalling. Biochem J 1993;296 (Pt 1):15-19.

14 Cline GW, Johnson K, Regittnig W, Perret P, Tozzo E, Xiao L, Damico C, Shulman GI: Effects of a novel glycogen synthase kinase-3 inhibitor on insulin-stimulated glucose metabolism in Zucker diabetic fatty (fa/fa) rats. Diabetes 2002;51:2903-2910.

15 Kaidanovich-Beilin O, Eldar-Finkelman H: Long-term treatment with novel glycogen synthase kinase-3 inhibitor improves glucose homeostasis in ob/ob mice: molecular characterization in liver and muscle. J Pharmacol Exp Ther 2006;316:17-24.

16 Benzler J, Ganjam GK, Kruger M, Pinkenburg O, Kutschke M, Stohr S, Steger J, Koch CE, Olkrug R, Schwartz MW, Shepherd PR, Grattan DR, Tups A: Hypothalamic glycogen-synthase-kinase 3beta has a central role in the regulation of food intake and glucose metabolism. Biochem J 2012.

17 Koch C, Augustine RA, Steger J, Ganjam GK, Benzler J, Pracht C, Lowe C, Schwartz MW, Shepherd PR, Anderson GM, Grattan DR, Tups A: Leptin rapidly improves glucose homeostasis in obese mice by increasing hypothalamic insulin sensitivity. J Neurosci 2010;30:16180-16187.

18 Mercer JG, Moar KM, Logie TJ, Findlay PA, Adam CL, Morgan PJ: Seasonally inappropriate body weight induced by food restriction: effect on hypothalamic gene expression in male Siberian hamsters. Endocrinology 2001;142:4173-4181.

19 Paxinos G, Franklin K.: The Mouse Brain in Stereotaxic Coordinates; San Diego, Academics, 2002.

20 Tups A, Anderson GM, Rizwan M, Augustine RA, Chaussade C, Shepherd PR, Grattan DR: Both p110alpha and p110beta isoforms of phosphatidylinositol 3-OH-kinase are required for insulin signalling in the hypothalamus. J Neuroendocrinol 2010;22:534-542.

21 Tamai K, Semenov M, Kato Y, Spokony R, Liu C, Katsuyama Y, Hess F, Saint-Jeannet JP, He X: LDL-receptor-related proteins in Wnt signal transduction. Nature 2000;407:530-535.

22 Morton GJ, Schwartz MW: The NPY/AgRP neuron and energy homeostasis. Int J Obes Relat Metab Disord 2001;25 Suppl 5:S56-S62.

23 Schwartz MW, Woods SC, Porte D, Jr., Seeley RJ, Baskin DG: Central nervous system control of food intake. Nature 2000;404:661-671.

24 van den Hoek AM, Voshol PJ, Karnekamp BN, Buijs RM, Romijn JA, Havekes LM, Pijl H: Intracerebroventricular neuropeptide Y infusion precludes inhibition of glucose and VLDL production by insulin. Diabetes 2004;53:2529-2534.

25 Cerpa W, Godoy JA, Alfaro I, Farias GG, Metcalfe MJ, Fuentealba R, Bonansco C, Inestrosa NC: Wnt-7a modulates the synaptic vesicle cycle and synaptic transmission in hippocampal neurons. J Biol Chem 2008;283:5918-5927.

26 Lyons JP, Mueller UW, Ji H, Everett C, Fang X, Hsieh JC, Barth AM, McCrea PD: Wnt-4 activates the canonical beta-catenin-mediated Wnt pathway and binds Frizzled-6 CRD: functional implications of Wnt/beta-catenin activity in kidney epithelial cells. Exp Cell Res 2004;298:369-387.

27 Jho EH, Zhang T, Domon C, Joo CK, Freund JN, Costantini F: Wnt/beta-catenin/Tcf signaling induces the transcription of Axin2, a negative regulator of the signaling pathway. Mol Cell Biol 2002;22:1172-1183.

28 Tetsu O, McCormick F: Beta-catenin regulates expression of cyclin D1 in colon carcinoma cells. Nature 1999;398:422-426.

29 German JP, Wisse BE, Thaler JP, Matsen ME, Taborsky GJ, Schwartz MW, Morton GJ: Insulin Resistance Induced by Uncontrolled Diabetes Is Mediated by Leptin Deficiency. Diabetes 2010;59:A410.

30 Hedbacker K, Birsoy K, Wysocki RW, Asilmaz E, Ahima RS, Farooqi IS, Friedman JM: Antidiabetic Effects of IGFBP2, a Leptin-Regulated Gene. Cell Metabolism 2010;11:11-22.

31 Li Z, Shen J, Wu WK, Yu X, Liang J, Qiu G, Liu J: Leptin induces cyclin D1 expression and proliferation of human nucleus pulposus cells via JAK/STAT, PI3K/Akt and MEK/ERK pathways. PLoS One 2012;7:e53176.

32 Valerio A, Ghisi V, Dossena M, Tonello C, Giordano A, Frontini A, Ferrario M, Pizzi M, Spano P, Carruba MO, Nisoli E: Leptin increases axonal growth cone size in developing mouse cortical neurons by convergent signals inactivating glycogen synthase kinase-3beta. J Biol Chem 2006;281:12950-12958.

33 Obici S, Feng Z, Karkanias G, Baskin DG, Rossetti L: Decreasing hypothalamic insulin receptors causes hyperphagia and insulin resistance in rats. Nat Neurosci 2002;5:566-572.

34 Obici S, Zhang BB, Karkanias G, Rossetti L: Hypothalamic insulin signaling is required for inhibition of glucose production. Nat Med 2002;8:1376-1382.

35 Gelling RW, Morton GJ, Morrison CD, Niswender KD, Myers MG, Jr., Rhodes CJ, Schwartz MW: Insulin action in the brain contributes to glucose lowering during insulin treatment of diabetes. Cell Metab 2006;3:67-73.

36 Koch L, Wunderlich FT, Seibler J, Konner AC, Hampel B, Irlenbusch S, Brabant G, Kahn CR, Schwenk F, Bruning JC: Central insulin action regulates peripheral glucose and fat metabolism in mice. J Clin Invest 2008;118:2132-2147.

37 Zhou T, Zhou KK, Lee K, Gao G, Lyons TJ, Kowluru R, Ma JX: The role of lipid peroxidation products and oxidative stress in activation of the canonical wingless-type MMTV integration site (WNT) pathway in a rat model of diabetic retinopathy. Diabetologia 2010.

38 Mani A, Radhakrishnan J, Wang H, Mani A, Mani MA, Nelson-Williams C, Carew KS, Mane S, Najmabadi H, Wu D, Lifton RP: LRP6 mutation in a family with early coronary disease and metabolic risk factors. Science 2007;315:1278-1282.

39 Jope RS, Johnson GV: The glamour and gloom of glycogen synthase kinase-3. Trends Biochem Sci 2004;29:95-102.

Figure legends

Figure 1. Genes encoding members of the WNT-pathway are expressed in the hypothalamus
Autoradiographs of wild-type mouse brain sections after *in-situ* hybridization to an antisense ^{35}S-labeled riboprobe binding to genes that are involved in WNT-signalling. Most genes whether encoding a ligand (WNT-4, WNT-7a), an antagonist (DKK-3) to the frizzled receptor, are part of the pathway (Axin-1, Dishevelled, GSK-3β, β-catenin, Frizzled-5, LRP-6 and TCF-7), or are target genes (Axin-2 and Cyclin-D1) are expressed in the ARC of the hypothalamus. Outside of the hypothalamus for some genes hybridization occurred in the hippocampus, cortex and thalamus. Representative for all respective sense riboprobes one image is shown (sense probe for Axin 1). Inserts depict binding of the riboprobes to the ARC. ARC: Arcuate nucleus; DKK-3: Dickkopf-3; GSK-3β: Glycogen synthase kinase 3 beta; LRP: low-density lipoprotein receptor-related protein; TCF-7: T cell specific transcription factor 7.

Figure 2. Differential mRNA regulation of ligands and target genes in the hypothalamic arcuate nucleus of Lep $^{+/+}$- and Lep$^{ob/ob}$ mice
For some genes, two examples of a WNT-receptor agonist [WNT-7a (**a**), WNT-4 (**b**)] and for two target genes of the WNT-pathway [Axin-2 (**c**), Cyclin-D (**d**)], differential gene expression between Lep $^{+/+}$- and Lep$^{ob/ob}$ mice was analyzed. Both, mRNA expression of target genes and agonist were down-regulated in the Lep$^{ob/ob}$ mice compared with the controls. An ip leptin injection (2mg/kg body weight) 2 hours before decapitation restored the decreased target gene expression of Axin-2 (**c**) and Cyclin-D1 (**d**) in Lep$^{ob/ob}$ mice. The upper panels depict autoradiographs of the respective genes whereas in the lower panels a bar graph generated from quantification of the signal in the ARC (5-6 animals in each group) of representative brain sections is shown. Inserts in the upper panels depict binding of the riboprobes to the ARC. ARC: arcuate nucleus; Lep$^{ob/ob}$ mice: leptin deficient mice; ip: intraperitoneal Means ± SEM, *$P \leq 0.05$, **$P \leq 0.01$.

Figure 3. Leptin interacts with the WNT-pathway at the level of the co-receptor LRP-6
a: Immunoreactivity of phospho-LRP-6 positive cells is decreased in the ARC of leptin deficient mice compared with lean wildtype mice. Leptin reversed the reduced number of phospho-LRP-6 (Ser1490) immunoreactive cells in the ARC of Lep$^{ob/ob}$ mice. Mice received either a leptin (2mg/kg) or a vehicle (PBS) ip injection 15 minutes before transcardial perfusion. Inserts depict representative images of phospho-LRP-6 immunoreactivity in the ARC of Lep$^{ob/ob}$ and control mice. A bar graph shows counted cells immunoreactive for phopho-LRP-6 in the ARC of representative sections of each animal (n= 5-6/group).
b: Immunoreactivity of phospho-LRP-6 positive cells decreased after DKK-1 administration. Wild-type mice received icv either DKK-1 (1µg in aCSF) or vehicle (aCSF), 15 minutes before transcardial

perfusion and immunohistochemistry was performed using anti-phospho-LRP-6 (n= 9/group). Phospho-LRP-6 (Ser1490) immunoreactive cells in the ARC decreased after DKK-1 injection (*P*= 0.019). Inserts depict representative images of phospho-LRP-6 immunoreactivity in the ARC. **c:** ICV injection of DKK-1 blocks the glucose lowering effect of leptin. ip GTT (1g glucose/kg) after ICV injection of DKK-1 (1µg in 1µl aCSF) and/or ip injection of leptin (2 mg/kg in PBS, n= 7 each group). 30 minutes after the ICV injection of DKK-1, leptin was injected, 30 min before glucose and blood glucose levels were measured. DKK-1 blocked the leptin effect and $Lep^{ob/ob}$ mice remained glucose intolerant, whereas leptin alone improved glucose tolerance in $Lep^{ob/ob}$ mice compared to the control group (n=7/group, *P*= 0.047).Vehicle/ leptin (black circles); DKK-1/ leptin (grey circles); Vehicle/ vehicle (white circles).

ARC: arcuate nucleus; DKK-1: Dickkopf-1; LRP: low-density lipoprotein receptor-related protein-6; ip: intraperitoneal. Data show means +/- SEM. **P*≤ 0.05, ***P*≤ 0.01.

Figure 4. Leptin activates WNT signalling via GSK-3β inhibition in NPY neurons

Immunoreactivity of phospho-GSK-3β (Ser9) positive cells increases after icv leptin administration. NPY-GFP mice received either leptin (2µg in 1µl aCSF) or vehicle (aCSF) 45 minutes before transcardial perfusion and immunohistochemistry was performed using anti-phospho-GSK-3β (n= 5/group). (**a**)The bar graph shows the counted cells positive for NPY-GFP cells. Leptin administration did not affect NPY staining. (**b**) Phosphorylation of GSK-3β (Ser9) increased after leptin administration. (**c**) The ratio of NPY and GSK-3β (Ser9) positive cells increased after leptin administration. Images show immunoreactive staining of cells, positive for GSK-3β (Ser9, red) in NPY neurons (green) after icv treatment with either vehicle or leptin. NPY: Neuropeptide Y; GFP**:** green fluorescent protein. Data show means +/- SEM. ***P*≤ 0.01.

Figure 5.

The WNT-pathway in the hypothalamus: Model proposing potential interactions of leptin, insulin and WNT-signalling in the hypothalamus.

a: In non diabetic, leptin-sensitive animals leptin activates LRP-6, resulting in inactivation of GSK-3β (This inactivation can also be induced artificially by administration of a GSK-3β inhibitor). Consequently a positive feedback loop might be triggered in which the phosphorylation of inhibitory phosphorylation sites on IRS-1 by GSK-3β is reduced. This modification on IRS-1 might result in activation of the IRS-PI3K pathway by insulin, resulting in increased phospho-AKT. Phospho-AKT in turn might enhance this mechanism by further inactivating GSK-3β.

b: In leptin-deficient mice leptin, no longer activates LRP-6. Enhanced GSK-3β activity will inhibit IRS-1 through phosphorylation on inhibitory sites. This in turn will lead to hypothalamic insulin resistance and subsequently to the development of type-2 diabetes. LepR: leptin receptor, IR: insulin receptor, JAK: Janus kinase, PI3K: phosphoinositide 3-kinase, IRS: insulin receptor substrate

Supplementary Table 1: Oligonucleotides used for cloning of the respective candidate genes for *in-situ* hybridization

Probes	***Primers***	***Oligonucleotides Sequence***	***Fragment Size, bp***	**GenBank Accession No.**
Axin-2	Forward	5´ -AAGCCCGCCACCAAGACCTACATA- 3´	265	158966712
	Reverse	5´ -TCGGCACACGTCCACTCCTCTTCT- 3´		
Axin-1	Forward	5´ -ACCGAAGGGAGATGCAGGAGAGTA- 3´	193	109730206
	Reverse	5´ -ATAGCGGGGTGGGAAATGGTG- 3´		
beta-catenin	Forward	5´ -GCCTGCCATCTGTGCTCTTCGTC- 3´	267	260166638
	Reverse	5´ -TGCGCCGCTGGGTGTC- 3´		
Cyclin-D1	Forward	5´ -GCGTGCAGAAGGAGATTGTG- 3´	230	27924088
	Reverse	5´ -CATTCCCTTGACTGCCGAGA- 3´		
DKK-3	Forward	5 ´-AATGAGACCAGCACGGAGAC- 3´	227	28374187
	Reverse	5´ -ATGGCTGGCAGGTGTACTTG- 3		
Dishevelled	Forward	5´ -GCGGCGGGAGCTGGGACTAC- 3´	223	13929169
	Reverse	5´ -GGTGATGCTGCTGAAGGAGGATGC- 3´		
Frizzled receptor- 5	Forward	5´ -TCCGGGGGCGAATGTCC- 3´	283	111160874
	Reverse	5´ -GATGGGGCGCTCAGGGTAG- 3´		
GSK-3 beta	Forward	5´ -CCGAGGAGAGCCCAATGTTTCA- 3´	219	158508595
	Reverse	5´ -TTTGCTCCCTTGTTGGTGTTCCTA- 3´		
LRP-6	Forward	5´ -GAGCGGCTATGGATGGAAGTG- 3´	297	315075272
	Reverse	5´ -CAAATGGCCCTGGATGATGG- 3´		
TCF-7	Forward	5´ -ATCGCACTCCTCGGCAGACATCA- 3´	265	145386571
	Reverse	5´ -GAAGGAGGGGAGCCAACAGGAGT- 3´		
WNT-4	Forward	5´ -TCCTCGTCTTCGCCGTGTTC- 3´	235	342672048
	Reverse	5´ -AACAGTTCCAGCGCCGGTTC- 3´		
WNT-7a	Forward	5´ -TCGGCTTCGCCAAGGTCTTC- 3´	205	144227223
	Reverse	5´ -CGAGAGCTAGGCTACGTGCT- 3´		

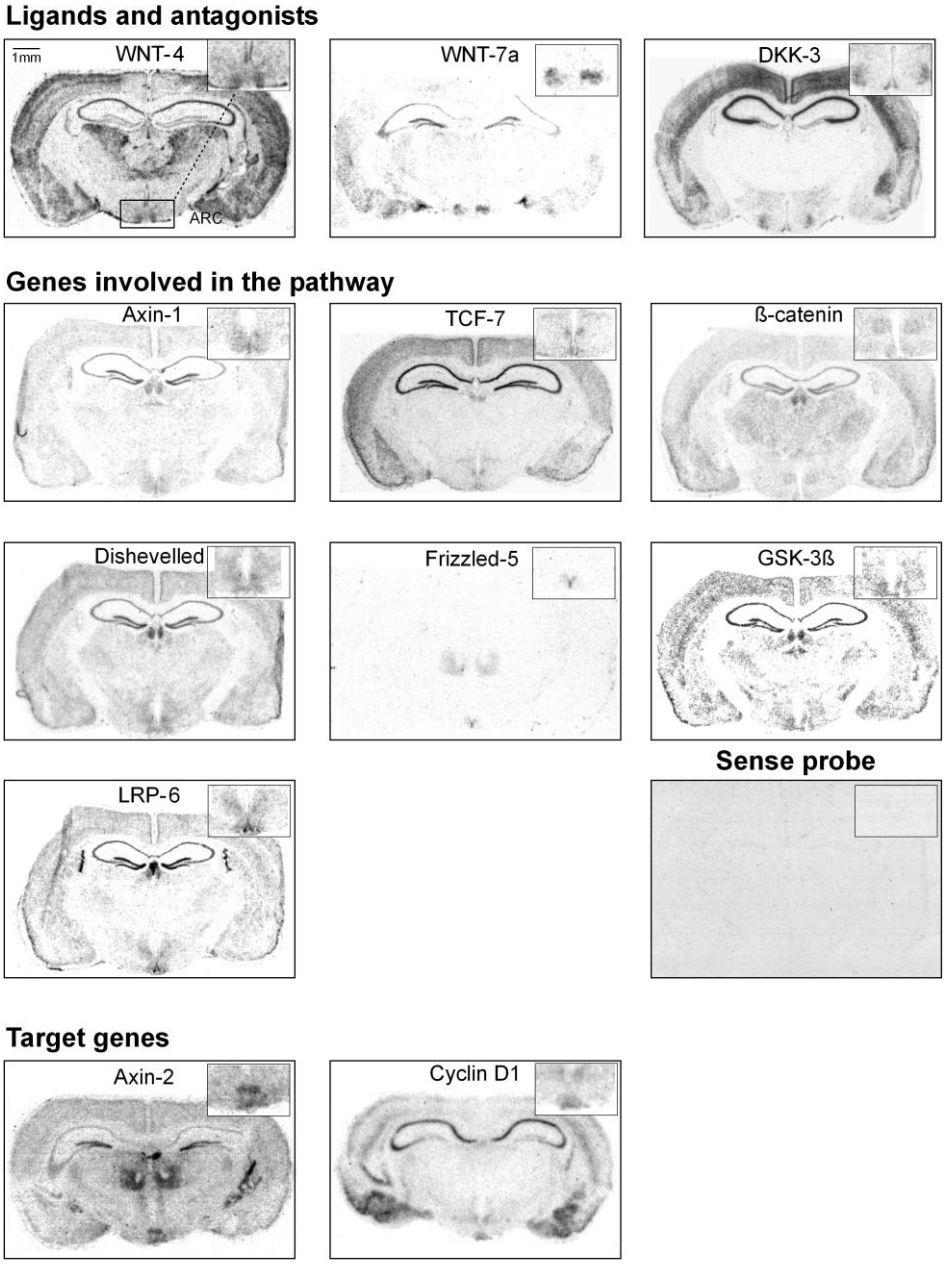
Ligands and antagonists
1mm
WNT-4
ARC
WNT-7a
DKK-3
Genes involved in the pathway
Axin-1
TCF-7
ß-catenin
Dishevelled
Frizzled-5
GSK-3ß
Sense probe
LRP-6
Target genes
Axin-2
Cyclin D1

Fig.1

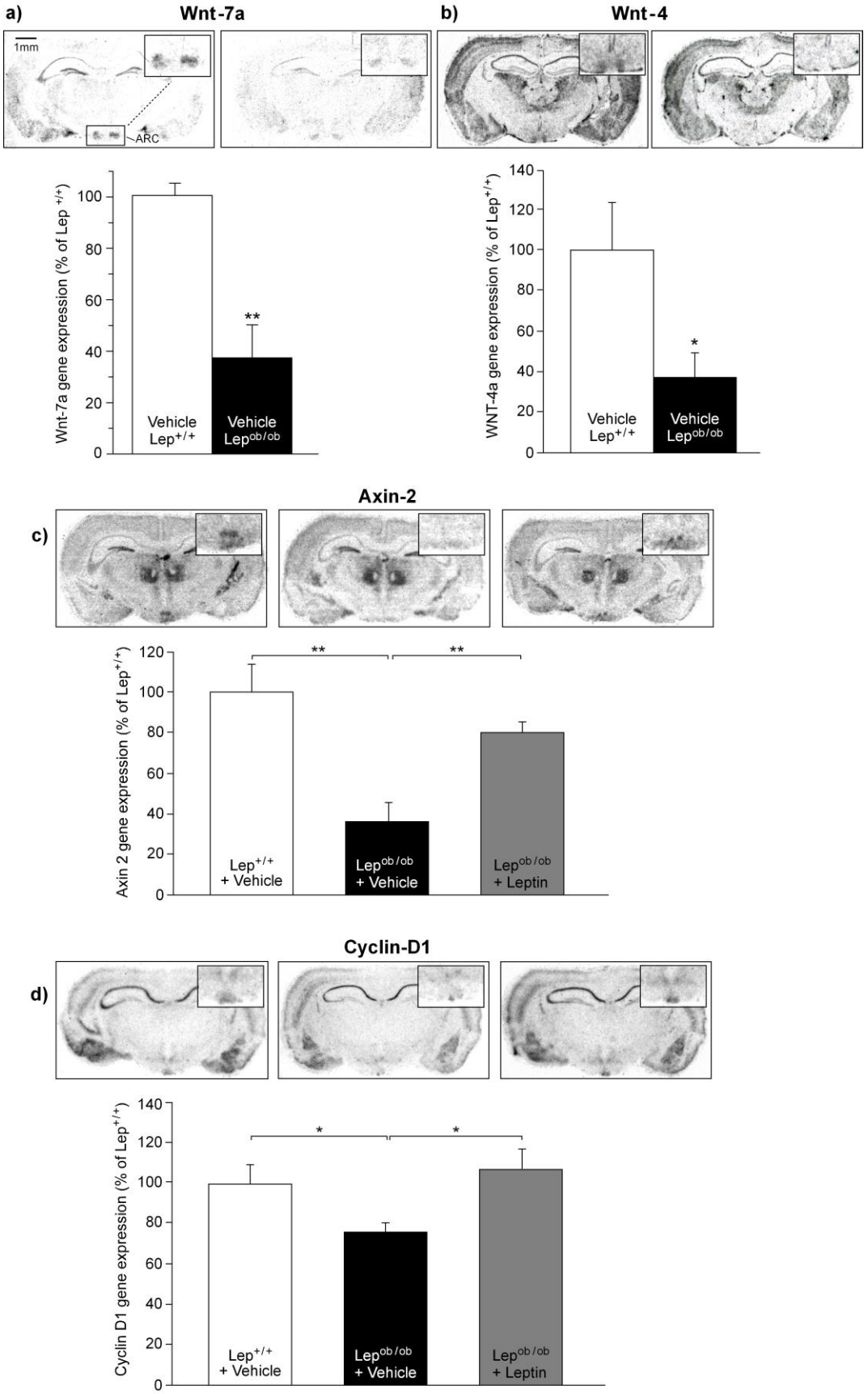
a)
Wnt-7a
1mm
ARC
b)
Wnt-4
Wnt-7a gene expression (% of Lep +/+)
Vehicle Lep+/+
Vehicle Lepob/ob
WNT-4a gene expression (% of Lep+/+)
c)
Axin-2
Axin 2 gene expression (% of Lep+/+)
Lep+/+ + Vehicle
Lepob/ob + Vehicle
Lepob/ob + Leptin
d)
Cyclin-D1
Cyclin D1 gene expression (% of Lep+/+)

Fig.2

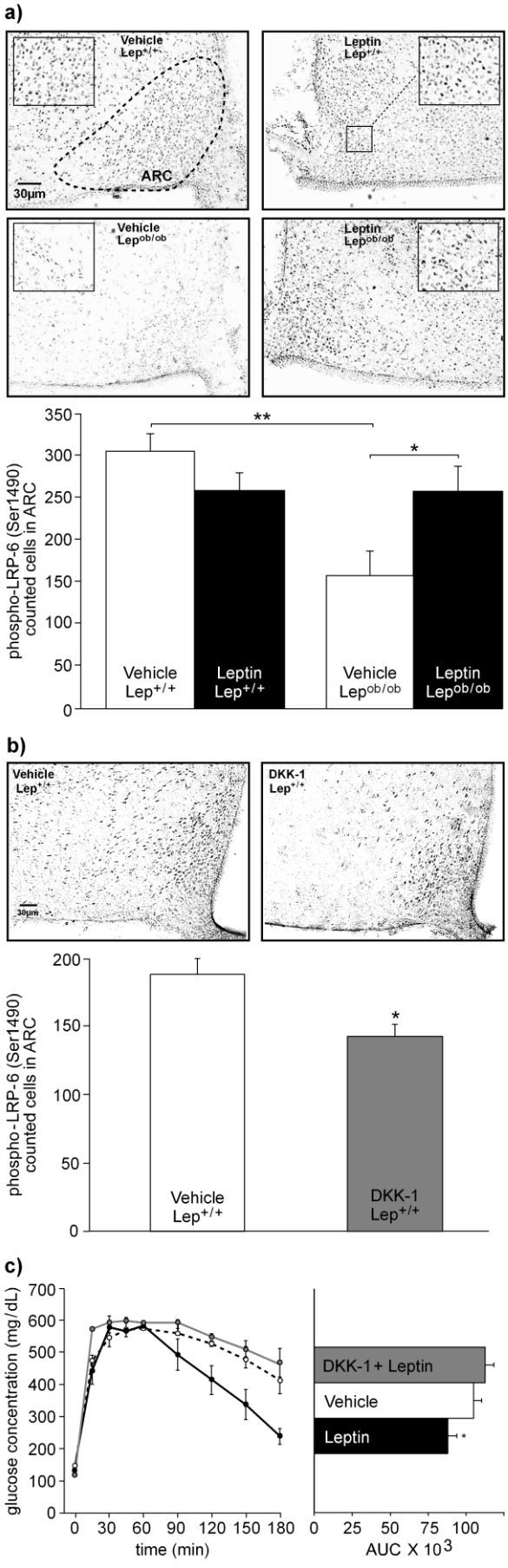
a)
Vehicle Lep+/+
Leptin Lep+/+
ARC
30µm
Vehicle Lepob/ob
Leptin Lepob/ob
phospho-LRP-6 (Ser1490) counted cells in ARC
350
300
250
200
150
100
50
0
**
*
Vehicle Lep+/+
Leptin Lep+/+
Vehicle Lepob/ob
Leptin Lepob/ob
b)
Vehicle Lep+/+
DKK-1 Lep+/+
30µm
phospho-LRP-6 (Ser1490) counted cells in ARC
200
150
100
50
0
*
Vehicle Lep+/+
DKK-1 Lep+/+
c)
glucose concentration (mg/dL)
700
600
500
400
300
200
100
0
0 30 60 90 120 150 180
time (min)
DKK-1 + Leptin
Vehicle
Leptin
*
0 25 50 75 100
AUC X 10 3

Fig.3

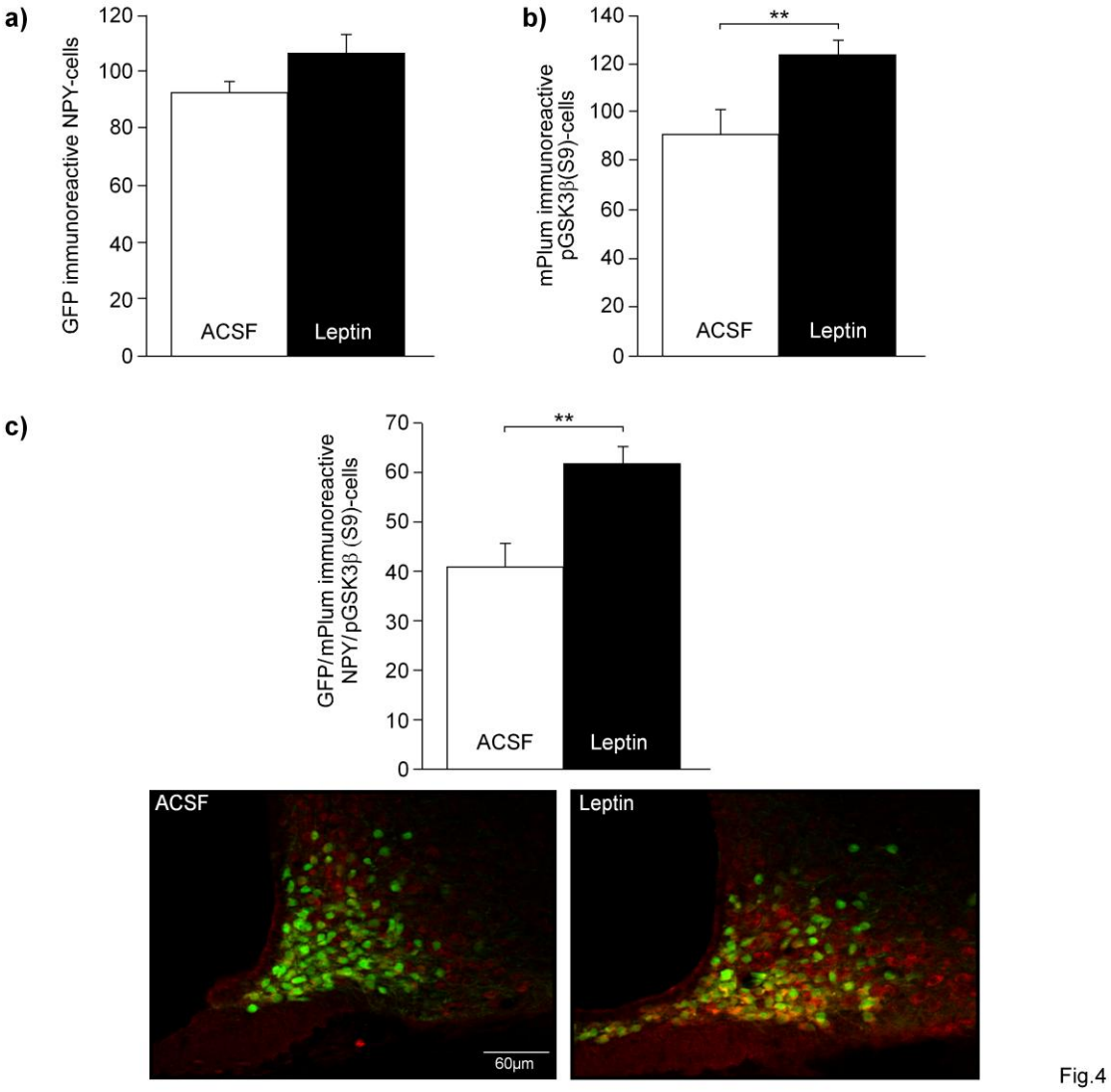
a)
GFP immunoreactive NPY-cells
120
100
80
60
40
20
0
ACSF
Leptin
b)
mPlum immunoreactive pGSK3β(S9)-cells
140
120
100
80
60
40
20
0
**
ACSF
Leptin
c)
GFP/mPlum immunoreactive NPY/pGSK3β (S9)-cells
70
60
50
40
30
20
10
0
**
ACSF
Leptin
ACSF
Leptin
60µm

Fig.4

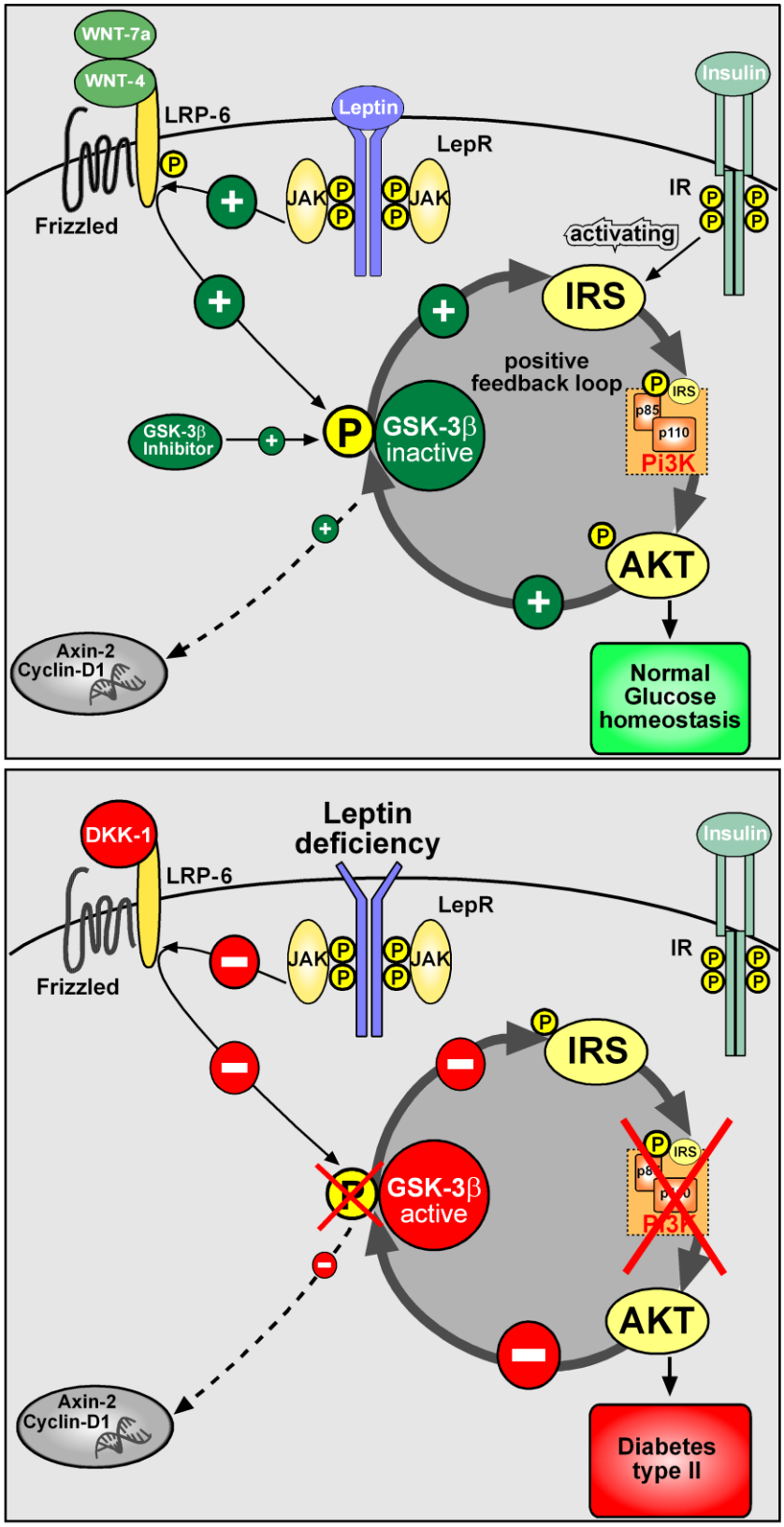
WNT-7a
WNT-4
LRP-6
Frizzled
Leptin
LepR
JAK
JAK
Insulin
IR
activating
IRS
positive
feedback loop
IRS
p85
p110
Pi3K
GSK-3β
Inhibitor
GSK-3β
inactive
AKT
Axin-2
Cyclin-D1
Normal
Glucose
homeostasis
DKK-1
Leptin
deficiency
LRP-6
Frizzled
LepR
JAK
JAK
Insulin
IR
IRS
GSK-3β
active
AKT
Axin-2
Cyclin-D1
Diabetes
type II

Fig.5

BJ Metabolism

Biochem. J. (2012) **447**, 175–184 (Printed in Great Britain) doi:10.1042/BJ20120834

ACCELERATED PUBLICATION

Hypothalamic glycogen synthase kinase 3β has a central role in the regulation of food intake and glucose metabolism

Jonas BENZLER*[1], Goutham K. GANJAM*[1], Manon KRÜGER*, Olaf PINKENBURG†, Maria KUTSCHKE‡, Sigrid STÖHR*, Juliane STEGER*, Christiane E. KOCH*, Rebecca ÖLKRUG*, Michael W. SCHWARTZ§, Peter R. SHEPHERD‖, David R. GRATTAN¶ and Alexander TUPS*[2]

*Department of Animal Physiology, Faculty of Biology, Philipps University Marburg, Marburg, Germany, †Department of Immunology, Faculty of Medicine, Philipps University Marburg, Marburg, Germany, ‡Institute for Diabetes and Obesity, Helmholtz Centre, Munich, Germany, §Diabetes and Obesity Center of Excellence, Department of Medicine, University of Washington, Seattle, WA, U.S.A., ‖Maurice Wilkins Centre for Molecular Biodiscovery and Department of Molecular Medicine and Pathology, University of Auckland, Auckland, New Zealand, and ¶Centre for Neuroendocrinology and Department of Anatomy and Structural Biology, University of Otago, Dunedin, New Zealand

GSK3β (glycogen synthase kinase 3β) is a ubiquitous kinase that plays a key role in multiple intracellular signalling pathways, and increased GSK3β activity is implicated in disorders ranging from cancer to Alzheimer's disease. In the present study, we provide the first evidence of increased hypothalamic signalling via GSK3β in leptin-deficient Lep$^{ob/ob}$ mice and show that intracerebroventricular injection of a GSK3β inhibitor acutely improves glucose tolerance in these mice. The beneficial effect of the GSK3β inhibitor was dependent on hypothalamic signalling via PI3K (phosphoinositide 3-kinase), a key intracellular mediator of both leptin and insulin action. Conversely, neuron-specific overexpression of GSK3β in the mediobasal hypothalamus exacerbated the hyperphagia, obesity and impairment of glucose tolerance induced by a high-fat diet, while having little effect in controls fed standard chow. These results demonstrate that increased hypothalamic GSK3β signalling contributes to deleterious effects of leptin deficiency and exacerbates high-fat diet-induced weight gain and glucose intolerance.

Key words: adeno-associated virus, arcuate nucleus, Dickkopf 1, food intake, high-fat diet, obesity, synapsin, Type II diabetes.

INTRODUCTION

Type II diabetes affects more than 165 million individuals and is increasing at an alarming rate [1]. Although a large number of papers has implicated the brain as a critical target for insulin regulation of systemic glucose metabolism [2–7], mechanisms underlying such insulin effects remain incompletely understood. Even less is known about the importance of altered neuronal insulin signalling in the pathogenesis of Type II diabetes. Studies focused on hypothalamic insulin signal transduction via the IRS (insulin receptor substrate)–PI3K (phosphoinositide 3-kinase) pathway suggest that it plays a critical role in CNS (central nervous system) regulation of peripheral glucose homoeostasis [5,8,9]. Leptin action in the brain similarly depends on intact IRS–PI3K signalling [9–11], but key neuronal mediators downstream of this pathway remain to be identified.

GSK3β (glycogen synthase kinase 3β) is a serine-threonine kinase that is phosphorylated and inhibited by protein kinase B (AKT) [12], a principal target of PI3K signalling. In addition to inhibiting cellular responses to insulin (for example, inhibition of GSK3β is required for insulin stimulation of glycogen synthesis), this enzyme also influences cell division, growth and development [13] as an endogenous inhibitor of canonical WNT signalling. The finding that systemic inhibition of GSK3β improves whole-body glucose homoeostasis [14-16] implies that GSK3β exerts a tonic inhibitory effect on glucose metabolism, but neither the mechanism(s) nor the specific tissue(s) involved in this effect are known. Some evidence points to GSK3β in skeletal muscle as a mediator of impaired glucose metabolism in diabetic mouse models [17,18], but activities of both AKT and GSK3β are also regulated in mouse brain in response to physiological changes of glucose [19]. In the present study we investigated whether an action in the brain might explain the deleterious effects of GSK3β signalling on peripheral glucose homoeostasis.

MATERIALS AND METHODS

Animals

All experiments used male mice that were purchased from Janvier. The animals were between 2- and 4-months-old and housed individually under standard conditions with a light/dark cycle of 12 h. All procedures were performed in accordance with the guidelines of the German Council of Animal Care. The ambient temperature for mice was 26 °C. Apart from the dark phase before the experiments, all animals had access to standard rodent diet, low-fat diet or HFD (high-fat diet) (containing 45 % fat) and water *ad libitum*. For the central administration of drugs, cannulae were

Abbreviations used: AAV, adeno-associated virus; aCSF, artificial cerebral spinal fluid; ARC, arcuate nucleus; CNS, central nervous system; DEXA, dual-emission X-ray absorptiometry; DKK-1, dickkopf 1; EGFP, enhanced green fluorescent protein; GSK3β, glycogen synthase kinase 3β; HA, haemagglutinin; HEK, human embryonic kidney; HFD, high-fat diet; ICV, intracerebroventricular; ipGTT, intraperitoneal glucose tolerance test; IRS, insulin receptor substrate; PEPCK, phosphoenolpyruvate carboxykinase 2; PI3K, phosphoinositide 3-kinase; SOCS-3, suppressor of cytokine signalling 3; WPRE, WHV (Woodchuck hepatitis virus) post-transcriptional regulatory element.

[1] These authors contributed equally to this work.
[2] To whom correspondence should be addressed (email alexander.tups@staff.uni-marburg.de).

stereotaxically implanted into the left lateral ventricle as described previously [9].

In situ hybridization

To determine the central expression of DKK-1 (dickkopf 1 homologue) and SOCS-3 (suppressor of cytokine signalling 3) we performed *in situ* hybridization on coronal brain sections. As previously described [20], forebrain sections (16 μm) were collected throughout the extent of the ARC (arcuate nucleus) on to a set of twelve slides, with twelve sections mounted on each slide. Accordingly, the slides spanned the hypothalamic region approximating from -2.8 to -1.22 mm relative to Bregma according to the atlas of the mouse brain [21]. *In situ* hybridizations and analysis was performed as described previously [20].

Glucose tolerance tests

We determined whether activation of GSK3β might impair glucose tolerance in lean mice. Therefore the WNT antagonist DKK-1 [1 μg in 1 μl of aCSF (artificial cerebral spinal fluid); R&D Systems, 5897-DK/CF] was administered ICV (intracerebroventricular) to one group ($n = 4$) of $Lep^{+/+}$ mice, whereas a second group ($n = 6$) received an ICV vehicle injection (aCSF). At 15 min later an ipGTT (intraperitoneal glucose tolerance test; 1 g of glucose/kg of body mass) was performed. To determine the blood glucose levels, the vena facialis was punctured and the glucose concentration was measured using a commercially available glucometer (Accu-Check Performa, Roche).

We next determined whether inhibition of GSK3β might improve glucose homoeostasis. Therefore the mice received a specifically designed inhibitor for GSK3β (AR-A014418, Calbiochem). To test whether central GSK3β inhibition affects hypothalamic PI3K, four groups of $Lep^{ob/ob}$ mice received two ICV injections (0.5 μl each), 30 min apart. The first group received vehicle (5 % DMSO/aCSF) followed by GSK3β inhibitor (0.5 nmol in 5 % DMSO/aCSF). The second group received isoform-specific PI3K inhibitors (0.1 nmol in 5 % DMSO/aCSF, PIK-75/TGX-221), since both isoforms are required for insulin signalling in the hypothalamus [22], followed by vehicle (5 % DMSO/aCSF). A third group received isoform-specific PI3K inhibitors, followed by GSK3β inhibitor, and the last group received two vehicle injections ($n = 4$–7). At 15 min after the second injection, an ipGTT was performed (1 g of glucose/kg of body mass) as described above.

To measure glucose tolerance after virus administration we performed two ipGTTs. The first one was performed on day 58 on chow diet (1 g of glucose/kg of body mass), whereas the second ipGTT was conducted at day 18 of the HFD (0.75 g of glucose/kg of body mass) as described above.

Food intake experiment

To test whether inhibition of central GSK3β affects food intake, we administered a GSK3β inhibitor (AR-A014418, Calbiochem) ICV in a separate group of 8-week-old $Lep^{ob/ob}$ mice. The mice were fasted for 16 h and weight matched. Mice received either a GSK3β inhibitor (0.5 nmol in 0.5 μl of aCSF/5 % DMSO) or vehicle injection (aCSF/5 % DMSO) 1 h before the beginning of the dark phase. Food intake was measured at 4 h and 24 h after administration ($n = 8$/group).

Immunohistochemistry

First we investigated the phosphorylation of GSK3β (Ser^{9}, catalogue number 9323) in the ARC of 8-week-old wild-type mice fed a HFD (containing 45 % fat) for 3 weeks. In addition, we also compared phosphorylation of GSK3β (Ser^{9}) in wild-type and $Lep^{ob/ob}$ mice. To do this the animals were fasted for 16 h and transcardial perfusion was performed. To determine any possible cross-talk between GSK3β and the IRS–PI3K pathway, we measured the effect of ICV GSK3β inhibitor on IRS-1 phosphorylation (Ser^{612}) and phospho-AKT (Ser^{473}) in the hypothalamic ARC. Accordingly, $Lep^{ob/ob}$ mice ($n = 10$/group) received either GSK3β inhibitor (AR-A014418, 0.5 nmol in 0.5 μl aCSF/5 % DMSO) or vehicle (aCSF/5 % DMSO) ICV 15 min before transcardial perfusion. Immunohistochemistry was performed using anti-(phospho-IRS-1 Ser^{612}) (catalogue number 3203) and anti-(phospho-AKT Ser^{473}) antibodies (catalogue number 4058). Immunohistochemistry was carried out on mouse brain coronal cryosections as described previously [9,22]. All antibodies were purchased from Cell Signaling Technology.

Recombinant adeno-associated viral vector generation and virus production

The human cDNA for *GSK3β* was subcloned from the eukaryotic expression vector pcDNA3-GSK3β HA (Addgene, 14753) into an AAV2-hSyn-EGFP-WPRE vector [23]. *GSK3β* cDNA along with an HA (haemagglutinin) tag coding sequence was amplified from the pcDNA3-GSK3β-HA plasmid by PCR (phusion DNA polymerase) using the forward, 5′-GCTAGCTAATACGACTCACTATAGG-3′ and reverse, 5′-TGTACACAATTTAGGTGACACTATCG-3′ primers. These primers contain suitable Nhe1 and BsrG1 restriction sites for cloning into the AAV (adeno-associated virus) construct. Amplified PCR product was first cloned into the pGemT easy cloning vector. The *GSK3β* cDNA fragment from pGemT easy vector was subcloned into Nhe1 and BsrG1 sites of AAV2-hSyn-EGFP-WPRE by replacing EGFP (enhanced green fluorescent protein) cDNA to obtain AAV2-hSyn-GSK3β-HA-WPRE. In this vector system the expression of GSK3β is under the control of the human synapsin-1 promoter to restrict the expression to neurons and WPRE [WHV (Woodchuck hepatitis virus) post-transcriptional regulatory element] facilitates long-term expression of the transgene. All molecular cloning procedures were performed in SURE2 bacterial cells to minimize the recombination events.

Recombinant AAV vectors of serotype 2 were produced by transfecting AAV *cis* plasmids encoding the gene of interest and a viral helper plasmid pDG [24] encoding *rep-2* (replication protein 2) and *cap-2* (capsid protein 2) genes into HEK (human embryonic kidney)-293 cells. Total cell lysates were collected after 48 h of transfection in AAV lysis buffer (50 mM Hepes with 150 mM NaCl, pH 7.6) by repeated freezing in liquid nitrogen and thawing at 37 °C. The cell lysates were cleared by centrifugation for 15 min at 4600 ***g*** at 4 °C to remove the cell debris. Unencapsulated nucleic acids were degraded by treating the cleared cell lysates with 250 units of benzonase (Sigma) for 90 min at 37 °C. AAV particles were purified in three step CsCl density gradient ultracentrifugation (rotor type SW41 at 15 °C), desalting and concentration by Amicon® Ultra Centrifugal filters (30 K MWCO UFC903008). The viral genome isolated by the Qiagen mini prep plasmid isolation kit was titrated by quantitative real-time PCR using the forward, 5′-CCTCAATCCAGCGGACCTTC-3′ and reverse, 5′-ACAGTGGGAGTGGCACCTTC-3′ primers.

Protein expression verification in primary cortical neuronal cells

Freshly isolated primary rat cortical neurons were plated at a density of 0.3 million cells on polyethyleneimine pre-coated plates and cultured in MEM$^{\oplus}$ medium as described previously [25]. After 4 h the cells were replenished with neurobasal medium [25] and were infected with 10^{10} vector genomes of purified AAV particles for 5 days. Total protein lysate (20 μg) from the cortical cells was used to verify the expression of GSK3β by Western blotting with an anti-HA tag antibody (catalogue number 2367, Cell Signaling Technology). The same cell lysates were used to analyse the phosphorylation of Tau protein with an anti-(phospho-Tau Ser^{396}) antibody (catalogue number 9632, Cell Signaling Technology) and total Tau with an anti-Tau antibody (catalogue number 4019, Cell Signaling Technology). The expression of EGFP control virus was verified by fluorescence light microscopy. To prove that the expression of human synapsin promoter controlled GSK3β is limited to neurons, we infected HEK-293 cells with 10^{10} vector genomes of EGFP and GSK3β viral particles. As a positive control we transfected HEK-293 cells with 5 μg of pcDNA3-GSK3β-HA plasmid [26]. After 3 days the total cell lysates were collected as described previously [27]. Total cell lysates (20 μg) were Western blotted with an anti-HA tag antibody.

Stereotaxic injections

Intracerebral injections were performed under isoflurane anaesthesia as described previously [9]. Stereotaxic co-ordinates to reach the ARC of hypothalamus are 1.5 mm posterior, $\pm$0.3 mm lateral and 6.1 mm ventral relative to Bregma. AAV2 particles, containing 4×10^{10} vector genomes, were injected into the ARC using a 0.5 μl Hamilton glass syringe for 2 min. The injection needle remained in place at each injection site for an additional 5 min to allow for diffusion and prevent backflow. The incision was sutured and the animals were placed under a heating lamp to recover from the surgery.

Body composition

To analyse their body composition, mice were anaesthetized with isoflurane (CP-Pharma) and were analysed via DEXA (dual-emission X-ray absorptiometry)-scan (Lunar PIXImus Densitometer; GE Medical Systems).

Metabolic measurement

We measured the effect on metabolic rate of regular chow and the HFD. Accordingly, carbon dioxide production (VCO_2) and oxygen consumption (VO_2) were measured in metabolic cages ($\sim$5 l vol.). Measurements were taken continuously for 2 days with a constant ambient temperature of 23 °C. The air flow in the cage was adjusted to $\sim$42 l/h and continuously monitored. The procedure has been described in detail previously [28].

Plasma insulin levels

We investigated whether blood insulin levels were affected by GSK3β overexpression. Accordingly, blood was collected by decapitation and plasma insulin was measured via a Rat/Mouse insulin ELISA kit (Millipore EZRMI-13K) according to the manufacturer's instructions.

Central inhibition of GSK3β decreased hepatic glucose production

To test whether inhibition of GSK3β in the brain affects gluconeogenesis, we performed pyruvate tolerance tests. Lep$^{ob/ob}$ mice received a single ICV injection of either GSK3β inhibitor (AR-A014418, Calbiochem, 0.5 nmol in 0.5 μl of aCSF/5 % DMSO, $n=5$) or vehicle (0.5 μl of aCSF/5 % DMSO, $n=11$). At 60 min before pyruvate was administered, blood glucose levels were measured as described above. To analyse the protein level of PEPCK (phosphoenolpyruvate carboxykinase 2) in the liver, three groups of Lep$^{ob/ob}$ mice ($n=4$–5/group) underwent the treatment regimen shown above with the exception that livers were removed 90 min after ICV treatment. Immunoblotting with 5 μg of total liver protein lysate was performed as described elsewhere [27] and normalized to β-actin.

Statistics

The data were analysed by one- or two-way ANOVA followed by a Holm–Sidak comparison test, as appropriate, using SigmaStat statistical software (Jandel). Where the data failed equal variance or normality tests, they were analysed by one-way ANOVA on ranks followed by Dunn's multiple comparison test. The results are presented as means $\pm$ S.E.M. and differences were considered significant if $P<0.05$.

RESULTS AND DISCUSSION

As a first step, we investigated whether activity of GSK3β is increased in the ARC, a key brain region for neuronal control of energy and glucose homoeostasis, during diet-induced obesity and leptin deficiency. It has been comprehensively established that activity of GSK3β is mediated via phosphorylation at Ser^9, a post-translational modification that is critical to inactivate the enzyme [12,29–32]. Furthermore, intact insulin signalling appears to involve inhibition of GSK3β phosphorylation at Ser^9 in the muscle [12,33]. Using an antibody specific against Ser^9 phosphorylation, we found that the number of phospho-GSK3β immunoreactive cells in this brain area was reduced in both models of impaired glucose homoeostasis (mice fed an HFD and Lep$^{ob/ob}$ mice) compared with their respective controls, suggesting that local GSK3β activity is increased in these animals (Figures 1a and 1b, $n=5$–6/group, $P=0.007$ and $P=0.026$ respectively). For a proof of concept, in extremely glucose intolerant Lep$^{ob/ob}$ mice we investigated whether central inhibition of GSK3β affects glucose homoeostasis. Consistent with this hypothesis, glucose tolerance in these animals was markedly improved following a single ICV injection of a GSK3β inhibitor (AR-A014418) relative to the ICV vehicle (Figure 1c, $n=4$–7/group, $P=0.016$). This effect cannot be attributed to changes of food intake or energy balance, since ICV injections were performed 15 min before ipGTT and the animals were not provided food during this time.

Since central insulin action is required for whole-body glucose homoeostasis [2–4,8,9,34] via a hypothalamic mechanism involving signal transduction via the PI3K pathway, we next asked whether pharmacological inhibition of central GSK3β restores impaired PI3K signalling in the ARC of Lep$^{ob/ob}$ mice. This was accomplished by histochemical analysis of the effect of ICV administration of a GSK3β inhibitor (AR-A014418) on the phosphorylation of IRS-1 (Ser^{612}) and AKT (Ser^{473}) in the ARC of Lep$^{ob/ob}$ mice. These markers were selected because serine phosphorylation of IRS-1 impairs signalling via PI3K, whereas phospho-AKT (Ser^{473}) is a marker of PI3K activation [9]. Following ICV injection, the GSK3β inhibitor acutely (within 15 min) decreased the number of phospho-IRS-1 (Ser^{612}) immunoreactive cells within the ARC of Lep$^{ob/ob}$ mice by

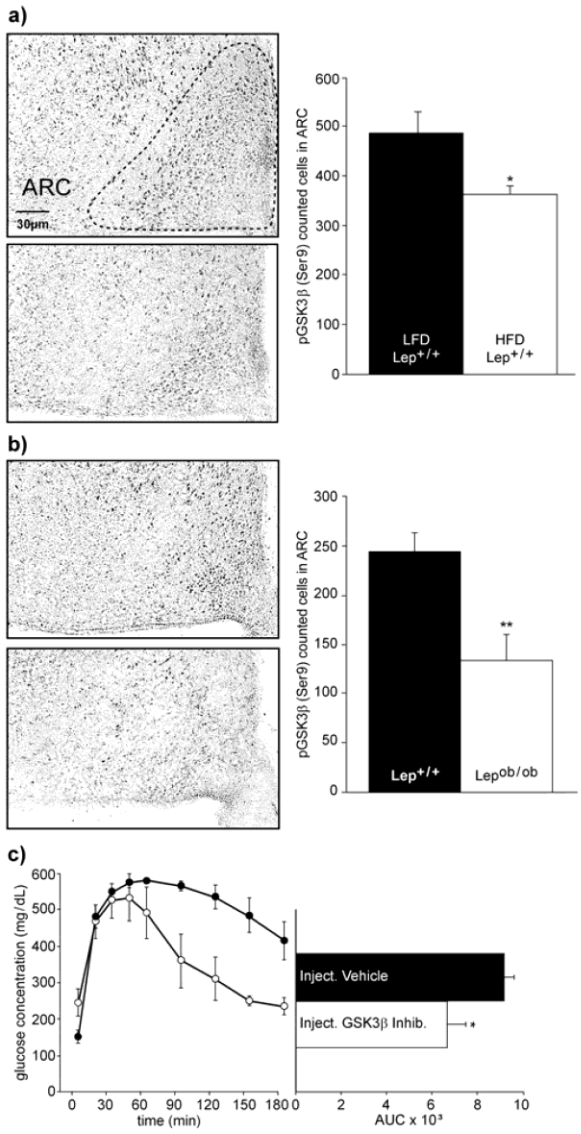

Figure 1 Phospho-GSK3β in the ARC during obesity and pharmacological inhibition of this enzyme

(**a**) Immunohistochemistry was performed on brain sections of mice fed an HFD compared with low-fat diet (LFD) mice. Inserts depict representative images of phospho-GSK3β (Ser^9) immunoreactivity in the ARC (phosphorylation at Ser^9 inactivates the enzyme). The histogram shows the counted phospho-GSK3β (Ser^9) cells in the ARC ($n = 5$–6/ group). (**b**) The same experiment, mentioned above, was performed on brain sections of wild-type and $Lep^{ob/ob}$ mice. The histogram shows the counted phospho-GSK3β (Ser^9) cells in the ARC ($n = 5$–6/ group). (**c**) A central injection of a GSK3β inhibitor improves glucose tolerance in $Lep^{ob/ob}$ mice. ipGTT was performed 15 min after administration of GSK3β inhibitor (○) or vehicle (●) into the lateral ventricle ($n = 4$–7 each group). Results are means ± S.E.M., $^*P \leqslant 0.05$ and $^{**}P \leqslant 0.01$. AUC, area under curve.

~20 % relative to vehicle-treated mice (Figure 2a, $P = 0.028$, $n = 10$/group), while increasing the number of phospho-AKT (Ser^{473}) immunoreactive cells in the ARC by ~3-fold, compared with the ICV vehicle (Figure 2b, $P \leqslant 0.001$, $n = 10$/group). Thus the glucose-lowering effects of central GSK3β are associated with increased hypothalamic IRS–PI3K signalling.

To determine whether the beneficial effect of central GSK3β inhibition depends on intact PI3K signalling, we determined if its effect on glucose tolerance is blocked by pharmacological inhibition of PI3K. Animals received an ICV injection of selective inhibitors of the PI3K catalytic subunits, p110α and p110β (PIK75 and TGX221) [22] with and without the GSK3β inhibitor, which was given 30 min later, followed by an ipGTT. Our findings that the metabolic improvement induced by the GSK3β inhibitor was fully blocked by co-administration of the PI3K p110α- and β-selective inhibitors (Figure 2c, $n = 4$–7/group) implicate increased PI3K signalling as a mediator of this beneficial effect.

We next investigated the effects of central inhibition of GSK3β on food intake in $Lep^{ob/ob}$ mice. Relative to the vehicle, ICV injection of the GSK3β inhibitor 30 min before the beginning of the dark phase induced a modest, but significant, reduction of 24 h food intake in these animals (− 15 % compared with the vehicle, $n = 8$/group, $P = 0.032$) (Figure 2d). These observations are consistent with published evidence that leptin administration increases hypothalamic IRS–PI3K signalling, and that leptin's ability to reduce food intake is prevented by central blockade of PI3K [10].

The above data collectively suggest that GSK3β is overactive in the hypothalamus of leptin-deficient mice, contributing to the diabetic state of these animals. Given the known role of the WNT pathway to inactivate GSK3β, we next investigated whether expression of DKK-1, a potent antagonist of the WNT pathway that activates GSK3β in neurons [35], might be up-regulated in the ARC of diabetic $Lep^{ob/ob}$ mice. As predicted, *DKK1* mRNA, as measured by *in situ* hybridization using an antisense riboprobe specific for DKK-1, was increased 3-fold in the ARC of diabetic $Lep^{ob/ob}$ mice (Figure 2e, $P = 0.008$) compared with wild-type controls. This observation suggests that increased hypothalamic GSK3β activity may be a consequence of increased DKK-1 in these animals. If this hypothesis is correct, interventions that increase neuronal DKK-1 signalling in normal animals should impair glucose homoeostasis. To test this hypothesis, we administered DKK-1 as an acute ICV injection to wild-type mice 15 min before an ipGTT was performed. Remarkably, the marked impairment of glucose homoeostasis induced by ICV injection of DKK-1 ($n = 4$–6, $P < 0.001$ compared with the controls) was comparable with that observed in $Lep^{ob/ob}$ mice (Figure 2f). On the basis of these findings, we infer that hypothalamic GSK3β activity in leptin-deficient mice: (i) arises at least in part from increased DKK-1 signalling and (ii) contributes to their impaired glucose metabolism. Further, metabolic benefit arising from reduced hypothalamic GSK3β action depends upon intact hypothalamic PI3K signalling, and increased brain signalling via either DKK-1 or GSK3β impairs systemic glucose homoeostasis.

As local inhibition of GSK3β in the brain improved glucose homoeostasis, the neuroanatomical identity of the underlying phenomenon remained limited due to ICV administration of the GSK3β inhibitor. Therefore we generated a viral construct enabling neuron-specific overexpression of functional GSK3β in the ARC, a key brain region for neuronal control of energy and glucose homoeostasis. This approach furthermore enables GSK3β overexpression in adult healthy mice, thereby circumventing potential defects in embryogenesis due to the ontogenic capacity of this enzyme. This was accomplished by cloning human *GSK3β* cDNA into the AAV2 vector. In contrast with adenoviruses, AAV2s do not cause adverse local immune responses and they have a higher transfection rate in the brain than lentiviruses [36,37]. To direct GSK3β expression selectively to neurons, transcription was directed by the human synapsin-1 promoter (Figure 3a). The ability of AAV2 vectors to drive selective neuronal expression of a transgene was

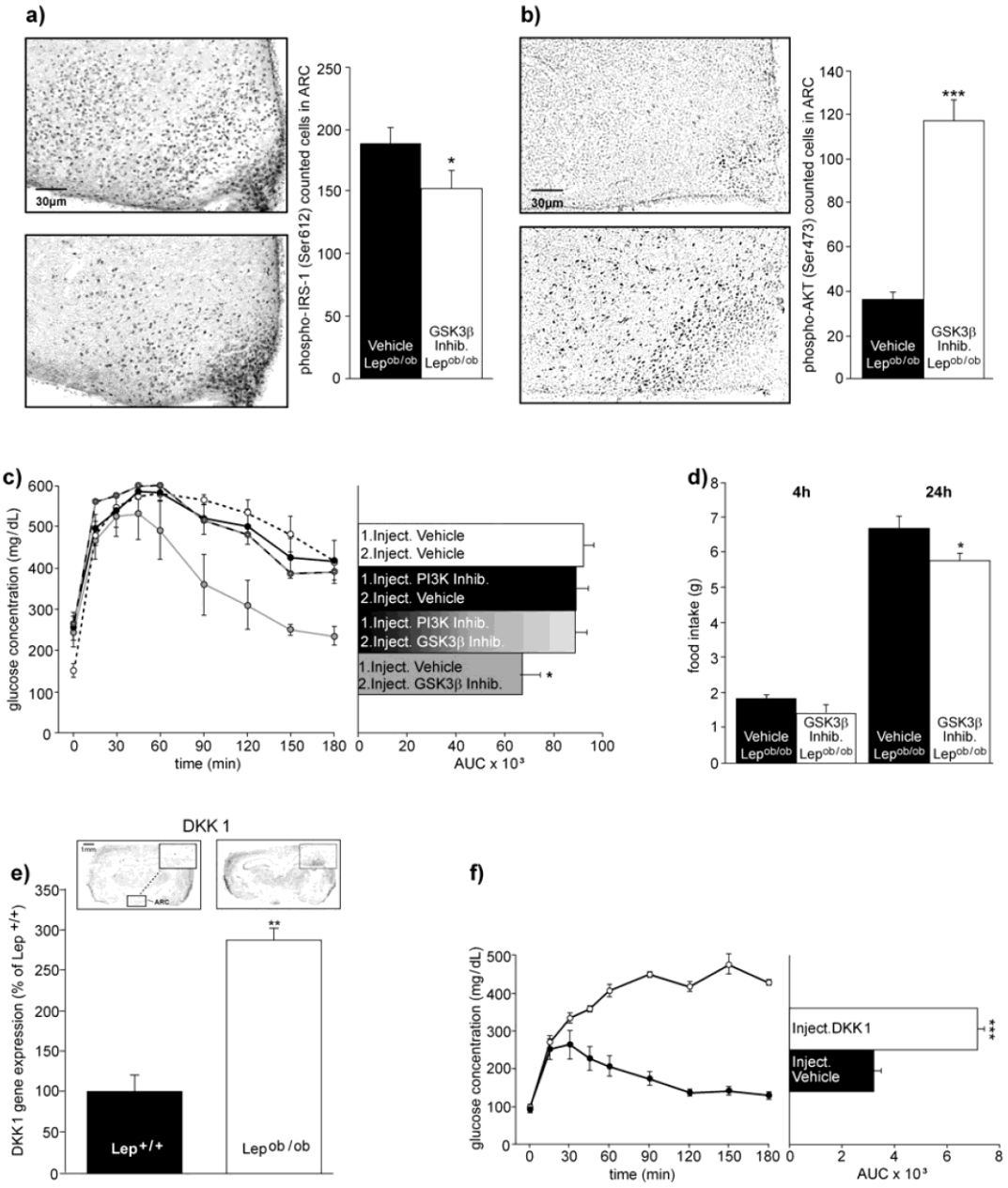

Figure 2 Pharmacological manipulation of GSK3β in the brain: effects on food intake and interaction with hypothalamic insulin signalling

(**a**) Immunohistochemistry was performed on brain sections of $Lep^{ob/ob}$ mice after central administration of a GSK3β inhibitor (Inhib.) or vehicle, 15 min before transcardial perfusion. Images are representative of phospho-IRS-1 (Ser^{612}) immunoreactivity in the ARC. The histogram shows the counted cells in the ARC that were immunoreactive for phospho-IRS-1 and were down-regulated after ICV injection of the GSK3β inhibitor ($n = 10$/group). (**b**) An additional set of brain sections of the experiment presented in (**e**) was analysed for phospho-AKT (Ser^{473}) immunoreactive cells in the ARC. The number of phospho-AKT (Ser^{473}) immunoreactive cells was increased after ICV injection of the GSK3β inhibitor. (**c**) Central improvement of glucose homoeostasis by the GSK3β inhibitor in $Lep^{ob/ob}$ mice was blocked by pre-treatment with isoform-specific PI3K inhibitors. The PI3K-inhibitor was injected ICV 30 min before GSK3β inhibitor injection (ICV) ($n = 4$–7 each group). (**d**) A single central injection of a GSK3β inhibitor decreased food intake in $Lep^{ob/ob}$ mice within 24 h by approximately 15 %. $Lep^{ob/ob}$ mice received a GSK3β inhibitor or vehicle injection ($n = 8$ each group) into the lateral ventricle and food intake was analysed after 4 h and 24 h. (**e**) Autoradiographs of mouse brain sections after *in situ* hybridization to an antisense ^{35}S-labelled riboprobe binding to the WNT antagonist DKK-1. Within the ARC gene expression was up-regulated in $Lep^{ob/ob}$ mice compared with the $Lep^{+/+}$ mice. The upper panels depict autoradiographs of the respective genes, whereas the lower panels show a histogram generated from quantification of the signal in the ARC ($n = 5$–6 animals in each group). (**f**) ICV administration of DKK-1 protein impairs glucose tolerance in wild-type mice ($Lep^{+/+}$ mice). DKK-1 protein (○, $n = 4$) or aCSF (●, $n = 6$) was administered 15 min before the ipGTT. Results are means ± S.E.M., $^{*}P \leqslant 0.05$, $^{**}P \leqslant 0.01$ and $^{***}P \leqslant 0.001$. AUC, area under curve.

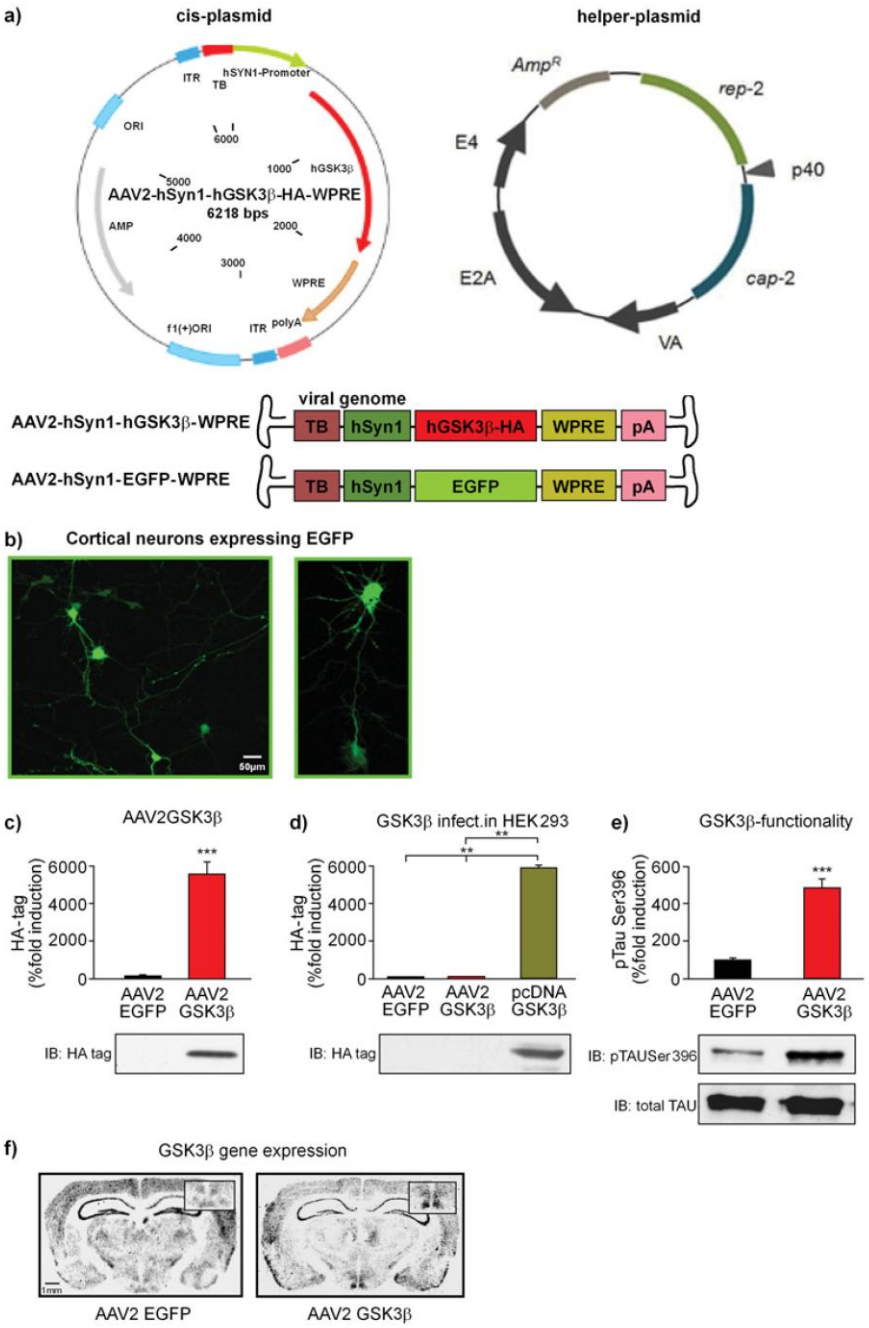

Figure 3 Neuron-specific AAV2-mediated overexpression of GSK3β in the ARC

(**a**) Schematic representation of *cis* and helper plasmid maps transfected into HEK-293 cells to produce AAV2–GSK3β (upper panels). Important elements of the viral genome are depicted in the lower panel. GSK3β transcription was controlled by the neuron-specific synapsin promoter. (**b**) Confocal image showing primary cortical neurons expressing EGFP after 5 days of AAV2–EGFP infection. (**c**) Confirmation of AAV2–GSK3β over-expression by immunoblotting of viral HA tag specific to AAV2–GSK3β in primary cortical neurons 5 days after infection. (**d**) In immunoblots of peripheral HEK-293 cells infection with neuron-specific AAV2–GSK3β was absent. Only cells transfected with pcDNA3-GSK3β led to an increase in the HA tag protein. (**e**) Immunoblot showing increased phospho-Tau (Ser^{396})/total Tau protein ratio in cortical neurons infected with AAV2–GSK3β. (**f**) Overexpression of AAV2–GSK3β *in vivo* was confirmed by *in situ* hybridizations. Shown are representative autoradiographs of mouse brain sections after *in situ* hybridization to an antisense ^{35}S-labelled riboprobe binding to GSK3β of AAV2–EFGP and AAV2–GSK3β mice. For validation each cell culture experiment was repeated three times and statistical analysis is represented in the histograms. Results are means $\pm$ S.E.M. $^{**}P \leqslant 0.01$ and $^{***}P \leqslant 0.001$. TB, transcriptional blocker; hSyn1, human synapsin1 promoter; hGSK3β, human GSK3β tagged with HA epitope; pA, poly A sequence from bovine growth hormone; ITR, inverted terminal repeat; IB, immunoblot.

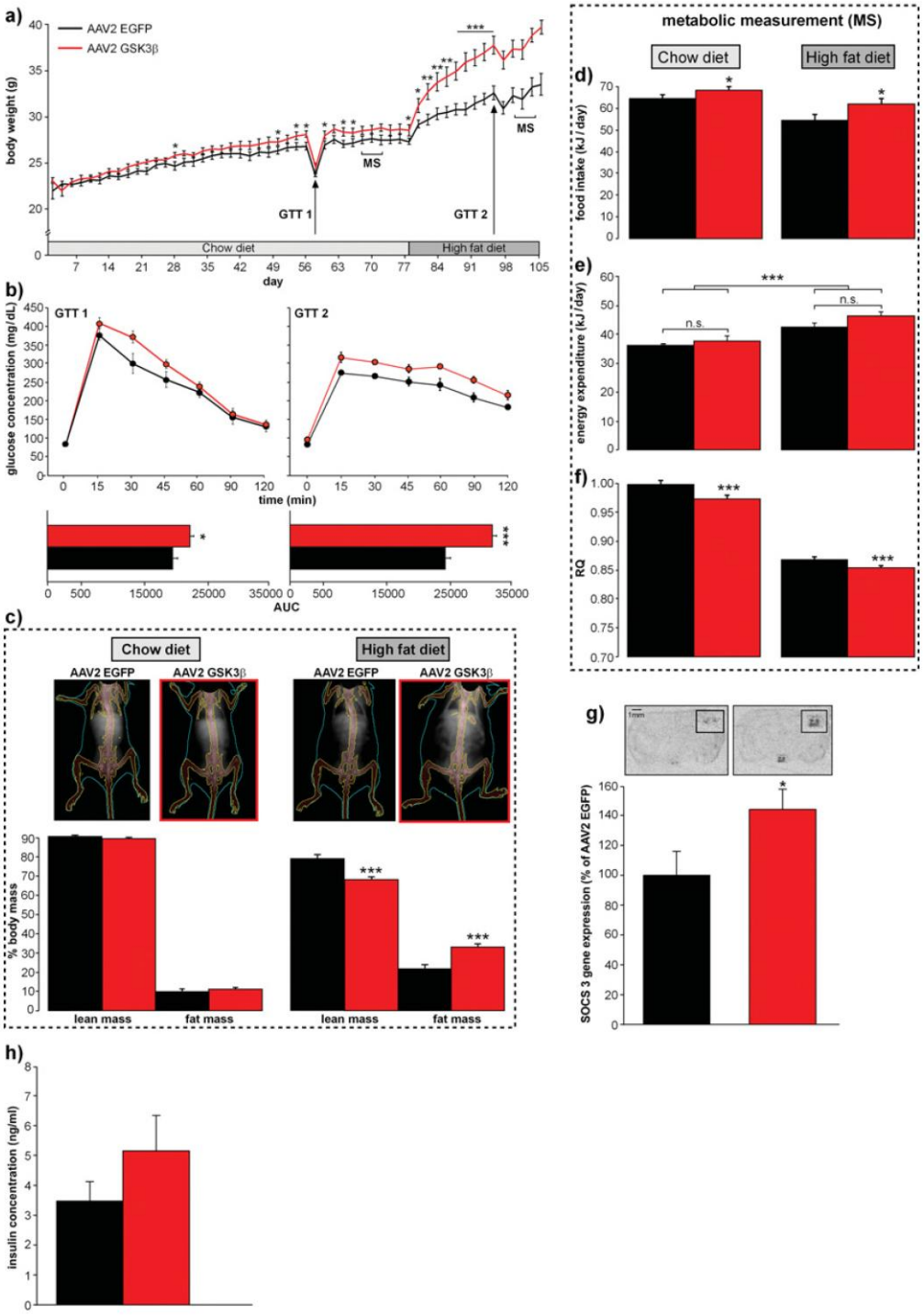

Figure 4 Neuron-specific AAV2-mediated overexpression of GSK3β in the ARC: effects on whole-body energy and glucose metabolism in mice

(**a**) Wild-type mice were stereotaxically injected into the bilateral halves of the ARC with 2×200 nl of AAV2 virus expressing EGFP ($n = 7$) as a control and GSK3β ($n = 8$). Shown are the body masses of EGFP- and GSK3β-overexpressing animals maintained on a chow diet (*ad libitum*) for 11 weeks followed by 18 days on an HFD (*ad libitum*). (**b**) Glucose tolerance tests 1 (GTT1) and 2 (GTT2) (upper panel) and associated area under the curve (AUC; lower panel). GTT1, performed on day 58 on chow diet after surgery, revealed impaired glucose tolerance in AAV2–GSK3β mice compared with AAV2–EGFP mice. After mice were switched to an HFD for 18 days GTT2 revealed exacerbated enhanced glucose intolerance in mice treated with AAV2–GSK3β compared with HFD-induced glucose

validated by infecting both primary cortical neurons (Figure 3c) and a peripheral cell line (HEK-293; Figure 3d) with AAV2 vectors expressing the fluorescent reporter EGFP (Figure 3b). As expected, viral-induced GSK3β overexpression occurred in neurons, but not HEK-293 cells. Following intraparenchymal injection of the AAV2–GSK3β vector into the ARC of wild-type mice, local overexpression of GSK3β was confirmed by *in situ* hybridization (Figure 3f), and increased GSK3β kinase activity was verified by measuring phospho-Tau content, a target of GSK3β in the brain [38]. In cultured primary cortical neurons, AAV2-mediated overexpression increased phospho-Tau protein 5-fold (Figure 3e, $P \leqslant 0.001$).

To investigate the effects of ARC-directed GSK3β overexpression on energy metabolism, we injected 10^{10} genomic units of either AAV2–GSK3β or a control AAV2 virus into the ARC of 8-week-old wild-type mice. On a standard chow diet, GSK3β overexpression induced a mild increase in body mass that was only intermittently and transiently significant over a time period of 78 days after injection (Figure 4a). Despite its minor effects on body mass, ARC-directed overexpression of GSK3β impaired glucose tolerance significantly relative to controls injected with AAV2–EGFP, based on an ipGTT performed on day 58 (Figure 4b, $P = 0.04$). After 78 days, both groups of mice were switched to an HFD for 18 days, which led to an increased body mass in both groups. However, the increase of body mass induced by the HFD was strikingly increased in AAV2–GSK3β mice compared with the controls, an effect that became significant within 2 days after the diet switch and reached a value 17 % greater than the controls by day 18 (Figure 4a). An ipGTT after 18 days on the HFD revealed that glucose tolerance had deteriorated markedly in the AAV2–GSK3β mice compared with the controls (Figure 4b, $P \leqslant 0.001$). DEXA analyses performed immediately after the ipGTT revealed significant reductions of relative lean mass ($P \leqslant 0.001$) and increases of relative fat mass ($P \leqslant 0.001$) in AAV2–GSK3β mice fed the HFD, but not in mice fed standard chow (Figure 4c). Cumulative food intake (kJ/day) was increased in AAV2–GSK3β mice compared with the AAV2–EGFP controls regardless of the diet (Figure 4d, $P \leqslant 0.05$), whereas energy expenditure was unaltered (Figure 4e). Lastly, the respiratory quotient (an indicator of substrate utilization) was reduced in AAV2–GSK3β mice on both the standard chow diet and HFD (Figure 4f, $P \leqslant 0.001$), suggesting preferential oxidation of lipid as a fuel.

Taken together, these data provide clear evidence that GSK3β signalling potently affects energy and glucose homoeostasis in a diet-sensitive manner via effects in the mediobasal hypothalamus. The striking increase in the body mass differential between AAV2–GSK3β and AAV2–EGFP mice after being fed the HFD probably involves increased food intake, whereas the metabolic rate was unchanged by hypothalamic GSK3β overexpression in the former mice. By comparison, the effects of neuronal GSK3β overexpression on the regular chow diet were modest, a discrepancy that might be explained by redundancy in components of the evolutionarily conserved WNT pathway, which may have partially compensated for the effects of increased GSK3β signalling on the chow diet. Interestingly, growing evidence indicates that consuming an HFD induces pro-inflammatory responses in the hypothalamus [39]. Combined with evidence that mediators of peripheral tissue inflammation [e.g. JNK (c-Jun N-terminal kinase)] also activate GSK3β [40], it is plausible that inflammation triggered by the HFD disrupts compensatory mechanisms that might be functional on the chow diet, thereby revealing potent deleterious effects of increased GSK3β activity.

This interpretation is strengthened by evidence of increased hypothalamic expression of SOCS3, which is induced during inflammation and suppresses leptin and insulin signalling [41,42], in AAV2–GSK3β mice compared with the controls while being fed an HFD (Figure 4g, $P = 0.02$). The possibilities that increased hypothalamic GSK3β signalling exacerbates inflammation and leptin resistance during HFD feeding and/or that hypothalamic inflammation increases local GSK3β activity are each consistent with the results of the present study and warrant additional study.

Our findings show that although activation of central GSK3β exacerbates the deleterious effects of HFD feeding on whole-body energy and glucose metabolism, there was only a trend towards increased serum insulin levels in AAV2–GSK3β mice relative to the controls (Figure 4h). A large number of papers suggest that hypothalamic insulin signalling is required for the inhibition of hepatic glucose production [3,4] and both hypothalamic insulin and leptin signalling appear to improve liver insulin sensitivity via a mechanism involving the vagus nerve [43]. To investigate whether central GSK3β activity opposes these effects and increases hepatic glucose output, we employed a strategy that involves an indirect measurement of hepatic glucose production using pyruvate as a substrate for gluconeogenesis, such that the observed glucose excursion reflects hepatic glucose output. $Lep^{ob/ob}$ mice received either GSK3β inhibitor or vehicle ICV 60 min before pyruvate was injected intraperitoneally and blood glucose levels were measured (Figure 5a). Leptin-deficient mice treated with the GSK3β inhibitor showed a significantly reduced glucose excursion compared with the vehicle ($P \leqslant 0.001$, $n = 5$–11/group). To further analyse the impact of central GSK3β inhibition on liver glucose metabolism, we measured the hepatic levels of PEPCK, which is rate-limiting for gluconeogenesis. $Lep^{ob/ob}$ mice received either GSK3β inhibitor or vehicle (aCSF) ICV 90 min before the liver was removed and immunoblotting was performed (Figure 5b) and normalized to the β-actin content. Central inhibition of GSK3β administration significantly decreased the amount of PEPCK protein in the liver compared with the vehicle-treated group ($P = 0.003$, $n = 4$–5/group), which is consistent with data obtained from hepatoma cells [44]. These results support a model in which GSK3β in the brain tonically favours increased plasma glucose levels via a mechanism that involves increased hepatic gluconeogenesis, a phenomenon that can be induced by local hypothalamic inhibition of PI3K [3] and is also observed in diabetic animals and humans [45,46].

Taken together, our data provide the first evidence that increased GSK3β signalling within the CNS drives hyperglycaemia and exerts deleterious effects on whole-body energy balance and glucose

intolerance in AAV2–EGFP mice. (**c**) DEXA scan images of representative animals with overexpression of AAV2–EGFP or AAV2–GSK3β mice on a chow diet and an HFD (upper panel). Body lean and fat mass did not change after treatment with AAV2–GSK3β virus on the chow diet. On the HFD, body lean mass was significantly reduced and body fat mass was increased accordingly after AAV2–GSK3β overexpression (lower panels). Values are expressed as the percentage of body mass. (**d**) AAV2–GSK3β over-expression in the ARC led to an increase in cumulative food intake in animals fed a chow diet or an HFD. Food intake is shown in kJ/day over the whole period of chow diet or an HFD. HFD led to a significant increase in energy expenditure (**e**), whereas GSK3β overexpression did not alter energy expenditure regardless of diet; respiratory quotient was reduced on both the chow diet and HFD after GSK3β overexpression (**f**). (**g**) GSK3β over-expression led to an increase in *SOCS3* gene expression in the ARC. Representative autoradiographies of coronal brain sections exposed to ^{35}S-labelled riboprobe against SOCS3. Insets depict localization within the ARC of mice treated with AAV2–EGFP (left-hand) or AAV2–GSK3β (right-hand). Semi-quantitative analyses of gene expression of *SOCS3* is represented in the histogram as the percentage of AAV2–EGFPb. (**h**) Plasma insulin levels as measured by ELISA were unaltered regardless of treatment with AAV20–EGFP or AAV20–GSK3β. Results are means $\pm$ S.E.M., $^{*}P \leqslant 0.05$, $^{**}P \leqslant 0.01$ and $^{***}P \leqslant 0.001$.

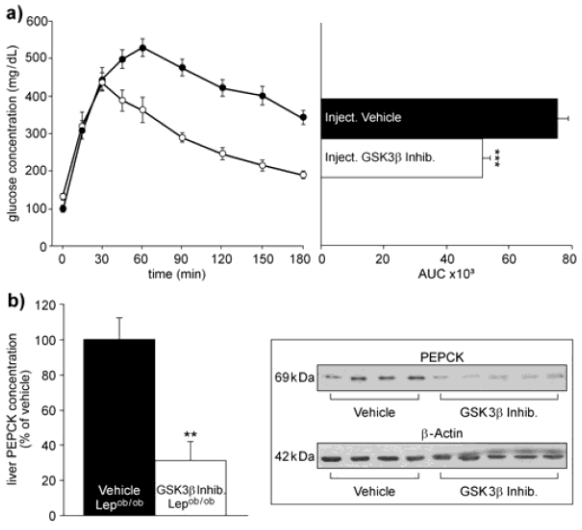

Figure 5 Central GSK3β regulates hepatic glucose production

(**a**) Shown are glucose concentrations (left-hand panel) and associated area under the curve (AUC; right-hand panel) during intraperitoneal pyruvate tolerance tests. A central injection of a GSK3β inhibitor decreased hepatic glucose production in $Lep^{ob/ob}$ mice. Pyruvate tolerance tests were performed 60 min after the administration of GSK3β inhibitor (○) or vehicle (●) into the lateral ventricle ($n = 5$–11/group). (**b**) Hepatic PEPCK levels were semi-quantitatively assessed by immunoblotting using a specific antibody against PEPCK 90 min after the central administration of either GSK3β inhibitor ($n = 5$) or vehicle ($n = 11$) and were normalized by β-actin. Results are means $\pm$ S.E.M., $^{**}P \leqslant 0.01$ and $^{***}P \leqslant 0.001$.

metabolism in the adult mouse, particularly in the setting of an HFD or genetic leptin deficiency. This, together with the notion that this enzyme sensitizes insulin signalling in the hypothalamus, further reinforces the concept that the brain is an essential organ in the maintenance of peripheral glucose homoeostasis. Aberrant GSK3β has also been associated with the pathogenesis of many human diseases, such as osteoporosis [47], atherosclerosis [48], cancer and Alzheimer's disease [49]. The proposed role of GSK3β in the brain in regulating peripheral glucose homoeostasis might constitute an important link between Type II diabetes and the pathogenesis of these other severe diseases.

AUTHOR CONTRIBUTION

Jonas Benzler carried out all of the experiments in Figures 1, 2 and 5, and helped to write the paper and develop the project. Goutham K. Ganjam and Manon Krüger generated the viral construct with technical support from Olaf Pinkenburg and performed the experiments in Figures 3 and 4. Maria Kutschke, Sigrid Stoehr and Juliane Steger provided technical support for all experiments. Christiane Koch helped performing the ipGTTs and Rebecca Oelkrug provided support for performing the metabolic measurements. Michael Schwartz helped to write and revise the paper. Peter R. Shepherd helped to write and revise the paper and gave advice on experiments. David R. Grattan helped to write and revise the paper and gave advice on developing the project. Alexander Tups was the principal investigator developed the project, supervised the research and wrote and revised the paper.

ACKNOWLEDGEMENT

We thank Professor James Woodgett (Samuel Lunenfeld Research Institute, Toronto, Canada) for providing the pcDNA3-GSK3β-HA vector.

FUNDING

This work was supported by the German Ministry of Education and Research [grant number 0315087 (to A.T.)].

REFERENCES

1 Chan, J. C., Malik, V., Jia, W., Kadowaki, T., Yajnik, C. S., Yoon, K. H. and Hu, F. B. (2009) Diabetes in Asia: epidemiology, risk factors, and pathophysiology. JAMA, J. Am. Med. Assoc. **301**, 2129–2140
2 Bruning, J. C., Gautam, D., Burks, D. J., Gillette, J., Schubert, M., Orban, P. C., Klein, R., Krone, W., Muller-Wieland, D. and Kahn, C. R. (2000) Role of brain insulin receptor in control of body weight and reproduction. Science **289**, 2122–2125
3 Obici, S., Zhang, B. B., Karkanias, G. and Rossetti, L. (2002) Hypothalamic insulin signaling is required for inhibition of glucose production. Nat. Med. *8* 1376–1382
4 Obici, S., Feng, Z., Karkanias, G., Baskin, D. G. and Rossetti, L. (2002) Decreasing hypothalamic insulin receptors causes hyperphagia and insulin resistance in rats. Nat. Neurosci. **5**, 566–572
5 Niswender, K. D., Morrison, C. D., Clegg, D. J., Olson, R., Baskin, D. G., Myers, Jr, M. G., Seeley, R. J. and Schwartz, M. W. (2003) Insulin activation of phosphatidylinositol 3-kinase in the hypothalamic arcuate nucleus: a key mediator of insulin-induced anorexia. Diabetes **52**, 227–231
6 Okamoto, H., Nakae, J., Kitamura, T., Park, B. C., Dragatsis, I. and Accili, D. (2004) Transgenic rescue of insulin receptor-deficient mice. J. Clin. Invest. **114**, 214–223
7 Okamoto, H., Obici, S., Accili, D. and Rossetti, L. (2005) Restoration of liver insulin signaling in Insr knockout mice fails to normalize hepatic insulin action. J. Clin. Invest. **115**, 1314–1322
8 Gelling, R. W., Morton, G. J., Morrison, C. D., Niswender, K. D., Myers, Jr, M. G., Rhodes, C. J. and Schwartz, M. W. (2006) Insulin action in the brain contributes to glucose lowering during insulin treatment of diabetes. Cell Metab. **3**, 67–73
9 Koch, C., Augustine, R. A., Steger, J., Ganjam, G. K., Benzler, J., Pracht, C., Lowe, C., Schwartz, M. W., Shepherd, P. R., Anderson, G. M. et al. (2010) Leptin rapidly improves glucose homeostasis in obese mice by increasing hypothalamic insulin sensitivity. J. Neurosci. **30**, 16180–16187
10 Niswender, K. D., Morton, G. J., Stearns, W. H., Rhodes, C. J., Myers, Jr, M. G. and Schwartz, M. W. (2001) Intracellular signalling. Key enzyme in leptin-induced anorexia. Nature **413**, 794–795
11 Zhao, A. Z., Huan, J. N., Gupta, S., Pal, R. and Sahu, A. (2002) A phosphatidylinositol 3-kinase phosphodiesterase 3B-cyclic AMP pathway in hypothalamic action of leptin on feeding. Nat. Neurosci. **5**, 727–728
12 Cross, D. A., Alessi, D. R., Cohen, P., Andjelkovich, M. and Hemmings, B. A. (1995) Inhibition of glycogen synthase kinase-3 by insulin mediated by protein kinase B. Nature **378**, 785–789
13 Hur, E. M. and Zhou, F. Q. (2010) GSK3 signalling in neural development. Nat. Rev. Neurosci. **11**, 539–551
14 Cline, G. W., Johnson, K., Regittnig, W., Perret, P., Tozzo, E., Xiao, L., Damico, C. and Shulman, G. I. (2002) Effects of a novel glycogen synthase kinase-3 inhibitor on insulin-stimulated glucose metabolism in Zucker diabetic fatty (fa/fa) rats. Diabetes **51**, 2903–2910
15 Kaidanovich-Beilin, O. and Eldar-Finkelman, H. (2006) Long-term treatment with novel glycogen synthase kinase-3 inhibitor improves glucose homeostasis in ob/ob mice: molecular characterization in liver and muscle. J. Pharmacol. Exp. Ther. **316**, 17–24
16 Rao, R., Hao, C. M., Redha, R., Wasserman, D. H., McGuinness, O. P. and Breyer, M. D. (2007) Glycogen synthase kinase 3 inhibition improves insulin-stimulated glucose metabolism but not hypertension in high-fat-fed C57BL/6J mice. Diabetologia **50**, 452–460
17 Eldar-Finkelman, H. (2002) Glycogen synthase kinase 3: an emerging therapeutic target. Trends Mol. Med. **8**, 126–132
18 Nikoulina, S. E., Ciaraldi, T. P., Mudaliar, S., Carter, L., Johnson, K. and Henry, R. R. (2002) Inhibition of glycogen synthase kinase 3 improves insulin action and glucose metabolism in human skeletal muscle. Diabetes **51**, 2190–2198
19 Clodfelder-Miller, B., De Sarno, P., Zmijewska, A. A., Song, L. and Jope, R. S. (2005) Physiological and pathological changes in glucose regulate brain Akt and glycogen synthase kinase-3. J. Biol. Chem. **280**, 39723–39731
20 Mercer, J. G., Moar, K. M., Logie, T. J., Findlay, P. A., Adam, C. L. and Morgan, P. J. (2001) Seasonally inappropriate body weight induced by food restriction: effect on hypothalamic gene expression in male Siberian hamsters. Endocrinology **142**, 4173–4181
21 Paxinos, G. and Franklin, K. (2002) The Mouse Brain in Stereotaxic Coordinates, Academics, San Diego
22 Tups, A., Anderson, G. M., Rizwan, M., Augustine, R. A., Chaussade, C., Shepherd, P. R. and Grattan, D. R. (2010) Both p110α and p110β isoforms of phosphatidylinositol 3-OH-kinase are required for insulin signalling in the hypothalamus. J. Neuroendocrinol. **22**, 534–542
23 Kugler, S., Lingor, P., Scholl, U., Zolotukhin, S. and Bahr, M. (2003) Differential transgene expression in brain cells *in vivo* and *in vitro* from AAV-2 vectors with small transcriptional control units. Virology **311**, 89–95

24 Grimm, D., Kay, M. A. and Kleinschmidt, J. A. (2003) Helper virus-free, optically controllable, and two-plasmid-based production of adeno-associated virus vectors of serotypes 1 to 6. Mol. Ther. **7**, 839–850
25 Culmsee, C., Zhu, C., Landshamer, S., Becattini, B., Wagner, E., Pellecchia, M., Blomgren, K. and Plesnila, N. (2005) Apoptosis-inducing factor triggered by poly(ADP-ribose) polymerase and Bid mediates neuronal cell death after oxygen-glucose deprivation and focal cerebral ischemia. J. Neurosci. **25**, 10262–10272
26 He, X., Saint-Jeannet, J. P., Woodgett, J. R., Varmus, H. E. and Dawid, I. B. (1995) Glycogen synthase kinase-3 and dorsoventral patterning in *Xenopus* embryos. Nature **374**, 617–622
27 Ganjam, G. K., Dimova, E. Y., Unterman, T. G. and Kietzmann, T. (2009) FoxO1 and HNF-4 are involved in regulation of hepatic glucokinase gene expression by resveratrol. J. Biol. Chem. **284**, 30783–30797
28 Heldmaier, G. and Ruf, T. (1992) Body temperature and metabolic rate during natural hypothermia in endotherms. J. Comp. Physiol. B **162**, 696–706
29 Sutherland, C., Leighton, I. A. and Cohen, P. (1993) Inactivation of glycogen synthase kinase-3β by phosphorylation: new kinase connections in insulin and growth-factor signalling. Biochem. J. **296**, 15–19
30 Stambolic, V. and Woodgett, J. R. (1994) Mitogen inactivation of glycogen synthase kinase-3β in intact cells via serine 9 phosphorylation. Biochem. J. **303**, 701–704
31 Dajani, R., Fraser, E., Roe, S. M., Young, N., Good, V., Dale, T. C. and Pearl, L. H. (2001) Crystal structure of glycogen synthase kinase 3β: structural basis for phosphate-primed substrate specificity and autoinhibition. Cell **105**, 721–732
32 Woodgett, J. R. (2001) Judging a protein by more than its name: GSK-3. Sci. STKE **2001**, re12
33 Shaw, M., Cohen, P. and Alessi, D. R. (1997) Further evidence that the inhibition of glycogen synthase kinase-3β by IGF-1 is mediated by PDK1/PKB-induced phosphorylation of Ser-9 and not by dephosphorylation of Tyr-216. FEBS Lett. **416**, 307–311
34 Koch, L., Wunderlich, F. T., Seibler, J., Konner, A. C., Hampel, B., Irlenbusch, S., Brabant, G., Kahn, C. R., Schwenk, F. and Bruning, J. C. (2008) Central insulin action regulates peripheral glucose and fat metabolism in mice. J. Clin. Invest **118**, 2132–2147
35 Scali, C., Caraci, F., Gianfriddo, M., Diodato, E., Roncarati, R., Pollio, G., Gaviraghi, G., Copani, A., Nicoletti, F., Terstappen, G. C. et al. (2006) Inhibition of Wnt signaling, modulation of Tau phosphorylation and induction of neuronal cell death by DKK1. Neurobiol. Dis. **24**, 254–265
36 Monahan, P. E. and Samulski, R. J. (2000) AAV vectors: is clinical success on the horizon? Gene Ther. **7**, 24–30
37 de Backer, M. W., Fitzsimons, C. P., Brans, M. A., Luijendijk, M. C., Garner, K. M., Vreugdenhil, E. and Adan, R. A. (2010) An adeno-associated viral vector transduces the rat hypothalamus and amygdala more efficient than a lentiviral vector. BMC Neurosci. **11**, 81
38 Sperber, B. R., Leight, S., Goedert, M. and Lee, V. M. (1995) Glycogen synthase kinase-3β phosphorylates tau protein at multiple sites in intact cells. Neurosci. Lett. **197**, 149–153
39 Posey, K. A., Clegg, D. J., Printz, R. L., Byun, J., Morton, G. J., Vivekanandan-Giri, A., Pennathur, S., Baskin, D. G., Heinecke, J. W., Woods, S. C. et al. (2009) Hypothalamic proinflammatory lipid accumulation, inflammation, and insulin resistance in rats fed a high-fat diet. Am. J. Physiol. Endocrinol. Metab **296**, E1003–E1012
40 Hu, D., Fang, W., Han, A., Gallagher, L., Davis, R. J., Xiong, B. and Yang, W. (2008) c-Jun N-terminal kinase 1 interacts with and negatively regulates Wnt/β-catenin signaling through GSK3β pathway. Carcinogenesis **29**, 2317–2324
41 Bjorbaek, C., Elmquist, J. K., Frantz, J. D., Shoelson, S. E. and Flier, J. S. (1998) Identification of SOCS-3 as a potential mediator of central leptin resistance. Mol. Cell **1**, 619–625
42 Tups, A., Ellis, C., Moar, K. M., Logie, T. J., Adam, C. L., Mercer, J. G. and Klingenspor, M. (2004) Photoperiodic regulation of leptin sensitivity in the Siberian hamster, *Phodopus sungorus*, is reflected in arcuate nucleus SOCS-3 (suppressor of cytokine signaling) gene expression. Endocrinology **145**, 1185–1193
43 German, J., Kim, F., Schwartz, G. J., Havel, P. J., Rhodes, C. J., Schwartz, M. W. and Morton, G. J. (2009) Hypothalamic leptin signaling regulates hepatic insulin sensitivity via a neurocircuit involving the vagus nerve. Endocrinology **150**, 4502–4511
44 Lochhead, P. A., Coghlan, M., Rice, S. Q. and Sutherland, C. (2001) Inhibition of GSK-3 selectively reduces glucose-6-phosphatase and phosphatase and phosphoenolypyruvate carboxykinase gene expression. Diabetes **50**, 937–946
45 Consoli, A., Nurjhan, N., Capani, F. and Gerich, J. (1989) Predominant role of gluconeogenesis in increased hepatic glucose production in NIDDM. Diabetes **38**, 550–557
46 Gerich, J. E. and Nurjhan, N. (1993) Gluconeogenesis in type 2 diabetes. Adv. Exp. Med. Biol. **334**, 253–258
47 Smith, E. and Frenkel, B. (2005) Glucocorticoids inhibit the transcriptional activity of LEF/TCF in differentiating osteoblasts in a glycogen synthase kinase-3β-dependent and -independent manner. J. Biol. Chem. **280**, 2388–2394
48 Robertson, L. A., Kim, A. J. and Werstuck, G. H. (2006) Mechanisms linking diabetes mellitus to the development of atherosclerosis: a role for endoplasmic reticulum stress and glycogen synthase kinase-3. Can. J. Physiol. Pharmacol. **84**, 39–48
49 Jope, R. S. and Johnson, G. V. (2004) The glamour and gloom of glycogen synthase kinase-3. Trends Biochem. Sci. **29**, 950–102

Received 22 May 2012/26 July 2012; accepted 1 August 2012
Published as BJ Immediate Publication 1 August 2012, doi:10.1042/BJ20120834

Journal of Neuroendocrinology

Journal of Neuroendocrinology, 2013, **25**, 446–454

ORIGINAL ARTICLE

Acute Inhibition of Central c-Jun N-terminal Kinase Restores Hypothalamic Insulin Signalling and Alleviates Glucose Intolerance in Diabetic Mice

J. Benzler, G. K. Ganjam, K. Legler, S. Stöhr, M. Krüger, J. Steger and A. Tups

Department of Animal Physiology, Faculty of Biology, Philipps University Marburg, Marburg, Germany.

Journal of Neuroendocrinology

The hypothalamus has been identified as a main insulin target tissue for regulating normal body weight and glucose metabolism. Recent observations suggest that c-Jun-N-terminal kinase (JNK)-signalling plays a crucial role in the development of obesity and insulin resistance because neuronal JNK-1 ablation in the mouse prevented high-fat diet-induced obesity (DIO) and increased energy expenditure, as well as insulin sensitivity. In the present study, we investigated whether central JNK inhibition is associated with sensitisation of hypothalamic insulin signalling in mice fed a high-fat diet for 3 weeks and in leptin-deficient mice. We determined whether i.c.v. injection of a pharmacological JNK-inhibitor (SP600125) improved impaired glucose homeostasis. By immunohistochemistry, we first observed that JNK activity was increased in the arcuate nucleus (ARC) and the ventromedial hypothalamus (VMH) in both mouse models, relative to normoglycaemic controls. This suggests that up-regulation of JNK in these regions is associated with glucose intolerance and obesity, independent of leptin levels. Acute i.c.v. injection of SP600125 ameliorated glucose tolerance within 30 min in both leptin-deficient and DIO mice. Given the acute nature of i.c.v. injections, these effects cannot be attributed to changes in food intake or energy balance. In a hypothalamic cell line, and in the ARC and VMH of leptin-deficient mice, JNK inhibition by SP600125 consistently improved impaired insulin signalling. This was determined by a reduction of phospho-insulin receptor substrate-1 [IRS-1(Ser612)] protein in a hypothalamic cell line and a decline in the number of pIRS-1(Ser612) immunoreactive cells in the ARC and VMH. Serine 612 phosphorylation of IRS-1 is assumed to negatively regulate insulin signalling. In leptin-deficient mice, in both nuclei, central inhibition of JNK increased the number of cells immunoreactive for phospho-Akt (Ser473) and phospho-GSK-3β (Ser9), which are important markers of insulin signalling. Collectively, our data suggest that the acute inhibition of central JNK improves impaired glucose homeostasis and is associated with sensitisation of hypothalamic insulin signalling.

Key words: type II diabetes, inflammation, obesity, high-fat diet, leptin-deficient mice, arcuate nuclues, ventromedial hypothalamus

doi: 10.1111/jne.12018

Correspondence to:
Dr A. Tups, Department of Animal Physiology, Faculty of Biology, Philipps University Marburg, Karl-von-Frisch Strasse 8, D-35043 Marburg, Germany (e-mail: alexander.tups@staff.uni-marburg.de).

Obesity represents a critical risk factor for the development of insulin resistance and, ultimately, type II diabetes (1,2). Despite the landmark discovery that identified the brain as being a critical insulin target tissue for the regulation of systemic glucose metabolism (3–9), the precise signalling mechanisms and the absolute contribution of the brain in the pathogenesis of type II diabetes are only poorly understood. It has been proposed that the hypothalamic insulin receptor substrate (IRS)-phosphatidylinositol 3-kinase (PI3K) pathway plays a critical role in the regulation of peripheral glucose homeostasis (5,10,11). Insulin and the adipokine leptin, which both improve glucose metabolism, activate signal transduction via the IRS-PI3K pathway (5,10–13). Although, the precise neuronal mechanisms contributing to insulin resistance are still incompletely understood, emerging evidence suggests that inflammation and altered lipid metabolism are associated with this metabolic disorder (14). In various animal models, inflammation, particularly in the

hypothalamus, has been established as a determining risk factor for the onset of obesity (15–17). One molecular correlate of hypothalamic inflammation is c-Jun N-terminal kinase (JNK) (18), which belongs to the mitogen-activated protein kinase family.

JNK consists of three different isoforms, JNK-1–3, and activation is associated with diet-induced obesity (DIO), which is mediated via different mechanisms (19–21). JNK-1 and JNK-2 are highly expressed in almost all cells and tissues (22), whereas the expression of JNK-3 is more restricted to the heart and the brain (23). Out of the three splice variants, the best characterised isoform is JNK-1. Up-regulation of JNK-1 can result in phosphorylation of IRS-1 and hence disrupted insulin signalling (23-27). Additionally, it has been demonstrated that JNK-1 deficient mice are protected against DIO and insulin resistance (23). Conditional inactivation of JNK-1 in numerous peripheral tissues (e.g. muscle or fat) improved insulin sensitivity in some insulin target regions (28,29); however, whether there is a key organ in which JNK disrupts whole body glucose homeostasis remains unknown. A large body of evidence suggests that the action of insulin in the central nervous system plays a potent role in the regulation of peripheral glucose homeostasis (3,8,9). Furthermore, hypothalamic JNK activation has been linked to hyperlipidaemia (30). Conclusively, central nervous system-targeted ablation of JNK-1 in mice prevented DIO and increased energy expenditure and insulin sensitivity associated with an activation of the hypothalamic-pituitary-thyroid axis (18,31). Despite recent advances, neither the precise molecular mechanism by which central JNK might mediate insulin resistance, nor the neuroanatomical target regions of the action of JNK have been identified so far.

In the present study, we identified hypothalamic key regions that are involved in the regulation of energy and glucose metabolism in which JNK activity is increased in a state of genetically (leptin-deficiency) or physiologically (DIO) induced glucose intolerance. We tested the hypothesis that acute manipulation of JNK in the brain could play a pivotal role in regulating peripheral glucose homeostasis. Using both *in vitro* and *in vivo* approaches, we show that acute inhibition of central JNK improves impaired glucose tolerance in leptin-deficient mice and mice on high-fat diet (HFD). Furthermore, we show that this acute glucose-lowering effect might be mediated via sensitising IRS-PI3K signalling in hypothalamic key regions. These data might further substantiate the hypothalamic inflammation theory and its implication in the maintenance of energy and glucose homeostasis.

Materials and methods

Animals

All procedures involving animals were licensed under German animal ethics legislation and received approval by the federal public authority for animal ethics. All experiments used male mice that were purchased from Janvier (Le Genest-Saint-Isle, France). All mice (wild-type and $Lep^{ob/ob}$ mice) were on the C57BL/6JRj genetic background. Animals were between 2 and 3 months old and were housed individually under a 12 : 12 h light/dark cycle. The ambient temperature for mice was 23 °C. Apart from the dark phase before the experiments, all animals had access to standard chow diet (containing 9% fat; catalogue number V1534, ssniff, Soest, Germany), unless stated otherwise. Standard chow diet, low-fat diet (LFD) or high-fat diet, (containing 10% or 45% fat, respectively; catalogue numbers D12450B and D12451, Research Diets, New Brunswick, NJ, USA), and water were available *ad lib.* For central administration of drugs, cannulae were stereotaxically implanted into the left lateral ventricle, as described previously (11).

Increased JNK activity: immunohistochemistry

To determine whether leptin deficiency leads to increased hypothalamic activity of JNK in key neuronal centres of body weight regulation, the arcuate nucleus (ARC) and the ventromedial hypothalamus (VMH), $Lep^{ob/ob}$ mice (n = 6) and respective wild-type controls (n = 5) were fasted for 16 h and weight matched before transcardial perfusion. Subsequently, immunohistochemistry was performed, using an anti-phospho-JNK antibody (Thr183/Tyr185, diluted 1 : 1000; catalogue number 4668), as a marker for JNK activation. Additionally, to $Lep^{ob/ob}$ mice, we also assessed whether high-fat feeding induces JNK activity in the ARC and VMH. Therefore, wild-type mice were fed a HFD for 3 weeks (n = 6) or low-fat diet (LFD; n = 5) prior to hypothalamic analysis of phospho-JNK. Before transcardial perfusion, mice were fasted for 16 h and weight matched. Immunohistochemistry was carried out on mouse brain coronal cryosections, as described previously (11,32). All antibodies were purchased from Cell Signaling Technology (Beverly, MA, USA). Section images were captured using a digital camera (SC20; Olympus, Hamburg, Germany) mounted on an Olympus microscope (BX-41; Olympus). For analysis of immunoreactivity, labelled cells were counted in three to four evenly-spaced, region-matched sections (35 μm thick) throughout the investigated nuclei (ARC: −2.3 to −1,5 mm relative to Bregma; VMH: −2,0 to −1,3 mm relative to Bregma). All cells immunoreactive within one of the bilateral halves of the ARC and VMH were counted by two investigators who were blinded to treatment, and multiplied by two to estimate the total number of immunoreactive cells per section.

Effect of JNK inhibition on insulin signalling in a hypothalamic cell line

In this experiment, we investigated whether JNK inhibition affects hypothalamic phospho-IRS-1 (Ser612) content, a molecule whose phosphorylation on Ser612 has been shown to negatively regulate insulin signaling (11,33,34). The adult mouse hypothalamic cell line (mHypoA-CLU190; CELLutions, Toronto, Canada) was maintained under standard conditions in an atmosphere of 16% O_2, 79% N_2, 5% CO_2 (v/v/v) in Dulbecco's modified Eagle's medium with 10% foetal bovine serum, 1% ciprofloxacin antibiotic and 0.5% non-essential amino acids. On the day of the experiment, cells were supplemented with fresh medium and were subjected to JNK-inhibitor (SP600125; 40 μM) for 30 min. Total protein was isolated after 30 min in RIPA lysis buffer containing phosphatase and protease inhibitors. Forty micrograms of the total protein lysates were used to analyse phospho-IRS (Ser612) levels by western blot as described previously (35).

Glucose tolerance tests

Using $Lep^{ob/ob}$ mice, we determined whether inactivation of central JNK might impair whole body glucose tolerance. Two different doses of the JNK-inhibitor were tested. In the first experiment, two groups of fasted (16 h), weight matched $Lep^{ob/ob}$ mice (n = 6), received either the JNK-inhibitor [2 nmol in 1 μl articifical cerebrospinal fluid (aCSF)/5% dimethylsulphoxide (DMSO) (SP600125) i.c.v.; n = 6] or an i.c.v. vehicle injection (aCSF/5% DMSO; n = 7). In the second experiment, one group of $Lep^{ob/ob}$ mice received the JNK-inhibitor (i.c.v.) in a higher concentration (5 nmol in 1 μl aCSF/5% DMSO; n = 5) or vehicle (aCSF/5% DMSO) using the same experimental design.

Thirty minutes later, an i.p. glucose tolerance test (i.p.-GTT; 1 g glucose/kg) was performed. To determine the blood glucose levels, the *Vena facialis* was repeatedly punctured and glucose concentration was measured using a commercially available glucometer (Accu-Check Performa; Roche, Mannheim, Germany). For statistical validation, the area under the curve was calculated.

Next, we investigated whether central inhibition of JNK also improves glucose tolerance in diet-induced obese and glucose intolerant mice. Therefore, mice were fed a HFD or a respective LFD for 3 weeks, fasted for 16 h and weight matched. We administered the JNK-inhibitor i.c.v. (5 nmol in 1 μl aCSF/5% DMSO) to one group of mice on a HFD (n = 6), whereas the second group on this diet received an i.c.v. vehicle injection (aCSF/5% DMSO). In addition, one group of mice was employed that were fed on LFD and received i.c.v. vehicle (aCSF/5% DMSO; n = 5) 30 min prior to the i.p.-GTT.

JNK inhibition restores IRS-PI3K signalling: Immunohistochemistry

We next investigated whether central inhibition of JNK restores impaired IRS-PI3K signalling, which is exhibited by $Lep^{ob/ob}$ mice. Therefore, $Lep^{ob/ob}$ mice received i.c.v. either a specific pharmacological JNK-inhibitor (SP600125; 5 nmol in 1 μl aCSF/5% DMSO; n = 9) or vehicle (1 μl aCSF/5% DMSO; n = 6) 30 min before transcardial perfusion and immunohistochemistry was performed as described above using anti-phospho-IRS-1 Ser612 (dilution 1 : 500; catalogue number 3203), anti-phospho-Akt Ser473 (dilution 1 : 500; catalogue number 4058) or anti-phospho GSK-3β Ser9 (dilution 1 : 1000; catalogue number 9323) antibodies. All antibodies were purchased from Cell Signaling Technology (Beverly, MA, USA).

Statistical analysis

Data were analysed by one-way ANOVA followed by a Holm–Sidak comparison test, as appropriate, using SigmaStat statistical software (Jandel, Erkrath, Germany). Where data failed equal variance or normality tests, they were analysed by one-way ANOVA on ranks followed by Dunn's multiple comparison test. Results are presented as the mean ± SEM. $P < 0.05$ was considered statistically significant.

Results

Analysis of JNK activity in the mediobasal hypothalamus of $Lep^{ob/ob}$ mice and mice fed a HFD

The investigated mice had a marked body weight differential between the $Lep^{ob/ob}$ background versus wild-type controls (41.5 g ± 0.4 versus 25.3 g ± 0.5, respectively; $P < 0.001$) and mice on a HFD versus mice on a LFD for 3 weeks, respectively (30.0 g ± 0.6 versus 27.6 g ± 0.5, respectively; $P = 0.007$). JNK activity in the hypothalamus was measured by immunohistochemistry of pJNK (Thr183/Tyr185). In $Lep^{ob/ob}$ mice and in mice on HFD, hypothalamic condensation of pJNK immunoreactivity was confined to the ARC and VMH, both key regions for neuronal control of energy- and glucose homeostasis. In extra-hypothalamic regions, immunoreactivity for JNK was found in the cortex and the habenular nucleus (data not shown). Immunoreactivity occurred within cell bodies, and cells positive for pJNK were counted. Within the ARC, both the $Lep^{ob/ob}$ genotype and DIO was associated with an approximate two-fold increase in the number of pJNK immunoreactive cells compared to their respective controls ($P < 0.001$; n = 5 or 6 per group) (Fig. 1A and B). Within the VMH, $Lep^{ob/ob}$ mice revealed an increase of more than three-fold (Fig. 1c), whereas mice on HFD exhibited a two-fold increase in the number of pJNK immunoreactive cells compared to their respective controls ($P = 0.018$, $P = 0.008$, n = 5 or 6 per group) (Fig. 1D).

Effect of JNK inhibition on insulin signalling in hypothalamic cells

We next investigated whether JNK inhibition affects phosphorylation of IRS-1 at Ser612, which has been described as a negative regulator of peripheral and central insulin signalling (11,33,34). In the hypothalamic adult mouse cell line (mHypoA-CLU190, CELLusions), 30 min of pre-treatment with the specific JNK-inhibitor (40 μM, SP600125) decreased the phosphorylation of IRS-1 by more than nine-fold compared to vehicle-treated cells ($P = 0.008$, n = 5 per group) (Fig. 2) as revealed by immunoblotting.

Acute inhibition of central JNK and glucose tolerance in mice

Having established that JNK activity is increased in the ARC and VMH of both, DIO and $Lep^{ob/ob}$ mice, and that inhibition of JNK decreases phosphorylation of IRS-1 (Ser612) *in vitro*, we next investigated whether central inhibition of JNK acutely influences whole body glucose homeostasis. Therefore, two doses of the JNK-inhibitor (2 nmol and 5 nmol in 1 μl aCSF) were injected i.c.v. in diabetic $Lep^{ob/ob}$ mice, 30 min prior to an i.p.-GTT. The lower dose (2 nmol) mildly improved glucose tolerance compared to the vehicle-treated group (n = 6 or 7 per group, $P = 0.032$) (Fig. 3A), whereas the higher dose (5 nmol) potently improved glucose tolerance in these mice (n = 5 or 6 per group, $P < 0.001$) (Fig. 3B). To exclude the possibility that this glucose-lowering effect is restricted to $Lep^{ob/ob}$ mice only, we also examined potential glucose-lowering properties of this substance during DIO. Intracebroventricular injection of the JNK-inhibitor (5 nmol) 30 min prior to the i.p.-GTT improved glucose tolerance in mice on HFD compared to vehicle-treated mice on the same diet (n = 5–7 per group, $P = 0.008$) (Fig. 3c). However, this treatment did not completely normalise glucose homeostasis because there was still a significant difference between the JNK-inhibitor treated mice on HFD and healthy vehicle-treated LFD mice ($P = 0.038$).

Acute inhibition of central JNK and insulin signalling in the hypothalamus

We next investigated whether the glucose-lowering properties of the JNK-inhibitor are mediated through interaction with hypothalamic IRS-PI3K signalling. This *in vivo* experiment was designed to confirm the *in vitro* observations in the hypothalamic cell line in which inhibition of JNK decreased phosphorylation of IRS (Ser612). $Lep^{ob/ob}$ mice received either a single i.c.v. injection of JNK-inhibitor (5 nmol in 1 μl aCSF) or vehicle (1 μl of aCSF) 30 min before transcardial perfusion and immunohistochemistry was performed. As observed in hypothalamic cells, the number of pIRS-1(Ser612)

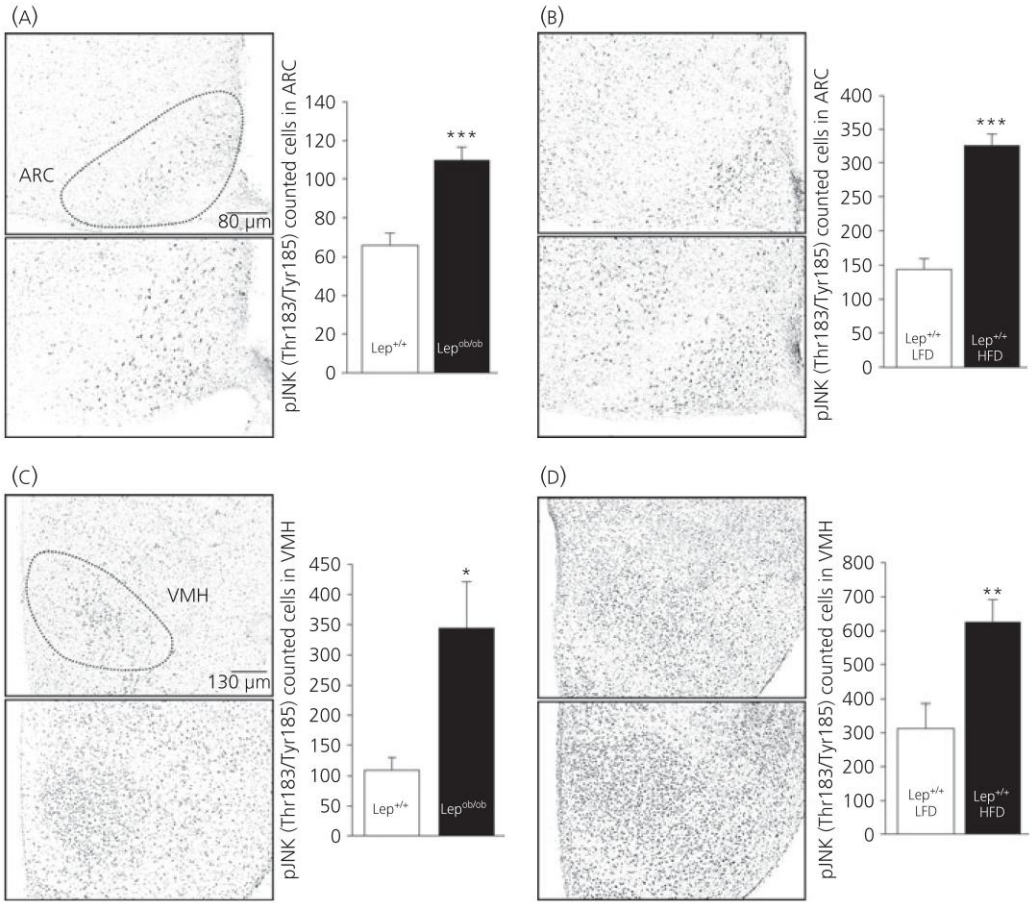

Fig. 1. Assessment of phospho-c-Jun-N-terminal kinase (JNK) activity in leptin-deficient mice and mice on a high-fat diet (HFD). Immunohistochemistry of phospho-JNK (Thr183/Tyr185), a marker for JNK activation, was performed on coronal brain sections of $Lep^{ob/ob}$ mice, their wild-type littermates and wild-type mice fed a HFD or a low-fat diet (LFD). The total number of phospho-JNK (Thr183/Tyr185) immunoreactive cells within the arcuate nucleus (ARC) and ventromedial hypothalamus (VMH) was counted in four region-matched sections of each animal. The number of phospho-JNK immunoreactive cells was increased in the ARC (A) and VMH (C) of $Lep^{ob/ob}$ mice compared to wild-type mice ($n = 5$ or 6 per group) and also during diet induced obesity in both nuclei (B and D, $n = 5$ or 6 per group). Data are the mean ± SEM, *$P \leq 0.05$, **$P \leq 0.01$, ***$P \leq 0.001$.

positive cells was strikingly reduced by the JNK-inhibitor in the ARC and the VMH compared to vehicle-treated $Lep^{ob/ob}$ mice. The magnitude of reduction was approximately two-fold in the ARC ($n = 6$–9 per group, $P < 0.001$) (Fig. 4A) and approximately four-fold in the VMH ($P = 0.002$) (Fig. 4A). Consistent with this decline of the inhibitory phosphorylation site of IRS-1, the i.c.v. JNK-inhibitor improved impaired PI3K signalling in these mice, as confirmed by a marked increase in the number of phospho-Akt (Ser473) immunoreactive cells in the ARC by 1.5-fold ($P < 0.001$) (Fig. 4B) and in the VMH by 2.5-fold ($P = 0.004$) (Fig. 4B).

It has been well established that intact insulin signalling appears to involve inhibition of GSK-3β via phosphorylation in muscle (36,37) and hypothalamus (38). Inactivation of GSK-3β is mainly accomplished by phosphorylation of GSK-3β at serine residue nine (39,40). To corroborate the finding that JNK inhibition leads to activation of insulin signaling in the hypothalamus, we measured pGSK-3β immunoreactive cells in the same experimental paradigm as shown above. Indeed, after JNK inhibition, the number of cells positive for phospho-GSK-3β was significantly increased by approximately 25% in the ARC and 40% in the VMH ($P = 0.03$, $P < 0.001$, $n = 6$–9 per group) (Fig. 4C).

Discussion

The hypothalamus represents a main insulin target tissue for regulating body weight and glucose metabolism. It was previously proposed that inflammatory changes occur in the hypothalamus of rodents that were fed a HFD (30). Subsequently, it has been established that DIO in rodents is associated with up-regulation of pro-inflammatory pathways in the hypothalamus, involving activation of signalling intermediates such as JNK and IKKβ/nuclear factor-κB (15,18,30,41). Moreover, peripheral inhibition of JNK-activity

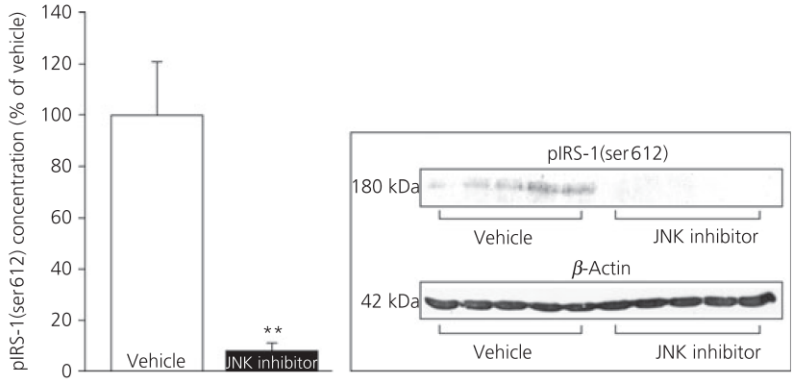

Fig. 2. Inhibition of c-Jun-N-terminal kinase (JNK) decreases phosphorylation of insulin-receptor substrate-1. Mouse hypothalamic cells (mHypoA-CLU190, CELLusions) were treated with vehicle or JNK inhibitor (SP600125, 40 μM) for 30 min. Phospho-insulin receptor substrate-1 (IRS-1) levels were semi-quantitatively assessed by immunoblotting using a specific antibody for phospho-IRS-1 (Ser612) and were normalised via β-actin. Values are plotted as the mean $\pm$ SEM of five repetitive experiments. **P $\leq$ 0.01.

protected against diet-induced insulin resistance (23,42–45). A conditional genetic inactivation of JNK-1 in the brain improved central and peripheral insulin sensitivity and whole body glucose metabolism, demonstrating that the hypothalamic JNK pathway plays an important role in the regulation of glucose homeostasis (18). Although powerful genetic data clearly established that the hypothalamus is the target site for JNK activity in the brain, the relative contribution of distinct nuclei contributing to the hypothalamic inflammation phenomenon remains to be unravelled.

In the present study, we demonstrate that JNK activity is markedly increased in glucose intolerant mice independent of whether this metabolic state was achieved by a mutation in the leptin gene or by DIO. Because the reasons for glucose derangements in $Lep^{ob/ob}$ mice and DIO mice are fundamentally different as a result of a lack of the cytokine leptin on the one hand and excessive circulating leptin concentrations associated with leptin resistance on the other, our data indicate that increased JNK activity is independent of leptin action. This concept is supported by a finding of increased JNK activity in the absence of endogenous leptin and, moreover, by a study performed by Münzberg *et al.* (2004) who reported a restriction of hypothalamic leptin resistance to the ARC during DIO in mice. Intriguingly, it was shown that, in mice fed a HFD, intracellular signalling of leptin in the VMH was functional, as demonstrated by the activation of STAT3 (46). Because JNK activity was increased in both hypothalamic regions in mice fed a HFD, our data suggest that increased activity of JNK at least in the VMH might not be involved in the development of leptin resistance.

We have previously shown that impaired central insulin signalling is associated with altered phosphorylation of IRS-1 (11). Using a pharmacological JNK-inhibitor, we tested the hypothesis that inhibition of JNK in a hypothalamic cell line reduces pIRS-1 (Ser612), whose inhibition has been recently demonstrated to be critical for central sensitisation of insulin signalling (11). We chose to pharmacologically inhibit JNK because it allows highly selective inhibition of JNK in the adult mouse brain. The specificity of SP600125 has been determined with > 300-fold selectivity for JNK over the related mitogen-activated kinases (47). Successful inhibition of JNK in the rat hypothalamus using this compound has also been described previously (30). Indeed, hypothalamic cells that were pre-treated with the JNK-inhibitor revealed a marked reduction in protein content of pIRS-1(Ser612), suggesting that JNK inhibition improves hypothalamic insulin signalling. Because impairment of central insulin signalling has been clearly shown to cause derangements in whole body glucose homeostasis (5,10,11), and because we demonstrated above that JNK activity is increased in glucose intolerant mice, we next hypothesised that central inhibition of JNK in these mice might improve their impaired whole body glucose homeostasis. In leptin-deficient mice, the JNK-inhibitor acutely (within 30 min) and dose dependently improved glucose tolerance. Using the higher dose (5 nmol), this result could be repeated in mice on HFD; however, the glucose-lowering effect appeared to be slightly smaller, which might be the result of less pronounced glucose intolerance in these mice compared to $Lep^{ob/ob}$ mice. Improvement in glucose tolerance via central JNK inhibition, using SP600125, is consistent with studies performed in mice exhibiting a neuronal JNK-1 knockout. However, the glucose-lowering capacity of the JNK-inhibitor in both $Lep^{ob/ob}$- and mice fed a HFD was of a greater magnitude compared to genetic ablation of the serine-kinase in mice fed a HFD (18,31). This discrepancy might be explained by the fact that the JNK-inhibitor blocks all three known JNK splice variants. Because neuronal ablation of JNK was restricted to the splice variant one, it is plausible that the other two isoforms are also involved in the central regulation of glucose homeostasis. Future studies are warranted to unravel the relative contribution of the three different splice variants to the neuroendocrine control of glucose metabolism.

The effect of the JNK-inhibitor on glucose tolerance was very acute, suggesting that it is not dependent on transcription of JNK target genes but rather through more rapid effects such as phosphorylation events or acute alterations in neuronal firing, including activation of the sympathetic outflow (48). Genetic ablation of central JNK-1 and chronic (18,31) large i.c.v. doses of SP600125

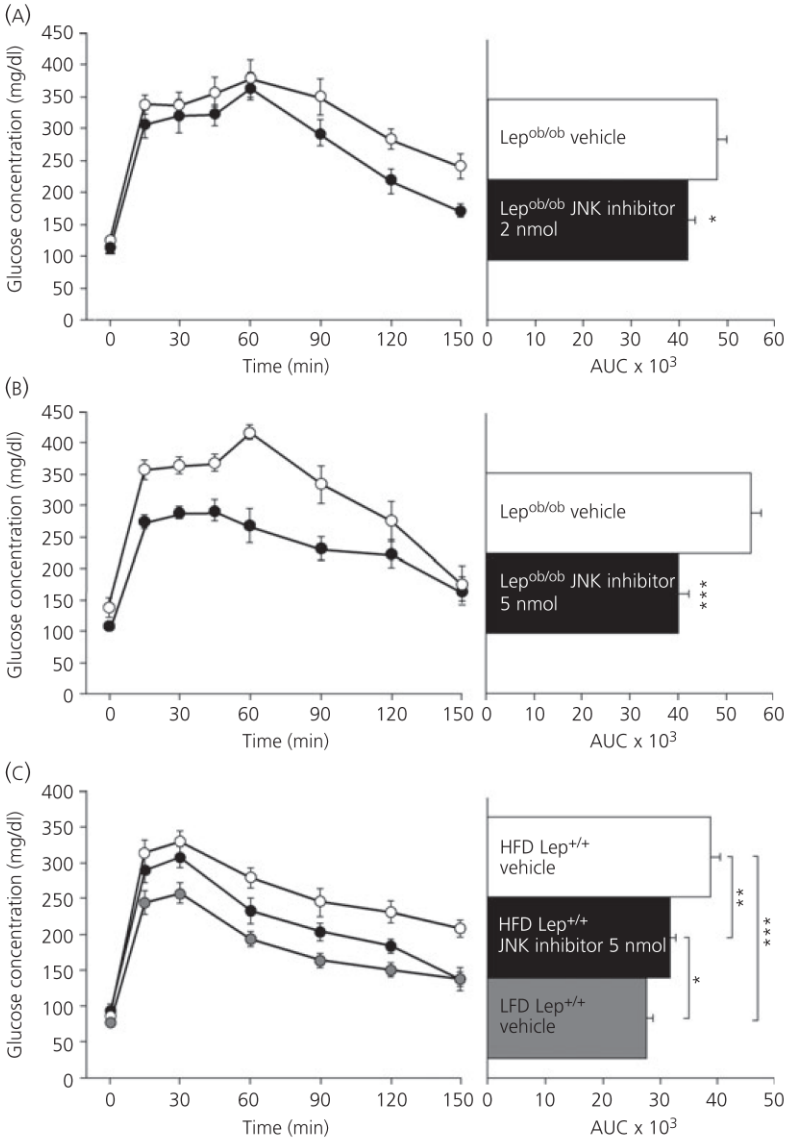

Fig. 3. Pharmacological inhibition of central c-Jun-N-terminal kinase (JNK) improves glucose tolerance. Shown are glucose concentrations (left) and associated area under the curve (AUC) (right) during an i.p. glucose tolerance test (i.p.-GTT). Central injection of the JNK inhibitor dose dependently improves glucose tolerance in Lep$^{ob/ob}$ mice. Intraperitoneal-GTT was performed 30 min after administration of the JNK inhibitor [2 nmol in 5% dimethylsulphoxide (DMSO)/artificial cerebrospinal fluid (aCSF), black circles] or vehicle (5% DMSO in aCSF, open circles) into the lateral ventricle (n = 6 or 7 per group). The JNK inhibitor was administered i.c.v. at 2 nmol (A) or 5 nmol (B) in 5% DMSO/aCSF (black circles). The same treatment also improves glucose tolerance in wild-type mice fed a high-fat diet for 3 weeks (black circles) compared to vehicle-treated mice (C, open circles, n = 5–7 per group) but with still attaining significant difference to mice on a low-fat diet (grey circles). Data show the mean ± SEM, *P $\leq$ 0.05, **P $\leq$ 0.01, ***P $\leq$ 0.001.

(23 μmol) twice daily for 1 week (30) were shown to improve insulin signalling in hypothalamic lysates. Whether these alterations in signalling events occur in important hypothalamic centres for the regulation of glucose homeostasis such as the ARC and VMH remains unresolved. Therefore, we sought to investigate whether post-translational modifications of essential molecules for central insulin signal transduction are modulated by i.c.v. JNK inhibition in these regions. Consistent with our result that pIRS-1(Ser612) was down-regulated in hypothalamic cells, we observed a reduction of pIRS-1(Ser612) immunoreactive cells in the ARC and VMH of Lep$^{ob/ob}$ mice after central inhibition of JNK. Down-regulation of this inhibitory phosphorylation site of IRS-1 was accompanied by an increased number of pAkt (Ser473) immunoreactive cells in both hypothalamic nuclei. Consistent with these findings, central

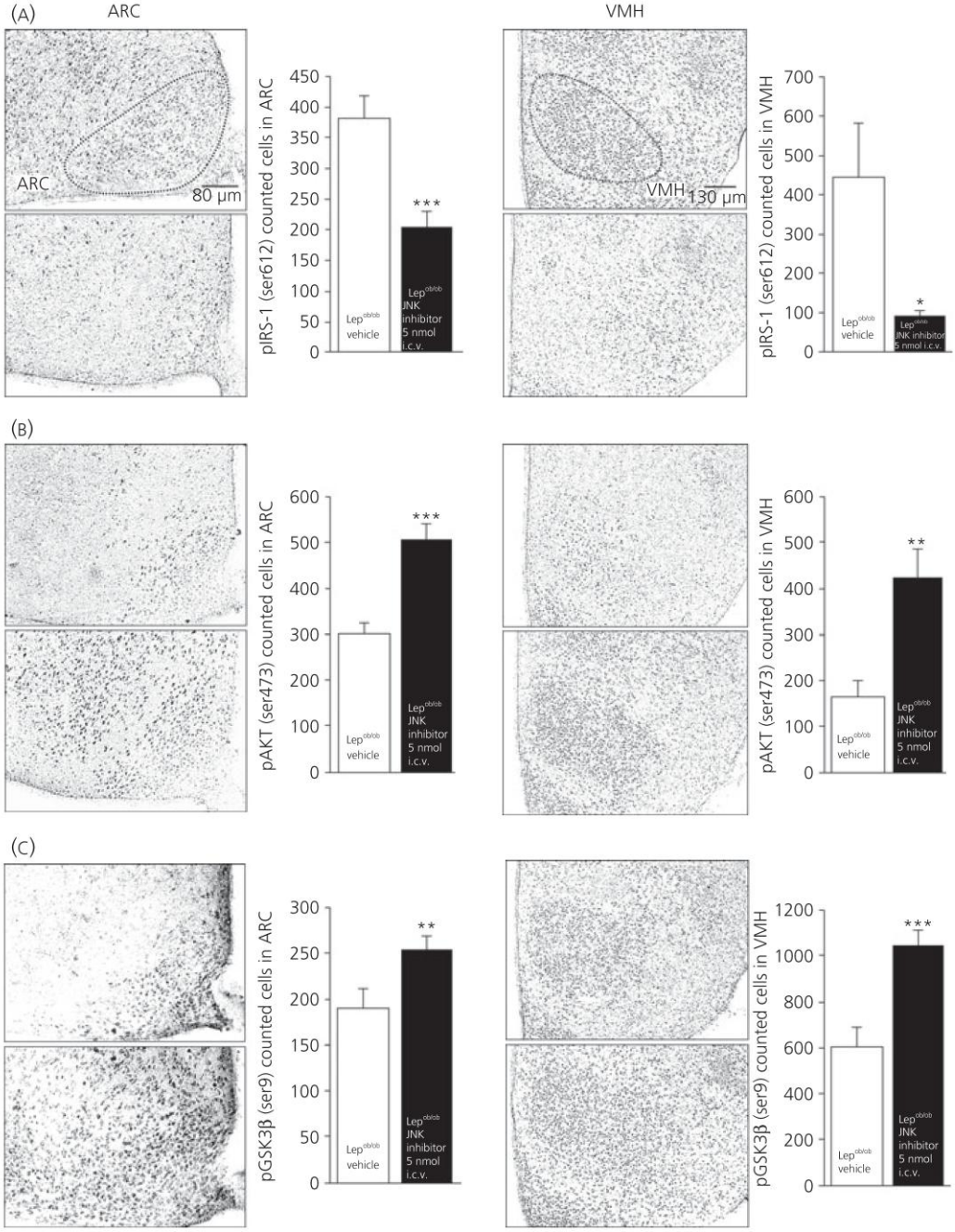

Fig. 4. Central inhibition of c-Jun-N-terminal kinase (JNK) improves deranged hypothalamic insulin signalling in leptin-deficient mice. Immunohistochemistry was performed on brain sections of $Lep^{ob/ob}$ mice after central administration of the JNK inhibitor [5 nmol in 5% dimethylsulphoxide (DMSO) in cerebrospinal fluid (aCSF)] or vehicle (5% DMSO in aCSF), 30 min before transcardial perfusion. Inserts depict representative images of immunoreactivity of important insulin signalling molecules in the arcuate nucleus (ARC) (left) and ventromedial hypothalamus (VMH) (right). The bar graph shows the counted cells in the ARC and VMH that were immunoreactive for (A) phospho-insulin receptor substrate-1 (IRS-1), (B) phospho-Akt (Ser473) and (C) phospho-GSK-3β (Ser9, n = 6–9 animals per group). Notably, JNK inhibition led to an improvement of insulin signalling in both hypothalamic nuclei. Data show the mean ± SEM. *$P \leq 0.05$; **$P \leq 0.01$; ***$P \leq 0.001$.

inactivation of JNK was associated with an increase in the number of pGSK-3β immunoreactive cells. GSK-3β serves as a downstream target of insulin signalling (36,37). Our studies clearly point towards the importance of the ARC and VMH in JNK signalling and its interaction with the insulin pathway. It has furthermore been shown that the neuropeptide Y/agouti-related peptide neurones are targets of the action of JNK (49). However, future studies are warranted to identify the neurochemical network that is involved in signal transduction of these pathways. Furthermore, it remains to be established whether other hypothalamic (such as the lateral and dorso-medial hypothalamus) or extra-hypothalamic regions reveal deranged JNK activity during obesity. For example, JNK has been associated with impaired insulin signalling in the hippocampus (50) and might therefore exaggerate impaired learning abilities that are caused by deranged insulin signalling in this brain region.

Taken together, in the present study, we demonstrate for the first time that, in physiological and genetic mouse models of obesity and glucose intolerance, JNK activity is similarly increased in the ARC and VMH, which are both important neuronal centres for the regulation of whole body glucose homeostasis. Hence, inflammation via JNK in the ARC and VMH appears to occur independent of absence of endogenous leptin ($Lep^{ob/ob}$ mice) or pathological hyperleptinaemia (DIO mice). Acute pharmacological inhibition of the JNK pathway in the adult mouse brain of these glucose intolerant mice improved whole body glucose homeostasis and was associated with improved insulin signalling in both hypothalamic regions independent of body weight changes. Reversing hypothalamic inflammation by pharmacological inhibition of pro-inflammatory pathways and possibly the development of novel isoform-specific JNK-inhibitors might be a promising novel tool to further unravelling the pathogenesis underlying obesity, diabetes and other associated diseases.

Acknowledgements

This study was funded by the German Ministry of Education and Research (reference number 0315087 to A.T.).

Received 28 September 2012,
revised 10 December 2012,
accepted 26 December 2012

References

1 Bastard JP, Maachi M, Lagathu C, Kim MJ, Caron M, Vidal H, Capeau J, Feve B. Recent advances in the relationship between obesity, inflammation, and insulin resistance. *Eur Cytokine Netw* 2006; **17**: 4–12.
2 Chan JC, Malik V, Jia W, Kadowaki T, Yajnik CS, Yoon KH, Hu FB. Diabetes in Asia: epidemiology, risk factors, and pathophysiology. *JAMA* 2009; **301**: 2129–2140.
3 Bruning JC, Gautam D, Burks DJ, Gillette J, Schubert M, Orban PC, Klein R, Krone W, Muller-Wieland D, Kahn CR. Role of brain insulin receptor in control of body weight and reproduction. *Science* 2000; **289**: 2122–2125.
4 Marks JL, Porte D Jr, Stahl WL, Baskin DG. Localization of insulin receptor mRNA in rat brain by in situ hybridization. *Endocrinology* 1990; **127**: 3234–3236.
5 Niswender KD, Morrison CD, Clegg DJ, Olson R, Baskin DG, Myers MG Jr, Seeley RJ, Schwartz MW. Insulin activation of phosphatidylinositol 3-kinase in the hypothalamic arcuate nucleus: a key mediator of insulin-induced anorexia. *Diabetes* 2003; **52**: 227–231.
6 Obici S, Zhang BB, Karkanias G, Rossetti L. Hypothalamic insulin signaling is required for inhibition of glucose production. *Nat Med* 2002; **8**: 1376–1382.
7 Obici S, Feng Z, Karkanias G, Baskin DG, Rossetti L. Decreasing hypothalamic insulin receptors causes hyperphagia and insulin resistance in rats. *Nat Neurosci* 2002; **5**: 566–572.
8 Okamoto H, Nakae J, Kitamura T, Park BC, Dragatsis I, Accili D. Transgenic rescue of insulin receptor-deficient mice. *J Clin Invest* 2004; **114**: 214–223.
9 Okamoto H, Obici S, Accili D, Rossetti L. Restoration of liver insulin signaling in Insr knockout mice fails to normalize hepatic insulin action. *J Clin Invest* 2005; **115**: 1314–1322.
10 Gelling RW, Morton GJ, Morrison CD, Niswender KD, Myers MG Jr, Rhodes CJ, Schwartz MW. Insulin action in the brain contributes to glucose lowering during insulin treatment of diabetes. *Cell Metab* 2006; **3**: 67–73.
11 Koch C, Augustine RA, Steger J, Ganjam GK, Benzler J, Pracht C, Lowe C, Schwartz MW, Shepherd PR, Anderson GM, Grattan DR, Tups A. Leptin rapidly improves glucose homeostasis in obese mice by increasing hypothalamic insulin sensitivity. *J Neurosci* 2010; **30**: 16180–16187.
12 Niswender KD, Morton GJ, Stearns WH, Rhodes CJ, Myers MG Jr, Schwartz MW. Intracellular signalling. Key enzyme in leptin-induced anorexia. *Nature* 2001; **413**: 794–795.
13 Zhao AZ, Huan JN, Gupta S, Pal R, Sahu A. A phosphatidylinositol 3-kinase phosphodiesterase 3B-cyclic AMP pathway in hypothalamic action of leptin on feeding. *Nat Neurosci* 2002; **5**: 727–728.
14 Boden G. Role of fatty acids in the pathogenesis of insulin resistance and NIDDM. *Diabetes* 1997; **46**: 3–10.
15 Posey KA, Clegg DJ, Printz RL, Byun J, Morton GJ, Vivekanandan-Giri A, Pennathur S, Baskin DG, Heinecke JW, Woods SC, Schwartz MW, Niswender KD. Hypothalamic proinflammatory lipid accumulation, inflammation, and insulin resistance in rats fed a high-fat diet. *Am J Physiol Endocrinol Metab* 2009; **296**: E1003–E1012.
16 Thaler JP, Schwartz MW. Minireview: inflammation and obesity pathogenesis: the hypothalamus heats up. *Endocrinology* 2010; **151**: 4109–4115.
17 Thaler JP, Yi CX, Schur EA, Guyenet SJ, Hwang BH, Dietrich MO, Zhao X, Sarruf DA, Izgur V, Maravilla KR, Nguyen HT, Fischer JD, Matsen ME, Wisse BE, Morton GJ, Horvath TL, Baskin DG, Tschop MH, Schwartz MW. Obesity is associated with hypothalamic injury in rodents and humans. *J Clin Invest* 2012; **122**: 153–162.
18 Belgardt BF, Mauer J, Wunderlich FT, Ernst MB, Pal M, Spohn G, Bronneke HS, Brodesser S, Hampel B, Schauss AC, Bruning JC. Hypothalamic and pituitary c-Jun N-terminal kinase 1 signaling coordinately regulates glucose metabolism. *Proc Natl Acad Sci USA* 2010; **107**: 6028–6033.
19 Hotamisligil GS. Inflammation and metabolic disorders. *Nature* 2006; **444**: 860–867.
20 Shoelson SE, Lee J, Goldfine AB. Inflammation and insulin resistance. *J Clin Invest* 2006; **116**: 1793–1801.
21 Weston CR, Davis RJ. The JNK signal transduction pathway. *Curr Opin Cell Biol* 2007; **19**: 142–149.
22 Davis RJ. Signal transduction by the JNK group of MAP kinases. *Cell* 2000; **103**: 239–252.
23 Hirosumi J, Tuncman G, Chang L, Gorgun CZ, Uysal KT, Maeda K, Karin M, Hotamisligil GS. A central role for JNK in obesity and insulin resistance. *Nature* 2002; **420**: 333–336.
24 Aguirre V, Uchida T, Yenush L, Davis R, White MF. The c-Jun NH(2)-terminal kinase promotes insulin resistance during association with insulin

receptor substrate-1 and phosphorylation of Ser(307). *J Biol Chem* 2000; **275**: 9047–9054.
25 Aguirre V, Werner ED, Giraud J, Lee YH, Shoelson SE, White MF. Phosphorylation of Ser307 in insulin receptor substrate-1 blocks interactions with the insulin receptor and inhibits insulin action. *J Biol Chem* 2002; **277**: 1531–1537.
26 Lee YH, Giraud J, Davis RJ, White MF. c-Jun N-terminal kinase (JNK) mediates feedback inhibition of the insulin signaling cascade. *J Biol Chem* 2003; **278**: 2896–2902.
27 Nguyen MT, Satoh H, Favelyukis S, Babendure JL, Imamura T, Sbodio JI, Zalevsky J, Dahiyat BI, Chi NW, Olefsky JM. JNK and tumor necrosis factor-alpha mediate free fatty acid-induced insulin resistance in 3T3-L1 adipocytes. *J Biol Chem* 2005; **280**: 35361–35371.
28 Sabio G, Das M, Mora A, Zhang Z, Jun JY, Ko HJ, Barrett T, Kim JK, Davis RJ. A stress signaling pathway in adipose tissue regulates hepatic insulin resistance. *Science* 2008; **322**: 1539–1543.
29 Sabio G, Kennedy NJ, Cavanagh-Kyros J, Jung DY, Ko HJ, Ong H, Barrett T, Kim JK, Davis RJ. Role of muscle c-Jun NH2-terminal kinase 1 in obesity-induced insulin resistance. *Mol Cell Biol* 2010; **30**: 106–115.
30 De Souza CT, Araujo EP, Bordin S, Ashimine R, Zollner RL, Boschero AC, Saad MJ, Velloso LA. Consumption of a fat-rich diet activates a proinflammatory response and induces insulin resistance in the hypothalamus. *Endocrinology* 2005; **146**: 4192–4199.
31 Sabio G, Cavanagh-Kyros J, Barrett T, Jung DY, Ko HJ, Ong H, Morel C, Mora A, Reilly J, Kim JK, Davis RJ. Role of the hypothalamic-pituitary-thyroid axis in metabolic regulation by JNK1. *Genes Dev* 2010; **24**: 256–264.
32 Tups A, Anderson GM, Rizwan M, Augustine RA, Chaussade C, Shepherd PR, Grattan DR. Both p110alpha and p110beta isoforms of phosphatidylinositol 3-OH-kinase are required for insulin signalling in the hypothalamus. *J Neuroendocrinol* 2010; **22**: 534–542.
33 De Fea K, Roth RA. Protein kinase C modulation of insulin receptor substrate-1 tyrosine phosphorylation requires serine 612. *Biochemistry* 1997; **36**: 12939–12947.
34 Zheng Y, Zhang W, Pendleton E, Leng S, Wu J, Chen R, Sun XJ. Improved insulin sensitivity by calorie restriction is associated with reduction of ERK and p70S6K activities in the liver of obese Zucker rats. *J Endocrinol* 2009; **203**: 337–347.
35 Ganjam GK, Dimova EY, Unterman TG, Kietzmann T. FoxO1 and HNF-4 are involved in regulation of hepatic glucokinase gene expression by resveratrol. *J Biol Chem* 2009; **284**: 30783–30797.
36 Cross DA, Alessi DR, Cohen P, Andjelkovich M, Hemmings BA. Inhibition of glycogen synthase kinase-3 by insulin mediated by protein kinase B. *Nature* 1995; **378**: 785–789.
37 Shaw M, Cohen P, Alessi DR. Further evidence that the inhibition of glycogen synthase kinase-3beta by IGF-1 is mediated by PDK1/PKB-induced phosphorylation of Ser-9 and not by dephosphorylation of Tyr-216. *FEBS Lett* 1997; **416**: 307–311.
38 Benzler J, Ganjam GK, Kruger M, Pinkenburg O, Kutschke M, Stohr S, Steger J, Koch CE, Olkrug R, Schwartz MW, Shepherd PR, Grattan DR, Tups A. Hypothalamic glycogen-synthase-kinase 3beta has a central role in the regulation of food intake and glucose metabolism. *Biochem J* 2012; **77**: 77–77.
39 Stambolic V, Woodgett JR. Mitogen inactivation of glycogen synthase kinase-3 beta in intact cells via serine nine phosphorylation. *Biochem J* 1994; **303**: 701–704.
40 Sutherland C, Leighton IA, Cohen P. Inactivation of glycogen synthase kinase-3 beta by phosphorylation: new kinase connections in insulin and growth-factor signalling. *Biochem J* 1993; **296**: 15–19.
41 Zhang X, Zhang G, Zhang H, Karin M, Bai H, Cai D. Hypothalamic IKKbeta/NF-kappaB and ER stress link overnutrition to energy imbalance and obesity. *Cell* 2008; **135**: 61–73.
42 Bennett BL, Satoh Y, Lewis AJ. JNK: a new therapeutic target for diabetes. *Curr Opin Pharmacol* 2003; **3**: 420–425.
43 Kaneto H, Kawamori D, Nakatani Y, Gorogawa S, Matsuoka TA. Oxidative stress and the JNK pathway as a potential therapeutic target for diabetes. *Drug News Perspect* 2004; **17**: 447–453.
44 Kaneto H, Nakatani Y, Miyatsuka T, Kawamori D, Matsuoka TA, Matsuhisa M, Kajimoto Y, Ichijo H, Yamasaki Y, Hori M. Possible novel therapy for diabetes with cell-permeable JNK-inhibitory peptide. *Nat Med* 2004; **10**: 1128–1132.
45 Nakatani Y, Kaneto H, Kawamori D, Hatazaki M, Miyatsuka T, Matsuoka TA, Kajimoto Y, Matsuhisa M, Yamasaki Y, Hori M. Modulation of the JNK pathway in liver affects insulin resistance status. *J Biol Chem* 2004; **279**: 45803–45809.
46 Munzberg H, Flier JS, Bjorbaek C. Region-specific leptin resistance within the hypothalamus of diet-induced obese mice. *Endocrinology* 2004; **145**: 4880–4889.
47 Bennett BL, Sasaki DT, Murray BW, O'Leary EC, Sakata ST, Xu W, Leisten JC, Motiwala A, Pierce S, Satoh Y, Bhagwat SS, Manning AM, Anderson DW. SP600125, an anthrapyrazolone inhibitor of Jun N-terminal kinase. *Proc Natl Acad Sci USA* 2001; **98**: 13681–13686.
48 Klieverik LP, Janssen SF, van Riel A, Foppen E, Bisschop PH, Serlie MJ, Boelen A, Ackermans MT, Sauerwein HP, Fliers E, Kalsbeek A. Thyroid hormone modulates glucose production via a sympathetic pathway from the hypothalamic paraventricular nucleus to the liver. *Proc Natl Acad Sci USA* 2009; **106**: 5966–5971.
49 Unger EK, Piper ML, Olofsson LE, Xu AW. Functional role of c-Jun-N-terminal kinase in feeding regulation. *Endocrinology* 2010; **151**: 671–682.
50 Junyent F, de Lemos L, Verdaguer E, Folch J, Ferrer I, Ortuno-Sahagun D, Beas-Zarate C, Romero R, Pallas M, Auladell C, Camins A. Gene expression profile in JNK3 null mice: a novel specific activation of the PI3K/AKT pathway. *J Neurochem* 2011; **117**: 244–252.

Central inhibition of NF-κB signalling improves glucose homeostasis in mice

Jonas Benzler*, Goutham K. Ganjam†, Christiane E. Koch*, Dominik Pretz*, Rebecca Oelkrug*, Christiane E. Koch*, Karen Legler*, Sigrid Stöhr*, Carsten Culmsee†, Lynda M. Williams° and Alexander Tups*

*Department of Animal Physiology, Faculty of Biology, Philipps University Marburg, Marburg, Germany

† Institute of Pharmacology and Clinical Pharmacy, Faculty of Pharmacy, Philipps University Marburg, Marburg, Germany

° Metabolic Health Group, Rowett Institute of Nutrition and Health, University of Aberdeen, Aberdeen AB21 9SB, United Kingdom

Proofs and correspondence to:
Dr. Alexander Tups
Department of Animal Physiology, Faculty of Biology, Philipps University Marburg, Karl-von-Frisch Str. 8 D-35043 Marburg, Germany
e-mail: alexander.tups@staff.uni-marburg.de

Keywords: Arcuate nucleus, IκBα, butein, inflammation, leptin, SOCS-3

Acknowledgments
This study was funded by the German Ministry of Education and Research (Ref. No: 0315087, to AT).

We thank William C. Hahn (Dana-Farber Cancer Institute, Boston, USA) for providing the pBabe-GFP-IKBalpha-mut (super repressor) vector.

Abstract

Metabolic inflammation in the central nervous system might be causative for the development of overnutrition-induced metabolic syndrome and related disorders such as obesity, leptin- and insulin - resistance and type II diabetes. Here we investigated whether nutritive and genetic inhibition of the central IKKβ/NF-κB pathway in DIO- and leptin deficient mice improves these metabolic impairments. A known prominent inhibitor of IKKβ/NF-κB signalling is the dietary flavonoid butein. We initially determined that oral and intracerebroventricular administration of this flavonoid acutely improved glucose tolerance and hypothalamic insulin signalling. The dose-dependent glucose lowering capacity was profound regardless of whether obesity was caused by leptin deficiency or high fat diet. To confirm the apparent central role of IKKβ/NF-κB signalling in the regulation of glucose- and energy homeostasis we genetically inhibited this pathway in neurons of the arcuate nucleus, the key centre for regulation of energy homeostasis, via specific AAV2-mediated over expression of IκBα, which inhibits NF-κB nuclear translocation. This treatment decelerated high fat diet-induced body weight gain, body fat mass accumulation, increased energy expenditure without altering food intake and reduced arcuate SOCS3 expression, suggesting enhanced leptin signalling. These results reinforce a specific role of pro-inflammatory IKKβ/NF-κB signalling in the development of DIO-induced co-morbidities.

Introduction

Obesity, as a consequence of overnutrition, reflects a high risk factor for the development of insulin resistance and ultimately type II diabetes (1;2). The hypothalamus represents a main insulin target tissue for regulating body weight and glucose metabolism (3-9). De Souza et al. proposed that inflammatory alterations occur in the hypothalamus of rodents that were fed a high fat diet (HFD) (10). Subsequently, it has been established that diet-induced obesity in rodents is associated with up-regulation of pro-inflammatory pathways in the hypothalamus, involving activation of signalling intermediates such as c-Jun N-terminal kinase and IκB kinase β (IKKβ) / nuclear factor-κB (NF-κB) (10-14). The IKKβ / NF-κB pathway, as a pro-inflammatory pathway, plays a pivotal role in classical immune response (15). In stationary state, NF-κB lingers in the cytoplasm in an inactive form and is bound to the inhibitory binding protein IκBα. A broad range of immune stimuli can activate the upstream kinase IKKβ, leading to IκBα phosphorylation (at Ser32 and Ser36) and degradation and subsequently to the release of NF-κB. Activated NF-κB enters the nucleus to induce transcription of target-genes that mediate diverse cellular processes such as immunity, inflammation, proliferation and apoptosis (16). It has been well established that HFD mediates metabolic inflammation in the central nerve system, particularly in the hypothalamus, which is associated with the development of overnutrition-induced metabolic syndrome and related disorders such as obesity, leptin- and insulin - resistance (10;13;14;17-19).

Secondary metabolites of herbs and spices are well known to act as an antioxidant, to reduce proinflammatory cytokines and to suppress inflammation (20) and are often used in traditional Chinese medicine. The flavonoid butein (3, 4, 2´, 4´ -tetrahydroxychalcone), which is found in herbs such as *Caragana jubata* and *Rhus verniciflua*, inhibits NF-κB signalling by direct blockade of the upstream kinase IKKβ (21).

In the current study we tested whether specific nutritive or genetic inhibition of IKKβ / NF-κB signalling in the brain improves glucose- and energy- metabolism during obesity. We first established that nutritive inhibition of IKKβ / NF-κB signalling via enteral or intracerebroventricular (icv) butein administration reveals potent glucose lowering properties independent as to whether obesity was caused by leptin deficiency or high fat feeding. These effects were associated with improved insulin-signalling involving the insulin receptor substrate (IRS)-phosphatidylinositol 3-kinase (PI3K) pathway in the arcuate nucleus (ARC), the key brain region required for the regulation of glucose- and energy homeostasis (5;22;23). To specifically inhibit downstream IKKβ / NF-κB signalling a AAV2 construct allowing overexpression of IκBα was generated that was specifically injected into the parentchyma of the ARC. By the replacement of the inhibitory phosphorylation sides Moreover, the inhibitory serine phosphorylation sites of IκBα were replaced by alanine [IκBα-mt (Serine 32 to Alanine, Serine 36 to Alanine)] hindering nuclear translocation of NF-κB and therefore inhibiting downstream signalling

events. Corroborating the essential role of central IKKβ / NF-κB signalling in the regulation of glucose- and energy homeostasis this treatment partially protected from high fat diet-induced metabolic impairments.

Materials and methods

All procedures were performed in accordance with national animal ethics legislation and received approval by the respective authorities for animal ethics All experiments used male mice (C57BL/6J) that were purchased from Janvier (Le Genest-Saint-Isle, France). The animals were seven weeks of age at the time of arcuate nucleus- directed AAV-2 IκBα-mt administration and housed individually under standard conditions with a light/dark cycle of 12h. The ambient temperature for mice was 23°C. All animals had access to standard chow diet (cat. no. V1534, ssniff®), low fat diet or high fat diet, (containing 10% or 60% fat respectively, cat. no. D12450B and D12492, Research Diets) as stated in the text and water *ad libitum.*For central administration of drugs**,** cannulae were stereotaxically implanted into the left lateral ventricle as described previously (23).

Stereotaxic injections

Intracerebral injections were performed under isoflurane anaesthesia as described previously (23). Stereotaxic co-ordinates to reach the hypothalamic ARC are 1.5mm posterior, ±0.3mm lateral and 6.1 mm ventral relative to Bregma. AAV2 particles, containing 4×10^{10} vector genomes, were injected into the ARC using a 0.5µl Hamilton glass syringe for 2min. The injection needle remained in place at each injection site for an additional 5min to allow for diffusion and prevent backflow. The incision was sutured and the animals were placed under a heating lamp to recover from the surgery.

Glucose tolerance tests / Insulin tolerance test

In a first approach, we analysed whether the flavonoid butein (0.08, 0.8, or 8mg/kg body weight in PBS containing 5% ethanol) is able to improve glucose tolerance. Therefore, 8 weeks old leptin deficient mice ($Lep^{ob/ob}$) were fasted for 16h and received butein orally. Sixty minutes later glucose (1.0g/kg) was intraperitoneally (ip) injected and a glucose tolerance test (GTT) was performed (n= 8/group). To determine the blood glucose levels, the *Vena facialis* was repeatedly punctured and glucose concentration was measured using a commercially available glucometer (Roche; Accu-Check Performa). For statistical validation the area under the curve was calculated.

We next determined whether the effect of butein on glucose homeostasis is mediated via a central mechanism. Therefore, $Lep^{ob/ob}$ mice were fasted for 16h and butein (5nmol in 1µl aCSF/ 5%DMSO) was icv injected, 30 minutes before glucose injection followed by an ipGTT as described above (n= 8/group).

We next investigated whether central administration of butein also improves glucose tolerance in diet-induced obese, glucose intolerant mice. Mice were fed a HFD or respective low fat diet (LFD) for three weeks, fasted for 16h and weight matched. Butein was adminsitered icv (5nmol in 1µl aCSF/5%DMSO) to one group of mice on HFD (n=6), whereas the second group received an icv vehicle injection (aCSF/5%DMSO). The cohort on the LFD received vehicle icv (aCSF/5%DMSO, n=5-7/group), 30 minutes prior to the ipGTT.

We investigated whether over-expression of hypothalamic IκBα-mt might improve glucose tolerance. Therefore, after 5 weeks of HFD, mice were fasted for 16 h and received ip glucose (1.5g glucose /kg body weight) and an ipGTT was performed as described above.
To determine whether IκBα-mt over-expression affects insulin sensitivity, an insulin tolerance test was performed. After 7 weeks on HFD, mice were fasted for 16h and received ip 1mg/kg insulin, 30 minutes before the insulin tolerance test was performed, and blood glucose values were analysed as described above.

Recombinant adeno-associated viral vector generation and virus production

The cDNA for IκBα-mt (Serine 32 to Alanine, Serine 36 to Alanine) was subcloned from the eukaryotic expression vector pBabe-GFP-IκB-alpha-mut (super repressor, Addgene, 15264) into an AAV2-hSyn-EGFP-WPRE vector (24). IκBα-mt cDNA was amplified from the plasmid by PCR (phusion DNA polymerase) using the forward, 5′- TTTAGCTAGCCCTCACTCCTTCTC -3′ and reverse, 5′- CAGTGTACACCACTGTGCTGGC -3′ primers. These primers contain suitable Nhe1 and BsrG1 restriction sites for cloning into the AAV (adeno-associated virus) construct. Amplified PCR product was first cloned into the pGemT easy cloning vector. The IκBα-mt cDNA fragment from pGemT easy vector was subcloned into Nhe1 and BsrG1 sites of AAV2-hSyn-EGFP-WPRE by replacing EGFP (enhanced green fluorescent protein) cDNA to obtain AAV2-hSyn-IκBα-mt-WPRE. In this vector system the expression of IκBα-mt is under the control of the human synapsin-1 promoter to restrict the expression to neurons and WPRE [WHV (Woodchuck hepatitis virus) post-transcriptional regulatory element] facilitates long-term expression of the transgene. All molecular cloning procedures were performed in SURE2 bacterial cells to minimize the recombination events. Virus transfection and production was performed as described previously (25). The ability of AAV2 vectors to drive neuronal expression of a transgene was validated by infecting differentiated LUHMES (human post-mitotic dopaminergic neurons) cells (Suppl Fig. 1a and b, $P<0.001$). Successful over-expression of IκBα-mt in the ARC was validated by *in-situ* hybridization and revealed 80% increase of IκBα expression in the ARC (Suppl Fig. 1c, $P< 0.001$).

Cell culture

Differentiated LUHMES (Lund human mesencephalic) cells (26) were used to investigate the expression of neuronal specific AAV2-hSyn-IκBα- mutant virus. LUHMES cells were proliferated on flasks (Nunclon DELTA surface) coated with 0.1mg/ml poly-L-lysine (Sigma-Aldrich) at 4°C overnight. For experiments 0.6 million cells were seeded on 6 well plates coated with 0.1mg/ml poly-L-lysine overnight and washed three times with sterile water followed by coating with 5 µg/ml fibronectin (Sigma-Aldrich) overnight in the incubator (37°C, 5% CO_2). Following 24 hours of plating the medium was exchanged with differentiation medium (DMEM/F12 with 1% N2-supplement, 1µg/ml tetracycline, 0.49 mg/ml dibutyryl cyclic AMP, Sigma-Aldrich, and 2 ng/ml

GDNF, R&D Systems). Four days after differentiation the medium was exchanged and infected with AAV2_EGFP as control and AAV2-hSyn- IκBα- mutant viruses at a concentration of 10^{10} GU/ml. After 5 days of infection the cells were lysed and the total protein was used to investigate the IκBα expression by westernblot.

Metabolic measurement

We measured the effect of the AAV-2 IκBα-mt on metabolic rate. Accordingly, carbon dioxide production (VCO_2) and oxygen consumption (VO_2) were measured in metabolic cages (~5 l vol.). Measurements were taken continuously for 24 hours with a constant ambient temperature of 23°C. The air flow in the cage was adjusted to ~42 l/h and continuously monitored. The procedure has been described in detail previously (27).

***In-situ* hybridization**

To determine the mRNA expression of IκBα and SOCS-3 (suppressor of cytokine signalling 3) in the ARC we performed *in-situ* hybridization on coronal brain sections. As previously described (28), forebrain sections (16 μm) were collected throughout the extent of the ARC on to a set of twelve slides, with twelve sections mounted on each slide. Accordingly, the slides spanned the hypothalamic region approximating from −2.8 to −1.22 mm relative to Bregma according to the atlas of the mouse brain (29). *In-situ* hybridizations and analysis was performed as described previously (28).

Body composition

To analyse body composition, mice were anaesthetized with isoflurane (CP-Pharma) and were analysed via DEXA (dual-emission X-ray absorptiometry)-scan (Lunar PIXImus Densitometer; GE Medical Systems).

Immunohistochemistry

For a possible interaction of butein with central insulin signalling, we investigated the phosphorylation of AKT in the ARC after butein treatment. Therefore, $Lep^{ob/ob}$ mice were fasted for 16 hours and received icv either butein (5nmol in 1µl aCSF/ 5% DMSO) or vehicle (1µl aCSF/ 5% DMSO) 30 minutes before transcardial perfusion (n= 7/group). Immunohistochemistry was carried out on mouse brain coronal cryosections as described previously (23;30), using an anti-(phospho-AKT Ser^{473}) antibody (Cell Signaling Technology, catalogue number 4058).

Statistics

The data were analysed by one way ANOVA followed by a Holm–Sidak comparison test, as appropriate, using SigmaStat statistical software (Jandel). Where data failed equal variance or normality tests, they were analysed by one-way ANOVA on ranks followed by Dunn's multiple

comparison test. The body weight data were analysed by Repeated Measurements two-way ANOVA. The results are presented as means±S.E.M. and differences were considered significant if $P \leq 0.05$.

Results

The flavonoid butein improves glucose homeostasis

Hypothalamic NF-κB signalling is associated with obesity and the impairment of insulin- and leptin signalling (13;14;17-19). As an intitial approach we tested whether nutritive inhibition of the of the IKKβ / NF-κB pathway.by butein affects glucose homeostasis.. Butein dose-dependently improved glucose tolerance in glucose intolerant, leptin deficient ($Lep^{ob/ob}$) mice as revealed by the ipGTT 60 min after oral administration.. The two lower doses (0.08mg/kg and 0.8mg/kg) revealed a trend towards improved glucose tolerance compared with the vehicle treated group whereas the higher dose (8mg/kg) significantly improved glucose tolerance in these mice relative to vehicle treated controls (Fig. 1a, n=8 animals/group, *P*= 0.009**)**. After this initial characterization, we sought to determine whether the effect of butein on glucose homeostasis was mediated through a central mechanism. Therefore, $Lep^{ob/ob}$ mice received icv butein (5nmol), 30 min prior to glucose and an ipGTT was performed. Indeed, acute icv administration of butein also improved glucose tolerance in $Lep^{ob/ob}$ mice compared with the $Lep^{ob/ob}$ vehicle treated group (Fig. 1b, n= 8/group, *P*= 0.007). We next investigated whether the glucose lowering properties of butein are mediated through interaction with hypothalamic insulin signalling. The number of cells positive for phospho-AKT (Ser^{473}) as a marker for PI3K activation (23),, was strikingly increased in the ARC after central administration of butein (5nmol in 1µl aCSF) by 66% relative to the vehicle (1µl in aCSF) treated $Lep^{ob/ob}$ mice (Fig. 1c, *P*= 0.003, n=7/group).

To verify that the glucose lowering capacity of butein is not restricted to $Lep^{ob/ob}$ mice, we assessed its effect on glucose homeostasis in DIO mice. Icv injection of butein (5nmol) 30 min prior to the ipGTT improved glucose tolerance significantly relative to the vehicle treated group on the same diet (*P*= 0.008) so profoundly that no difference could be detected to the vehicle treated cohort on the LFD group (Fig. 1d, n= 5-7/group).

Over expression of IκBα-mt decelerates diet induced obesity

The ARC represents a key brain region for neuronal control of energy and glucose homeostasis. To test whether NF-κB- mediated inflammation in the ARC affects glucose- and energy- homeostasis, we inhibited NF-κB signalling via ARC-directed injection of $4*10^{10}$ genomic units of either AAV2–IκBα-mt (n= 6) or a control AAV2 virus (n=10) into 8-week-old wild-type mice. Neuron specific expression of IκBα-mt mRNA was facilitated by the human synapsin-1 promoter to restrict the expression to neurons. After 12 days on standard chow diet, both groups of mice did not differ in body weight and were switched to HFD for 50 days (Fig. 2a). Immediately after the shift to HFD, an elevation of the body weight trajectory occurred in both groups. However, the increase in body weight induced by the HFD was decelerated in AAV2– IκBα-mt mice compared with the mice that received the control virus. This effect became significant within 17 days after receiving the HFD and reached a plateau value of 10% less than the controls by day 38 which was sustained until the end of the study.

DEXA analysis revealed a significant reduction of body fat mass (Fig. 2b, *P*= 0.027) by approximately 35% of the IκBα-mt group relative to the control cohort, whereas lean mass, bone mineral content (BMC) and bone mineral density (BMD) was not unaltered (Fig. 2c, d and e) by adeno-associated over expression of IκBα-mt in the ARC.

Over expression of IκBα-mt improves glucose homeostasis

Basal blood glucose levels were lower in the AAV2– IκBα-mt mice compared with the HFD controls (Fig. 3a, *P*= 0.033). To determine whether NF-κB signalling in the ARC alters neuronal control of glucose homoeostasis, we performed an ipGTT in these mice on the 48th day after viral injection Viral over-expression of IκBα-mt in the ARC improved glucose tolerance in comparison with the controls (Fig. 3b, *P*= 0.011). Furthermore, the insulin tolerance test revealed that the clearance rate of glucose was significantly increased in the AAV2– IκBα-mt mice relative to the AAV2-EGFP mice (Fig. 3c, *P*= 0.027).

Metabolic measurements

The mediobasal hypothalamus regulates energy balance by adjusting food intake to the metabolic needs (3;5-7;9). To explore whether ARC-directed IκBα over-expression alters metabolism, various metabolic markers were assessed. During the period of the metabolic measurements (day 33 - 34 after viral injection) no difference in food intake between AAV2– IκBα-mt- (3.00g ± 0.2g / 24h)and AAV2-EGFP- mice (2.92g ± 0.09g /24h) could be detected (Fig. 4a). However, average metabolic rate, measured as oxygen consumption, was increased by 13% in AAV2– IκBα-mt mice (90.2 ± 4.5 ml O_2 h^{-1}) relative to the AAV2-EGFP mice (79.5 ± 2.7 ml O_2 h^{-1}, Fig. 4b, *P*= 0.049). Furthermore, daily energy expenditure in these mice was also elevated by 13% (43.3 ± 2.2 kJ/g) relative to AAV2-EGFP controls (38.2 ± 1.3 kJ/g, Fig. 4c, *P*= 0.049), whereas the respiratory quotient was not different between the group (AAV2– IκBα-mt, 0.84 ± 0.008 vs. AAV2-EGFP, 0.85 ± 0.002, Fig 4d). In addition, resting metabolic rate (RMR) was elevated in the AAV2– IκBα-mt group (70.5 ± 2.4 ml O_2 h^{-1}) relative to AAV2-EGFP controls (62.0 ± 2.1 ml O_2 h^{-1}, Fig 4e, *P*= 0.038) which equals a 14% increase. A correction for the influence of body weight by calculating the RMR/g body weight revealed an increase in RMR of 27% in AAV2– IκBα-mt mice (2.3 ± 0.07 ml O_2 h^{-1} g^{-1}) relative to the AAV2-EGFP controls (1.8 ± 0.06 ml O_2 h^{-1} g^{-1},Fig. 4f, *P*= 0.006). To exclude that the detected metabolic changes are not secondarily based on altered activity between the groups, the maximal oxygen consumption was assessed. Complying with unaltered activity the maximal oxygen consumption did not differ between AAV2– IκBα-mt mice (173.8 ± 17.4 ml O_2 h^{-1}) relative to the AAV2-EGFP controls mice (153.1 ± 8.8 ml O_2 h^{-1}, Fig. 4 g).

Arcuate gene expression of suppressor of cytokine signalling 3 is decreased in response to ARC-directed IκBα-mt over-expression

To test whether Arc-directed adeno-associated viral over-expression of IκBα-mt might alter leptin sensitivity on a molecular level, we investigated the expression of suppressor of cytokine signalling 3 (SOCS-3), as the most prominent inhibitor of leptin signalling (31;32). *In-situ* hybridization analysis revealed that SOCS-3 mRNA was decreased by 35% in the ARC of AAV-2 IκBα-mt mice relative to controls (Fig. 4, P=0.029).

Discussion

Obesity and related metabolic disorders are largely the result of overconsumption of energy dense foods which are high in sugar and long chain saturated fats. Diet-induced obesity leads to insulin resistance with numerous studies showing that both obesity and insulin resistance are related to the presence of a low-grade inflammatory state (33). Some studies have shown that obesity is associated with inflammation in the hypothalamus (10-14), the central regulator of whole body energy- and glucose homeostasis (3-9). It appears that saturated fatty acids may directly activate the toll-like-receptor-4 (34) which subsequently leads to the activation of the downstream JNK and IKKβ/NF-κB cascade (13;19;35). In particular modulation of the IKKβ / NF-κB pathway at the level of IKKβ and the upstream adaptor regulatory protein MyD88 suggested that this cascade, once activated induces diet-induced resistance to the adiposity signals leptin and insulin (14;18).

While accumulating evidence supports the hypothalamic inflammation theory, studies involving a nutritive and genetherapeutic approach to functionally assess whether direct inhibition of this cascade leads to metabolic improvements, are scarce. As a nutritive intervention strategy to combat experimental glucose intolerance in genetic and dietary mouse-models of obesity we identified the flavonoid butein as a potent glucose lowering agent. Dose dependent enteral and icv application of butein improved glucose tolerance at a similar magnitude in $Lep^{ob/ob}$ -mice (Fig. 1a and b), suggesting that the glucose lowering effect of this substance is mediated via central signalling events. Indeed, we identified activation of central insulin signalling as demonstrated by an increase in the number of cells positive for phospho-AKT (Ser473, Fig. 1c) upon icv butein administration within the ARC which supports this hypothesis. The very potent glucose lowering potential of butein is supported by the finding that HFD-induced glucose intolerance was reversed after icv butein administration (Fig. 1d). Since the anti-inflammatory properties of butein are mediated via inhibition of the IKKβ / NF-κB pathway (21) we tested the hypothesis as to whether chronic genetherapeutic inactivation of this cascade in neurons of the ARC might prevent HFD-induced metabolic derangements in mice. As a genetherapeutic intervention we over-expressed the regulatory molecule IκBα, which lingers NF-κB in the cytoplasm. Constitutive binding of NF-κB to IκBα was facilitated by the generation of a mutant IκBα construct which can not be phosphorylated by the upstream kinase IKKβ due to exchange of the inhibitory phosphorylation sites Serine 32 and Serine 36 to Alanine. Adverse effects by viral induced inflammation were circumvented by the use of AAV2 which do not cause adverse local immune in contrast with e.g. adenovirus (36). Indeed, ARC-directed over-expression of IκBα-mt partially protected from HFD-induced weight gain (Fig. 2a) which was exclusively caused by a reduction in body fat mass (Fig. 2b), without changes in body lean mass, BMC and BMD (Fig. 2c, d and e). Notably, parallel to the effects of butein also chronic inactivation of the NF-κB pathway in the ARC improved glucose tolerance and additionally led to a reduction in basal blood glucose levels (Fig. 3a and b), confirming the therapeutic glucose lowering potential of central IKKβ / NF-κB pathway inhibition. Although also systemic low grade inflammation involving IKKβ / NF-κB cascade is

associated with high fat feeding, blockade of this pathway exclusively in neurons of the ARC is sufficient to ameliorate HFD-induced glucose- and insulin- intolerance, confirming the central role of this brain region in regulating whole body glucose homeostasis.

Since food intake did not differ between the AAV2- IκBα-mt- and AAV2-EGPF- mice (Fig. 4a) we hypothesized that the catabolic effects of IκBα-mt over-expression must be assigned to an increase in energy expenditure. Indeed, average metabolic rate, measured as oxygen consumption, and energy expenditure were increased in the AAV2- IκBα-mt mice relative to the AAV2-EGPF- mice (Fig. 4b and c). The respiratory quotient was unaltered between both groups (Fig. 4d), suggesting that the observed effects are not based on different substrate utilization. To distinguish whether the increased energy expenditure is due to an elevated basal energy requirement or altered physical activity, we measured RMR and maximal oxygen consumption. While ARC-directed over-expression of IκBα-mt led to a marked increase in RMR (Fig. 4e and f), maximal oxygen consumption was unaltered (Fig. 4g), suggesting a selective elevation in basal energy requirement by blockade of the NF-κB pathway in the ARC, without changing physical activity. The ARC-directed IκBα-mt over-expression, which was restricted to neurons led to the profound metabolic alterations. This suggests that neuronal inflammation, involving the IKKβ / NF-κB pathway, contributes to the development of DIO-induced metabolic syndrome. However, whether IKKβ / NF-κB signalling in different neuron populations within the ARC differentially alter glucose- and energy- metabolism remains to be identified in future studies.

Some of the glucose lowering effects of butein were similar to leptin, which contributes to the maintenance of glucose homeostasis (23;37-40). For instance, we recently showed that leptin exhibits a potent acute glucose lowering capacity in leptin deficient mice, which was associated with an increased number of pAKT immunoreactive cells in the ARC, thereby sensitizing insulin action (23). It is plausible that diet-induced hypothalamic inflammation leads to relative leptin insensitivity, involving NF-κB-mediated transcription of the most prominent leptin inhibitor, SOCS-3 (31;32), which is a target gene regulated by this transcription factor (14). Inhibition of IKKβ / NF-κB signalling in the ARC was associated with a reduction of SOCS-3 expression in this nucleus (Fig. 5). This together with the fact that leptin increases energy expenditure and oxygen consumption (41) supports the speculation that the catabolic actions of this metabolic manipulation might be mediated by restoration of leptin sensitivity, despite ongoing high fat feeding. Future studies focusing on the possible restoration of leptin singalling by inhibition of hypothalamic inflammation are urgently required.

Taken together, combining nutritive and genetherapeutic inhibition of the central IKKβ / NF-κB pathway our data strongly support the hypothalamic inflammation theory and might provide novel tools to combat HFD-induced metabolic disorders.

Reference List

1. Bastard,JP, Maachi,M, Lagathu,C, Kim,MJ, Caron,M, Vidal,H, Capeau,J, Feve,B: Recent advances in the relationship between obesity, inflammation, and insulin resistance. *Eur Cytokine Netw* 17:4-12, 2006

2. Chan,JC, Malik,V, Jia,W, Kadowaki,T, Yajnik,CS, Yoon,KH, Hu,FB: Diabetes in Asia: epidemiology, risk factors, and pathophysiology. *JAMA* 301:2129-2140, 2009

3. Bruning,JC, Gautam,D, Burks,DJ, Gillette,J, Schubert,M, Orban,PC, Klein,R, Krone,W, Muller-Wieland,D, Kahn,CR: Role of brain insulin receptor in control of body weight and reproduction. *Science* 289:2122-2125, 2000

4. Marks,JL, Porte,D, Jr., Stahl,WL, Baskin,DG: Localization of insulin receptor mRNA in rat brain by in situ hybridization. *Endocrinology* 127:3234-3236, 1990

5. Niswender,KD, Morrison,CD, Clegg,DJ, Olson,R, Baskin,DG, Myers,MG, Jr., Seeley,RJ, Schwartz,MW: Insulin activation of phosphatidylinositol 3-kinase in the hypothalamic arcuate nucleus: a key mediator of insulin-induced anorexia. *Diabetes* 52:227-231, 2003

6. Obici,S, Zhang,BB, Karkanias,G, Rossetti,L: Hypothalamic insulin signaling is required for inhibition of glucose production. *Nat Med* 8:1376-1382, 2002

7. Obici,S, Feng,Z, Karkanias,G, Baskin,DG, Rossetti,L: Decreasing hypothalamic insulin receptors causes hyperphagia and insulin resistance in rats. *Nat Neurosci* 5:566-572, 2002

8. Okamoto,H, Nakae,J, Kitamura,T, Park,BC, Dragatsis,I, Accili,D: Transgenic rescue of insulin receptor-deficient mice. *Journal of Clinical Investigation* 114:214-223, 2004

9. Okamoto,H, Obici,S, Accili,D, Rossetti,L: Restoration of liver insulin signaling in Insr knockout mice fails to normalize hepatic insulin action. *Journal of Clinical Investigation* 115:1314-1322, 2005

10. De Souza,CT, Araujo,EP, Bordin,S, Ashimine,R, Zollner,RL, Boschero,AC, Saad,MJ, Velloso,LA: Consumption of a fat-rich diet activates a proinflammatory response and induces insulin resistance in the hypothalamus. *Endocrinology* 146:4192-4199, 2005

11. Belgardt,BF, Mauer,J, Wunderlich,FT, Ernst,MB, Pal,M, Spohn,G, Bronneke,HS, Brodesser,S, Hampel,B, Schauss,AC, Bruning,JC: Hypothalamic and pituitary c-Jun N-terminal kinase 1 signaling coordinately regulates glucose metabolism. *Proc Natl Acad Sci U S A* 107:6028-6033, 2010

12. Benzler,J, Ganjam,GK, Legler,K, Stohr,S, Kruger,M, Steger,J, Tups,A: Acute Inhibition of Central c-Jun N-terminal Kinase Restores Hypothalamic Insulin Signalling and Alleviates Glucose Intolerance in Diabetic Mice. *J Neuroendocrinol* 25:446-454, 2013

13. Posey,KA, Clegg,DJ, Printz,RL, Byun,J, Morton,GJ, Vivekanandan-Giri,A, Pennathur,S, Baskin,DG, Heinecke,JW, Woods,SC, Schwartz,MW, Niswender,KD: Hypothalamic proinflammatory lipid accumulation, inflammation, and insulin resistance in rats fed a high-fat diet. *Am J Physiol Endocrinol Metab* 296:E1003-E1012, 2009

14. Zhang,X, Zhang,G, Zhang,H, Karin,M, Bai,H, Cai,D: Hypothalamic IKKbeta/NF-kappaB and ER stress link overnutrition to energy imbalance and obesity. *Cell* 135:61-73, 2008

15. Baeuerle,PA, Baltimore,D: NF-kappa B: ten years after. *Cell* 87:13-20, 1996

16. Vaughan,S, Jat,PS: Deciphering the role of nuclear factor-kappaB in cellular senescence. *Aging (Albany NY)* 3:913-919, 2011

17. Cai,D: NFkappaB-mediated metabolic inflammation in peripheral tissues versus central nervous system. *Cell Cycle* 8:2542-2548, 2009

18. Kleinridders,A, Schenten,D, Konner,AC, Belgardt,BF, Mauer,J, Okamura,T, Wunderlich,FT, Medzhitov,R, Bruning,JC: MyD88 signaling in the CNS is required for development of fatty acid-induced leptin resistance and diet-induced obesity. *Cell Metab* 10:249-259, 2009

19. Thaler,JP, Yi,CX, Schur,EA, Guyenet,SJ, Hwang,BH, Dietrich,MO, Zhao,X, Sarruf,DA, Izgur,V, Maravilla,KR, Nguyen,HT, Fischer,JD, Matsen,ME, Wisse,BE, Morton,GJ, Horvath,TL, Baskin,DG, Tschop,MH, Schwartz,MW: Obesity is associated with hypothalamic injury in rodents and humans. *J Clin Invest* 122:153-162, 2012

20. Chuang,CC, McIntosh,MK: Potential mechanisms by which polyphenol-rich grapes prevent obesity-mediated inflammation and metabolic diseases. *Annu Rev Nutr* 31:155-176, 2011

21. Pandey,MK, Sandur,SK, Sung,B, Sethi,G, Kunnumakkara,AB, Aggarwal,BB: Butein, a tetrahydroxychalcone, inhibits nuclear factor (NF)-kappaB and NF-kappaB-regulated gene expression through direct inhibition of IkappaBalpha kinase beta on cysteine 179 residue. *J Biol Chem* 282:17340-17350, 2007

22. Gelling,RW, Morton,GJ, Morrison,CD, Niswender,KD, Myers,MG, Jr., Rhodes,CJ, Schwartz,MW: Insulin action in the brain contributes to glucose lowering during insulin treatment of diabetes. *Cell Metab* 3:67-73, 2006

23. Koch,C, Augustine,RA, Steger,J, Ganjam,GK, Benzler,J, Pracht,C, Lowe,C, Schwartz,MW, Shepherd,PR, Anderson,GM, Grattan,DR, Tups,A: Leptin rapidly improves glucose homeostasis in obese mice by increasing hypothalamic insulin sensitivity. *J Neurosci* 30:16180-16187, 2010

24. Kugler,S, Lingor,P, Scholl,U, Zolotukhin,S, Bahr,M: Differential transgene expression in brain cells in vivo and in vitro from AAV-2 vectors with small transcriptional control units. *Virology* 311:89-95, 2003

25. Benzler,J, Ganjam,GK, Kruger,M, Pinkenburg,O, Kutschke,M, Stohr,S, Steger,J, Koch,CE, Olkrug,R, Schwartz,MW, Shepherd,PR, Grattan,DR, Tups,A: Hypothalamic glycogen-synthase-kinase 3beta has a central role in the regulation of food intake and glucose metabolism. *Biochem J* 2012

26. Lotharius,J, Falsig,J, van,BJ, Payne,S, Dringen,R, Brundin,P, Leist,M: Progressive degeneration of human mesencephalic neuron-derived cells triggered by dopamine-dependent oxidative stress is dependent on the mixed-lineage kinase pathway. *J Neurosci* 25:6329-6342, 2005

27. Heldmaier,G, Ruf,T: Body temperature and metabolic rate during natural hypothermia in endotherms. *J Comp Physiol B* 162:696-706, 1992

28. Mercer,JG, Moar,KM, Logie,TJ, Findlay,PA, Adam,CL, Morgan,PJ: Seasonally inappropriate body weight induced by food restriction: effect on hypothalamic gene expression in male Siberian hamsters. *Endocrinology* 142:4173-4181, 2001

29. Paxinos G and Franklin K. The Mouse Brain in Stereotaxic Coordinates. (2). 2002. San Diego, Academics.
Ref Type: Catalog

30. Tups,A, Anderson,GM, Rizwan,M, Augustine,RA, Chaussade,C, Shepherd,PR, Grattan,DR: Both p110alpha and p110beta isoforms of phosphatidylinositol 3-OH-kinase are required for insulin signalling in the hypothalamus. *J Neuroendocrinol* 22:534-542, 2010

31. Bjorbaek,C, Elmquist,JK, Frantz,JD, Shoelson,SE, Flier,JS: Identification of SOCS-3 as a potential mediator of central leptin resistance. *Mol Cell* 1:619-625, 1998

32. Tups,A, Ellis,C, Moar,KM, Logie,TJ, Adam,CL, Mercer,JG, Klingenspor,M: Photoperiodic regulation of leptin sensitivity in the Siberian hamster, Phodopus sungorus, is reflected in arcuate nucleus SOCS-3 (suppressor of cytokine signaling) gene expression. *Endocrinology* 145:1185-1193, 2004

33. Hotamisligil,GS: Inflammation and metabolic disorders. *Nature* 444:860-867, 2006

34. Milanski,M, Degasperi,G, Coope,A, Morari,J, Denis,R, Cintra,DE, Tsukumo,DM, Anhe,G, Amaral,ME, Takahashi,HK, Curi,R, Oliveira,HC, Carvalheira,JB, Bordin,S, Saad,MJ, Velloso,LA: Saturated fatty acids produce an inflammatory response predominantly through the activation of TLR4 signaling in hypothalamus: implications for the pathogenesis of obesity. *J Neurosci* 29:359-370, 2009

35. Thaler,JP, Schwartz,MW: Minireview: Inflammation and obesity pathogenesis: the hypothalamus heats up. *Endocrinology* 151:4109-4115, 2010

36. Monahan,PE, Samulski,RJ: AAV vectors: is clinical success on the horizon? *Gene Ther* 7:24-30, 2000

37. Kievit,P, Howard,JK, Badman,MK, Balthasar,N, Coppari,R, Mori,H, Lee,CE, Elmquist,JK, Yoshimura,A, Flier,JS: Enhanced leptin sensitivity and improved glucose homeostasis in mice lacking suppressor of cytokine signaling-3 in POMC-expressing cells. *Cell Metab* 4:123-132, 2006

38. Hill,JW, Williams,KW, Ye,C, Luo,J, Balthasar,N, Coppari,R, Cowley,MA, Cantley,LC, Lowell,BB, Elmquist,JK: Acute effects of leptin require PI3K signaling in hypothalamic proopiomelanocortin neurons in mice. *J Clin Invest* 118:1796-1805, 2008

39. German,J, Kim,F, Schwartz,GJ, Havel,PJ, Rhodes,CJ, Schwartz,MW, Morton,GJ: Hypothalamic leptin signaling regulates hepatic insulin sensitivity via a neurocircuit involving the vagus nerve. *Endocrinology* 150:4502-4511, 2009

40. Hedbacker,K, Birsoy,K, Wysocki,RW, Asilmaz,E, Ahima,RS, Farooqi,IS, Friedman,JM: Antidiabetic Effects of IGFBP2, a Leptin-Regulated Gene. *Cell Metabolism* 11:11-22, 2010

41. Hwa,JJ, Fawzi,AB, Graziano,MP, Ghibaudi,L, Williams,P, Van,HM, Davis,H, Rudinski,M, Sybertz,E, Strader,CD: Leptin increases energy expenditure and selectively promotes fat metabolism in ob/ob mice. *Am J Physiol* 272:R1204-R1209, 1997

Figure legends

Figure 1. The chalcone butein improved glucose tolerance.

a: Leptin deficient mice received oral, via stomach tube, butein in three different concentrations (0.08 mg/kg body weight in PBS/ 5% ethanol, black circles, 0.8mg/kg, dark grey circles, 8mg/kg, light grey circles) 1h before ipGTT was performed. Oral administration of butein dose dependently improved glucose tolerance in $Lep^{ob/ob}$ compared with vehicle treated mice (open circles, n=8/group). Shown are glucose concentrations (left panel) and associated area under the curve (right panel) during ipGTT.

b: A central injection of the butein improved glucose tolerance in $Lep^{ob/ob}$ mice. IpGTT was performed 30 min after administration of butein (5nmol in 5%DMSO/aCSF, black circles) or vehicle (5%DMSO in aCSF, open circles) into the lateral ventricle (n= 8/group).

c: Icv administration of butein increased hypothalamic insulin signalling. Immunohistochemistry was performed on brain sections of $Lep^{ob/ob}$ mice after central administration of butein (5nmol in 5%DMSO in aCSF) or vehicle (5%DMSO in aCSF), 30 minutes before transcardial perfusion. Inserts depict representative images of immunoreactivity of phospho-AKT (Ser473) in the ARC. The bar graph shows the counted cells in the ARC that were immunoreactive for phospho-AKT (Ser473)

d: The same treatment, as used in leptin deficient mice, also improved glucose tolerance in wild-type mice fed a high fat diet for three weeks (black circles) compared with vehicle treated mice (grey circles) without significant difference to mice on LFD (open circles, n=5-7/group). ip: intraperitoneal; GTT: glucose tolerance test; icv: intracerebroventricular; aCSF: artificial cerebral spinal fluid; HFD: high fat diet; LFD low fat diet; $Lep^{ob/ob}$ mice: leptin-deficient mice. Data show means ± SEM, $^{**}P \leq 0.01$, $^{***}P \leq 0.001$.

Figure 2. Neuron-specific AAV2-mediated over-expression of IκBα-mt in the ARC decelerated diet induced obesity

a: Wild-type mice were stereotaxically injected into the bilateral halves of the ARC with 2×250nl of AAV2 virus expressing IκBα-mt (n=6) or EGFP as a control (n=10). Shown are the body masses of EGFP- and IκBα-mt –over-expressing animals maintained on a chow diet (*ad libitum*) for 12 days followed by 50 days on an HFD (*ad libitum*).

b: DEXA scan revealed that body fat mass decelerated after treatment with AAV2– IκBα-mt virus on HFD (**b**), whereas lean mass(**c**), bone mineral density (BMD, **d**) and bone mineral content (BMC, **e**) did not change. ARC: Arcuate nucleus; AAV: adeno-associated virus; IκBα-mt: IκBα –mutant; DEXA: dual-emission X-ray absorptiometry; HFD: high fat diet; GTT: glucose tolerance test; ITT: insulin tolerance test; MS: metabolic measurements. Results are means±S.E.M., $^{*}P \leq 0.05$.

Figure 3. Over-expression of IκBα-mt in the ARC improved whole body glucose homeostasis

a: After 36 days of HFD, mice over-expressing IκBα-mt exhibit decreased blood glucose levels. The glucose tolerance test (**b**) performed on day 48 after surgery on HFD, revealed improved glucose

tolerance in AAV2– IκBα-mt mice compared with AAV2–EGFP mice. Mice over-expressing IκBα-mt exhibit enhanced insulin sensitivity as the insulin tolerance test (**c**) demonstrated. Shown are glucose concentrations (left panel) and associated area under the curve (right panel) during ip-GTT. ARC: Arcuate nucleus; AAV: adeno-associated virus; IκBα-mt: IκBα –mutant; HFD: high fat diet. Results are means±S.E.M., **P*≤0.05.

Figure 4. Metabolic measurements

After 3 weeks of HFD the metabolic measurements revealed that food intake (**a**) was not affected. Average metabolic rate (**b**) and energy expenditure (**c**) were increased in the AAV2 IκBα-mt mice compared with the AAV2–EGFP mice, whereas respiratory quotient (**d**) was unaltered. Mice over-expressing IκBα-mt in the ARC show elevated resting metabolic rate (**e**) and resting metabolic rate /g body weight (**f**) compared with vehicle treated mice, while maximal oxygen consumption was not affected (**g**). ARC: Arcuate nucleus; AAV: adeno-associated virus; IκBα-mt: IκBα –mutant; HFD: high fat diet. Results are means±S.E.M., **P*≤0.05, ****P*≤ 0.001.

Figure 5. ARC directed neuronal over-expression of IκBα-mt decreased SOCS-3 mRNA expression

IκBα-mt over-expression led to a decrease in SOCS-3 gene expression in the ARC. Representative autoradiographies of coronal brain sections exposed to ^{35}S-labelled riboprobe against SOCS-3. Insets depict localization within the ARC of mice treated with AAV2–EGFP or an AAV2– IκBα-mt. Semi-quantitative analysis of gene expression of SOCS-3 is presented in the bar graph as percentage of AAV2–EGFP. ARC: Arcuate nucleus; AAV: adeno-associated virus; IκBα-mt: IκBα –mutant; SOCS-3: suppressor of cytokine signalling 3. Results are means±S.E.M., **P*≤0.05.

Suppl Fig.: Validation of AAV2- IκBα-mt expression

IκBα transcription was controlled by the neuron-specific synapsin promoter. (**a**) Confocal image showing LUHMES cells expressing EGFP after 5days of AAV2–EGFP infection. (**b**) Confirmation of AAV2– IκBα-mt over-expression by immunoblotting of total IκBα in primary cortical neurons 5 days after infection. The bar graph and the western blot show that the over-expression markedly increases the protein content of IκBα, whereas it was almost absent in the AAV2–EGFP treated cells (**c**) Over-expression of AAV2– IκBα.mt *in-vivo* was confirmed by *in-situ* hybridizations and revealed an 80% increase of IκBα in the mediobasal hypothalamus. Shown are representative autoradiographs of mouse brain sections after *in -itu* hybridization to an antisense ^{35}S-labelled riboprobe binding to IκBα of AAV2–EFGP and AAV2– IκBα-mt mice. For validation each cell culture experiment was repeated four times and statistical analysis is represented in the histograms. Results are means±S.E.M. ****P*≤0.001.

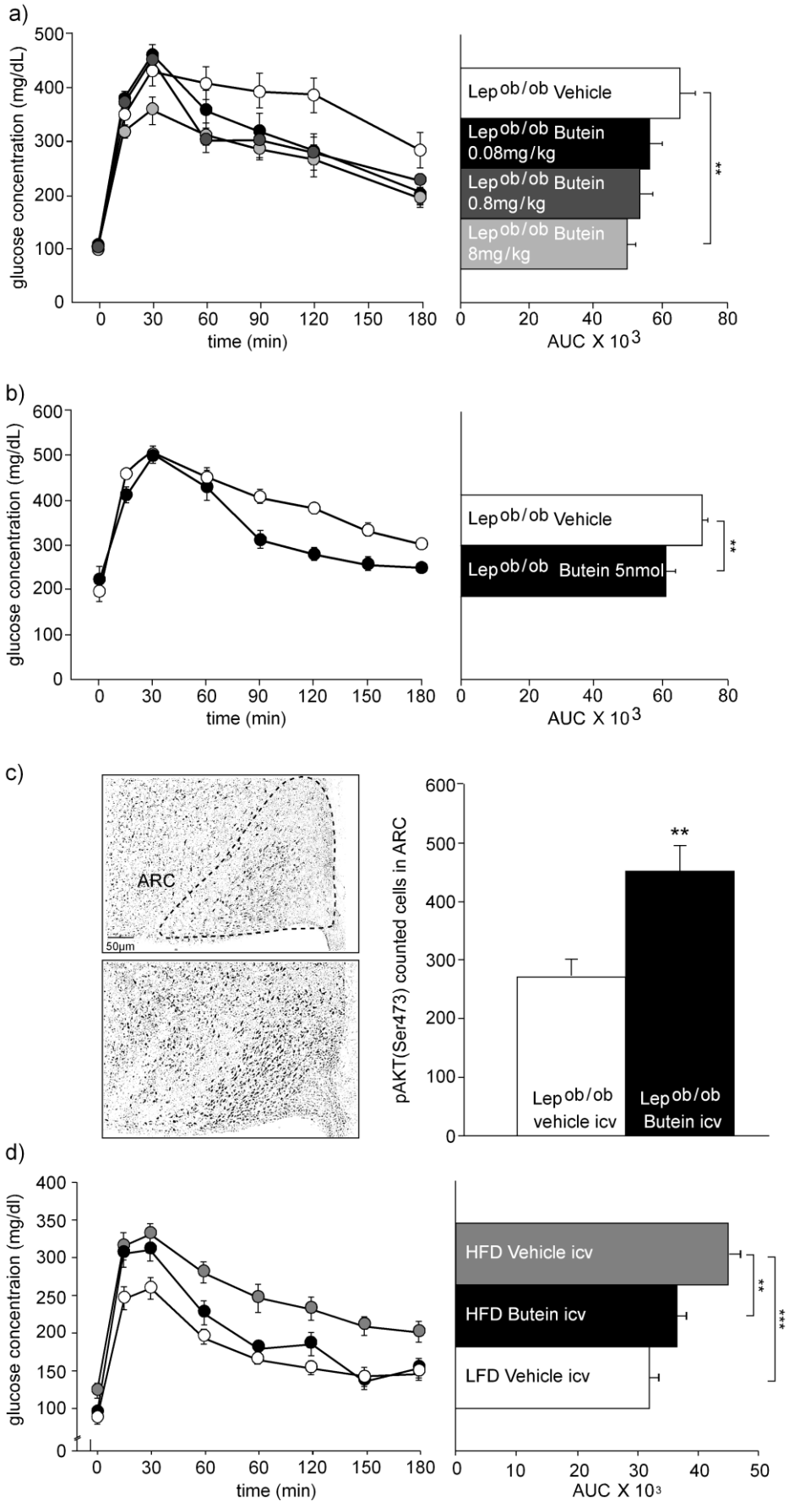
a)
glucose concentration (mg/dL)
time (min)
Lep ob/ob Vehicle
Lep ob/ob Butein 0.08mg/kg
Lep ob/ob Butein 0.8mg/kg
Lep ob/ob Butein 8mg/kg
AUC X 10 3
b)
glucose concentration (mg/dL)
time (min)
Lep ob/ob Vehicle
Lep ob/ob Butein 5nmol
AUC X 10 3
c)
ARC
50µm
pAKT(Ser473) counted cells in ARC
Lep ob/ob vehicle icv
Lep ob/ob Butein icv
d)
glucose concentraion (mg/dl)
time (min)
HFD Vehicle icv
HFD Butein icv
LFD Vehicle icv
AUC X 10 3

Fig.1

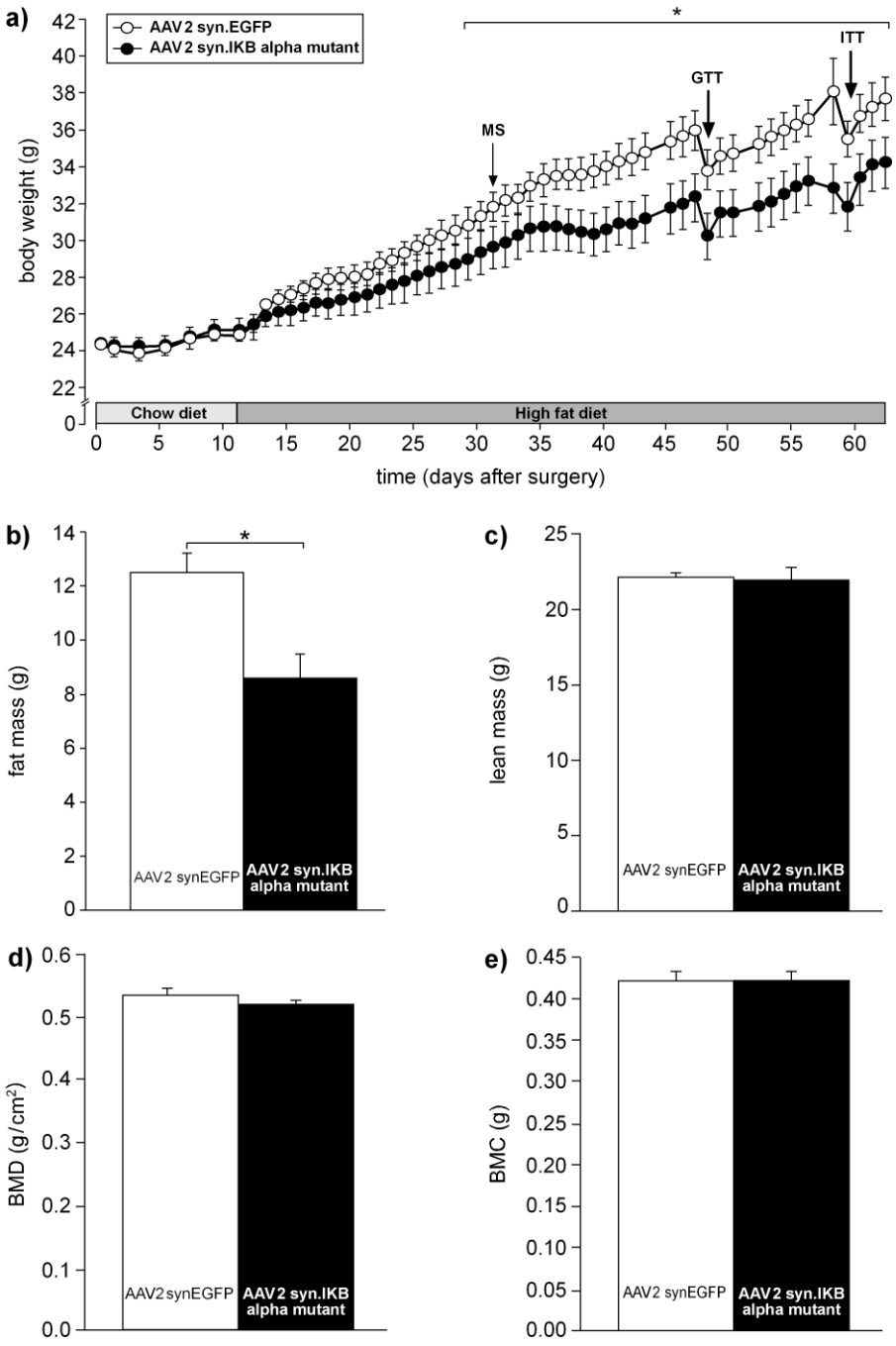
a)
AAV2 syn.EGFP
AAV2 syn.IKB alpha mutant
body weight (g)
time (days after surgery)
MS
GTT
ITT
*
Chow diet
High fat diet
b)
fat mass (g)
c)
lean mass (g)
d)
BMD (g/cm²)
e)
BMC (g)
AAV2 synEGFP
AAV2 syn.IKB alpha mutant

Fig.2

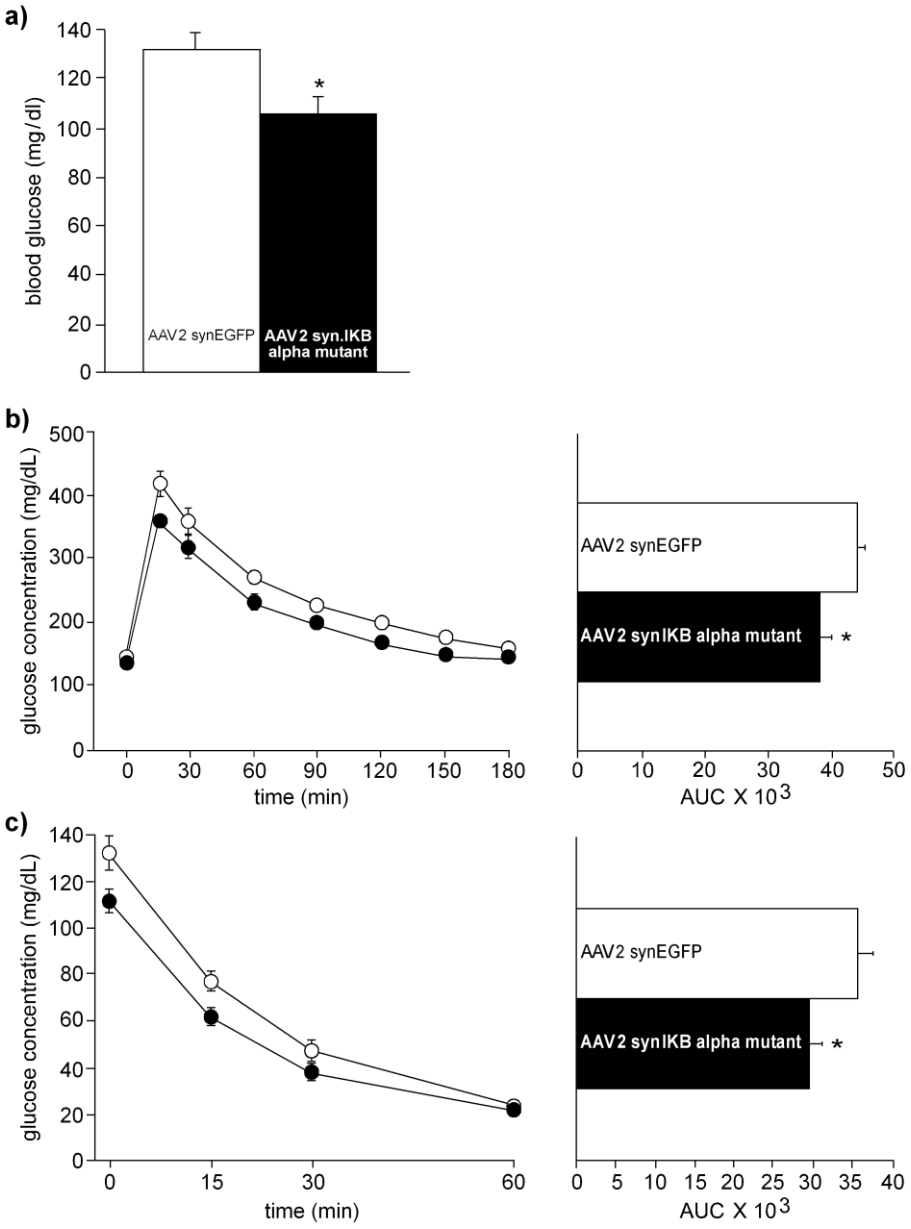
a)
blood glucose (mg/dl)
140
120
100
80
60
40
20
0
*
AAV2 synEGFP
AAV2 syn.IKB alpha mutant
b)
glucose concentration (mg/dL)
500
400
300
200
100
0
0 30 60 90 120 150 180
time (min)
AAV2 synEGFP
AAV2 synIKB alpha mutant
*
0 10 20 30 40 50
AUC X 10 3
c)
glucose concentration (mg/dL)
140
120
100
80
60
40
20
0
0 15 30 60
time (min)
AAV2 synEGFP
AAV2 synIKB alpha mutant
*
0 5 10 15 20 25 30 35 40
AUC X 10 3

Fig.3

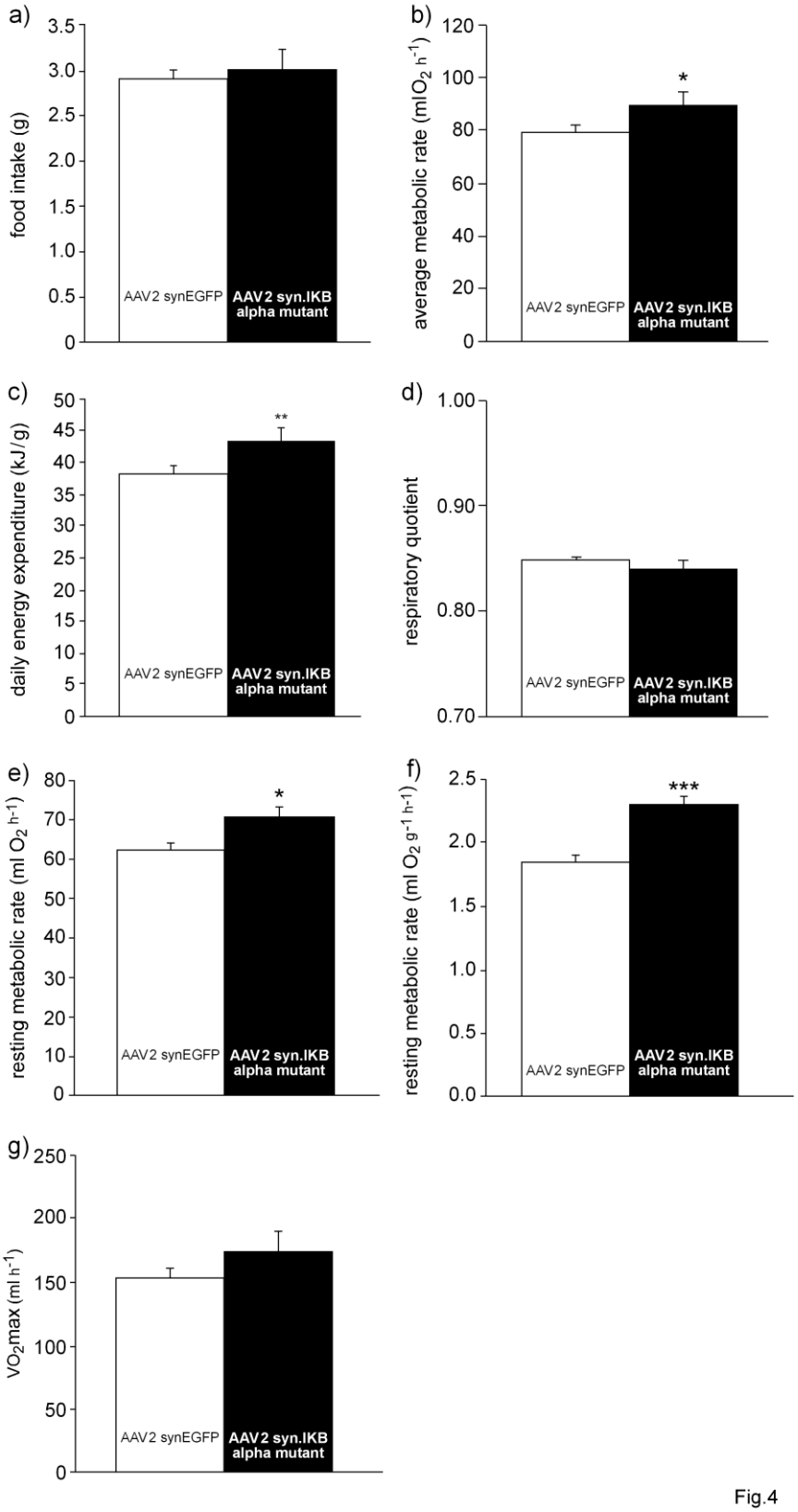
a)
food intake (g)
3.5
3.0
2.5
2.0
1.5
1.0
0.5
0
AAV2 synEGFP
AAV2 syn.IKB alpha mutant
b)
average metabolic rate (mlO_2 h^{-1})
120
100
80
60
40
20
0
*
AAV2 synEGFP
AAV2 syn.IKB alpha mutant
c)
daily energy expenditure (kJ/g)
50
45
40
35
30
25
20
15
10
5
0
**
AAV2 synEGFP
AAV2 syn.IKB alpha mutant
d)
respiratory quotient
1.00
0.90
0.80
0.70
AAV2 synEGFP
AAV2 syn.IKB alpha mutant
e)
resting metabolic rate (ml O_2 h^{-1})
80
70
60
50
40
30
20
10
0
*
AAV2 synEGFP
AAV2 syn.IKB alpha mutant
f)
resting metabolic rate (ml O_2 g^{-1} h^{-1})
2.5
2.0
1.5
1.0
0.5
0.0
***
AAV2 synEGFP
AAV2 syn.IKB alpha mutant
g)
VO_2max (ml h^{-1})
250
200
150
100
50
0
AAV2 synEGFP
AAV2 syn.IKB alpha mutant

Fig.4

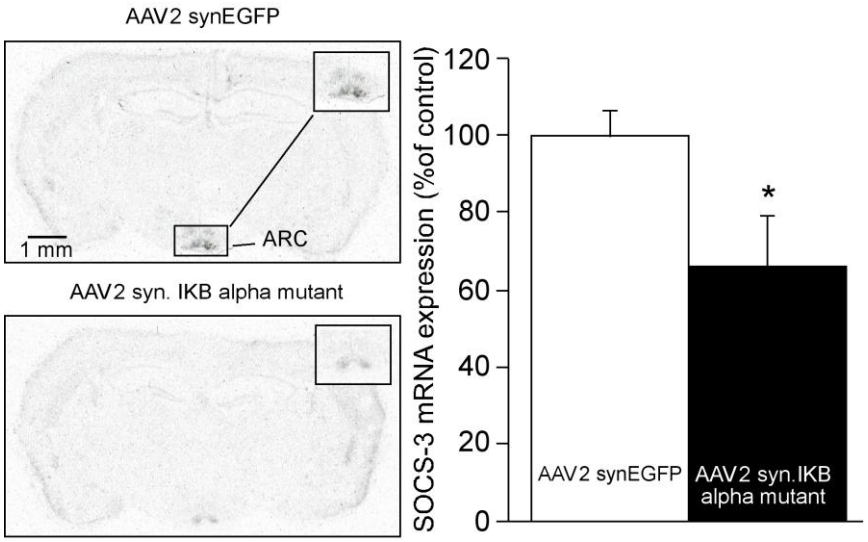
AAV2 synEGFP
1 mm
ARC
AAV2 syn. IKB alpha mutant
SOCS-3 mRNA expression (%of control)
120
100
80
60
40
20
0
*
AAV2 synEGFP
AAV2 syn.IKB alpha mutant

Fig.5

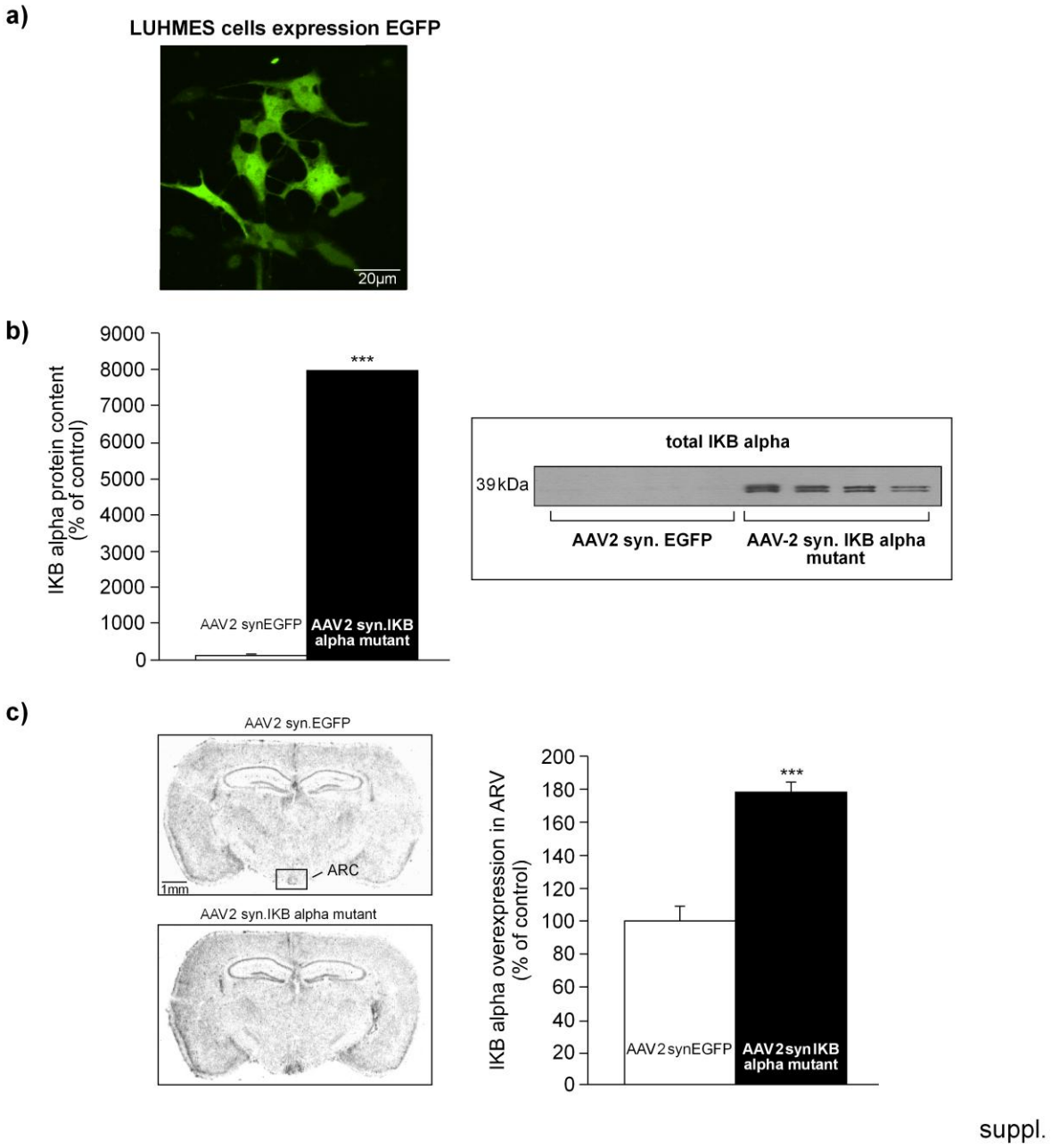
a)
LUHMES cells expression EGFP
20µm
b)
IKB alpha protein content (% of control)
9000
8000
7000
6000
5000
4000
3000
2000
1000
0
***
AAV2 synEGFP
AAV2 syn.IKB alpha mutant
total IKB alpha
39kDa
AAV2 syn. EGFP
AAV-2 syn. IKB alpha mutant
c)
AAV2 syn.EGFP
ARC
1mm
AAV2 syn.IKB alpha mutant
IKB alpha overexpression in ARV (% of control)
200
180
160
140
120
100
80
60
40
20
0
***
AAV2synEGFP
AAV2synIKB alpha mutant

suppl.

Central Adiponectin Acutely Improves Glucose Tolerance in Male Mice (Abbreviated Title: Adiponectin and Hypothalamus)

Christiane E. Koch[1], Chrishanthi Lowe[1], Karen Legler[1], Jonas Benzler[1], Juliane Steger[1], David R. Grattan[3], Lynda M. Williams[2] and Alexander Tups[1]

[1]Department of Animal Physiology, Faculty of Biology, Philipps University Marburg, D-35043 Marburg, Germany

[2] Metabolic Health Group, Rowett Institute of Nutrition and Health, University of Aberdeen, Aberdeen AB21 9SB, United Kingdom

[3]Centre for Neuroendocrinology and Department of Anatomy and Structural Biology, University of Otago, Dunedin, New Zealand

Proofs and correspondence to:
Dr. Alexander Tups
Department of Animal Physiology, Faculty of Biology, Philipps University Marburg, Karl-von-Frisch Str. 8 D-35043 Marburg, Germany
e-mail: alexander.tups@staff.uni-marburg.de

Keywords: diabetes type II, high fat diet, arcuate nucleus, obesity, insulin, inflammation
Acknowledgments: This study was funded by the German Ministry of Education and Research (Ref. No: 0315087, to AT). LMW was funded by RESAS.

Disclosure Summary: The authors have nothing to disclose

Abstract

Adiponectin, an adipocyte-derived hormone, regulates glucose and lipid metabolism. It is also anti-inflammatory. During obesity, adiponectin levels and sensitivity are reduced. While the action of adiponectin in the periphery is well established the neuroendocrine role of adiponectin is largely unknown. To address this we analyzed the expression of adiponectin and the two adiponectin receptors (AdipoR1 and AdipoR2) in response to fasting (AdipoR1) and to diet-induced and genetic obesity. We also investigated the acute impact of adiponectin on central regulation of glucose homeostasis. Adiponectin (1µg) was injected intracerebroventricularly (ICV) and glucose tolerance tests were performed in dietary and genetic obese mice. Finally, the influence of ICV adiponectin administration on central signalling cascades regulating glucose homeostasis and on markers of hypothalamic inflammation was assessed. Gene expression of *adiponectin* and *AdipoR1* was down-regulated in the arcuate nucleus (ARC) of fasted mice. High-fat (HF) feeding increased *AdipoR1* and *AdipoR2* gene expression in this region. In mice on a HF diet and in leptin deficient mice acute ICV adiponectin improved glucose tolerance 60 min after injection, whereas normoglycemia in control mice was unaffected. ICV adiponectin increased pAKT, decreased pAMPK and did not change pSTAT3 immunoreactivity. In HF fed mice, ICV adiponectin reversed parameters of hypothalamic inflammation and insulin resistance as determined by the number of pGSK-3β(Ser9) and pJNK(Thr183/Tyr185) immunoreactive cells in the ARC and ventromedial hypothalamus. This study demonstrates that the insulin sensitising properties of adiponectin are at least partially based on a neuroendocrine mechanism that involves centrally synthesised adiponectin.

Introduction

Obesity and its co-morbidities, especially type II diabetes, have emerged as major medical problems of modern societies (1). Obesity is associated with a profound drop in circulating adiponectin levels (2). Adiponectin, which is a potent anti-inflammatory and insulin sensitizing hormone, is at present, the only adipokine where circulating concentrations inversely correlate with the body fat mass (3-5). It is plausible that the obesity-associated decrease of the insulin sensitizing hormone adiponectin links obesity with insulin insensitivity and the development of type II diabetes. Based on the insulin sensitising properties of adiponectin, this hormone could be an important therapeutic target for metabolic disorders.

While peripheral actions of adiponectin have been thoroughly investigated, studies investigating the central properties of this hormone in mediating the regulation of energy balance and glucose metabolism are rare. Adiponectin is one of the most abundant hormones in the circulation of non-obese individuals, and is found in the cerebrospinal fluid (CSF) at a concentration approximately 0.1 % those in the circulation. Nonetheless, in comparison to other circulating fat derived hormones, such as leptin, this CSF concentration is remarkably high (6-9). Adiponectin is detectable in the serum as full-length trimers and hexamers either pooled, as low molecular weight adiponectin (LMW) or as high molecular weight (HMW) adiponectin multimers or globular adiponectin (gAD) which is generated by cleavage of the full-length adiponectin monomers (10-13). The globular form of adiponectin has been shown to activate signalling events in hypothalamic neurons and appears to have the highest binding affinity for the adiponectin receptor 1 (AdipoR1) (14). A high binding affinity of AdipoR2 for gAD has also been found but is lower than that for AdipoR1.

In the periphery adiponectin has been shown to activate AMP-activated protein kinase (AMPK) (14), a master switch involved in the regulation of a number of different metabolic processes, including carbohydrate, lipid and protein metabolism and aging (15). Emerging evidence suggests that adiponectin acts in the brain to decrease body weight mainly by stimulating energy expenditure and reducing food intake (16;17). However, together with the origin of adiponectin in the CSF, the nature of signalling pathways involved in this phenomenon remain incompletely understood. It is still a matter of debate as to whether adiponectin reaches the brain via passage through the blood brain barrier (BBB) or whether it is directly expressed in the brain (8). Several recent studies suggest that adiponectin is biologically active in the brain as intracerebroventricular (ICV) administration leads to an increase in cFos positive cells in the hypothalamus and activation of signalling typical of insulin stimulation of the PI3K (Phosphoinositide 3-kinase) in rats (16). The effects of adiponectin in the CNS seem to be mediated via the AdipoR1 (16). Central inhibition of AdipoR1 decreases adiponectin-induced activation of PI3K, whereas inhibition of AdipoR2 appears not to affect insulin signalling in the hypothalamus (16).

Adiponectin has also been described to act as anti-inflammatory hormone. We recently demonstrated that diet-induced obesity (DIO) in mice is associated with increased pro-inflammatory signalling in the mediobasal hypothalamus (MBH) involving phospho-c-Jun N-terminal kinases (pJNK) (18) and phospho-glycogen synthase kinase 3 (pGSK3) (19). We therefore hypothesised that the effect of adiponectin in the hypothalamus may be via an inhibition of hypothalamic inflammation.

Thus, the aim of the current study was to look more closely at the central actions of adiponectin particularly its glucose lowering, insulin sensitizing and anti-inflammatory properties. To measure the effects of obesity on adiponectin and adiponectin receptor expression in the hypothalamus we used two models of obesity; leptin deficient, $Lep^{ob/ob}$ mice and DIO mice fed a high-fat (HF) diet either containing 45% or 60% fat by energy. The effect of fasting on the hypothalamic adiponectin system was also tested. Specifically we measured gene expression of *adiponectin*, *AdipoR1*, *AdipoR2* and adaptor protein containing pleckstrin homology domain, phosphotyrosine binding domain, and leucine zipper motif 1(*APPL1*), an important mediator linking adiponectin and insulin signalling. We used *in situ* hybridization to look at gene expression in the ARC, a key region in the mediobasal hypothalamus (MBH) that is involved in the regulation of energy and glucose homeostasis. Furthermore, we investigated the glucose-lowering properties of ICV adiponectin in these mice assessing the effect of central adiponectin on PI3K and AMPK immunoreactivity in the ARC and ventromedial hypothalamus (VMH). Finally, we investigated whether ICV adiponectin could acutely reverse the elevated pro-inflammatory signals seen in DIO mice in the MBH

Materials and Methods

Animals

All procedures involving animals were carried out under national animal ethics legislation and received approval by the respective authorities for animal ethics. Male C57BL/6JRj wild-type ($Lep^{+/+}$) and $Lep^{ob/ob}$ mice were purchased from Janvier (Le Genest-Saint-Isle; France). They were housed individually under a 12/12 light/dark cycle h and an ambient temperature of 23°C. All mice had *ad libitum* access to food and water except for the period of food withdrawal prior to the experiments (overnight fasting for 16 h). Mice were fed either a low fat diet (LF); with 10% energy from fat (Kcal), a moderate high fat diet (mHF) with 45% from fat or a high-fat diet (HF) with 60% from fat (D12450B, D12451 and D12492: respectively Research Diets; Brunswick; New Jersey).

Analysis of gene expression of the adiponectin system in the mediobasal hypothalamus

Using *in situ* hybridization (20), we analyzed whether fasting influences central gene expression of *adiponectin (accession no. NM_145221.2)*, *AdipoR1 (accession no. NM_028320.3)* and the adaptor protein *APPL1 (accession no. AF304466.1).* Mice were divided into two groups, the first group were fed *ad libitum* and the second group fasted for 16 h prior to decapitation (n = 6 – 7).

Additionally, we characterized whether the expression patterns of *AdipoR*, *AdipoR2 (accession no. NM_197985.3)* and *APPL1* were influenced by diet and/or genotype. Eight week old wild-type mice were divided into three groups and were fed a LF, a mHF (45 %) or a HF (60 %) diet for 4 weeks. To analyze the influence of genetic obesity, a group of eight week old $Lep^{ob/ob}$ mice fed a LF diet were used (n = 4-6 mice/group). Mice were killed, brains removed and frozen on dry ice. For *in situ* hybridization brains were cryosectioned at 16µm. The sequences of the primers to generate the specific amplicons are provided (Table 1).

Tabe1: Genes with their primer sequences used for riboprobe derivation

Gene	Primer sequence
Adiponectin Receptor 1 forward:	5'GGCTGAAAGACAACGACTAC3' (20bp)
Adiponectin Receptor 1 reverse:	5' GGAAGAACATCCCGAAGAC3' (20bp)
Adiponectin Receptor 2 forward:	5' GGGCACCAACTTGATGATAC3' (20bp)
Adiponectin Receptor 2 reverse:	5' CCTTCCCACACCTTACAAAC3' (20bp)
Adiponectin forward:	5' GGAATGACAGGAGCTGAAGG3'(20bp)
Adiponectin reverse:	5' GTCCCGGAATGTTGCAGTAG3'(20bp)
APPL1 forward:	5' CCGATTCCTTGGTTCATATGG3'(20bp)
APPL1 reverse:	5' CACGGCAATGGAAATGTGAG3'(20bp)

Acute action of centrally administered adiponectin on glucose tolerance and hepatic glucose production

Using three different obese and glucose intolerant mouse models, we investigated whether centrally administered adiponectin improves glucose tolerance in these mice. The procedure was identical in each experiment. One hour prior to an intraperitoneal glucose tolerance test (ipGTT) all mice received either an ICV injection of adiponectin (1µg in PBS) or vehicle (PBS). Blood was collected by puncturing the *V. facials* and glucose concentration was measured at defined time points using a glucometer [Roche; Accu-Check Performa; (21)]. To test whether ICV administered adiponectin alters hepatic glucose output, we performed a pyruvate tolerance test in $Lep^{ob/ob}$ mice on LFD (see experiment 1).

In experiment 1 the effect of ICV adiponectin on glucose tolerance of eight week old normoglycemic wild-type- (n = 7 - 8 mice/group) or leptin-deficient, glucose intolerant $Lep^{ob/ob}$ mice (n = 9 - 11 mice/group) on LFD was analyzed. For the ipGTT, mice received 1 g glucose/kg body weight.

To further asses whether ICV adiponectin alters hepatic glucose output, $Lep^{ob/ob}$ mice received an ip pyruvate injection (1.5 mg/kg) sixty minutes prior to acute ICV injection of either adiponectin (1µg adiponectin in PBS; n = 5) or vehicle (PBS; n = 6). Blood glucose levels were measured as stated above.

In experiment 2 we analyzed whether ICV adiponectin improves the impaired glucose tolerance during diet-induced obesity. Wild-type mice received either a LFD or a HFD for 4 weeks (n = 5 - 7 mice/group). An ipGTT (1 g glucose/kg body weight) was then carried out with either ICV adiponectin or vehicle pre-treatment as described above.

In the third experiment, we analyzed the effect of central adiponectin in an extreme setting of obesity; $Lep^{ob/ob}$ mice fed a 60% HFD. After 10 days of HF feeding an ipGTT (0.75 g glucose/kg body weight) with either adiponectin or vehicle pre-treatment was performed as described above (adiponectin n = 9; vehicle n = 23).

Acute effects of ICV adiponectin on central signalling cascades involved in energy balance and glucose metabolism

To identify the molecular mechanisms of central adiponectin action, hypothalamic signalling cascades which are involved in the regulation of energy and glucose metabolism were analyzed. Mice were treated centrally with either adiponectin or vehicle (n = 5-6 mice/group). One hour after ICV injections, mice were anesthetized with pentobarbital (Narcoren; Merial GmbH) and perfused with 0.9% saline containing heparin followed by 4% paraformaldehyde in 0.1M phosphate buffer, pH 7.4. Brains were removed and stored in the same solution for about 5 hours followed by dehydration (in 30% sucrose/0.1 M phosphate buffer). When brains had sunk, they were frozen in isopentane cooled over dry ice for 1 min, and sectioned coronally at 35 µm. Brain slices were collected in a series of four and stored in cryoprotectant at -20°C. Free-floating sections were incubated in H_2O_2 diluted in 0.1M phosphate buffer followed by incubation in blocking solution (5% normal goat serum, 0.5% Triton X-100 in phosphate buffer) for 60 min. Sections were incubated with the primary antibody overnight at

4°C diluted in blocking-solution [anti-pAKT(Ser473) 1:500 ; anti-pAMPK(Thr172) 1:500; Cell Signalling Technology]. After an overnight incubation and rinsing, sections were incubated with a secondary goat anti-rabbit antibody for 1-2 h. For pAKT(Ser473) sections were incubated with a biotinylated secondary antibody (1:500 in blocking solution containing 3 % normal goat serum, 0.5% Triton X-100) followed by ABC solution (Vector Laboratories) for 1 h. To detect pAMPK(Thr172), sections were incubated with a HRP-conjugated secondary goat anti-rabbit antibody overnight (1:500 in blocking solution containing 3 % normal goat serum, 0.5% Triton X-100). Finally, the signal was developed by nickel-diaminobenzidine solution (Vector Laboratories), giving a grey/black precipitate. Immunoreactive cells in the ARC and the VMH were counted by two investigators blinded to the treatments.

For phospho-signal transducer and activator of transcription 3 (pSTAT3) immunostaining an antigen retrieval step was necessary. Prior to the blocking step detailed above, sections were pre-treated with 1% NaOH and 1% H_2O_2 for 20 min, followed by 0.3% glycine for 10 min and by incubation in 0.03% SDS for 10 min (22). The primary antibody for pSTAT3(Tyr705) (Cell Signalling Technology) was diluted 1:3000 in blocking solution followed by a biotinylated secondary antibody diluted 1:1000 using the ABC protocol.

Acute effects of ICV adiponectin on phospho-JNK(Thr183/Tyr185) and phospho-GSK3β(Ser9) immunoreactivity in the mediobasal hypothalamus in diet-induced obesity

Wild-type mice were divided into three groups (n = 5 mice/group). One group were fed a LF diet, and two groups fed a HF diet. After 4 weeks on diet, one group of HF mice was injected centrally, as described above with adiponectin and the second HF group was injected with vehicle. One hour after injection, mice were perfused with 4% paraformaldehyde/phosphate buffer under pentobarbital anaesthesia and brains were removed, sectioned and analyzed by immunohistochemistry as detailed above. A specific antibody against pJNK(Thr183/Tyr185) or pGSK3β(Ser9) (both diluted 1:1000 in blocking solution, anti-pJNK and anti-pGSK3β (Cell Signalling Technology) was used, using the protocol specific for the HRP-conjugated secondary antibody as described above.

Results

Central expression pattern of genes involved in adiponectin signal transduction

The level of gene expression of *adiponectin, AdipoR1* and *APPL1* in the ARC was dependent on the feeding status of the mice (Fig.1). In *ad libitum* fed wild-type mice, adiponectin expression was detected in the hypothalamic ARC. After food deprivation for 16 h adiponectin gene expression was markedly reduced (n = 6 - 7 mice/group; *ad libitum vs* food deprived $P < 0.001$). Gene expression of *AdipoR1* and *APPL1* in the ARC was increased in fasted mice compared with *ad libitum* fed controls. The magnitude of changes in mRNA expression was 1.8-fold for *AdipoR1* ($P = 0.039$; Fig. 1b) and 4-fold for *APPL1* ($P = 0.019$; Fig.1c) in food deprived mice compared with controls.

We next tested whether diet or genotype may also affect gene expression of adiponectin signalling components (Fig.2; n = 4-6 mice/group). Expression of *AdipoR1* in the ARC was increased in mice fed HFD (60%) over 2-fold compared with LF controls ($P = 0.008$). In mice fed mHF (45%), expression of *AdipoR1* was markedly increased in this brain region reaching 3 times that in LF controls (LF *vs.* mHF, $P = 0.001$; Fig. 2a). There was a significant difference in *AdipoR1* gene expression between mice on mHF and HF (mHF *vs.* HF, $P = 0.025$; Fig.2a). The lack of endogenous leptin had no effect on central *AdipoR1* gene expression in $Lep^{ob/ob}$ mice compared with wild-type controls (Fig.2a).

The gene expression of the second adiponectin receptor *AdipoR2* was unaffected in mice fed the 60 % HF diet, however, gene expression of mice on mHF (45%) was doubled compared with LF mice (LF *vs.* mHF; $P = 0.007$; Fig.2b). As with *AdipoR1* expression in the ARC, lack of leptin did not affect gene expression of *AdipoR2* (Fig.2b) in this region. *AdipoR2* expression was comparable in wild-type and $Lep^{ob/ob}$ mice on LFD.

The downstream target of adiponection signalling, *APPL1*, was neither influenced by diet nor by genotype (data not shown).

Acute actions of ICV adiponectin on glucose tolerance and hepatic glucose production

Having established that gene expression of *adiponectin*, its receptors and the adaptor protein *APPL1* were influenced by feeding status and partially by diet, we next investigated whether ICV adiponectin could modulate impaired glucose tolerance during HF *vs.* LF feeding in wild-type and in $Lep^{ob/ob}$ mice. In all mouse models of obesity used, ICV adiponectin consistently improved the impaired glucose tolerance (Fig.3). In glucose intolerant $Lep^{ob/ob}$ mice fed a LF diet (n= 9-11 mice/group) acute ICV adiponectin markedly improved glucose tolerance. The AUC in these mice was significantly decreased compared with vehicle treated $Lep^{ob/ob}$ mice ($P = 0.01$; Fig.3a).

In normoglycemic wild-type mice fed a LF diet ICV adiponectin had no effect and did not lead to hypoglycaemia (Fig.3a; n = 7-8 mice/group).

Additionally, in glucose intolerant Lep$^{ob/ob}$ mice the effect of ICV adiponectin on hepatic glucose production (n = 5-6 mice/group) using a pyruvate tolerance test was tested. By using pyruvate, a substrate for gluconeogenesis, it is possible to measure the rate of glucose production reflecting hepatic glucose output. Central adiponectin application led to a significantly reduced glucose excursion compared with the vehicle treated Lep$^{ob/ob}$ mice (P = 0.006; Fig. 3b).

Next we investigated whether the glucose lowering properties of ICV adiponectin are also present in DIO mice. As expected, four weeks of HF feeding significantly impaired the glucose tolerance of mice (LF vehicle *vs.* HF vehicle P < 0.001; Fig.3c). Centrally-administered adiponectin 60 min prior to an ipGTT acutely improved the impaired glucose tolerance in these mice (HF adiponectin *vs.* HF vehicle P = 0.002; n = 5-7 mice/group) so that the glucose clearance rate was comparable to that observed in normoglycemic mice on LF diet (LF vehicle *vs.* HF adiponectin = n.s, HF vehicle *vs.* LF vehicle P < 0.001).

We next tested whether central adiponectin can also improve glucose tolerance in mice in an extreme state of obesity and glucose intolerance; Lep$^{ob/ob}$ mice fed a HF diet. Consistent with the findings above, ICV adiponectin, in these mice, robustly improved glucose tolerance. The calculated AUC of DIO Lep$^{ob/ob}$ mice treated centrally with adiponectin was significantly decreased compared with vehicle treated controls (P = 0.045; Fig.3c; n = 9-23 mice/group).

Acute effects of centrally-administered adiponectin on central signalling cascades involved in energy regulation and glucose metabolism

Since centrally-administered adiponectin exhibited potent glucose-lowering properties; we next investigated the underlying neurochemical mechanism in the glucose intolerant Lep$^{ob/ob}$ mouse. ICV adiponectin led to a non significant 1.7-fold increase in the number of pAKT(Ser473) immunoreactive cells in the ARC of Lep$^{ob/ob}$ mice relative to vehicle (vehicle *vs* adiponectin P = 0.065; Fig. 4a; n = 5-6 mice/group). In the VMH we observed a significant 2.4-fold increase in the number of pAKT(Ser473) immunoreactive cells in adiponectin treated Lep$^{ob/ob}$ mice compared with controls (vehicle *vs.* adiponectin P = 0.02; Fig. 4b; n = 5-6 mice/group).

The number of pAMPK(Thr172) immunoreactive cells was significantly reduced by 1.5-fold in the ARC (P = 0.018) and by 2.5-fold in the VMH (P = 0.005) after ICV adiponectin treatment compared with vehicle (Fig. 4c, d, n = 13 / group).
In contrast to the rise in pAKT immunoreactivity and the decrease in pAMPK, the number of pSTAT3(Try705) immunoreactive cells in both hypothalamic nuclei was unaffected by adiponectin treatment and only very few pSTAT3(Try705) immunoreactive cells were detected in the ARC (Fig. 4e), whereas staining in the VMH was undetectable (data not shown).

Acute effects of ICV adiponectin on pro-inflammatory signalling in DIO

To identify whether adiponectin affects pro-inflammatory signalling in the MBH in obesity, we investigated the pattern of pJNK(Thr183/Tyr185) and pGSK3β(Ser9) immunoreactivity after acute ICV adiponectin administration (n = 5 / group). This experiment was performed in DIO mice which exhibit increased pro-inflammatory signalling. We previously reported that HFD feeding leads to an increase in the number of pJNK(Thr183/Tyr185) and a decrease in the number of pGSK3β(Ser9) immunoreactive cells in regions of the MBH (18;19) which is associated with activation of pro-inflammatory signalling pathways.

Consistent with our previous findings (18), HF feeding was associated with an increase in the number of pJNK(Thr183/Tyr185) cells in the ARC (P = 0.001) and VMH (P = 0.043) compared with control mice on LF diet (Fig. 5a,b). ICV adiponectin acutely reduced the elevated number of pJNK(Thr183/Tyr185) positive cells in the ARC of these mice (HF vehicle *vs.* HF adiponectin, P = 0.019). Notably, in the ARC, the number of pJNK(Thr183/Tyr185) positive cells was reversed to levels of LF after this treatment (P = 0.06; Fig. 5a). In the VMH, centrally administered adiponectin totally reversed the diet-induced increase in pJNK(Thr183/Tyr185) immunoreactive cells to levels exhibited by LF mice (HF vehicle *vs.* HF adiponectin; P = 0.045; Fig.5b). Consistent with previous findings (19), HF feeding led to a decrease in the number of pGSK3β(Ser9) immunoreactive cells in the ARC (HF vehicle *vs.* LF vehicle P = 0.026; Fig.5c) and VMH (HF vehicle *vs.* LF vehicle P = 0.002; Fig.5d) by approximately 30 % indicating an elevated GSK3 activity in these mice. ICV adiponectin totally reversed these diet-induced alterations in the number of pGSK3β(Ser9) positive cells in the ARC (HF vehicle *vs.* HF adiponectin P < 0.001; Fig.5c) and VMH (HF vehicle *vs.* HF adiponectin P = 0.012; Fig.5d) to levels seen in mice on the LF diet.

Discussion

It is well established that the anti-inflammatory hormone adiponectin sensitizes the action of insulin in peripheral tissues (23;24). Circulating adiponectin levels are inversely correlated with the size of body fat stores thereby linking obesity to insulin insensitivity and the development of type II diabetes (3;25). Although peripheral effects of adiponectin on glucose- and energy metabolism are well characterised, the precise action of adiponectin in the CNS remains uncertain (25). While some evidence suggests that adiponectin acts centrally to control metabolism, it has not yet been satisfactorily determined whether adiponectin is expressed in the brain. Neumeier M *et al*. described adiponectin to be 1000-fold lower in mouse and human cerebrospinal fluid (CSF) than in the peripheral circulation (8). Compared with other hormones e.g. leptin (~ 100 pg/ml), the absolute adiponectin concentration in CSF (~100ng/ml) is still about 1000-fold higher suggesting a potent biological activity of adiponectin in the brain (17). Despite this high concentration of adiponectin in the CSF, *adiponectin* gene expression has not been detected in the human brain indicating transport across the blood brain barrier must occur (8). In contrast to humans, emerging evidence suggests that *adiponectin* is expressed in the brain of mice (26). These apparent controversial findings might be explained by the regulation of *adiponectin g*ene expression by feeding status. In our experiments, *adiponectin* expression was only detectable in the ARC of *ad libitum* fed mice, whereas fasting led to a reduction in gene expression levels which was virtually undetectable. The physiological relevance of *adiponectin* expression in the hypothalamus remains uncertain. Bauche *et al*. suggested that adiponectin might regulate its own expression as transient over-expression of adiponectin in young mice was associated with a decreased *adiponectin* gene expression, protein content in fat depots and serum adiponectin during adulthood (27). This potential auto-regulation of the adiponectin gene may account for the down-regulation of central *adiponectin* expression seen after 16 h food deprivation in the present study as CSF concentrations of adiponectin were reported to be elevated after 8 h fasting in mice.

It was reported that central injection of adiponectin robustly reduces food intake (16) and increases energy expenditure (17). Thus, down-regulation of *adiponectin* gene expression in the ARC after fasting might compensate for the catabolic action of adiponectin in the MBH. This indicates a regulatory mechanism distinct from the reported peripheral regulation processes. In the periphery, during fasting or caloric restriction, circulating adiponectin and expression in adipose tissue is elevated, which may convey the beneficial properties of adiponectin on whole body glucose and energy homeostasis (28;29).

In contrast to *adiponectin*, *AdipoR1* expression appears to be similarly regulated in peripheral and central insulin target regions. Caloric restriction significantly increased the expression of *AdipoR1* in liver and skeletal muscle (30;31). We found that fasting was also associated with increased *AdipoR1*

gene expression in the ARC. HF feeding, however, was also associated with increased *AdipoR1* expression in the ARC, intriguingly this effect was exacerbated in mice on the 45% fat diet compared with those on the 60% fat diet. The 45% fat diet was also effective in increasing *AdipoR2* gene expression in the ARC whereas on the 60% fat diet no change was observed compared with the LFD controls. A DIO-associated increase in central *AdipoR1* is in line with data derived from studies in the periphery, where HF feeding was associated with an increase in *AdipoR1* expression in liver and skeletal muscle of HF fed rodents compared with LF controls (32;33). Apart from nutrition-related regulation of *AdipoR1* and *AdipoR2*, we also investigated whether the central expression of these receptors is regulated by endogenous leptin. Surprisingly, in our study *AdipoR1* and *AdipoR2* expression in the ARC was not different in the ARC of Lep$^{ob/ob}$ compared with wild-type mice, although circulating adiponectin levels and the expression of the peripheral adiponectin receptors have been reported to be significantly reduced in these mice. In contrast, Kubota *et al*. reported that central expression of *AdipoR1* and *AdipoR2* was significantly decreased in Lep$^{ob/ob}$ mice compared with wild-type mice (34). This apparent discrepancy may be explained by termination of the experiments during a different circadian phase (35;36). Gene expression of the adaptor protein *APPL1* was only affected by nutritional status. Acute 16 h fasting increased the expression of *APPL1*, whereas dietary fat content or endogenous leptin levels did not affect the expression indicating that mRNA expression of this adaptor protein is not affected by HF diet or leptin treatment.

Having established that adiponectin and adiponectin receptor expression are regulated by acute feeding conditions and chronic HF feeding, we hypothesised an important role for central adiponectin in the regulation of whole body glucose homeostasis. In agreement with this hypothesis, ICV adiponectin acutely improved glucose tolerance in Lep$^{ob/ob}$ mice. This finding is consistent with a study by Qi *et al*. who demonstrated that ICV adiponectin improved basal blood glucose levels in these mice (17). Intriguingly, in wild-type mice fed a HF diet that exhibit profound central leptin resistance in terms of its glucose lowering potential (Koch CE; unpublished data), central adiponectin potently improved glucose homeostasis. It has been reported that peripheral adiponectin sensitivity was reduced in mice fed a HF diet. Also in the case of extreme obesity and glucose intolerance, as exhibited by Lep$^{ob/ob}$ mice fed a HFD for 10 days, adiponectin retained its glucose lowering properties.

We next investigated whether ICV adiponectin affects hypothalamic insulin signalling and pro-inflammatory pathways. Coope *et al*. had previously shown that central adiponectin elevates protein levels of the insulin signalling target pAKT(Ser473) in rat hypothalamic lysates (16). Using immunohistochemistry, we demonstrated that in mice ICV adiponectin increased the number of pAKT(Ser473) positive cells in the ARC and VMH. Interestingly, the most documented molecular target of adiponectin, pAMPK(Thr172), was inversely regulated by adiponectin, with the number of pAMPK(Thr172) cells decreased in these regions compared with vehicle-treated mice. This down-

regulation of pAMPK(Thr172) in response to ICV adiponectin in the MBH is in contrast to peripheral action of this hormone and one previous study that investigated the central effects of adiponectin on AMPK after peripheral administration of the hormone (34). These differences could be explained by an opposite action of adiponectin in the periphery and in the brain. Our findings clearly show reduced AMPK activity after ICV adiponectin administration which agrees with the general catabolic action of central adiponectin similar to both central insulin and leptin which have a potent catabolic action and reduce pAMPK(Thr172) in the MBH (37).

The known catabolic action of central adiponectin appears to be independent of the JAK2/STAT3 pathway which mediates the anorexgenic effect of leptin as ICV adiponectin did not affect the number of pSTAT3(Tyr705) immunoreactive cells in the ARC or VMH. Thus, it is likely that the catabolic function of adiponectin is mediated by hypothalamic AMPK which is known to be involved in the regulation of food intake (37).

As previously described adiponectin improves glucose intolerance in mice fed a HF diet. Since HF feeding is associated with inflammation in the MBH (38), we hypothesised that central adiponectin may reverse the HFD induction of important pro-inflammatory markers, such as JNK and GSK3 (18;19). Consistent with this hypothesis, ICV administration of adiponectin, lowered the HF induced increase in the number of pJNK immunoreactive cells in the ARC and VMH. Also the reduced number of pGSK3 immunoreactive cells seen in HFD mice was fully reversed by ICV adiponectin. We have previously shown that increased activity of JNK and GSK3 in the MBH is associated with impaired whole body glucose homeostasis (18;19). Therefore, it is plausible that one of the ways in which adiponectin exerts its glucose-lowering properties is by reversing pro-inflammatory signalling in the MBH. Taken together these data clearly demonstrate that adiponectin plays a crucial role in the neuroendocrine regulation of glucose homeostasis providing an important link in the interaction of obesity and insulin insensitivity.

Reference List

1. **Chan JC, Malik V, Jia W, Kadowaki T, Yajnik CS, Yoon KH, Hu FB** 2009 Diabetes in Asia: epidemiology, risk factors, and pathophysiology. JAMA 301:2129-2140

2. **Trayhurn P, Beattie JH** 2001 Physiological role of adipose tissue: white adipose tissue as an endocrine and secretory organ. Proc Nutr Soc 60:329-339

3. **Arita Y, Kihara S, Ouchi N, Takahashi M, Maeda K, Miyagawa J, Hotta K, Shimomura I, Nakamura T, Miyaoka K, Kuriyama H, Nishida M, Yamashita S, Okubo K, Matsubara K, Muraguchi M, Ohmoto Y, Funahashi T, Matsuzawa Y** 1999 Paradoxical decrease of an adipose-specific protein, adiponectin, in obesity. Biochem Biophys Res Commun 257:79-83

4. **Hotta K, Funahashi T, Bodkin NL, Ortmeyer HK, Arita Y, Hansen BC, Matsuzawa Y** 2001 Circulating concentrations of the adipocyte protein adiponectin are decreased in parallel with reduced insulin sensitivity during the progression to type 2 diabetes in rhesus monkeys. Diabetes 50:1126-1133

5. **Hu E, Liang P, Spiegelman BM** 1996 AdipoQ is a novel adipose-specific gene dysregulated in obesity. J Biol Chem 271:10697-10703

6. **Ebinuma H, Miida T, Yamauchi T, Hada Y, Hara K, Kubota N, Kadowaki T** 2007 Improved ELISA for selective measurement of adiponectin multimers and identification of adiponectin in human cerebrospinal fluid. Clin Chem 53:1541-1544

7. **Kusminski CM, McTernan PG, Schraw T, Kos K, O'Hare JP, Ahima R, Kumar S, Scherer PE** 2007 Adiponectin complexes in human cerebrospinal fluid: distinct complex distribution from serum. Diabetologia 50:634-642

8. **Neumeier M, Weigert J, Buettner R, Wanninger J, Schaffler A, Muller AM, Killian S, Sauerbruch S, Schlachetzki F, Steinbrecher A, Aslanidis C, Scholmerich J, Buechler C** 2007 Detection of adiponectin in cerebrospinal fluid in humans. Am J Physiol Endocrinol Metab 293:E965-E969

9. **Yildiz BO, Suchard MA, Wong ML, McCann SM, Licinio J** 2004 Alterations in the dynamics of circulating ghrelin, adiponectin, and leptin in human obesity. Proc Natl Acad Sci U S A 101:10434-10439

10. **Fruebis J, Tsao TS, Javorschi S, Ebbets-Reed D, Erickson MR, Yen FT, Bihain BE, Lodish HF** 2001 Proteolytic cleavage product of 30-kDa adipocyte complement-related protein increases fatty acid oxidation in muscle and causes weight loss in mice. Proc Natl Acad Sci U S A 98:2005-2010

11. **Nakano Y, Tobe T, Choi-Miura NH, Mazda T, Tomita M** 1996 Isolation and characterization of GBP28, a novel gelatin-binding protein purified from human plasma. J Biochem 120:803-812

12. **Waki H, Yamauchi T, Kamon J, Ito Y, Uchida S, Kita S, Hara K, Hada Y, Vasseur F, Froguel P, Kimura S, Nagai R, Kadowaki T** 2003 Impaired multimerization of human adiponectin mutants associated with diabetes. Molecular structure and multimer formation of adiponectin. J Biol Chem 278:40352-40363

13. **Waki H, Yamauchi T, Kamon J, Kita S, Ito Y, Hada Y, Uchida S, Tsuchida A, Takekawa S, Kadowaki T** 2005 Generation of globular fragment of adiponectin by leukocyte elastase secreted by monocytic cell line THP-1. Endocrinology 146:790-796

14. **Yamauchi T, Kamon J, Minokoshi Y, Ito Y, Waki H, Uchida S, Yamashita S, Noda M, Kita S, Ueki K, Eto K, Akanuma Y, Froguel P, Foufelle F, Ferre P, Carling D, Kimura S, Nagai R, Kahn BB, Kadowaki T** 2002 Adiponectin stimulates glucose utilization and fatty-acid oxidation by activating AMP-activated protein kinase. Nat Med 8:1288-1295

15. **Minokoshi Y, Alquier T, Furukawa N, Kim YB, Lee A, Xue B, Mu J, Foufelle F, Ferre P, Birnbaum MJ, Stuck BJ, Kahn BB** 2004 AMP-kinase regulates food intake by responding to hormonal and nutrient signals in the hypothalamus. Nature 428:569-574

16. **Coope A, Milanski M, Araujo EP, Tambascia M, Saad MJ, Geloneze B, Velloso LA** 2008 AdipoR1 mediates the anorexigenic and insulin/leptin-like actions of adiponectin in the hypothalamus. FEBS Lett 582:1471-1476

17. **Qi Y, Takahashi N, Hileman SM, Patel HR, Berg AH, Pajvani UB, Scherer PE, Ahima RS** 2004 Adiponectin acts in the brain to decrease body weight. Nat Med 10:524-529

18. **Benzler J, Ganjam GK, Legler K, Stohr S, Kruger M, Steger J, Tups A** 2013 Acute inhibition of central c-Jun N-terminal kinase restores hypothalamic insulin signalling and alleviates glucose intolerance in diabetic mice. J Neuroendocrinol 25:446-454

19. **Benzler J, Ganjam GK, Kruger M, Pinkenburg O, Kutschke M, Stohr S, Steger J, Koch CE, Olkrug R, Schwartz MW, Shepherd PR, Grattan DR, Tups A** 2012 Hypothalamic glycogen synthase kinase 3beta has a central role in the regulation of food intake and glucose metabolism. Biochem J 447:175-184

20. **Mercer JG, Moar KM, Logie TJ, Findlay PA, Adam CL, Morgan PJ** 2001 Seasonally inappropriate body weight induced by food restriction: effect on hypothalamic gene expression in male Siberian hamsters. Endocrinology 142:4173-4181

21. **Koch C, Augustine RA, Steger J, Ganjam GK, Benzler J, Pracht C, Lowe C, Schwartz MW, Shepherd PR, Anderson GM, Grattan DR, Tups A** 2010 Leptin rapidly improves glucose homeostasis in obese mice by increasing hypothalamic insulin sensitivity. J Neurosci 30:16180-16187

22. **Munzberg H, Huo L, Nillni EA, Hollenberg AN, Bjorbaek C** 2003 Role of signal transducer and activator of transcription 3 in regulation of hypothalamic proopiomelanocortin gene expression by leptin. Endocrinology 144:2121-2131

23. **Kubota N, Terauchi Y, Yamauchi T, Kubota T, Moroi M, Matsui J, Eto K, Yamashita T, Kamon J, Satoh H, Yano W, Froguel P, Nagai R, Kimura S, Kadowaki T, Noda T** 2002 Disruption of adiponectin causes insulin resistance and neointimal formation. J Biol Chem 277:25863-25866

24. **Maeda N, Shimomura I, Kishida K, Nishizawa H, Matsuda M, Nagaretani H, Furuyama N, Kondo H, Takahashi M, Arita Y, Komuro R, Ouchi N, Kihara S, Tochino Y, Okutomi K, Horie M, Takeda S, Aoyama T, Funahashi T, Matsuzawa Y** 2002 Diet-induced insulin resistance in mice lacking adiponectin/ACRP30. Nat Med 8:731-737

25. **Thundyil J, Pavlovski D, Sobey CG, Arumugam TV** 2012 Adiponectin receptor signalling in the brain. Br J Pharmacol 165:313-327

26. **Wilkinson M, Brown R, Imran SA, Ur E** 2007 Adipokine gene expression in brain and pituitary gland. Neuroendocrinology 86:191-209

27. **Bauche IB, it El MS, Rezsohazy R, Funahashi T, Maeda N, Miranda LM, Brichard SM** 2006 Adiponectin downregulates its own production and the expression of its AdipoR2 receptor in transgenic mice. Biochem Biophys Res Commun 345:1414-1424

28. **Ding Q, Ash C, Mracek T, Merry B, Bing C** 2012 Caloric restriction increases adiponectin expression by adipose tissue and prevents the inhibitory effect of insulin on circulating adiponectin in rats. J Nutr Biochem 23:867-874

29. **Niemann B, Silber RE, Rohrbach S** 2008 Age-specific effects of short- and long-term caloric restriction on the expression of adiponectin and adiponectin receptors: influence of intensity of food restriction. Exp Gerontol 43:706-713

30. **de OC, de Mattos AB, Biz C, Oyama LM, Ribeiro EB, do Nascimento CM** 2011 High-fat diet and glucocorticoid treatment cause hyperglycemia associated with adiponectin receptor alterations. Lipids Health Dis 10:11

31. **Huang H, Iida KT, Sone H, Yokoo T, Yamada N, Ajisaka R** 2006 The effect of exercise training on adiponectin receptor expression in KKAy obese/diabetic mice. J Endocrinol 189:643-653

32. **Bullen JW, Jr., Bluher S, Kelesidis T, Mantzoros CS** 2007 Regulation of adiponectin and its receptors in response to development of diet-induced obesity in mice. Am J Physiol Endocrinol Metab 292:E1079-E1086

33. **Tsuchida A, Yamauchi T, Ito Y, Hada Y, Maki T, Takekawa S, Kamon J, Kobayashi M, Suzuki R, Hara K, Kubota N, Terauchi Y, Froguel P, Nakae J, Kasuga M, Accili D, Tobe K, Ueki K, Nagai R, Kadowaki T** 2004 Insulin/Foxo1 pathway regulates expression levels of adiponectin receptors and adiponectin sensitivity. J Biol Chem 279:30817-30822

34. **Kubota N, Yano W, Kubota T, Yamauchi T, Itoh S, Kumagai H, Kozono H, Takamoto I, Okamoto S, Shiuchi T, Suzuki R, Satoh H, Tsuchida A, Moroi M, Sugi K, Noda T, Ebinuma H, Ueta Y, Kondo T, Araki E, Ezaki O, Nagai R, Tobe K, Terauchi Y, Ueki K, Minokoshi Y, Kadowaki T** 2007 Adiponectin stimulates AMP-activated protein kinase in the hypothalamus and increases food intake. Cell Metab 6:55-68

35. **Barnea M, Madar Z, Froy O** 2010 High-fat diet followed by fasting disrupts circadian expression of adiponectin signaling pathway in muscle and adipose tissue. Obesity (Silver Spring) 18:230-238

36. **Bluher M, Fasshauer M, Kralisch S, Schon MR, Krohn K, Paschke R** 2005 Regulation of adiponectin receptor R1 and R2 gene expression in adipocytes of C57BL/6 mice. Biochem Biophys Res Commun 329:1127-1132

37. **Andersson U, Filipsson K, Abbott CR, Woods A, Smith K, Bloom SR, Carling D, Small CJ** 2004 AMP-activated protein kinase plays a role in the control of food intake. J Biol Chem 279:12005-12008

38. **Posey KA, Clegg DJ, Printz RL, Byun J, Morton GJ, Vivekanandan-Giri A, Pennathur S, Baskin DG, Heinecke JW, Woods SC, Schwartz MW, Niswender KD** 2009 Hypothalamic proinflammatory lipid accumulation, inflammation, and insulin resistance in rats fed a high-fat diet. Am J Physiol Endocrinol Metab 296:E1003-E1012

Figure Legends

Fig1: Gene expression of *adiponectin*, the receptor *AdipoR1* and the adaptor protein *APPL1 in the arcuate nucleus* of either *ad libitum* or food deprived mice.

Adiponectin, AdipoR1 and APPL1 gene expression in the ARC is regulated by feeding status. Autoradiographs depicting *in situ* hybridization with antisense ^{35}S-labelled riboprobes to *adiponectin* (a), *AdipoR1* (b) *and APPL1* (c) mRNA signal in *ad libitum* fed (upper left panels) and food deprived (lower left panels) mice. The right panels show a bar graph generated from quantification of the respective signal in the arcuate nucleus.

Means +/- SEM of the quantified signal; **P < 0.01; ***P < 0.001

Fig2: Gene expression pattern of *AdipoR1* and *AdipoR2* in the arcuate nucleus of wild-type mice fed low and high fat diets and leptin deficient mice on low fat diet.

AdipoR1 and APPL1 gene expression in the ARC are affected by dietary fat content. Gene expression of AdipoR1 (a) and AdipoR2 (b) in the arcuate nuclues of wildtype mice fed low and high fat diets (45% and 60% fat content, for 4 weeks) and Lep$^{ob/ob}$ mice on low fat diet.

The bar chart shows the means +/- SEM of the quantified *in situ* hybridization signal; *P < 0.05; **P < 0.01; ***P < 0.001

Fig3: Effect of centrally administered adiponectin on glucose tolerance in mice with genetically and/or diet-induced impaired energy and glucose metabolism.

Central adiponectin lowers peripheral glucose levels. a) Intraperitoneal glucose tolerance test in Lep$^{ob/ob}$ mice and respective wildtype controls that were either ICV injected with adiponectin (1µg in aCSF) or vehicle (aCSF). b) Pyruvate tolerance test of Lep$^{ob/ob}$ mice and respective wildtype controls either ICV injected with adiponectin (1µg in aCSF) or vehicle (aCSF). c) Intraperitoneal glucose tolerance tests of wildtype mice on low fat diet (ICV injected with vehicle (aCSF)) and of wildtype mice fed high fat diet (60% fat) ICV injected with either adiponectin (1µg in aCSF) or vehicle (aCSF). d) Intraperitoneal glucose tolerance tests after either adiponectin (1µg in aCSF) or vehicle (aCSF) ICV injection in Lep$^{ob/ob}$ mice on high fat diet (60% fat, 10 days. Adiponection and vehicle were injected 60 min prior to all tests. Shown are ipGTTs (left panels) and respective AUCs (right panels).

Data show means +/- SEM; *P < 0.05; **P < 0.01; ***P < 0.001

Fig4: Impact of centrally administered adiponectin on hypothalamic insulin and leptin signalling pathways.

Compared with vehicle treated controls centrally administered adiponectin (1µg) partially increases the number of pAKT(Ser473) (a, b) and reduces the number of pAMPK(Thr172) (c,d)

immunopositive cells in the ARC and VMH of $Lep^{ob/ob}$ mice while pSTAT3(Tyr705) (e) immunreactivity remains unaltered. Mice received either adiponectin (1µg in aCSF) or vehicle (aCSF) 60 min prior to transcardial perfusion. Representative images show pAKT(Ser473), pAMPK(Thr172) and pSTAT3(Tyr705) immunoreactivity in the ARC and VMH. Immunoreactive cells counted in the respective region are shown in bar charts.
Bar charts show means +/- SEM; *P < 0.05; **P < 0.01

Fig5: Central adiponectin reduces inflammatory signalling in the mediobasal hypothalamus during diet induced obesity.

High-fat feeding (60% fat) increases the number of pJNK(Thr183/Tyr185) and reduces the number of pGSK3β(Ser9) counted cells in the ARC and VMH of wild-type mice while central adiponectin (1µg in aCSF) reverses this effect. Wildtype mice were fed the high fat diet for 4 weeks. Mice received either adiponectin (1µg in aCSF) or vehicle (aCSF) 60 min prior to transcardial perfusion. Representative images show pJNK(Thr183/Tyr185), and pGSK3β(Ser9) and immunoreactivity in the ARC and VMH. Immunoreactive cells counted in the respective region are shown in bar charts.
Bar charts show means +/- SEM; *P < 0.05; **P < 0.01; ***P < 0.001

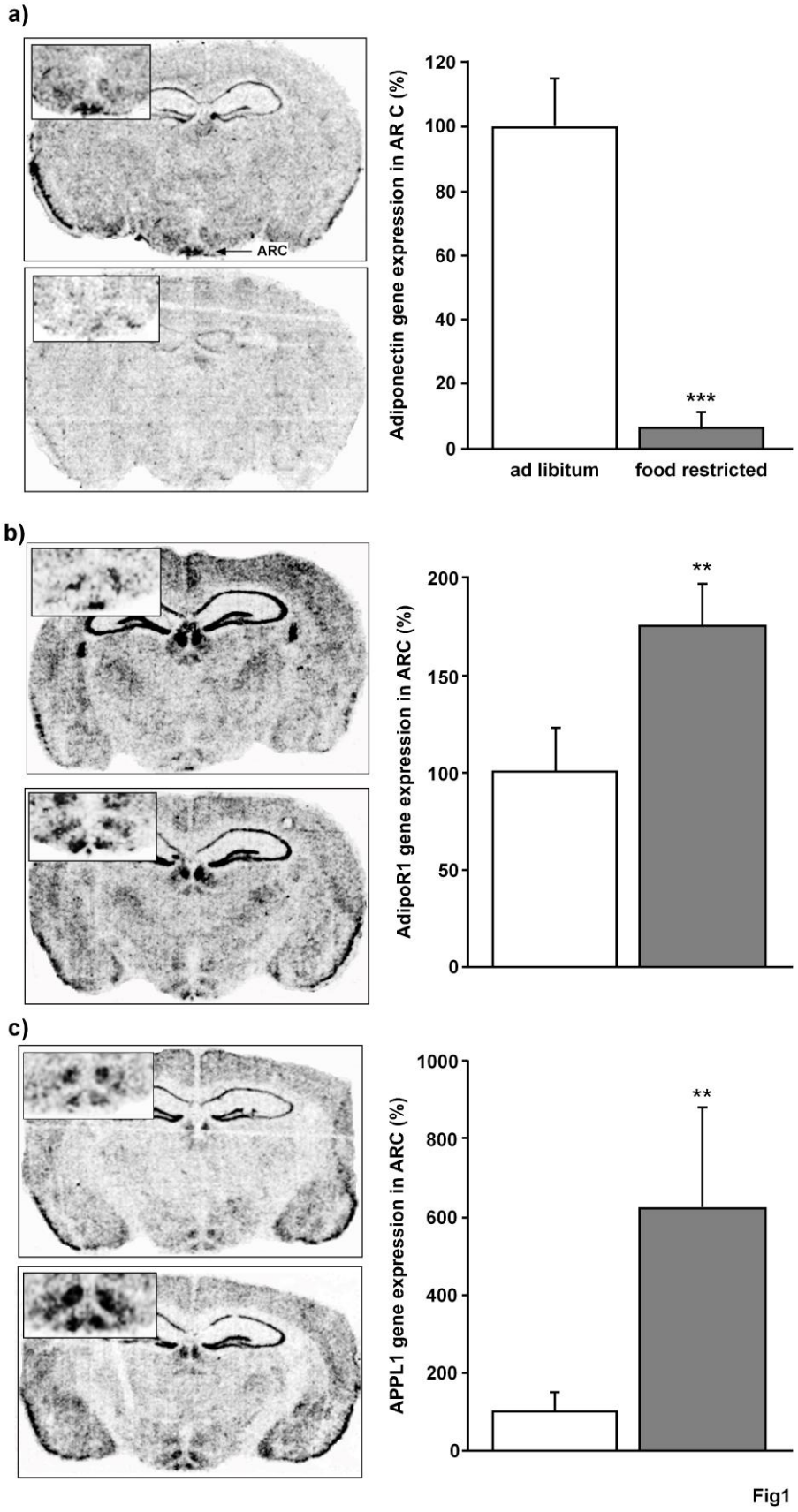
a)
ARC
Adiponectin gene expression in AR C (%)
120
100
80
60
40
20
0
***
ad libitum
food restricted
b)
AdipoR1 gene expression in ARC (%)
200
150
100
50
0
**
c)
APPL1 gene expression in ARC (%)
1000
800
600
400
200
0
**

Fig1

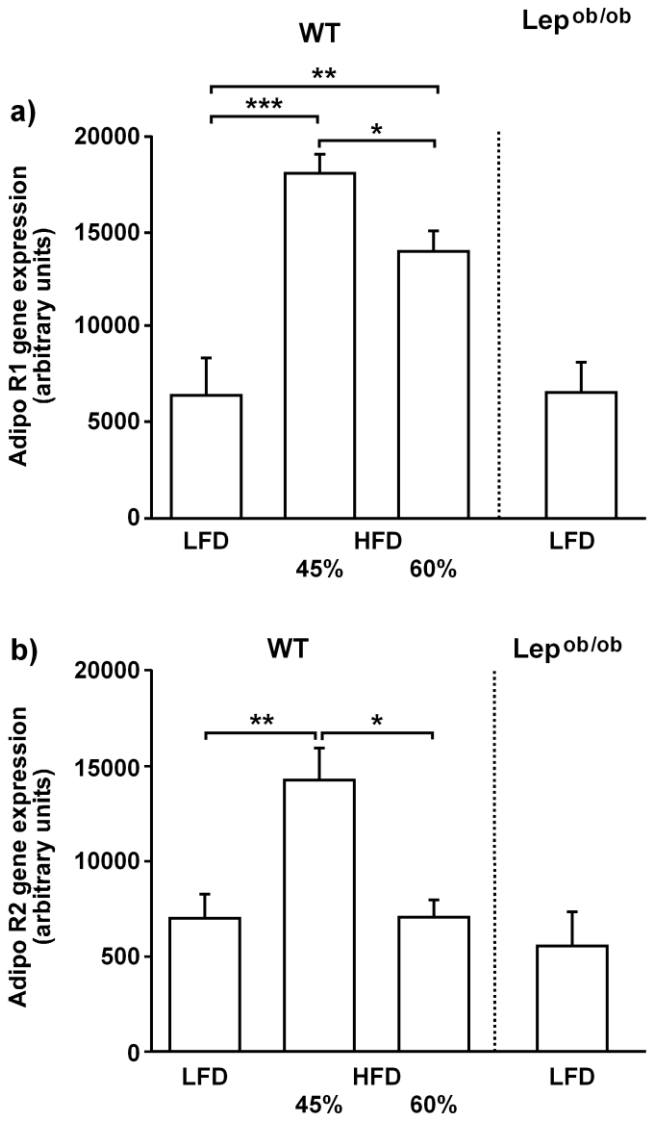
a)
WT
Lep ob/ob
**
***
*
Adipo R1 gene expression (arbitrary units)
20000
15000
10000
5000
0
LFD
HFD
45%
60%
LFD
b)
WT
Lep ob/ob
**
*
Adipo R2 gene expression (arbitrary units)
20000
15000
10000
500
0
LFD
HFD
45%
60%
LFD

Fig.2

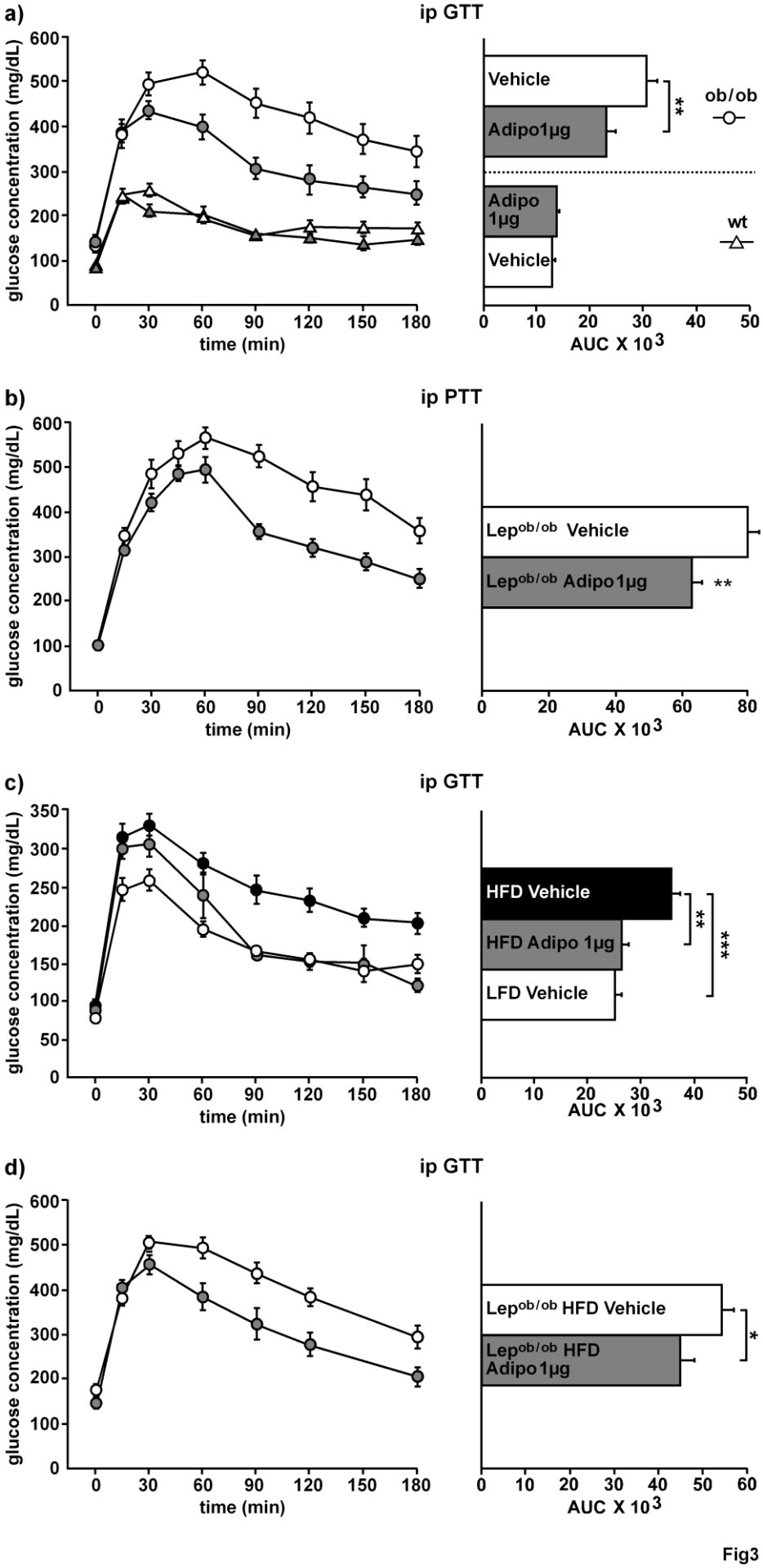
a)
ip GTT
glucose concentration (mg/dL)
time (min)
Vehicle
Adipo1µg
ob/ob
Adipo 1µg
Vehicle
wt
AUC X 10 3
b)
ip PTT
Lepob/ob Vehicle
Lepob/ob Adipo1µg
c)
ip GTT
HFD Vehicle
HFD Adipo 1µg
LFD Vehicle
d)
ip GTT
Lepob/ob HFD Vehicle
Lepob/ob HFD Adipo1µg

Fig3

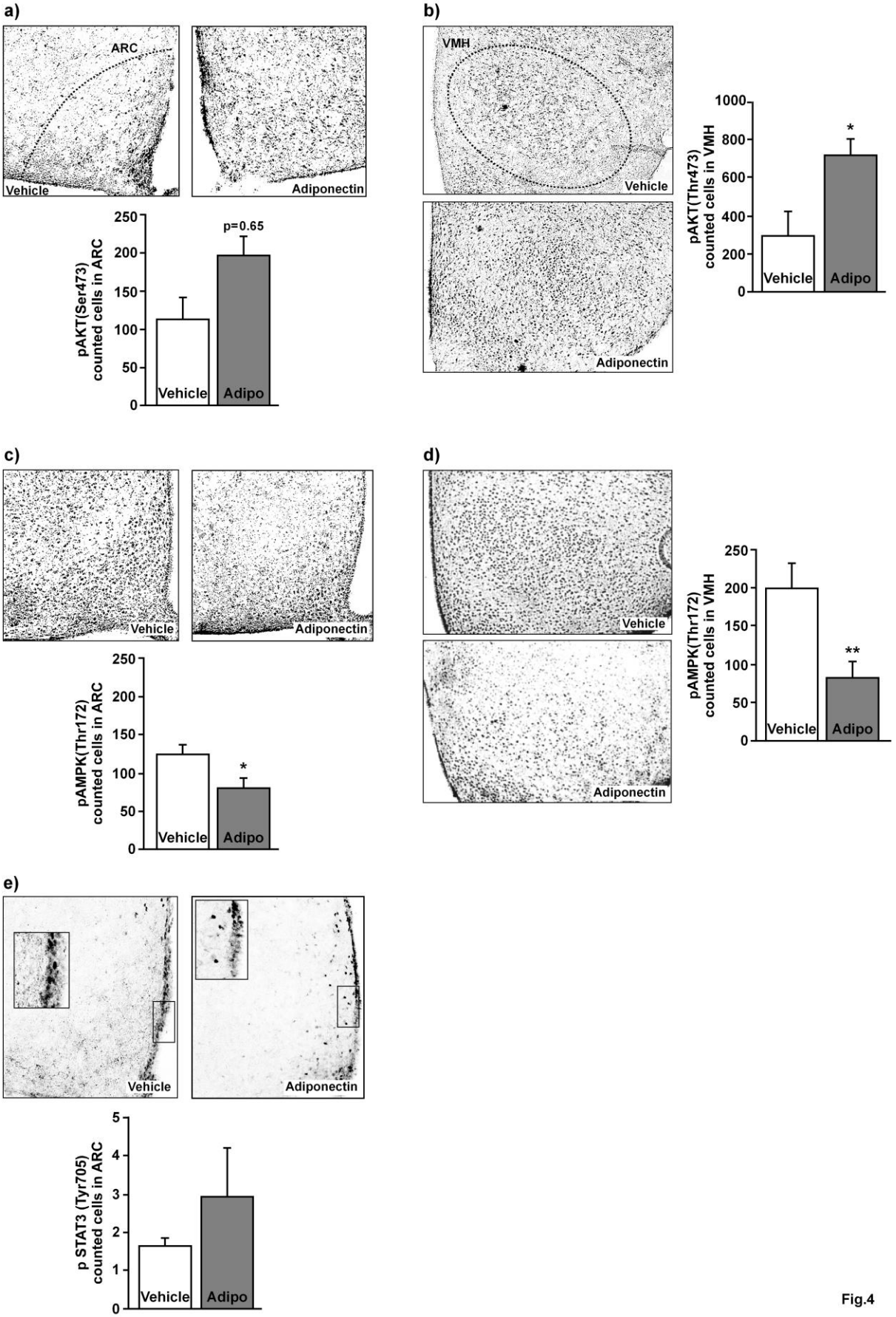
a)
ARC
Vehicle
Adiponectin
pAKT(Ser473) counted cells in ARC
p=0.65
Vehicle
Adipo
b)
VMH
Vehicle
Adiponectin
pAKT(Thr473) counted cells in VMH
*
Vehicle
Adipo
c)
Vehicle
Adiponectin
pAMPK(Thr172) counted cells in ARC
*
Vehicle
Adipo
d)
Vehicle
Adiponectin
pAMPK(Thr172) counted cells in VMH
**
Vehicle
Adipo
e)
Vehicle
Adiponectin
p STAT3 (Tyr705) counted cells in ARC
Vehicle
Adipo

Fig.4

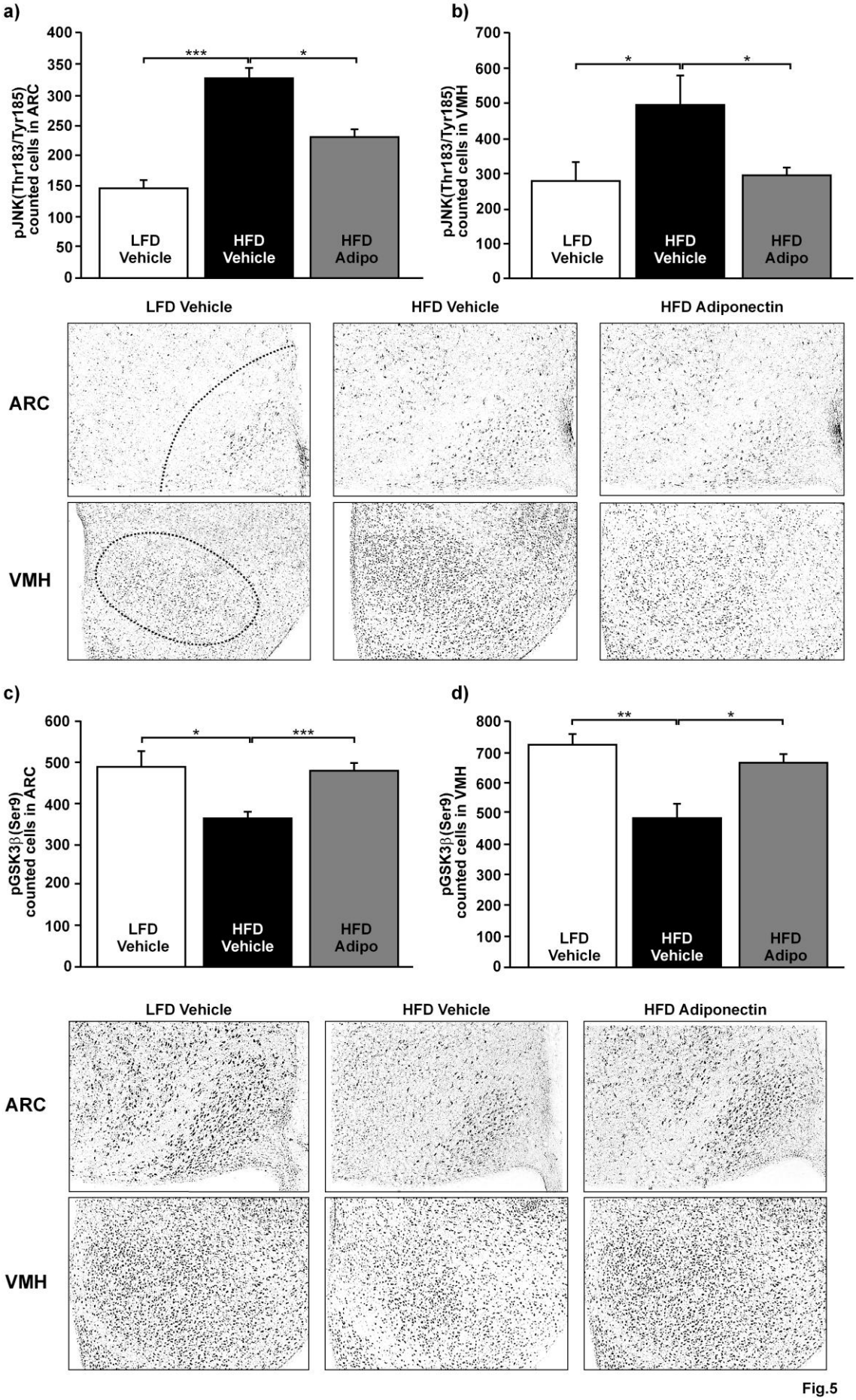
a)
pJNK(Thr183/Tyr185) counted cells in ARC
400
350
300
250
200
150
100
50
0
***
*
LFD Vehicle
HFD Vehicle
HFD Adipo
b)
pJNK(Thr183/Tyr185) counted cells in VMH
700
600
500
400
300
200
100
0
*
*
LFD Vehicle
HFD Vehicle
HFD Adipo
LFD Vehicle
HFD Vehicle
HFD Adiponectin
ARC
VMH
c)
pGSK3β(Ser9) counted cells in ARC
600
500
400
300
200
100
0
*
***
LFD Vehicle
HFD Vehicle
HFD Adipo
d)
pGSK3β(Ser9) counted cells in VMH
800
700
600
500
400
300
200
100
0
**
*
LFD Vehicle
HFD Vehicle
HFD Adipo
LFD Vehicle
HFD Vehicle
HFD Adiponectin
ARC
VMH

Fig.5

J Comp Physiol B
DOI 10.1007/s00360-013-0772-1

ORIGINAL PAPER

Overexpression of suppressor of cytokine signaling 3 in the arcuate nucleus of juvenile *Phodopus sungorus* alters seasonal body weight changes

Goutham K. Ganjam · Jonas Benzler · Olaf Pinkenburg · Alisa Boucsein · Sigrid Stöhr · Juliane Steger · Carsten Culmsee · Perry Barrett · Alexander Tups

Received: 17 January 2013 / Revised: 9 June 2013 / Accepted: 14 June 2013

Abstract The profound seasonal cycle in body weight exhibited by the Djungarian hamster (*Phodopus sungorus*) is associated with the development of hypothalamic leptin resistance during long day photoperiod (LD, 16:8 h light dark cycle), when body weight is elevated relative to short day photoperiod (SD, 8:16 h light dark cycle). We previously have shown that this seasonal change in physiology is associated with higher levels of mRNA for the potent inhibitor of leptin signaling, suppressor of cytokine signaling-3 (SOCS3), in the arcuate nucleus (ARC) of LD hamsters relative to hamsters in SD. The alteration in SOCS3 gene expression preceded the body weight change suggesting that SOCS3 might be the molecular switch of seasonal body weight changes. To functionally characterize the role of SOCS3 in seasonal body weight regulation, we injected SOCS3 expressing recombinant adeno-associated virus type-2 (rAAV2-SOCS3) constructs into the ARC of leptin sensitive SD hamsters immediately after weaning. Hamsters that received rAAV2 expressing enhanced green fluorescent protein (rAAV2-EGFP) served as controls. ARC-directed SOCS3 overexpression led to a significant increase in body weight over a period of 12 weeks without fully restoring the LD phenotype. This increase was partially due to elevated brown and white adipose tissue mass. Gene expression of pro-opiomelanocortin was increased while thyroid hormone converting enzyme DIO3 mRNA levels were reduced in SD hamsters with SOCS3 overexpression. In conclusion, our data suggest that ARC-directed SOCS3 overexpression partially overcomes the profound seasonal body weight cycle exhibited by the hamster which is associated with altered pro-opiomelanocortin and DIO3 gene expression.

Keywords Adeno-associated virus · SOCS3 · Arcuate nucleus · Body weight · POMC · Deiodinase

Communicated by G. Heldmaier.

G. K. Ganjam (✉) · J. Benzler · A. Boucsein · S. Stöhr · J. Steger · A. Tups
Department of Animal Physiology, Faculty of Biology, Philipps University Marburg, Karl-von-Frisch Str. 8, 35043 Marburg, Germany
e-mail: ganjam@staff.uni-marburg.de

A. Tups
e-mail: alexander.tups@staff.uni-marburg.de

G. K. Ganjam · C. Culmsee
Institute of Pharmacology and Clinical Pharmacy, Faculty of Pharmacy, Philipps University Marburg, Marburg, Germany

O. Pinkenburg
Department of Immunology, Faculty of Medicine, Philipps University Marburg, Marburg, Germany

P. Barrett
Rowett Institute, University of Aberdeen, Bucksburn, Aberdeen, UK

Introduction

Much of our knowledge about the neuroendocrine regulation of energy balance has come from valuable studies of genetically or dietary obese mice and rats. State of the art CNS-targeted genetic manipulations that are contributing significantly to further unravel the complex neuroendocrine regulation of energy balance are mostly limited to studies in mice, rodents that are rarely adapted to physiologically induced positive energy balance in their natural habitat. A fascinating rodent model to expand our knowledge about the dynamic long-term regulation of body weight is the Djungarian hamster (*Phodopus sungorus*), also known as

Published online: 17 July 2013

the Siberian hamster. This species exhibits a remarkable seasonal body weight cycle over the course of a year. During natural winter or in laboratory short day photoperiod conditions (SD, 8:16 h light dark cycle) the hamster's body weight trajectory reaches its nadir with about 30–40 % of values in long day photoperiod (LD, 16:8 h light dark cycle), more than half of this loss being due to a reduction of adipose tissue mass (Klingenspor et al. 2000). Consequently, this loss in body fat leads to decreased leptin gene expression and lowered circulating leptin concentrations. This seasonal variation in body weight is associated with a profound seasonal cycle in leptin sensitivity. Despite the anticipated high anorectic tone, LD hamsters increase their food intake indicating resistance to leptin in this photoperiod. Twice daily leptin injections at supraphysiological doses or chronic leptin infusion at physiological doses either caused a more profound decline in body fat in SD than in LD or even failed to induce a catabolic response in LD hamsters (Klingenspor et al. 2000). Mounting evidence suggests that alterations in leptin signaling in the hypothalamus are driven by seasonal variation in melatonin levels acting at the pars tuberalis and translated as a variation in thyroid hormone levels in the hypothalamus. Hypothalamic thyroid hormone is then responsible for the seasonal change in food intake and body weight exhibited by the hamster (Herwig et al. 2009; Lerchl and Schlatt 1993; Murphy et al. 2012).

The hypothalamic arcuate nucleus (ARC) has been intensively investigated as an important integrative center for mediation of the leptin signal in this species (Rousseau et al. 2003). Leptin transmits its signal by the long form of the leptin receptor (LRb) and activates the Janus kinase 2-signal transducer and activator of transcription 3 (JAK2-STAT3) pathway. This occurs via a series of phosphorylation events which lead to activation of the transcription factor STAT3 (Baumann et al. 1996; Tartaglia 1997; White et al. 1997), whose activation in the ARC is photoperiodically regulated (Tups et al. 2012). Amongst others, the transcription of two important target genes, the melanocortin precursor pro-opiomelanocortin (POMC) and the suppressor of cytokine signaling 3 (SOCS3) is activated by STAT3 (Bjorbaek et al. 1998; Munzberg et al. 2003; Myers 2004; Ramadoss et al. 2009). SOCS3 has been characterized as a putative mediator of central leptin resistance, it suppresses signaling downstream of the leptin receptor by inhibition of STAT3 phosphorylation (Bjorbaek et al. 1998). We previously demonstrated that SOCS3 gene expression in the ARC of *P. sungorus* was highly regulated by photoperiod (Tups et al. 2004; Tups et al. 2006; Tups 2009). In LD photoperiod, SOCS3 mRNA levels were relatively high compared to SD photoperiod in juvenile and adult hamsters demonstrating leptin resistance in LD at a molecular level. Increased levels of arcuate SOCS3 in LD were reversible when hamsters were transferred to SD (Tups et al. 2006). Furthermore, we demonstrated that photoperiod-induced changes in SOCS3 preceded subsequent alterations in body weight by about 3 weeks. These experiments suggested that SOCS3 might act as a molecular switch for the seasonal body weight change in *P. sungorus*.

In the current study, we functionally manipulated SOCS3 expression in the ARC to provide evidence for the hypothesis that SOCS3 is a potent driver of seasonal body weight changes. We mimicked LD conditions by overexpressing the SOCS3 gene in the ARC of SD acclimated juvenile hamsters using recombinant adeno-associated virus type 2 (AAV2) as a carrier. In juvenile SD hamsters this treatment led to a partial increase in body weight, a trend towards increased body fat mass and alterations in the hypothalamic profile of gene expression of important components of the neuroendocrine network of body weight regulation. These data substantiate the hypothesis that SOCS3 plays an important role in driving seasonal adaptations in *P. sungorus*.

Methods

Animals

Djungarian hamsters (*P. sungorus*) drawn from the breeding colony at the Biology Department of the University Marburg (Germany) were maintained in accordance with the guidelines of the Germany Council of Animal Care. Only male hamsters were used in this study. All hamsters were weaned at the age of 3 weeks in LD and were housed individually with ad libitum access to standard chow diet and water for a period of 12 weeks. Irrespective of the photoperiod, the animals were maintained at an ambient temperature of 23 °C. AAV2 constructs were stereotaxically injected into the bilateral halves of ARC immediately after weaning (at the age of 3 weeks) and hamsters were divided into three groups: AAV2-EGFP ($n = 10$) and AAV2-SOCS3 ($n = 10$) in SD photoperiod and AAV2-EGFP ($n = 7$) as control group in LD. Body weight was recorded once a week for up to 12 weeks. After 12 weeks when animals reached their complete adulthood, they were sacrificed and fat depots and the brains were collected for further analysis.

Recombinant adeno-associated viral vector generation and virus production

The mouse cDNA for SOCS3 was excised by BamH1 and Sal1 from eukaryotic expression vector pCMV-SOCS3-FLAG (Ueki et al. 2004) and subcloned into AAV2-CMV-LUC-IRES-EGFP vector by replacing the luciferase (LUC)

gene to obtain AAV2-CMV-SOCS3-IRES-EGFP. The EGFP control AAV2-CMV-EGFP-WPRE vector was generated by subcloning the EGFP-WPRE fragment from the AAV2-hSyn-EGFP-WPRE vector (Kugler et al. 2003) into BamH1 and BsrG1 sites of the AAV2-CMV-LUC-IRES-EGFP vector (Fig. 1a). The positive clones were verified by sequencing using forward 5′- TGACGCAAAT GGGCGGTAGG-3′ and reverse 5′-GTGGATACGCTGCT TTAATGCC-3′ primers. For convenience, we used the abbreviation AAV2-EGFP instead of AAV2-CMV-EGFP-WPRE for control virus and AAV2-SOCS3 instead of AAV2-CMV-SOCS3-IRES-EGFP for SOCS3 virus in this manuscript. All molecular cloning procedures were performed in SURE2 bacterial cells to minimize the recombination events. Recombinant AAV (rAAV) vectors of serotype 2 were produced by transfecting AAV cis-plasmids encoding gene of interest and viral helper plasmid pDG encoding *rep-2 and cap-2* genes (Grimm and Kay 2003; Grimm et al. 2003) into HEK 293 cells. Total cell lysates were collected after 48 h of transfection in AAV lysis buffer (50-mM HEPES and 150-mM NaCl, pH 7.6) by repeated freezing in liquid nitrogen and thawing at 37 °C. The cell lysates were cleared by centrifugation for 15 min at 5,000 rpm to remove the cell debris. Unencapsulated nucleic acids were degraded by treating the cleared cell lysates with 250 U of benzonase (sigma) for 90 min at 37 °C. rAAV particles were purified in three-step CsCl density gradient ultracentrifugation and desalted by overnight dialysis in PBS followed by concentration using Amicon® ultra centrifugal filters (30 K MWCO #UFC903008) (Benzler et al. 2012). To determine the number of transducing units (TU), the purified and concentrated viral particles were serially diluted and infected to HEK293 cells on a 92-well cell culture plate. After 3 days of infection the number of EGFP expressing cells was counted and the titer was calculated accordingly (AAV2-EGFP 1.0×10^{10} and AAV2-SOCS3-EGFP 9×10^{11} TU/ml).

Cell culture and viral expression verification

Recombinant AAV2 generation and expression analysis were performed in human embryonic kidney cells (HEK 293) that were maintained in DMEM supplemented with 10 % FBS, 1 % ciprofloxacin antibiotics and 0.5 % non-essential amino acids under standard conditions in an atmosphere of 16 % O_2, 79 % N_2, and 5 % CO_2 (v/v/v). Purified AAV2-EGFP and AAV2-SOCS3 viral particles were infected at a concentration of 10^{10} TU to 0.3×10^6 HEK293 cells. After 3 days of infection, expression of EGFP, a common feature of both the control- and SOCS3 overexpressing virus, was observed under a inverted fluorescence microscope (Olympus IX81). In order to analyze the SOCS3 protein expression, virus-infected HEK 293 cells were lysed using Ripa lysis buffer (50-mM Tris–Cl, 150-mM NaCl, 1-mM EDTA, 1 % NP-40, 0.25 % sodium deoxycholate, 1-mM sodium orthovanadate) including phosphatase inhibitors (1-mM Na_3VO_4, 20-mM NaF) and a protease inhibitor tablet (Roche; Basel, Switzerland). Twenty micrograms of the total protein lysate were used to verify the expression of SOCS3 by Western blot using a SOCS3 antibody specific for SOCS3 (Cell signaling # 2923).

The AAV2-mediated EGFP expression was further confirmed in primary rat cortical neurons. Freshly isolated primary rat cortical neurons were plated at a density of 0.3 million cells on polyethyleneimine precoated plates and cultured in modified Eagles medium (MEM) supplemented with 10 % serum, 1-mM HEPES, 55-mM glucose, 26-mM $NaHCO_3$, 30-mM KCl, 1-mM sodium pyruvate, 1.2-mM L-glutamine, and 0.1 % gentamicin (10 mg/ml) as described earlier (Culmsee et al. 2005). After 4 h, MEM medium was replaced with neurobasal medium (Invitrogen #21103) supplemented with 4.8-mM HEPES, 1.2-mM L-glutamine, 0.1 % gentamicin (10 mg/ml), 10× B27 (serum supplement) as explained previously (Culmsee et al. 2005) and infected with rAAV particles at a concentration of 10^{10} TU. Five days later, the neuronal EGFP expression was analyzed by confocal microscopy (Leica TCS sp2).

In situ hybridization for SOCS3, NPY, POMC, CART, DIO2, and DIO3 following overexpression of SOCS3

To verify hypothalamic overexpression of SOCS3 and determine its effect on POMC, neuropeptide Y (NPY), cocaine and amphetamine-regulated transcript (CART), deiodinase-2 (DIO2) and -3 (DIO3) mRNA, gene expression of these important components of the neuroendocrine network of seasonal body weight regulation was analyzed by in situ hybridization. After 12 weeks in LD and SD, respectively, brains were isolated and frozen in dry ice. Coronal forebrain sections (16 μm) of hamsters were collected throughout the extent of the ARC approximately from −2.7 to −0.8 mm relative to Bregma according to the atlas of the mouse brain (Paxinos and Franklin 1997) onto a set of ten slides, with 12 sections mounted on each slide. The brain sections were probed with antisense riboprobes complementary to the above-mentioned genes. Radiolabelled antisense probes were generated by in vitro transcription from cloned cDNA templates using T3, T7, and SP6 RNA polymerases in the presence of ^{35}S-UTP. All riboprobes used in this study were generated as described earlier: SOCS3 (Tups et al. 2004), NPY, POMC (Mercer et al. 2000), CART (Mercer et al. 2003), DIO2 and DIO3 (Herwig et al. 2009). In situ hybridizations and analysis was performed as previously described (Mercer et al. 2000).

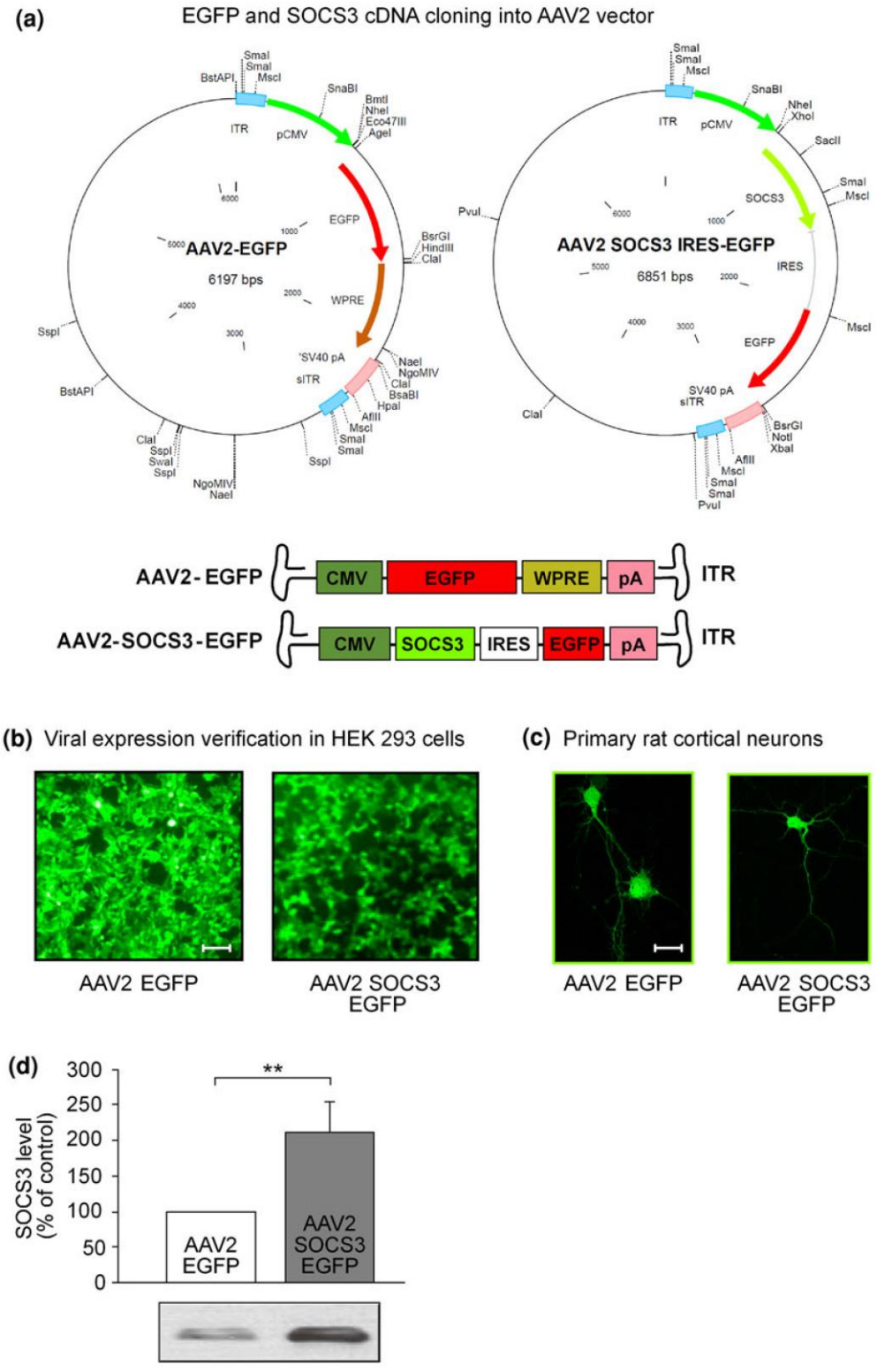
(a)
EGFP and SOCS3 cDNA cloning into AAV2 vector
AAV2-EGFP
6197 bps
ITR
pCMV
EGFP
WPRE
SV40 pA
sITR
AAV2 SOCS3 IRES-EGFP
6851 bps
SOCS3
IRES
EGFP
SV40 pA
sITR
AAV2-EGFP
CMV
EGFP
WPRE
pA
ITR
AAV2-SOCS3-EGFP
CMV
SOCS3
IRES
EGFP
pA
ITR
(b) Viral expression verification in HEK 293 cells
AAV2 EGFP
AAV2 SOCS3 EGFP
(c) Primary rat cortical neurons
AAV2 EGFP
AAV2 SOCS3 EGFP
(d)
SOCS3 level (% of control)
300
250
200
150
100
50
0
**
AAV2 EGFP
AAV2 SOCS3 EGFP

◀ **Fig. 1** Recombinant AAV2-mediated overexpression of SOCS3 in the ARC: generation and validation of the viral construct. **a** Schematic representation of AAV cis-plasmids transfected into HEK 293 cells to produce AAV2-SOCS3 and AAV2-EGFP (*upper panel*). Important elements of the viral genome are depicted in the *lower panel*. Both EGFP and SOCS3 transcription was regulated by the CMV promoter. **b** Inverted fluorescence microscopic images showing HEK 293 cells expressing EGFP after 3 days of AAV2-EGFP (*left panel*) and AAV2-SOCS3 (*right panel*) infection (*scale bar* 35 μm). **c** Confocal images showing rat primary cortical neurons expressing EGFP after 5 days of AAV2-EGFP (*left panel*) and AAV2-SOCS3 (*right panel*) infection (*scale bar* 50 μm). **d** Confirmation of AAV2-SOCS3 overexpression by immunoblotting of total cell lysates from virus-infected HEK 293 cells with a specific SOCS3 antibody. For validation, each cell culture experiment was repeated three times and statistical analysis is represented in the *bar charts*. Data show mean ± SEM $^{**}p \leq 0.01$; *CMV* cytomegalo virus promoter; *SOCS3* mouse suppressor of cytokine signaling 3; *EGFP* enhanced green fluorescent protein; *IRES* internal ribosome entry site; *WPRE* woodchuck hepatitis virus (WHP) post-transcriptional regulatory element; *pA* poly A sequence from bovine growth hormone; *ITR* inverted terminal repeat

Stereotaxic injections

Stereotaxic injections were performed under isoflurane anesthesia. Stereotaxic coordinates to inject rAAV particles into the ARC of the hypothalamus were 1.0-mm posterior, ±0.35-mm lateral, and 7.25-mm ventral relative to Bregma. AAV2 particles containing 10^8 TU (1 μl each side) were injected bilaterally into the ARC using a 1.0-μl Hamilton glass syringe over a time period of 2 min. The injection needle remained in place at each injection site for additional 5 min before slow removal. The skin was sutured and animals were placed under a heating lamp to recover from the surgery.

Adipose tissue collection

Twelve weeks after AAV injection, the hamsters were sacrificed to collect white and brown adipose tissue depots. The weights of inguinal white adipose tissue, retroperitoneal white adipose tissue, epididymal white adipose tissue, and interscapular brown adipose tissue were monitored. The degree of body adiposity was determined by calculating the total weight of the dissected white adipose tissue depots.

Pelage score

Pelage score was counted based on the six different stages of color patterns as explained previously in (Figala et al. 1973). The score was obtained at the time of the injection of viral particles and before termination of the experiment, respectively.

Statistics

Body weight data were analyzed using two-way repeated measures ANOVA. All other data were analyzed by one-way ANOVA followed by Holm-Sidak comparison test, as appropriate, using SigmaStat statistical software (Jandel, Erkrath, Germany). Where data failed equal variance or normality tests, they were analyzed by one-way ANOVA on ranks followed by Dunn's multiple comparison test. Results are presented as mean ± SEM, and differences were considered significant if $p < 0.05$.

Results

Experimental verification of functionality of recombinant AAV2 in vitro

The functionality of recombinant AAV virus constructs was tested in cell culture. EGFP expression was observed in both HEK 293 and primary rat cortical neurons infected with AAV2-EGFP and AAV2-SOCS3 viral particles. Both in HEK 293 cells and in rat primary cortical neurons viral infection was confirmed by profound expression of EGFP (Fig. 1b, c). Viral SOCS3 overexpression was further confirmed by Western blot using total cell lysates from HEK 293 cells. Cells infected with SOCS3 virus showed more than twofold induction in the SOCS3 protein level compared to EGFP controls (Fig. 1d).

SOCS3 overexpression in the ARC induces a mild body weight change in juvenile short day hamsters

The ARC-directed overexpression of SOCS3 immediately after weaning at an age of 3 weeks prevented a complete acclimation to SD. As previously shown following transfer from LD to SD on the day of weaning (Hoffmann 1978), a differential marked body weight was established between the groups from the second week onwards in opposite photoperiods. LD acclimation led to an increase of 13 % relative to AAV2-EGFP SD controls after 12-week-acclimation ($p \leq 0.01$). The elevation of body weight trajectory in AAV2-SOCS3 relative to AAV2-EGFP SD hamsters became significant from the fourth week onwards ($p \leq 0.05$) and was maintained until week 12 [two-way repeated measures ANOVA, $p \leq 0.01$; (Fig. 2)]. The difference in body weight between AAV2-EGFP in LD to AAV2-SOCS3 in SD was still significant after 12 weeks ($p \leq 0.001$).

SOCS3 overexpression is associated with altered gene expression of neuropeptides and thyroid hormone converting enzymes

Following an in vitro validation of viral expression, at the end of the in vivo experiment successful overexpression of

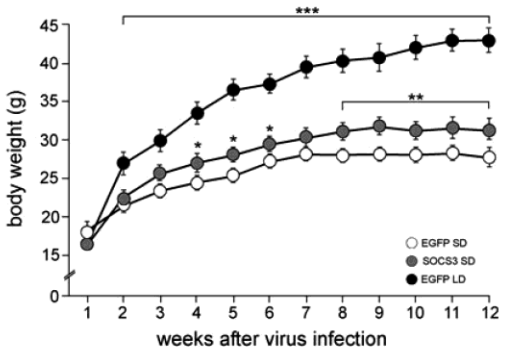

Fig. 2 AAV2-mediated overexpression of SOCS3 in the ARC: Effects on body weight. 3-week-old juvenile male hamsters were stereotaxically injected with the AAV2-EGFP and AAV2-SOCS3 viral particles bilaterally as mentioned above. Immediately after gene transfer one group of hamsters receiving AAV2-EGFP was maintained in LD photoperiod (*gray circle*; $n = 7$), and the other two groups receiving AAV2-EGFP (*white circles*; $n = 10$) and AAV2-SOCS3 (*black circles*; $n = 10$) were shifted to SD photoperiod. All the hamsters were maintained on chow diet (ad libitum) for 12 weeks. Body weight measurements were collected once weekly for a period of 12 weeks after the gene transfer. Data show mean ± SEM $^{*}p \leq 0.05$; $^{**}p \leq 0.01$; $^{***}p \leq 0.001$

SOCS3 in the ARC was additionally validated by in situ hybridization (Fig. 3a). SOCS3 mRNA expression was markedly increased by 1.9-fold in AAV2-SOCS3 SD hamsters compared with AAV2-EGFP SD hamsters ($p = 0.007$). As expected, LD photoperiod was associated with an induction of SOCS3 gene expression in AAV2-EGFP LD compared with AAV2-EGFP SD control hamsters ($p = 0.005$) after 12 weeks exposure.

We next tested whether increased body weight after ARC-directed SOCS3 overexpression is associated with alterations in gene expression of prominent neuropeptides and thyroid hormone converting enzymes in the ARC that are involved in the regulation of energy homeostasis. Messenger RNA levels of the neuropeptide precursor POMC were significantly elevated by 3.3-fold in the ARC of AAV2-EGFP LD hamsters relative to AAV2-EGFP SD hamsters ($p \leq 0.001$). ARC-directed overexpression of SOCS3 was associated with a twofold increase of POMC mRNA levels relative to AAV2-EGFP controls in SD [$p \leq 0.001$; (Fig. 3b)]. However, there was still a significant difference between the AAV2-EGFP LD and AAV-SOCS3 SD hamsters ($p \leq 0.001$). Cocaine and amphetamine-regulated transcript in the ARC was significantly increased by 1.3-fold in AAV2-SOCS3 SD hamsters compared with AAV2-EGFP SD control animals [$p \leq 0.01$; (Fig. 3c)]. However, there was no significant difference between AAV2-EGFP SD and AAV2-EGFP LD hamsters in arcuate CART gene expression. Neuropeptide Y (NPY) mRNA levels in the ARC were not altered by SOCS3 overexpression, but by photoperiod. NPY mRNA was significantly increased by 1.3-fold in AAV2-EGFP LD hamsters compared with AAV2-EGFP SD hamsters [$p = 0.005$; (Fig. 3d)]. Besides the neuropeptides known to be involved in body weight regulation, also processing of thyroid hormones was reported to be involved in seasonal body weight regulation. Hence, we investigated the effect of SOCS3 overexpression on gene regulation of two thyroid hormone converting enzymes DIO2 and DIO3 in the ARC. In situ hybridization revealed that gene expression of both enzymes was localized in the hypothalamic ependymal layer surrounding the third ventricle. DIO2 mRNA levels were unaffected by photoperiod and by SOCS3 overexpression (Fig. 3e). However, there was a significant difference between AAV2-SOCS3 SD and AAV2-EGFP LD hamsters ($p = 0.003$). In contrast, DIO3 mRNA levels were markedly elevated in the ARC of AAV2-EGFP SD hamsters compared with AAV2-EGFP LD ($p \leq 0.001$) hamsters with gene expression levels being below the detection limit (Fig. 3f). Interestingly, SOCS3 overexpression was associated with a decrease by approximately 40 % [$p = 0.013$; (Fig. 3f)].

Effect of ARC-directed SOCS3 overexpression on body fat composition and testis weight

Since AAV2-SOCS3 SD hamsters showed a significant increase in body weight, we analyzed the body fat pad weights. LD photoperiod acclimation was associated with an increase in body fat pad weight by 2.4-fold of retroperitoneal (Fig. 4a) and inguinal (Fig. 4b), 3.6-fold of epididymal white adipose tissue (WAT) (Fig. 4c), 2.7-fold of total WAT (Fig. 4e), and 1.6-fold of interscapular brown adipose tissue (BAT) (Fig. 4e) compared to AAV2-EGFP SD hamsters ($p \leq 0.001$). AAV2-SOCS3 SD hamsters showed a trend towards an increase in the retroperitoneal, inguinal and epididymal, and total WAT mass in comparison with AAV2-EGFP SD hamsters (Fig. 4a–d). In contrast to WAT, in interscapular BAT mass, a significant increase of 1.7-fold was observed after ARC-directed SOCS3 overexpression [$p \leq 0.001$ (Fig. 4e)]. Acclimation to SD was associated with a profound reduction in testes weight ($p \leq 0.001$) that was unaltered by ARC-directed SOCS3 overexpression (Fig. 4f).

Hypothalamic SOCS3 overexpression does not alter seasonal pelage score

Pelage score was counted based on the published data in (Figala et al. 1973). At the time of viral injection, all hamsters were 3-week-old and their pelage score was similar in all three groups. After 12 weeks of SD photoperiod exposure, both AAV2-EGFP SD and AAV2-SOCS3 SD hamsters maintained their pale pelage color, whereas

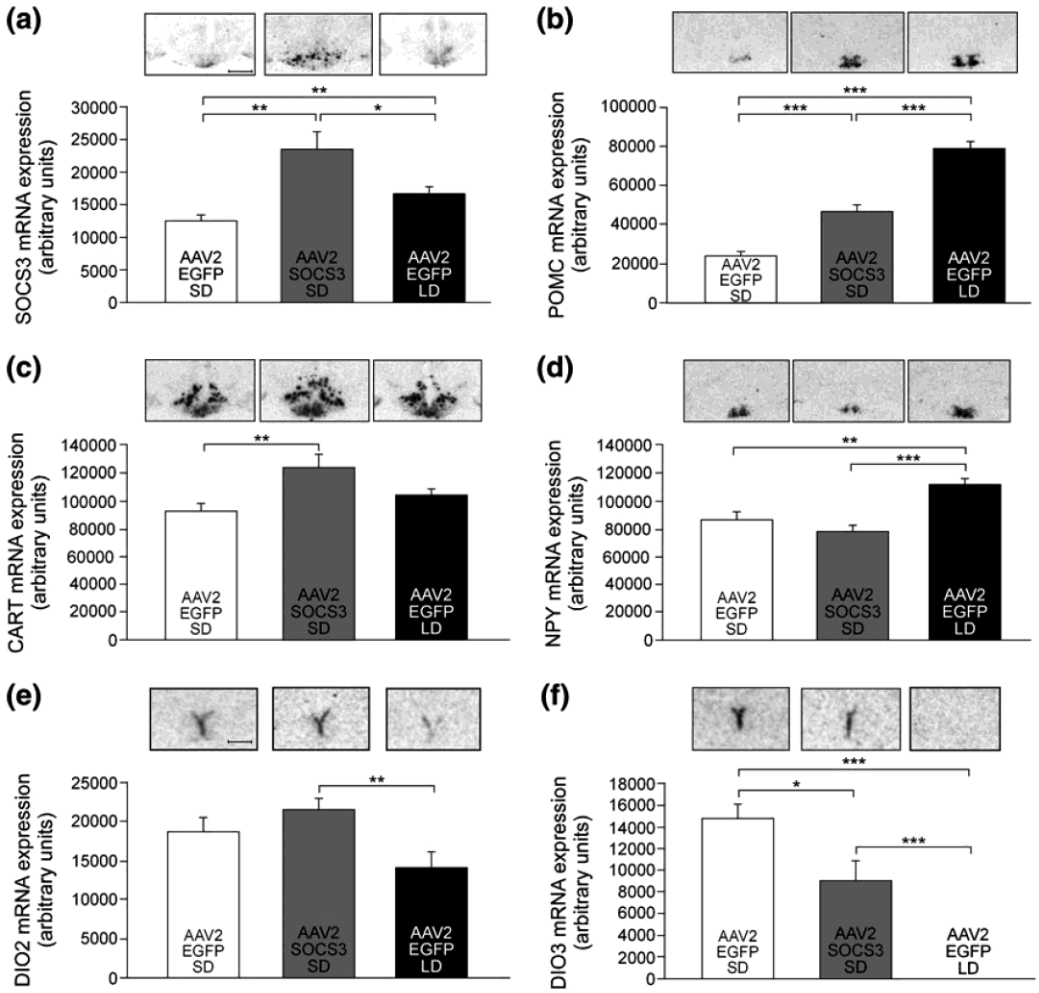

Fig. 3 Effect of SOCS3 overexpression on neuropeptide and thyroid hormone converting enzyme gene expression. Autoradiographs depicting the hypothalamic region of hamster brain sections after in situ hybridization to an antisense ^{35}S-labeled riboprobe binding to the mRNAs of **a** *SOCS3* ($n = 7$–10), **b** *POMC* ($n = 7$–9), **c** *CART* ($n = 7$–10), **d** *NPY* ($n = 7$–10) (*scale bar* 1 mm) and thyroid hormone converting enzyme mRNAs, **e** *Dio2* ($n = 7$–10), **f** *Dio3* ($n = 7$–10) (*scale bar* 300 μM). The *upper panels* depict autoradiographs of the respective genes, whereas the *lower panels* show a bar graph generated from quantification of the signal in the ARC for SOCS3, neuropeptides and *Dio2* and *Dio3* in the ependymal layer. Data show mean ± SEM $*p \leq 0.05$; $**p \leq 0.01$; $***p \leq 0.001$ by one-way ANOVA

AAV2-EGFP hamsters acclimated to LD for a period of 12 weeks became considerably dark (Fig. 5).

Discussion

Leptin resistance is regarded as an important contributing factor in the development of obesity. Much of our knowledge about this phenomenon has derived from studies in rodents that were genetically modified or imposed to positive or negative energy balance. Studies in animal models that reveal natural, physiological, and reversible leptin resistance are scarce. The best studied mammal that reveals a profound seasonal cycle in body weight and leptin resistance is the Djungarian hamster. This species synchronizes its physiology and behavior to the seasonally programmed signal imposed by photoperiod which is exemplified by an increase of body weight in a summer-like photoperiod as compared to body weight reduction in a winter-like photoperiod. Previous findings by us and others suggested that SOCS3 might be a central player in mediating seasonal leptin resistance. In our previous studies, changes in SOCS3 gene expression clearly preceded the chronic body weight change induced by photoperiod.

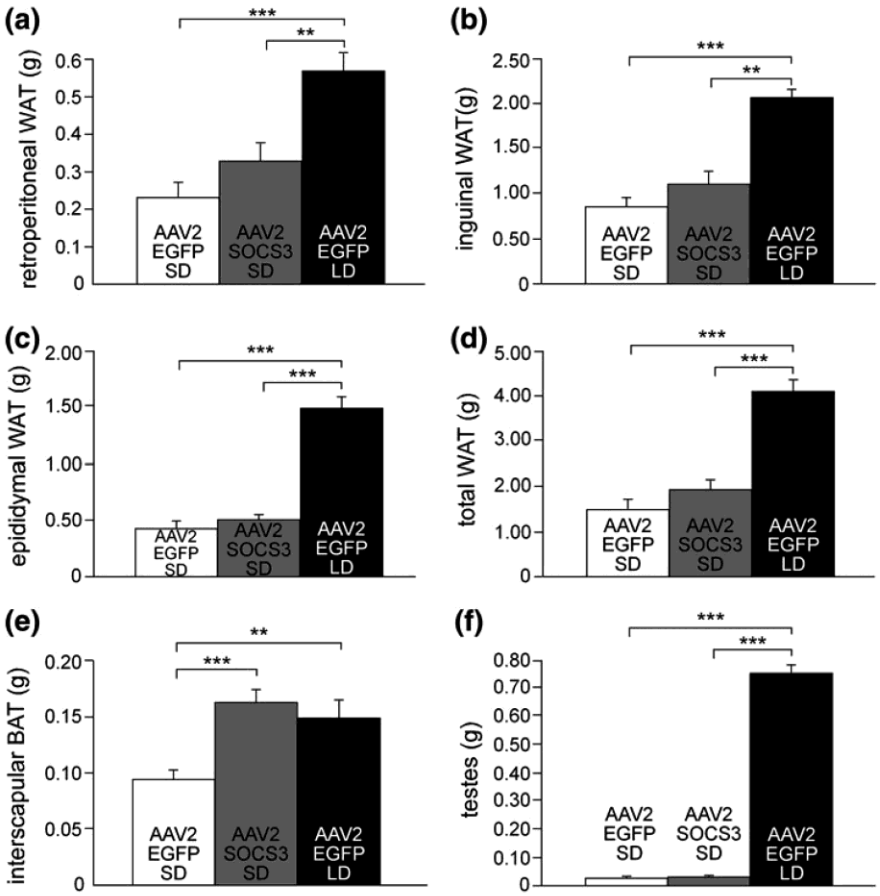

Fig. 4 Effect of SOCS3 overexpression on body fat composition and testis weight. Tissue weights from the respective groups of hamsters ($n = 7$–10) were determined post-mortally. **a** Retroperitoneal WAT, **b** inguinal WAT, **c** epididymal WAT, **d** total WAT, **e** interscapular BAT, and **f** paired testes. Data show mean ± SEM
$^{**}p < 0.01$;$^{***}p < 0.001$

SOCS3 mRNA levels were increased in LD as compared to SD and this differential became significantly established 2 weeks after acclimation to opposite photoperiods (Tups et al. 2004; Tups et al. 2006). These findings strongly suggested that SOCS3 acts as a molecular switch for seasonal body weight changes. However, functional studies dealing with the involvement of SOCS3 in seasonal leptin resistance are challenging, since no transgenic seasonal hamster models are available.

In the current study, we genetically manipulated SOCS3 in the ARC of juvenile SD hamsters using AAV2-mediated gene transfer to functionally alter central SOCS3 gene expression. Consistent with our hypothesis that SOCS3 triggers seasonal body weight changes, this manipulation led to an increase in body weight; however, surprisingly hamsters did not completely reach the body weight trajectory of SOCS3 control hamsters. Although SOCS3 overexpression did not fully reverse SD body weight adaptation, to our knowledge this is the first genetic manipulation in the hamster that partially overcame the profound seasonal physiology exhibited by the hamster. An elegant study that utilized gene transfer in the hamster by overexpressing the orexigenic neuropeptide agouti related peptide (AgRP) in the ARC revealed that AgRP overexpression, indeed increased the body weight but failed to override the seasonal body weight cycle (Jethwa et al. 2010). The incomplete increase in body weight observed after ARC-directed SOCS3 overexpression in SD might be explained by redundant pathways that compensate SOCS3 overexpression. From a teleological perspective this is not unlikely since the seasonal body weight cycle exhibited by the hamster is critical for the survival of the species as a whole which implies the existence of redundant mechanisms that regulate this fundamental phenomenon. However, given the small size of the hamster ARC it is also possible that AAV2-mediated overexpression of SOCS3 might affect adjacent hypothalamic areas and different neuronal populations. Future studies are required to further delineate the role of SOCS3 in specific neuronal populations, such as POMC or NPY neurons and its implication in seasonal body weight regulation. Nevertheless, the partial increase in body weight that we observed after ARC-directed SOCS3 overexpression was in line with a trend towards an increase in total WAT and a complete

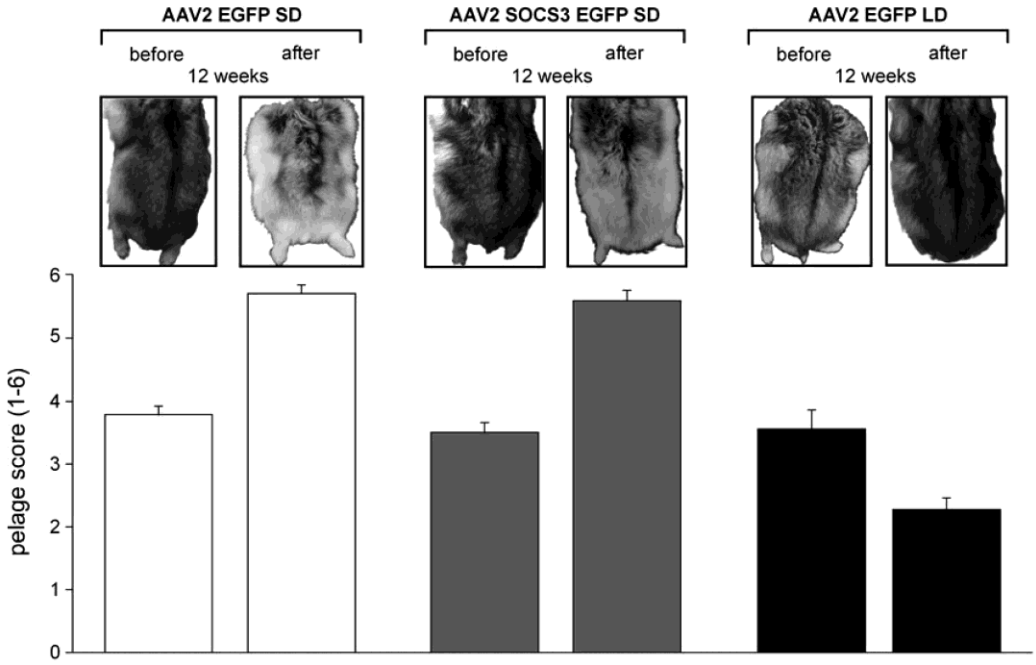

Fig. 5 Hypothalamic SOCS3 overexpression does not alter seasonal pelage score. Pelage score (1 = summer, 6 = winter) counted prior to and after 12 weeks of the viral mediated gene transfer. Hamster photos on the *top* of each bar chart show fur *color* differences at the beginning and after 12 weeks of the experiment, whereas the bar chart depicts the calculated pelage score. Data show mean ± SEM on $n = 7$–10 animals/group

restoration of BAT mass compared with LD hamsters. Consistent to our observation, in mice brain-specific deletion of SOCS3 led to the opposite effect, a reduction in body fat; however, BAT mass was unaltered (Kievit et al. 2006; Metlakunta et al. 2011).

The SOCS3 overexpression led to a partial increase in body weight in SD hamsters and did not induce testicular development, suggesting that this trait is regulated independent of SOCS3. SOCS3 overexpression in SD hamsters did not lead to a change in fur color and this was expected since changes in fur color appear to be largely mediated via alterations in pituitary prolactin secretion and only to some extent by gonadal steroid hormone secretion (Duncan and Goldman 1984a, b).

The ARC-directed SOCS3 overexpression was associated with a significant alteration in the gene expression profile of important components of the neurochemical network of energy balance in the ARC. Pro-opiomelanocortin mRNA was increased in LD hamsters relative to SD hamsters which is in agreement with previous findings (Mercer et al. 2000). Intriguingly, POMC mRNA was partially increased to LD levels in AAV2-SOCS3 SD hamsters suggesting that POMC might be involved in mediating the partial body weight response. Since POMC is the precursor of neuropeptides involved in body weight regulation and post-translational modification of POMC might be critical for seasonal body weight responses, we measured mRNA in the ARC of one POMC converting enzyme, the prohormone convertase 2 (PC2). However, ARC-directed SOCS3 overexpression did not alter PC2 gene expression relative to SD control hamsters (data not shown). Future studies are warranted to measure the impact of ARC-directed SOCS3 overexpression on POMC-derived neuropeptides and the consequence for seasonal body weight regulation. We investigated mRNA levels of another neuropeptide that has been described to be involved in seasonal body weight regulation, CART. AAV2-SOCS3 SD hamsters revealed a significant increase of CART mRNA in the ARC compared with AAV2-EGFP SD hamsters. CART has previously been shown to be anorexigenic (Kristensen et al. 1998) and may have opposed a larger increase in body weight anticipated of SOCS3 overexpression. We did not observe differential gene expression of CART between LD and SD EGFP hamsters in our study; however, the role of CART in mediating seasonal body weight responses has not been fully addressed. Our findings are consistent with Robson et al. (2002), who did not detect a difference in CART mRNA levels between LD and SD in adult male hamsters (Robson et al. 2002). However, in juvenile female hamster

exposure to SD and LD for 14 days only was associated with increased CART mRNA levels in SD hamsters (Mercer et al. 2003). These opposing findings suggest either gender or age specific differences in seasonal regulation of CART mRNA in the ARC. The analysis of an orexigenic neuropeptide, NPY, surprisingly revealed increased mRNA levels in LD-EGFP relative to SD hamsters that were, however, unaltered by SOCS3 overexpression. In contrast to previous reports that did not detect seasonal differences in NPY mRNA expression in the ARC, these data indicate that NPY might play a specific role in seasonal body weight regulation at this particular time point of 12 weeks acclimation.

Emerging evidence suggests that thyroid hormone action within the hypothalamus is involved in driving seasonal body weight adaptations. Particularly, type 2 and 3 deidoinase enzymes in tanycytes surrounding the third ventricle in the mediobasal hypothalamus appear to regulate thyroid hormone concentrations in the hypothalamus via catalyzing enzyme reactions that determine the availability of active triiodothyronine in the hypothalamus (Barrett et al. 2007; Herwig et al. 2008) Consistent with Barrett et al. (2007), DIO2 levels were unaffected by photoperiod, whereas DIO3 mRNA levels were markedly altered. In tanycytes of LD hamsters, gene expression of the latter enzyme was absent in comparison with SD hamsters that revealed abundant expression in this region. ARC-directed SOCS3 overexpression in SD was associated with a significant reduction in DIO3 mRNA levels suggesting that SOCS3 alters thyroid hormone availability in the hypothalamus. Levels were, however, still significantly higher than in LD hamsters which is in line with the partial effect of SOCS3 overexpression on body weight. It is plausible that thyroid hormone converting enzymes, such as DIO3 represent an important downstream relay system that converts SOCS3-mediated leptin resistance into a behavioral response. Our findings suggest that there may be a negative feedback mechanism to ependymal cells of the third ventricle, and therefore could play a role in alterations in thyroid hormone availability that are associated with changes in seasonal physiology. Future studies are required to identify the primary cue that triggers the physiological transition from one photoperiod to the other and to identify the hierarchy and timing of hormonal cues that trigger seasonal changes in physiology.

Acknowledgments This study was funded by the German Ministry of Education and Research (Ref. No: 0315087, to AT). Isolation and culturing of primary rat cortical cells was performed with support of Sandra Engel under supervision of Prof. Carsten Culmsee at the Institute of Pharmacology and Clinical Pharmacy, Philipps University of Marburg.

References

Barrett P, Ebling FJ, Schuhler S, Wilson D, Ross AW, Warner A, Jethwa P, Boelen A, Visser TJ, Ozanne DM, Archer ZA, Mercer JG, Morgan PJ (2007) Hypothalamic thyroid hormone catabolism acts as a gatekeeper for the seasonal control of body weight and reproduction. Endocrinology 148:3608–3617

Baumann H, Morella KK, White DW, Dembski M, Bailon PS, Kim H, Lai CF, Tartaglia LA (1996) The full-length leptin receptor has signaling capabilities of interleukin 6-type cytokine receptors. Proc Natl Acad Sci USA 93:8374–8378

Benzler J, Ganjam GK, Kruger M, Pinkenburg O, Kutschke M, Stohr S, Steger J, Koch CE, Olkrug R, Schwartz MW, Shepherd PR, Grattan DR, Tups A (2012) Hypothalamic glycogen synthase kinase 3beta has a central role in the regulation of food intake and glucose metabolism. Biochem J 447:175–184

Bjorbaek C, Elmquist JK, Frantz JD, Shoelson SE, Flier JS (1998) Identification of SOCS-3 as a potential mediator of central leptin resistance. Mol Cell 1:619–625

Culmsee C, Zhu C, Landshamer S, Becattini B, Wagner E, Pellecchia M, Blomgren K, Plesnila N (2005) Apoptosis-inducing factor triggered by poly(ADP-ribose) polymerase and Bid mediates neuronal cell death after oxygen–glucose deprivation and focal cerebral ischemia. J Neurosci 25:10262–10272

Duncan MJ, Goldman BD (1984a) Hormonal regulation of the annual pelage color cycle in the Djungarian hamster, *Phodopus sungorus*. I. Role of the gonads and pituitary. J Exp Zool 230:89–95

Duncan MJ, Goldman BD (1984b) Hormonal regulation of the annual pelage color cycle in the Djungarian hamster, *Phodopus sungorus*. II. Role of prolactin. J Exp Zool 230:97–103

Figala J, Hoffmann K, Goldau G (1973) Annual cycle in Djungarian hamster *Phodopus sungorus* Pallas. Oecologia 12:89–118

Grimm D, Kay MA (2003) From virus evolution to vector revolution: use of naturally occurring serotypes of adeno-associated virus (AAV) as novel vectors for human gene therapy. Curr Gene Ther 3:281–304

Grimm D, Kay MA, Kleinschmidt JA (2003) Helper virus-free, optically controllable, and two-plasmid-based production of adeno-associated virus vectors of serotypes 1 to 6. Mol Ther 7:839–850

Herwig A, Ross AW, Nilaweera KN, Morgan PJ, Barrett P (2008) Hypothalamic thyroid hormone in energy balance regulation. Obes Facts 1:71–79

Herwig A, Wilson D, Logie TJ, Boelen A, Morgan PJ, Mercer JG, Barrett P (2009) Photoperiod and acute energy deficits interact on components of the thyroid hormone system in hypothalamic tanycytes of the Siberian hamster. Am J Physiol Regul Integr Comp Physiol 296:R1307–R1315

Hoffmann K (1978) Effects of short photoperiods on puberty, growth and moult in the Djungarian hamster (*Phodopus sungorus*). J Reprod Fertil 54:29–35

Jethwa PH, Warner A, Fowler MJ, Murphy M, de Backer MW, Adan RA, Barrett P, Brameld JM, Ebling FJ (2010) Short-days induce weight loss in Siberian hamsters despite overexpression of the agouti-related peptide gene. J Neuroendocrinol 22:564–575

Kievit P, Howard JK, Badman MK, Balthasar N, Coppari R, Mori H, Lee CE, Elmquist JK, Yoshimura A, Flier JS (2006) Enhanced leptin sensitivity and improved glucose homeostasis in mice lacking suppressor of cytokine signaling-3 in POMC-expressing cells. Cell Metab 4:123–132

Klingenspor M, Niggemann H, Heldmaier G (2000) Modulation of leptin sensitivity by short photoperiod acclimation in the Djungarian hamster, *Phodopus sungorus*. J Comp Physiol B 170:37–43

Kristensen P, Judge ME, Thim L, Ribel U, Christjansen KN, Wulff BS, Clausen JT, Jensen PB, Madsen OD, Vrang N, Larsen PJ, Hastrup S (1998) Hypothalamic CART is a new anorectic peptide regulated by leptin. Nature 393:72–76

Kugler S, Kilic E, Bahr M (2003) Human synapsin 1 gene promoter confers highly neuron-specific long-term transgene expression from an adenoviral vector in the adult rat brain depending on the transduced area. Gene Ther 10:337–347

Lerchl A, Schlatt S (1993) Influence of photoperiod on pineal melatonin synthesis, fur color, body weight, and reproductive function in the female Djungarian hamster, *Phodopus sungorus*. Neuroendocrinology 57:359–364

Mercer JG, Moar KM, Ross AW, Hoggard N, Morgan PJ (2000) Photoperiod regulates arcuate nucleus POMC, AGRP, and leptin receptor mRNA in Siberian hamster hypothalamus. Am J Physiol Regul Integr Comp Physiol 278:R271–R281

Mercer JG, Ellis C, Moar KM, Logie TJ, Morgan PJ, Adam CL (2003) Early regulation of hypothalamic arcuate nucleus CART gene expression by short photoperiod in the Siberian hamster. Regul Pept 111:129–136

Metlakunta AS, Sahu M, Yasukawa H, Dhillon SS, Belsham DD, Yoshimura A, Sahu A (2011) Neuronal suppressor of cytokine signaling-3 deficiency enhances hypothalamic leptin-dependent phosphatidylinositol 3-kinase signaling. Am J Physiol Regul Integr Comp Physiol 300:R1185–R1193

Munzberg H, Huo L, Nillni EA, Hollenberg AN, Bjorbaek C (2003) Role of signal transducer and activator of transcription 3 in regulation of hypothalamic proopiomelanocortin gene expression by leptin. Endocrinology 144:2121–2131

Murphy M, Jethwa PH, Warner A, Barrett P, Nilaweera KN, Brameld JM, Ebling FJ (2012) Effects of manipulating hypothalamic triiodothyronine concentrations on seasonal body weight and torpor cycles in Siberian hamsters. Endocrinology 153:101–112

Myers MG Jr (2004) Leptin receptor signaling and the regulation of mammalian physiology. Recent Prog Horm Res 59:287–304

Paxinos G, Franklin KBJ (1997) The mouse brain in stereotaxic coordinates. Academic press, Harcourt Brace and Co., San Diego

Ramadoss P, Unger-Smith NE, Lam FS, Hollenberg AN (2009) STAT3 targets the regulatory regions of gluconeogenic genes in vivo. Mol Endocrinol 23:827–837

Robson AJ, Rousseau K, Loudon AS, Ebling FJ (2002) Cocaine and amphetamine-regulated transcript mRNA regulation in the hypothalamus in lean and obese rodents. J Neuroendocrinol 14:697–709

Rousseau K, Atcha Z, Loudon AS (2003) Leptin and seasonal mammals. J Neuroendocrinol 15:409–414

Tartaglia LA (1997) The leptin receptor. J Biol Chem 272:6093–6096

Tups A (2009) Physiological models of leptin resistance. J Neuroendocrinol 21:961–971

Tups A, Ellis C, Moar KM, Logie TJ, Adam CL, Mercer JG, Klingenspor M (2004) Photoperiodic regulation of leptin sensitivity in the Siberian hamster, *Phodopus sungorus*, is reflected in arcuate nucleus SOCS-3 (suppressor of cytokine signaling) gene expression. Endocrinology 145:1185–1193

Tups A, Barrett P, Ross AW, Morgan PJ, Klingenspor M, Mercer JG (2006) The suppressor of cytokine signalling 3, SOCS3, may be one critical modulator of seasonal body weight changes in the Siberian hamster, *Phodopus sungorus*. J Neuroendocrinol 18:139–145

Tups A, Stohr S, Helwig M, Barrett P, Krol E, Schachtner J, Mercer JG, Klingenspor M (2012) Seasonal leptin resistance is associated with impaired signalling via JAK2-STAT3 but not ERK, possibly mediated by reduced hypothalamic GRB2 protein. J Comp Physiol B 182:553–567

Ueki K, Kondo T, Kahn CR (2004) Suppressor of cytokine signaling 1 (SOCS-1) and SOCS-3 cause insulin resistance through inhibition of tyrosine phosphorylation of insulin receptor substrate proteins by discrete mechanisms. Mol Cell Biol 24:5434–5446

White DW, Kuropatwinski KK, Devos R, Baumann H, Tartaglia LA (1997) Leptin receptor (OB-R) signaling. Cytoplasmic domain mutational analysis and evidence for receptor homo-oligomerization. J Biol Chem 272:4065–4071

The time course and mechanisms contributing to ghrelin resistance after high fat diet exposure

Dana I Briggs[1], Sarah H Lockie[1], Jonas Benzler[4], Qunli Wu[1,2], Andrew J Hoy[3], Moyra B Lemus[1], Romana Stark[1], Harold A Coleman[1], Helena C Parkington[1], Alexande Tups[4], Zane B Andrews[1]

[1] Department of Physiology, Monash University, Wellington Rd, Clayton, Victoria, Australia

[2] Traditional Chinese Medicine Department, Peking Union Medical College Hospital, No.1 Shuaifuyuan Wangfujing, Dongcheng District, Beijing, China 100730

[3] Department of Physiology, Bosch Institute, The University of Sydney, New South Wales, Australia

[4] Department of Animal Physiology, Faculty of Biology, Phillips University, Marburg, D-35043 Marburg, Germany.

Corresponding Author: Zane B. Andrews
Tel. +61 399058165, Fax. +61 399029500
Email: zane.andrews@monash.edu

Running Title: Time course and mechanisms of ghrelin resistance

Keywords: Ghrelin resistance, NPY, AgRP, Leptin,
Word Count: (excluding figure legends and references) 4204
Words in Abstract: 248
Number of Tables: 1
Number of Figures: 5

Disclosure Statement: The authors have nothing to disclose.

Acknowledgements:

This work was supported by a Monash Fellowship, Monash University, Australia; an Australia Research Council Future Fellowship (FT100100966) and NHMRC project grants (NHMRC 1011274, 10030037) to ZBA; and an NHMRC Postgraduate Scholarship to DIB.

ABSTRACT

We have previously demonstrated that 12 weeks of high fat diet (HFD)-feeding causes ghrelin resistance in arcuate neuropeptide Y (NPY)/agouti-related peptide (AgRP) neurons. In the current study, we investigated the timecourse over which this occurs. We show that after three weeks of HFD-feeding, neither peripheral nor central ghrelin increases food intake. At this time, ghrelin does not activate NPY neurons as demonstrated by a lack of Fos-immunoreactivity. Whole-cell patch clamp electrophysiology confirmed that NPY neurons from mice fed a HFD for three weeks do not increase firing in response to ghrelin. We show that leptin-deficient obese *ob/ob* mice are still ghrelin-sensitive but become ghrelin-resistant when central leptin is co-administered. We observed increased plasma leptin in mice fed a HFD for 3 weeks, this suggests that hyperleptinemia contributes to ghrelin resistance in NPY/AgRP neurons. As these neurons express the leptin receptor (ObR), we examined leptin-induced pSTAT-3 in NPY neurons. After three weeks of HFD-feeding when NPY/AgRP neurons become resistant to ghrelin, ~40% of NPY neurons express pSTAT-3 in response to leptin compared to ~70% in chow-fed animals. We also examined hypothalamic gliosis in HFD and chow-fed mice and ob/ob mice or lean controls. HFD mice exhibited increased GFAP-positive cells compared with chow-fed mice suggesting that hypothalamic gliosis underlies ghrelin resistance. In further support of this, obese but ghrelin sensitive ob/ob mice did not show an increase in GFAP-positive cells compared to wild type controls. We conclude that hyperleptinemia after 3 weeks of HF feeding initiates ghrelin resistance by suppressing NPY/AgRP function and causing hypothalamic gliosis.

INTRODUCTION

Ghrelin is a stomach-derived orexigenic hormone that stimulates feeding and weight gain to regulate energy homeostasis (1-3). Ghrelin's effects on food intake and energy homeostasis primarily occur via arcuate neuropeptide Y (NPY)/Agouti-related peptide (AgRP) neurons. Ghrelin administration induces NPY/AgRP action potential firing (4, 5), which increases NPY and AgRP peptide release from nerve terminals in the paraventricular nucleus (PVN). NPY and AgRP increase food intake by activating Y receptors and antagonizing melanocortin 4 receptor (MC4R)-containing neurons, respectively (6-8). Ghrelin also increases NPY and AgRP mRNA concentrations in order to maintain sufficient peptide pools for release (9-11). The stimulatory effects of ghrelin on orexigenic NPY/AgRP neurons are complemented by increased inhibitory GABAergic post-synaptic inputs onto anorexigenic pro-opiomelanocortin (POMC) neurons (4, 5).

We previously demonstrated that diet-induced obesity (DIO) suppresses the neuroendocrine ghrelin axis and causes ghrelin resistance in arcuate NPY/AgRP neurons (12). Twelve weeks of HFD-feeding causes central ghrelin resistance that affects not only the hypothalamic appetite-regulating NPY/AgRP neurons, but also other functions of ghrelin, as demonstrated by a lack of growth hormone release in response to central ghrelin administration. Ghrelin did not induce AgRP or NPY secretion in hypothalamic explants from DIO mice but NPY induced normal feeding in both control and DIO mice, indicating that downstream NPY/AgRP neural targets remain intact. Therefore, defective NPY/AgRP neuronal function causes ghrelin resistance in hypothalamic appetite-regulating pathways. Others have also shown that ghrelin-induced hyperphagia is blunted by exposure to a high fat diet (HFD) (13-15). Interestingly, defective NPY/AgRP function suppresses the responsiveness to other orexigenic stimuli, such as fasting (16, 17). The lack of appropriate feeding responses in DIO mice is likely caused by NPY/AgRP dysfunction and impaired hypothalamic circuits regulating appetite (18, 19), however the mechanism by which NPY/AgRP neurons become resistant to orexigenic stimuli remains unclear.

Recent studies indicate that HFD feeding increases GFAP-positive cells in the hypothalamic arcuate nucleus and these GFAP-positive cells ensheathe NPY/AgRP and POMC forming physical barriers to nutrient and hormone stimuli in the plasma (20). Hypothalamic gliosis and inflammation was observed within 1 week of HFD feeding in both rats and mice prior to the onest of substantial weight gain suggesting that hypothalamic gliosis and inflammation is a cause rather than a consequence of significant weight gain (21). Furthermore, the same studies presented evidence to show increased hypothalamic gliosis, as assessed by MRI, in obese humans (21). Thus, one potential mechanism leading to hypothalamic ghrelin resistance and hormonal resistance in general is hypothalamic gliosis.

In the current study, we aimed to characterise the time course over which ghrelin resistance develops in NPY/AgRP neurons during HFD-exposure, in order to identify mechanisms that contribute to this phenomenon. We found that 3 weeks of HFD-feeding induces ghrelin resistance in arcuate NPY/AgRP neurons, and this is associated with an increase in plasma leptin. As ghrelin and leptin have a reciprocal relationship in the plasma and leptin suppresses NPY neuronal function (22, 23), we hypothesized that hyperleptinemia caused by HFD-feeding and hypothalamic gliosis contributes to NPY/AgRP dysfunction and resultant ghrelin resistance.

MATERIALS AND METHODS

Animals

Male C57/Bl6 (Monash Animal Services, Victoria, Australia) and NPY-GFP (B6.FVB-Tg(Npy-hr*GFP*)1Lowl/J; stock number 006417; The Jackson Laboratory, Maine, USA; both ~8 weeks old) were group housed (5 per cage) under controlled conditions (21^{o}C and 12:12 hour light/dark cycle) and maintained on either a chow diet or a high fat diet *ad libitum* (for diet composition see Table 1) with free access to tap water for 12 weeks. *ob/ob*-NPY-GFP mice were generated by crossing *ob*/+ mice with NPY-GFP mice. *Ob*/+ mice on a C57/Bl6 background and lean wild-type (WT) mice were obtained from Monash University Animal Services. Experiments were conducted in accordance with the Monash University Animal Ethics Committee guidelines.

Table 1 Nutritional content of chow and high fat diets for C57Bl6 and NPY-GFP mice

	CHOW DIET BARASTOC, 8720610	**HIGH FAT DIET SPECIALTY FEEDS SF04-001**
Protein	22%	22.6%
Total Fat	9%	23.5%
Crude Fibre	3.2%	5.4%
AD Fibre	4.4%	5.4%
Digestible Energy	13.2 MJ/kg	19 MJ/Kg

For feeding experiments, *ob/ob* mice (~8 weeks old; Janvier, Le Genest-Saint-Isle, France); were housed individually under standard conditions (temperature 23C with 12:12 hour light/dark cycle) and maintained on a chow diet. Experiments were conducted in accordance with the Philipps University of Marburg Animal Ethics Committee guidelines.

Glucose tolerance test

For intraperitoneal glucose tolerance tests (ipGTT), a tail tip blood sample was taken from fasted mice (5 hours). Blood glucose concentration was immediately measured with ACCU-CHEK® Active (Roche Diagnostics GmbH, Tokyo, Japan), after which d-glucose was injected (50% solution; 2 g/kg, i.p.). Additional samples for blood glucose were taken at 15, 30, 60 and 90 min after injection.

Cannulation of the lateral ventricle

Animals were anaesthetized with isoflurane/oxygen. The guide cannula was inserted 1.0 mm lateral and 0.3 mm rostral to bregma to a depth of 2 mm before being embedded in dental cement. The cannula was sealed at the external opening with a dummy cannula. Animals were housed individually

following surgery, and body weight and food intake were measured to monitor recovery. All animals were given 7 days to recover before experimental manipulations.

Food intake experiments

To assess the effect of peripheral ghrelin on feeding behaviour, non-fasted C57Bl6 mice received an i.p. injection of ghrelin (1mg/kg; SC1357, NeoMPS, Strasbourg, France) or vehicle (sterile saline) just prior to the onset of the dark phase (1800 hours). Food intake was measured 5 hours later. To assess the effect of central ghrelin on feeding behaviour, non-fasted C57Bl6 mice received an i.c.v injection of ghrelin (1 µg/µl; volume 1.5 µl; SC1357, NeoMPS, Strasbourg, France) or vehicle (artificial cerebrospinal fluid; aCSF) at the onset of the light phase (0800 hours). Food intake was measured 5 hours later.

To assess how leptin modulates ghrelin-induced feeding behaviour in *ob/ob* mice, non-fasted animals received an i.c.v. injection of aCSF or recombinant mouse leptin (4 µg/µl; 498-OB, R&D systems, Wiesbaden-Norderstedt, Germany). Food was removed and 1-hour later mice received either aCSF or ghrelin (1 µg/µl; volume 2 µl; SC1357, NeoMPS, Strasbourg, France). Food was measured 4 hours later.

Enzyme-linked immunosorbent assay (ELISA) of acylated ghrelin, total ghrelin, insulin and leptin

Trunk blood was collected into EDTA tubes treated with Pefabloc SC (Roche Applied Science, Mannheim, Germany) to achieve a final concentration of 1 mg/ml. Blood was centrifuged and collected plasma was acidified with HCl (final concentration 0.05 N).

Acylated (EZRGRA-90K) and total (EZRGRT-91K Millipore, Billerica, MA, USA) ghrelin in mouse plasma was measured as per kit instructions. Leptin in mouse plasma was measured as per kit instructions (Mouse Leptin ELISA Kit # No: 90030, Crystal Chem, Inc, Downers Grove, IL, USA) and insulin was measured by an in-house ELISA assay developed by the Monash Obesity and Diabetes Institute. Mice were fasted for 6 hours before collection of plasma insulin.

Immunohistochemistry

Animals were deeply anaesthetized with isoflurane and perfused with 0.05 M phosphate buffered saline (PBS), followed by 4% paraformaldehyde. Brains were post-fixed in 4% paraformaldehyde overnight at 4^{o}C then placed in 30% sucrose. Brains were cut at 40 µm on a cryostat, and every fourth section through the hypothalamus was collected and stored in cryoprotectant at -20^{o}C.

Brains of chow- and HFD-fed NPY-GFP mice were analysed for Fos protein expression in NPY neurons 60 minutes after i.c.v. ghrelin administration (1.5 µg in 1.5 µl aCSF). Sections were washed in 0.1 M PB and incubated with 1% hydrogen peroxide (H_2O_2) for 15 minutes to prevent endogenous

peroxidase activity and blocked for 1 hour with 5% normal horse serum (NHS) in 0.3% Triton 0.1 M PB. Sections were incubated with c-Fos rabbit polyclonal IgG (#sc-52 Santa Cruz Biotechnology, Inc, San Cruz CA, U.S.A) at 1:5000 in diluent of 1% NHS in 0.3% Triton in 0.1 M PB. After incubation the sections were washed and incubated with AlexaFluor® goat anti-rabbit 594 antibody (A-11037, Invitrogen Corporation, Carlsbad CA, USA) at 1:500 in 0.3% Triton in 0.1 M PB. Sections were then washed, mounted and coverslipped. We quantified Fos-positive NPY neurons in the arcuate nucleus (Br -1.22 to -2.54).

Chow- and HFD-fed NPY-GFP mice that were fasted overnight were analysed for pSTAT-3 protein expression in NPY neurons 45 minutes after i.p. leptin (1mg/kg) administration. Sections were washed in 0.1 M PB and incubated with 0.5% sodium borohydride for 15 minutes, and 1% NaOH and 1% H_2O_2 for 20 minutes to prevent endogenous peroxidase activity. Sections were then washed with 0.3% glycine for 10 minutes and 0.03% sodium dodecyl sulphate for 10 minutes before being blocked for 1 hour with goat anti-mouse antibody. Sections were then blocked with 3% NHS in 0.25% Triton 0.1 M PB and 0.02% sodium acetate for 1 hour.

Sections were incubated with pSTAT-3 (Tyr705)(D3A7) XP® Rabbit monoclonal IgG (#9145, Cell Signalling Technology Inc, Danvers, MA, USA) at 1:5000 in diluent of 1% NHS in 0.3% Triton in 0.1 M PB. After incubation the sections were washed and incubated with AlexaFluor® goat anti-rabbit 594 antibody (A-11012, Invitrogen) at 1:400 in 0.3% Triton in 0.1 M PB. Sections were then washed, mounted and coverslipped. We quantified pSTAT-3-positive NPY neurons in the arcuate nucleus (Br -1.22 to -2.54). For GFAP immunohistohistochemistry, sections were incubated in primary antibody at 1:1000 (Abcam 7260). After primary antibody incubation all sections were thoroughly washed and incubated with AlexaFluor® goat anti-rabbit 594 antibody (A-11012, Invitrogen) at 1:400 in 0.3% Triton in 0.1 M PB. Sections were then washed, mounted and coverslipped.

Brain regions were identified using a mouse brain atlas. Cells were visualized by a Zeiss Apotome microscope and immunoreactive cells were counted using a grid eye piece from serial sections through the arcuate nucleus (every fourth section), the first section was chosen randomly. To estimate GFAP fiber number and length we used Image J to generate concentric circles and known distances, calibrated to pixelation in the scale bar. Concentric circles at 10, 20, 30, 40, 50, 60 and 70 microns were placed over the center of the GFAP-positive cells and fibre intercepts were marked. Both the number of fibre intercepts and fibre length were estimated in this manner.

Electrophysiology

Mice were deeply anaesthetized with isoflurane (0900-1000 hours). Brains were rapidly removed into ice-cold aCSF containing (in mM): sucrose 206, KCl 3, $MgCl_2$ 6, $CaCl_2$ 0.5, NaH_2PO_4 1.25, $NaHCO_3$

25, glucose 10.6, and continuously bubbled with carbogen (O_2 95% and CO_2 5%). A tissue block containing the mediobasal hypothalamus was mounted on a vibrating microtome (Campden Integraslice, UK) and coronal slices (250 µm thick) were cut in sucrose aCSF. The slices were moved to a chamber filled with gassed aCSF containing (in mM): NaCl 125, KCl 3, $MgCl_2$ 1, $CaCl_2$ 2.5, NaH_2PO_4 1.25, $NaHCO_3$ 25, and glucose 10.6 in a water bath at 35°C. After 30 minutes the aCSF containing the slices was placed at room temperature. After 1 hour a slice was transferred to a recording chamber mounted on an upright microscope (Leica DMLSF) equipped with infrared–differential interference contrast (DIC) and fluorescence optics and was continuously superfused at 7 ml/minute with gassed aCSF at 32°C. Ghrelin or leptin was applied at close range at 100 µl/minute via polyethylene tubing (0.28 mm inside diameter) positioned ~300 µm upstream of the neuron under study. Control aCSF was superfused through this tube continuously, with stop-flow and exchange to ghrelin-containing aCSF for 1 minute. GFP-expressing NPY neurons were identified by brief exposure to blue excitation light from a lamp using a 40× water-immersion lens and a long-pass dichroic filter block.

Whole-cell current-clamp recordings were made using pipettes with 3–5 MΩ resistance after filling with solution containing (in mM): KCl 15, K gluconate 115, $MgCl_2$ 1, HEPES 10, EGTA 0.3, $MgCl_2$ 1.2 and 1 ATP, adjusted to pH 7.2 using KOH. NPY neurons in the arcuate were first identified under fluorescence, and DIC was subsequently used to obtain a seal on these cells. After a Giga ohm seal had been obtained, a gentle negative pressure was applied to break through into whole-cell configuration.

A L/M EPC7 patch-clamp amplifier (List, Germany) and pClamp 9 software (Axon Instruments, USA) were used for data acquisition and analysis. The spike frequency and resting potential were the mean values from at least 2 minutes of stable recording before drug application.

Statistical analyses

Data are presented as mean ± SEM. Statistical significance was determined by Student's t test, a Fisher's exact test or a two factor ANOVA followed by a Bonferonni's post hoc test using GraphPad Prism 5.00 (GraphPad Software, San Diego California USA). $p < 0.05$ was considered statistically significant.

RESULTS

High fat diet causes metabolic disturbances

One week of HFD-feeding increased body weight (Fig. 1), which was maintained throughout the duration of the study. At this time HFD-fed mice showed impaired glucose tolerance as demonstrated by an increased AUC during an i.p.GTT (Fig. 1).

Three weeks of high fat diet feeding causes ghrelin resistance in NPY/AgRP neurons

We have previously demonstrated that 12 weeks of HFD-feeding causes ghrelin resistance in arcuate NPY/AgRP neurons (12). To determine the timeframe over which this occurs, we assessed i.p. ghrelin-induced food intake in adult male C57Bl6 mice after 0, 1, 2 and 3 weeks exposure to a HFD (Fig 2A-D). Ghrelin (1mg/kg i.p.) was injected immediately prior to the onset of the dark phase (1800 hours) and food intake was measured 5 hours later. After 2 weeks of HFD-feeding, ghrelin failed to significantly increase food intake. However, there was a trend towards increased food intake, indicating only partial ghrelin resistance. After 3 weeks of HFD-feeding, animals showed no response to ghrelin treatment, and hence were considered ghrelin resistant. This effect was sustained at 6, 9 and 12 weeks of HFD-feeding (data not shown).

To establish that ghrelin resistance induced by three weeks of HFD-feeding is a centrally mediated phenomenon, we administered ghrelin (1.5 µg) directly into the lateral ventricle at the onset of the light phase (0800 hours) and measured food intake 5 hours later. We confirmed that i.c.v ghrelin completely fails to induce feeding after 3 weeks on a HFD (Fig. 2E). Mice fed a HFD for 3 weeks also had reduced plasma total ghrelin and acylated ghrelin compared with age-matched chow fed mice (Fig. 2F-G), indicating suppression of the neuroendocrine ghrelin axis similar to ghrelin resistance seen at 12 weeks of age (Fig. 2F-G)(12).

Normally, ghrelin activates arcuate NPY/AgRP neurons to stimulate food intake (4, 12, 24, 25). To determine whether ghrelin activates NPY/AgRP neurons after 3 weeks of HFD-feeding, we used c-fos, the protein product of the immediate-early gene *Fos*, to identify and localize activated neurons. We administered i.c.v. vehicle or ghrelin (1.5µg) directly into the lateral ventricle of NPY-GFP mice fed chow or a HFD for three weeks at the onset of the light phase (0900 hours) and perfused them 60 minutes later. We used immunohistochemistry to identify ghrelin-induced Fos-positive NPY neurons in the arcuate and found that ghrelin induced Fos-IR in NPY neurons of chow-fed but not high fat-fed mice (Fig. 3A).

These results demonstrate that after 3 weeks of HFD-feeding, ghrelin does not activate NPY/AgRP neurons to stimulate feeding, supporting our previous observation of ghrelin resistance in NPY/AgRP neurons (12). We confirmed our finding of ghrelin resistance in these neurons using whole cell patch-

clamp electrophysiology. Ghrelin increased firing of 10/11 NPY neurons from chow-fed mice, but only 4/12 neurons from HFD-fed mice (Fig. 3B), confirming that NPY neurons are ghrelin resistant after three weeks exposure to a HFD. Collectively, these data show that ghrelin resistance occurs after just 3 weeks of HFD-feeding and this effect is mediated specifically in NPY/AgRP neurons.

Leptin contributes to ghrelin resistance in NPY/AgRP neurons

In order to understand changes in key metabolic hormones at the onset of ghrelin resistance, we measured fasting leptin and insulin levels in the plasma at 3 weeks of HFD. Fasting plasma insulin was unchanged but plasma leptin was increased after 3 weeks on a HFD (Fig 4A&B), which was associated with an increase in body weight (Fig 1). Based on these results, we hypothesized that elevated plasma leptin at 3 weeks on a HFD contributes to reduced ghrelin sensitivity in DIO. We therefore invesitagted whether leptin or insulin suppresses the ability of NPY neurons to respond to ghrelin. NPY neurons contain the long form of the leptin receptor (ObR) and insulin receptor substrate, and leptin or insulin directly inhibits NPY gene expression and firing (22, 26-30). We used obese and glucose intolerant *ob/ob* mice to assess the relationship between these two hormones. Ghrelin increased food intake in *ob/ob* mice, and leptin but not insulin i.c.v. pre-treatment abolished this effect. These results indicate that leptin-deficient obese mice are ghrelin sensitive and confirm that leptin, but not insulin, suppresses ghrelin's orexigenic effects (Fig. 4C). Further, this highlights that ghrelin resistance is unrelated to obesity or glucose intolerance *per se*, as *ob/ob* mice are obese and glucose intolerant (31) but remain ghrelin sensitive. Additional electrophysiology experiments showed that ghrelin increased and insulin or leptin decreased NPY action potential frequency (Fig 4D), similar to previous reports (32). However, in the presence of leptin, ghrelin did not increase NPY firing, while ghrelin modestly increases NPY firing in the presence of insulin (Fig 4D).

These results suggest that hyperleptinemia during DIO contributes to ghrelin resistance and NPY/AgRP neuronal dysfunction. However, as DIO causes leptin resistance in some neuronal populations, it was therefore important to determine if leptin signalling in NPY/AgRP neurons still occurs after three weeks of HFD-feeding. Leptin-induced STAT-3 phosphorylation was decreased specifically in NPY neurons in mice fed a HFD for three weeks compared to controls. Approximately 40% of NPY neurons still express pSTAT-3 in response to leptin, as compared to ~70% of NPY neurons from control mice (Fig. 4.E). Thus, NPY neurons are largely leptin-sensitive at the time they become ghrelin resistant and leptin may contribute to ghrelin resistance in NPY neurons.

Hypothalamic gliosis underlies ghrelin resistance

Recent studies show that HFD induces hypothalamic gliosis (20, 21), in which GFAP-positive cells ensheathe POMC and NPY neurons (20). Horvath and colleagues postulated that these changes underlie hormonal resistance during DIO. In order to test the potential role of hypothalamic gliosis as a contributing factor to ghrelin resistance we counted GFAP-positive cells from serial sections

throughout the arcuate nucleus. Three weeks of HFD, which induces ghrelin resistance, increased the number of GFAP-positive cells in the arcuate nucleus compared to chow-fed mice and also increased GFAP fibre length and fibre projections (Fig 5A&B). We also examined GFAP cell number in obese *ob/ob*-NPY GFP mice, which are not ghrelin resistant. There was no significant difference in GFAP-positive cells in *ob/ob*-NPY GFP mice compared with lean controls. HFD mice are ghrelin resistant and exhibit hypothalamic gliosis, whereas *ob/ob* mice are ghrelin sensitive and do not exhibit hypothalamic gliosis, thus our results suggest that hypothalamic gliosis, as assessed by GFAP positive cells may contribute to ghrelin resistance.

DISCUSSION

In the current study, we examined the time-course over which HFD-feeding causes ghrelin resistance in NPY/AgRP neurons. We show that ghrelin resistance occurs after only 3 weeks of HFD-feeding. At this time, both central or peripheral ghrelin fails to induce food intake and central ghrelin does not induce Fos-IR in NPY neurons or action potential firing in NPY neurons. Collectively, these data show that HFD-feeding renders NPY neurons unresponsive to ghrelin after only 3 weeks, an effect that is caused by diet-induced hyperleptinemia through actions on NPY neuron firing and hypothalamic gliosis. It is well established that the homeostatic circuits regulating food intake are impaired by chronic exposure to a HFD (19, 33), but in this study we examined the acute effects of HFD-exposure in order to identify the mechanisms that contribute to hormone resistance in the early stages of DIO. This is an important consideration for ongoing studies as most mouse models of DIO involve 10-37 weeks of HFD feeding (34-39) even though body weight and glucose tolerance are affected after only 1 week of HFD.

We observed the onset of ghrelin resistance in NPY neurons at 3 weeks, as NPY neurons failed to show c-fos or to increase action potential activity in response to ghrelin. At 3 weeks of age, we also observed elevated plasma leptin and no difference in insulin in DIO mice compared with chow mice. Because leptin suppresses appetite, leptin receptors are found on NPY neurons in the arcuate nucleus (40), and leptin suppresses NPY/AgRP gene expression and transcription (29, 41) through nuclear exclusion of FOXO1 (42, 43), we examined whether diet-induced hyperleptinemia contributed to ghrelin resistance. To answer this question we used a physiological approach, utilizing the leptin-deficient *ob/ob* mouse. Despite the severe obesity and glucose intolerance, i.c.v. ghrelin still increased food intake in *ob/ob* mice, which was completely prevented by 1 hour pre-treatment with i.c.v. leptin, but not insulin. Moreover, electrophysiological studies showed that leptin pre-treatment hyperpolarizes NPY neurons and inhibits their ability to respond to ghrelin, whereas ghrelin still modestly increased action potential firing in the presence of insulin. This provides physiological evidence that leptin, but not insulin, prevents ghrelin-induced food intake by impairing NPY neuronal function. In support of this interaction, leptin suppressed ghrelin-induced activation of isolated NPY neurons *in vitro* (22) and c-fos expression in the arcuate nucleus (44). In the ventromedial arcuate nucleus, which contains primarily NPY neurons (45), 90 ± 5% of ObR-expressing neurons co-express the ghrelin receptor (GHSR) (46). Taken together, these data suggest that diet-induced hyperleptinemia contributes to ghrelin resistance in arcuate NPY/AgRP neurons rather than obesity or glucose intolerance *per se*.

We speculate that leptin and ghrelin reciprocally regulate NPY neurons in opposing directions. Perello and colleagues showed that leptin regulates food intake and appetite normally in GHSR wild type and knockout mice, whereas leptin-deficient Zucker rats are more sensitive to GHSR agonist-mediated c-fos induction in the arcuate nucleus (44) and our results illustrate leptin suppresses ghrelin-induced food intake in *ob/ob* mice. These results suggest an hierarchical regulation of NPY function by leptin over ghrelin and we hypothesize leptin provides some level of tonic inhibition over NPY/AgRP

neurons that restricts ghrelin-induced food intake. Fasting is a metabolic state characterized by low insulin and leptin levels, and ghrelin is dramatically more effective at increasing appetite in the fasted state (24, 44). Moreover, high leptin levels and insulin levels characterize the diet-induced obese state and NPY/AgRP neurons are unresponsive to ghrelin in this condition(12).

It is currently unknown as to why leptin but not insulin inhibited ghrelin's ability to increase food intake in *ob/ob* mice or action potential firing in NPY mice. Although both insulin and leptin target NPY neurons, it is possible that different subpopulations of leptin- or insulin-sensitive NPY neurons exist. Recent studies show that there are different leptin sensitive and insulin sensitive subpopulations of POMC neurons (47), supporting the idea that different hormone-sensitive subpopulations of NPY neurons also exist.

Importantly, we determined the level of leptin resistance in NPY neurons of mice on HFD for 3 weeks by measuring the number of NPY-GFP neurons containing leptin-induced phosphorylation of STAT-3. We observed that leptin still signals in NPY neurons after HFD although not with the same effectiveness as chow-fed mice (70% in chow vs 40% in HFD mice). This suggests that mice remain at least partially leptin-sensitive after three weeks of HFD, and obesity-related hyperleptinemia may therefore contribute to ghrelin resistance by inhibiting NPY neuronal function. This is further evidence of selective leptin resistance in the hypothalamus as previously reported (48, 49).

Recent studies show that DIO promotes hypothalamic gliosis and structural rewiring within appetite-regulating circuits, which promotes inflammation and exacerbates the obesogenic state (20, 21). Further, Horvath and colleagues highlighted that DIO causes hypothalamic gliosis, in which GFAP-positive fibres surround and ensheathe NPY and POMC neurons forming significant physical barriers to hormones or nutrient stimuli in the plasma. We found that 3 weeks of HFD feeding, which caused ghrelin resistance, increased body weight, glucose intolerance and hyperleptinemia, induced hypothalamic gliosis in terms of GFAP-positive cell number and fibre projection number and length. However, ghrelin-sensitive obese *ob/ob* mice did not show signs of hypothalamic gliosis. These results again strengthen the notion that neither obesity nor glucose intolerance underlie hypothalamic gliosis and subsequent ghrelin resistance but rather point towards hyperleptinemia and/or HFD as primary causes of hypothalamic gliosis. Indeed, leptin modifies astrocyte-specific glutamate and glucose transporters (50), DIO elevates leptin receptor expression in hypothalamic astrocytes (51, 52) and leptin regulates astrocyte morphology (53). These studies show that hyperleptinemia is a driving force behind HFD-induced hypothalamic gliosis and the lack of gliosis in leptin-deficient *ob/ob* mice helps to maintain ghrelin sensitivity. However, there is presumably an acute effect of leptin on NPY neuronal firing, independent of changes in the gliosis given that 1-hour leptin pre-treatment to *ob/ob* mice prevents ghrelin-induced food intake. The suppressive effect of diet-induced hyperleptinemia also extends to other orexigenic stimuli, as reduced activation of arcuate neurons to fasting is associated with hyperleptinemia in obese mice (54). We suggest that defective NPY/AgRP neuronal function is responsible for suppressing the appropriate responses to physiological cues about energy

status and feeding requirements at the level of the hypothalamic circuitry. Studies from obese humans support this; clinical studies reveal that many obese patients do not recognize a pattern between their food consumption and sensations of hunger (55). Clearly, the homeostatic regulation of food intake is impaired in DIO and defective NPY/AgRP function is confounded by other DIO-induced variables, including impaired POMC function, selective leptin resistance and hypothalamic structural rewiring.

In summary, our data show that ghrelin resistance in NPY/AgRP occurs by 3 weeks of HFD-feeding in mice and suggest that ghrelin resistance in NPY/AgRP occurs as a result of increased plasma leptin and hypothalamic gliosis brought about by acute exposure to a HFD.

References

1. Andrews, Z. B. (2011) Central mechanisms involved in the orexigenic actions of ghrelin. *Peptides* 32, 2248-2255
2. Kojima, M., Hosoda, H., Date, Y., Nakazato, M., Matsuo, H., and Kangawa, K. (1999) Ghrelin is a growth-hormone-releasing acylated peptide from stomach. *Nature* 402, 656-660
3. Tschop, M., Smiley, D. L., and Heiman, M. L. (2000) Ghrelin induces adiposity in rodents. *Nature* 407, 908-913
4. Andrews, Z. B., Liu, Z. W., Walllingford, N., Erion, D. M., Borok, E., Friedman, J. M., Tschop, M. H., Shanabrough, M., Cline, G., Shulman, G. I., Coppola, A., Gao, X. B., Horvath, T. L., and Diano, S. (2008) UCP2 mediates ghrelin's action on NPY/AgRP neurons by lowering free radicals. *Nature* 454, 846-851
5. Cowley, M. A., Smith, R. G., Diano, S., Tschop, M., Pronchuk, N., Grove, K. L., Strasburger, C. J., Bidlingmaier, M., Esterman, M., Heiman, M. L., Garcia-Segura, L. M., Nillni, E. A., Mendez, P., Low, M. J., Sotonyi, P., Friedman, J. M., Liu, H., Pinto, S., Colmers, W. F., Cone, R. D., and Horvath, T. L. (2003) The distribution and mechanism of action of ghrelin in the CNS demonstrates a novel hypothalamic circuit regulating energy homeostasis. *Neuron* 37, 649-661
6. Morgan, D. G., Small, C. J., Abusnana, S., Turton, M., Gunn, I., Heath, M., Rossi, M., Goldstone, A. P., O'Shea, D., Meeran, K., Ghatei, M., Smith, D. M., and Bloom, S. (1998) The NPY Y1 receptor antagonist BIBP 3226 blocks NPY induced feeding via a non-specific mechanism. *Regul Pept* 75-76, 377-382
7. Nijenhuis, W. A., Oosterom, J., and Adan, R. A. (2001) AgRP(83-132) acts as an inverse agonist on the human-melanocortin-4 receptor. *Mol Endocrinol* 15, 164-171
8. Wolak, M. L., DeJoseph, M. R., Cator, A. D., Mokashi, A. S., Brownfield, M. S., and Urban, J. H. (2003) Comparative distribution of neuropeptide Y Y1 and Y5 receptors in the rat brain by using immunohistochemistry. *J Comp Neurol* 464, 285-311
9. Kamegai, J., Tamura, H., Shimizu, T., Ishii, S., Sugihara, H., and Wakabayashi, I. (2000) Central effect of ghrelin, an endogenous growth hormone secretagogue, on hypothalamic peptide gene expression. *Endocrinology* 141, 4797-4800
10. Kamegai, J., Tamura, H., Shimizu, T., Ishii, S., Sugihara, H., and Wakabayashi, I. (2001) Chronic central infusion of ghrelin increases hypothalamic neuropeptide Y and Agouti-related protein mRNA levels and body weight in rats. *Diabetes* 50, 2438-2443
11. Nakazato, M., Murakami, N., Date, Y., Kojima, M., Matsuo, H., Kangawa, K., and Matsukura, S. (2001) A role for ghrelin in the central regulation of feeding. *Nature* 409, 194-198

12. Briggs, D. I., Enriori, P. J., Lemus, M. B., Cowley, M. A., and Andrews, Z. B. (2010) Diet-induced obesity causes ghrelin resistance in arcuate NPY/AgRP neurons. *Endocrinology* 151, 4745-4755
13. Gardiner, J. V., Campbell, D., Patterson, M., Kent, A., Ghatei, M. A., Bloom, S. R., and Bewick, G. A. (2010) The hyperphagic effect of ghrelin is inhibited in mice by a diet high in fat. *Gastroenterology* 138, 2468-2476, 2476 e2461
14. Perez-Tilve, D., Heppner, K., Kirchner, H., Lockie, S. H., Woods, S. C., Smiley, D. L., Tschop, M., and Pfluger, P. (2011) Ghrelin-induced adiposity is independent of orexigenic effects. *FASEB J* 25, 2814-2822
15. Perreault, M., Istrate, N., Wang, L., Nichols, A. J., Tozzo, E., and Stricker-Krongrad, A. (2004) Resistance to the orexigenic effect of ghrelin in dietary-induced obesity in mice: reversal upon weight loss. *Int J Obes Relat Metab Disord* 28, 879-885
16. Becskei, C., Lutz, T. A., and Riediger, T. (2009) Blunted fasting-induced hypothalamic activation and refeeding hyperphagia in late-onset obesity. *Neuroendocrinology* 90, 371-382
17. Briggs, D. I., Lemus, M. B., Kua, E., and Andrews, Z. B. (2011) Diet-induced obesity attenuates fasting-induced hyperphagia. *J Neuroendocrinol*
18. Bouret, S. G., Draper, S. J., and Simerly, R. B. (2004) Formation of projection pathways from the arcuate nucleus of the hypothalamus to hypothalamic regions implicated in the neural control of feeding behavior in mice. *J Neurosci* 24, 2797-2805
19. Bouret, S. G., Gorski, J. N., Patterson, C. M., Chen, S., Levin, B. E., and Simerly, R. B. (2008) Hypothalamic neural projections are permanently disrupted in diet-induced obese rats. *Cell Metab* 7, 179-185
20. Horvath, T. L., Sarman, B., Garcia-Caceres, C., Enriori, P. J., Sotonyi, P., Shanabrough, M., Borok, E., Argente, J., Chowen, J. A., Perez-Tilve, D., Pfluger, P. T., Bronneke, H. S., Levin, B. E., Diano, S., Cowley, M. A., and Tschop, M. H. (2010) Synaptic input organization of the melanocortin system predicts diet-induced hypothalamic reactive gliosis and obesity. *Proceedings of the National Academy of Sciences of the United States of America* 107, 14875-14880
21. Thaler, J. P., Yi, C. X., Schur, E. A., Guyenet, S. J., Hwang, B. H., Dietrich, M. O., Zhao, X., Sarruf, D. A., Izgur, V., Maravilla, K. R., Nguyen, H. T., Fischer, J. D., Matsen, M. E., Wisse, B. E., Morton, G. J., Horvath, T. L., Baskin, D. G., Tschop, M. H., and Schwartz, M. W. (2012) Obesity is associated with hypothalamic injury in rodents and humans. *J Clin Invest* 122, 153-162
22. Kohno, D., Nakata, M., Maekawa, F., Fujiwara, K., Maejima, Y., Kuramochi, M., Shimazaki, T., Okano, H., Onaka, T., and Yada, T. (2007) Leptin suppresses ghrelin-induced activation of neuropeptide Y neurons in the arcuate nucleus via phosphatidylinositol 3-kinase- and phosphodiesterase 3-mediated pathway. *Endocrinology* 148, 2251-2263

23. Tschop, M., Weyer, C., Tataranni, P. A., Devanarayan, V., Ravussin, E., and Heiman, M. L. (2001) Circulating ghrelin levels are decreased in human obesity. *Diabetes* 50, 707-709

24. Hewson, A. K., and Dickson, S. L. (2000) Systemic administration of ghrelin induces Fos and Egr-1 proteins in the hypothalamic arcuate nucleus of fasted and fed rats. *J Neuroendocrinol* 12, 1047-1049

25. Wang, L., Saint-Pierre, D. H., and Tache, Y. (2002) Peripheral ghrelin selectively increases Fos expression in neuropeptide Y - synthesizing neurons in mouse hypothalamic arcuate nucleus. *Neurosci Lett* 325, 47-51

26. Baskin, D. G., Breininger, J. F., and Schwartz, M. W. (1999) Leptin receptor mRNA identifies a subpopulation of neuropeptide Y neurons activated by fasting in rat hypothalamus. *Diabetes* 48, 828-833

27. Konner, A. C., Janoschek, R., Plum, L., Jordan, S. D., Rother, E., Ma, X., Xu, C., Enriori, P., Hampel, B., Barsh, G. S., Kahn, C. R., Cowley, M. A., Ashcroft, F. M., and Bruning, J. C. (2007) Insulin action in AgRP-expressing neurons is required for suppression of hepatic glucose production. *Cell Metab* 5, 438-449

28. Pardini, A. W., Nguyen, H. T., Figlewicz, D. P., Baskin, D. G., Williams, D. L., Kim, F., and Schwartz, M. W. (2006) Distribution of insulin receptor substrate-2 in brain areas involved in energy homeostasis. *Brain Res* 1112, 169-178

29. Schwartz, M. W., Erickson, J. C., Baskin, D. G., and Palmiter, R. D. (1998) Effect of fasting and leptin deficiency on hypothalamic neuropeptide Y gene transcription in vivo revealed by expression of a lacZ reporter gene. *Endocrinology* 139, 2629-2635

30. Schwartz, M. W., Sipols, A. J., Marks, J. L., Sanacora, G., White, J. D., Scheurink, A., Kahn, S. E., Baskin, D. G., Woods, S. C., Figlewicz, D. P., and et al. (1992) Inhibition of hypothalamic neuropeptide Y gene expression by insulin. *Endocrinology* 130, 3608-3616

31. Flatt, P. R., and Bailey, C. J. (1981) Development of glucose intolerance and impaired plasma insulin response to glucose in obese hyperglycaemic (ob/ob) mice. *Horm Metab Res* 13, 556-560

32. Konner, A. C., Hess, S., Tovar, S., Mesaros, A., Sanchez-Lasheras, C., Evers, N., Verhagen, L. A., Bronneke, H. S., Kleinridders, A., Hampel, B., Kloppenburg, P., and Bruning, J. C. (2011) Role for insulin signaling in catecholaminergic neurons in control of energy homeostasis. *Cell metabolism* 13, 720-728

33. Kohsaka, A., Laposky, A. D., Ramsey, K. M., Estrada, C., Joshu, C., Kobayashi, Y., Turek, F. W., and Bass, J. (2007) High-fat diet disrupts behavioral and molecular circadian rhythms in mice. *Cell metabolism* 6, 414-421

34. Dzamko, N., van Denderen, B. J., Hevener, A. L., Jorgensen, S. B., Honeyman, J., Galic, S., Chen, Z. P., Watt, M. J., Campbell, D. J., Steinberg, G. R., and Kemp, B. E. (2010) AMPK

beta1 deletion reduces appetite, preventing obesity and hepatic insulin resistance. *J Biol Chem* 285, 115-122

35. Enriori, P. J., Evans, A. E., Sinnayah, P., Jobst, E. E., Tonelli-Lemos, L., Billes, S. K., Glavas, M. M., Grayson, B. E., Perello, M., Nillni, E. A., Grove, K. L., and Cowley, M. A. (2007) Diet-induced obesity causes severe but reversible leptin resistance in arcuate melanocortin neurons. *Cell Metab* 5, 181-194
36. Martin, T. L., Alquier, T., Asakura, K., Furukawa, N., Preitner, F., and Kahn, B. B. (2006) Diet-induced obesity alters AMP kinase activity in hypothalamus and skeletal muscle. *J Biol Chem* 281, 18933-18941
37. Pistell, P. J., Morrison, C. D., Gupta, S., Knight, A. G., Keller, J. N., Ingram, D. K., and Bruce-Keller, A. J. (2009) Cognitive impairment following high fat diet consumption is associated with brain inflammation. *J Neuroimmunol*
38. Zigman, J. M., Nakano, Y., Coppari, R., Balthasar, N., Marcus, J. N., Lee, C. E., Jones, J. E., Deysher, A. E., Waxman, A. R., White, R. D., Williams, T. D., Lachey, J. L., Seeley, R. J., Lowell, B. B., and Elmquist, J. K. (2005) Mice lacking ghrelin receptors resist the development of diet-induced obesity. *The Journal of clinical investigation* 115, 3564-3572
39. Ueno, N., Asakawa, A., and Inui, A. (2007) Blunted metabolic response to fasting in obese mice. *Endocrine* 32, 192-196
40. Draper, S., Kirigiti, M., Glavas, M., Grayson, B., Chong, C. N., Jiang, B., Smith, M. S., Zeltser, L. M., and Grove, K. L. (2010) Differential gene expression between neuropeptide Y expressing neurons of the dorsomedial nucleus of the hypothalamus and the arcuate nucleus: microarray analysis study. *Brain Res* 1350, 139-150
41. Morrison, C. D., Morton, G. J., Niswender, K. D., Gelling, R. W., and Schwartz, M. W. (2005) Leptin inhibits hypothalamic Npy and Agrp gene expression via a mechanism that requires phosphatidylinositol 3-OH-kinase signaling. *Am J Physiol Endocrinol Metab* 289, E1051-1057
42. Kitamura, T., Feng, Y., Kitamura, Y. I., Chua, S. C., Jr., Xu, A. W., Barsh, G. S., Rossetti, L., and Accili, D. (2006) Forkhead protein FoxO1 mediates Agrp-dependent effects of leptin on food intake. *Nat Med* 12, 534-540
43. Fukuda, M., Jones, J. E., Olson, D., Hill, J., Lee, C. E., Gautron, L., Choi, M., Zigman, J. M., Lowell, B. B., and Elmquist, J. K. (2008) Monitoring FoxO1 localization in chemically identified neurons. *J Neurosci* 28, 13640-13648
44. Hewson, A. K., Tung, L. Y., Connell, D. W., Tookman, L., and Dickson, S. L. (2002) The rat arcuate nucleus integrates peripheral signals provided by leptin, insulin, and a ghrelin mimetic. *Diabetes* 51, 3412-3419

45. Elias, C. F., Aschkenasi, C., Lee, C., Kelly, J., Ahima, R. S., Bjorbaek, C., Flier, J. S., Saper, C. B., and Elmquist, J. K. (1999) Leptin differentially regulates NPY and POMC neurons projecting to the lateral hypothalamic area. *Neuron* 23, 775-786

46. Perello, M., Scott, M. M., Sakata, I., Lee, C. E., Chuang, J. C., Osborne-Lawrence, S., Rovinsky, S. A., Elmquist, J. K., and Zigman, J. M. (2012) Functional implications of limited leptin receptor and ghrelin receptor coexpression in the brain. *The Journal of comparative neurology* 520, 281-294

47. Williams, K. W., Margatho, L. O., Lee, C. E., Choi, M., Lee, S., Scott, M. M., Elias, C. F., and Elmquist, J. K. (2010) Segregation of acute leptin and insulin effects in distinct populations of arcuate proopiomelanocortin neurons. *The Journal of neuroscience : the official journal of the Society for Neuroscience* 30, 2472-2479

48. Munzberg, H., Flier, J. S., and Bjorbaek, C. (2004) Region-specific leptin resistance within the hypothalamus of diet-induced obese mice. *Endocrinology* 145, 4880-4889

49. Enriori, P. J., Sinnayah, P., Simonds, S. E., Garcia Rudaz, C., and Cowley, M. A. (2011) Leptin action in the dorsomedial hypothalamus increases sympathetic tone to brown adipose tissue in spite of systemic leptin resistance. *J Neurosci* 31, 12189-12197

50. Fuente-Martin, E., Garcia-Caceres, C., Granado, M., de Ceballos, M. L., Sanchez-Garrido, M. A., Sarman, B., Liu, Z. W., Dietrich, M. O., Tena-Sempere, M., Argente-Arizon, P., Diaz, F., Argente, J., Horvath, T. L., and Chowen, J. A. (2012) Leptin regulates glutamate and glucose transporters in hypothalamic astrocytes. *J Clin Invest* 122, 3900-3913

51. Pan, W., Hsuchou, H., He, Y., Sakharkar, A., Cain, C., Yu, C., and Kastin, A. J. (2008) Astrocyte leptin receptor (ObR) and leptin transport in adult-onset obese mice. *Endocrinology* 149, 2798-2806

52. Hsuchou, H., He, Y., Kastin, A. J., Tu, H., Markadakis, E. N., Rogers, R. C., Fossier, P. B., and Pan, W. (2009) Obesity induces functional astrocytic leptin receptors in hypothalamus. *Brain : a journal of neurology* 132, 889-902

53. Garcia-Caceres, C., Fuente-Martin, E., Burgos-Ramos, E., Granado, M., Frago, L. M., Barrios, V., Horvath, T., Argente, J., and Chowen, J. A. (2011) Differential acute and chronic effects of leptin on hypothalamic astrocyte morphology and synaptic protein levels. *Endocrinology* 152, 1809-1818

54. Becskei, C., Lutz, T. A., and Riediger, T. (2010) Reduced fasting-induced activation of hypothalamic arcuate neurons is associated with hyperleptinemia and increased leptin sensitivity in obese mice. *Am J Physiol Regul Integr Comp Physiol* 299, R632-641

55. Barkeling, B., King, N. A., Naslund, E., and Blundell, J. E. (2007) Characterization of obese individuals who claim to detect no relationship between their eating pattern and sensations of hunger or fullness. *Int J Obes (Lond)* 31, 435-439

Figure legends

Figure 1: Body weight and glucose tolerance were measured in chow- and HFD-fed animals every week until the onset of ghrelin resistance (as determined by ghrelin-induced food intake). For weekly body weight analysis * $p < 0.05$ compared with chow by Student's t test (n=7-11). Glucose tolerance tests were performed weekly (n=5-6). Blood glucose response to bolus glucose administration (2g/kg, i.p.) was measured over 90 minutes and corresponding AUC analysis (n=4-6). *, $p < 0.05$ vs chow by two-way repeated measures ANOVA and Student's t test for GTT and AUC, respectively. All data are mean ± SEM.

Figure 2: Three weeks of HFD-feeding causes ghrelin resistance. (A-D) Exogenous ghrelin was administered weekly i.p. (1 mg/kg) at the end (1800 hours) of the light phase and food intake was measured over 5 h (n = 5-10). (E) To determine whether ghrelin resistance was centrally mediated, food intake was measured in response to i.c.v ghrelin after 3 weeks of chow- or HFD-feeding. Exogenous ghrelin was administered i.c.v. (1 µg/µl, injection vol 1.5 µl) at the beginning (0800 h) of the light phase and food intake was measured over 5 h (n = 5-10). All data are presented as milli joules (mJ) of energy consumed per animal. *, $p < 0.05$ vs. corresponding vehicle-treated control by two way ANOVA with Bonferonni's post hoc test. (E-G) Peripheral acylated ghrelin and total ghrelin in the plasma of mice fed a HFD for 3 weeks and chow-fed controls. *, $p < 0.05$ compared to chow by student's t test (n=6). Data are mean ± SEM.

Figure 3: Ghrelin resistance occurs in NPY/AgRP neurons after 3 weeks of HFD-feeding. (A) The presence of Fos was used as a surrogate marker of neuronal activation in mice after i.c.v. injection of ghrelin in mice after 3 weeks of chow-fed control and HFD-feeding (n=5-6). Fos-immunoreactive NPY-GFP neurons were quantified 60 minutes after i.c.v. injection of ghrelin (1 µg/µl, injection vol 1.5 µl) or aCSF in the arcuate nucleus of NPY-GFP mice. Representative images of Fos-immunoreactivity in the arcuate nucleus of mice on chow diet or HFD treated with aCSF or ghrelin. All data are mean ± SEM. *, $p < 0.05$ by two-way ANOVA with Bonferonni's post hoc test. (B) Whole-cell patch clamp electrophysiology was used to determine whether NPY neurons increased firing in response to ghrelin. In slices of arcuate nucleus, GFP-expressing NPY neurons responded to ghrelin (1 or 3 nM) with a robust increase in action potential firing (10 of 11 cells from 5 mice) in slices from normal chow fed mice. In contrast, only 4 of 12 NPY arcuate neurons (n = 6 mice) responded to ghrelin application in HFD mice. *, $p < 0.05$ by Fisher's exact test. Representative traces of NPY neuronal firing in the arcuate nucleus in mice on chow diet or HFD treated with ghrelin.

Figure 4: Leptin contributes to ghrelin resistance. Fasting plasma leptin (A) or insulin (B) concentrations of mice fed chow or HFD for 3 weeks (n=6). (C) To assess how leptin or insulin modulates ghrelin-induced feeding behaviour in *ob/ob* mice, non-fasted animals received an i.c.v.

injection of aCSF, leptin (4 µg/ µl in 2 µl) or insulin (5 µU/µl in 2 µl). Food was removed and 1-hour later mice received either aCSF or ghrelin (1 µg/µl in 2 µl). Food was returned then measured 4 hours later (n=6-8). *, p<0.05 by one-way ANOVA with Bonferonni's post hoc test. (D) Ghrelin increased and insulin or leptin suppressed action potential (AP) spike frequency as a percentage of basal firing rates. The addition of ghrelin with insulin modestly increased action potential firing in NPY neurons whereas the addition of ghrelin with leptin did not increase action potential firing in NPY neurons. Ghrelin alone reduces action potential amplitude, however the presence of insulin or leptin prevented the ability of ghrelin to reduce action potential amplitude. ψ, p<0.05 by Student's t-test (Insulin vs Ghrelin in Insulin). (E) The presence of pSTAT-3 was used as a marker of leptin signaling in chow- or HFD-fed mice. Chow- and HFD-fed mice were fasted overnight and analysed for pSTAT-3 protein expression in the arcuate nucleus of NPY-GFP mice 45 minutes after i.p. leptin (1mg/kg) or aCSF (n=5). #, p<0.05 High fat vs chow by two-way ANOVA with Bonferonni's post hoc test. (F) Representative images of arcuate nucleus pSTAT3-immunoreactivity in mice on chow diet or HFD treated with aCSF or leptin. All data are mean ± SEM. *, p < 0.05 by two-way ANOVA with Bonferonni's post hoc test or Student's t test (vs. chow).

Figure 5: Hypothalamic gliosis contributes to ghrelin resistance after 3 weeks high fat diet (HFD). (A) Mice on a HFD for 3 weeks show hypothalamic gliosis, as assessed by an increase in GFAP-positive cells in the arcuate nucleus of the hypothalamus. (B) HFD exposure for 3 weeks also increased the number of fibre projections and fibre projection length of GFAP-positive cells in the arcuate nucleus of the hypothalamus. (C) Representative images showing increased GFAP cell number and fibre projections in mice fed HFD for 3 weeks. (D) Even though ob/ob mice are obese and glucose intolerant they do not show an increase GFAP-positive cell number relative to lean WT mice, suggesting hyperleptinemia associated with HF-feeding contributes to hypothalamic gliosis. (E) Representative images showing GFAP-positive cells in lean WT and ob/ob-NPY GFP mice. All data are mean ± SEM. *, p < 0.05 by two-way ANOVA with Bonferonni's post hoc test (vs. chow in panel B). *, p < 0.05 by Student's t-test in panel A.

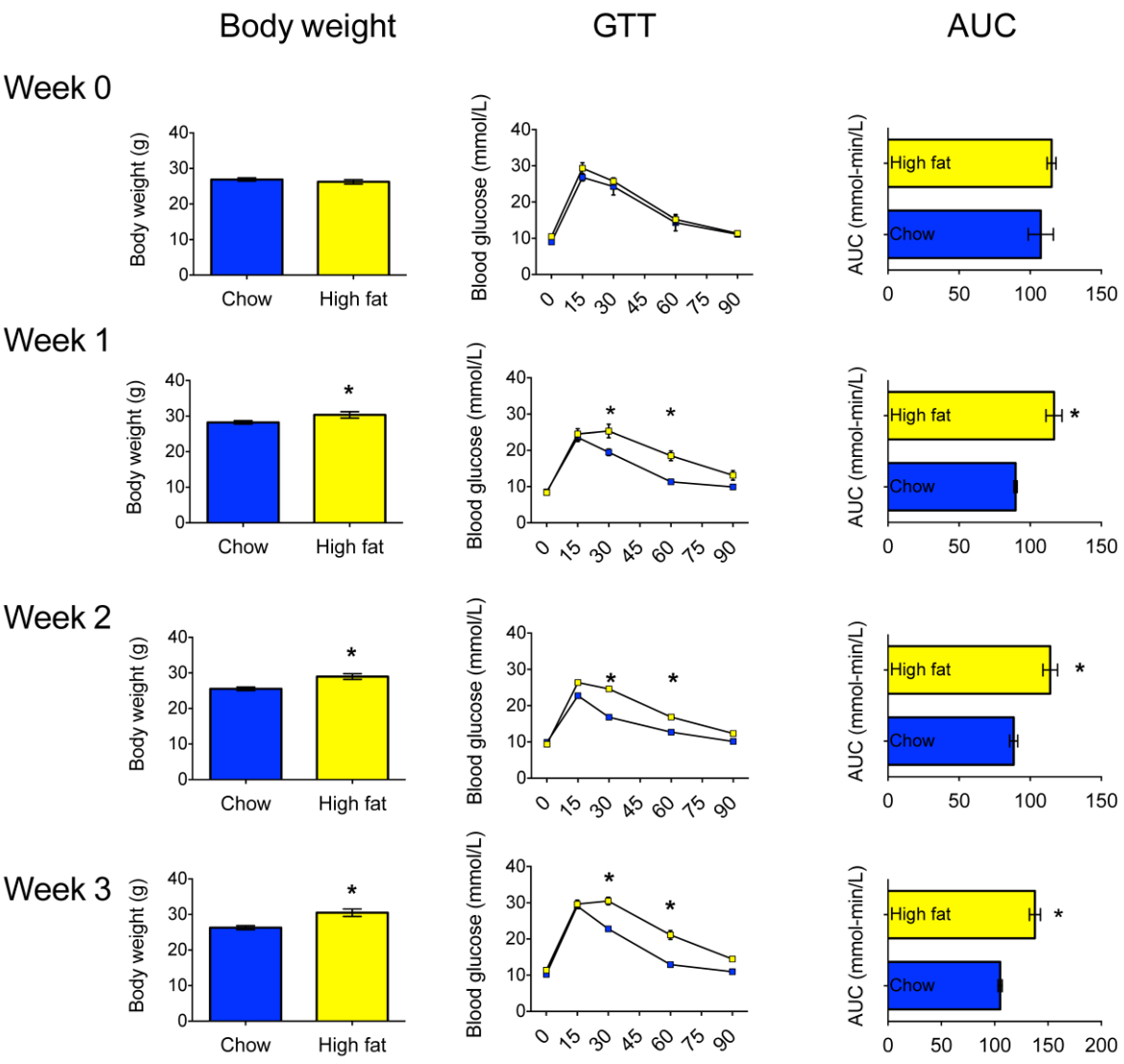

Fig 1- Briggs et al

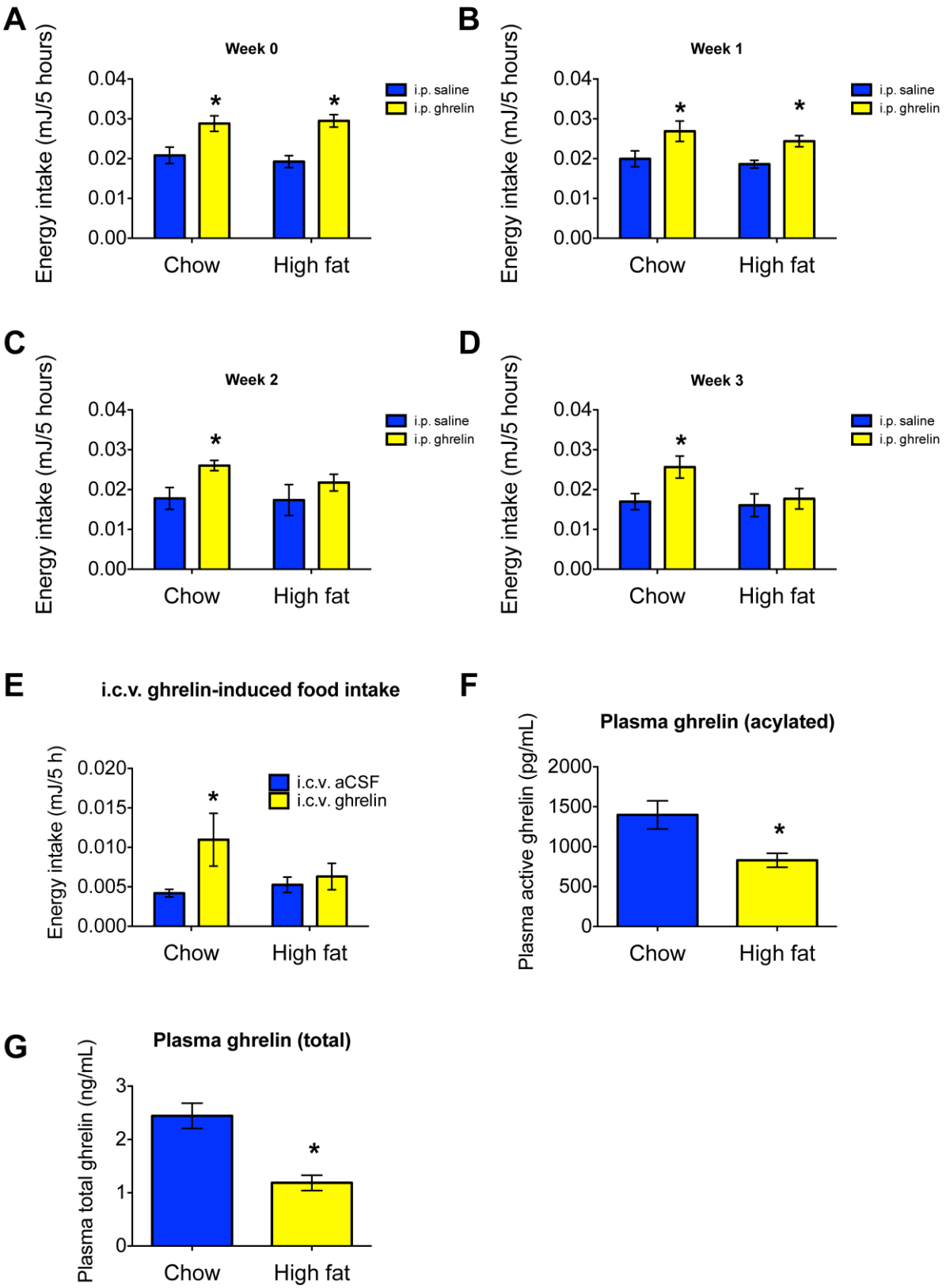

Fig 2 - Briggs et al

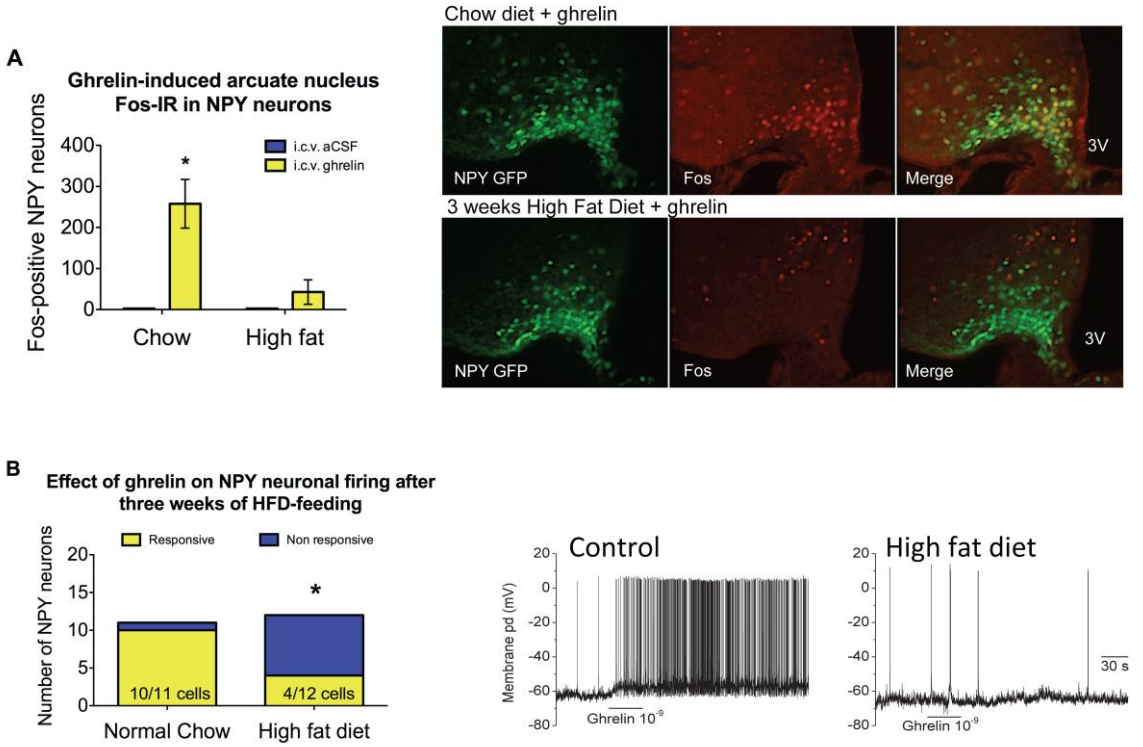

Figure 3 - Briggs et al

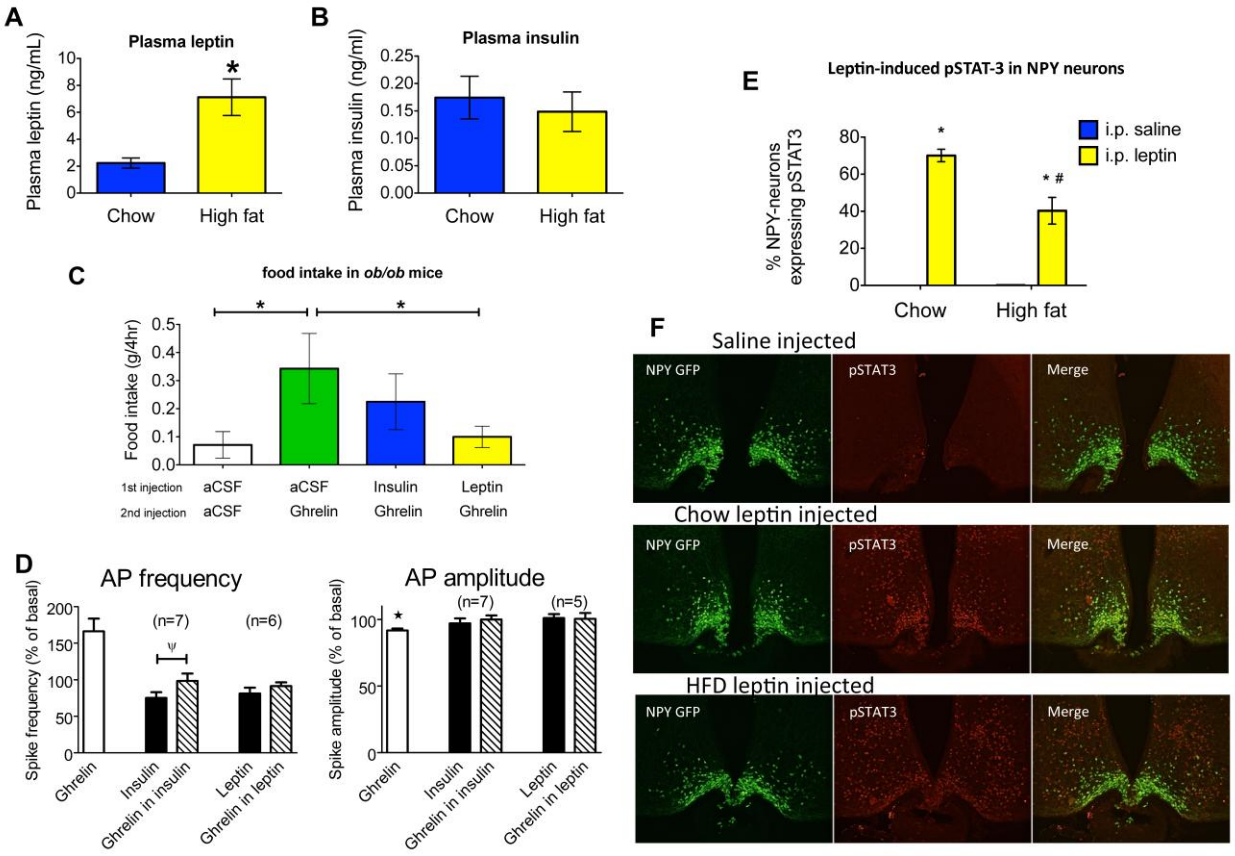

Figure 4 - Briggs et al

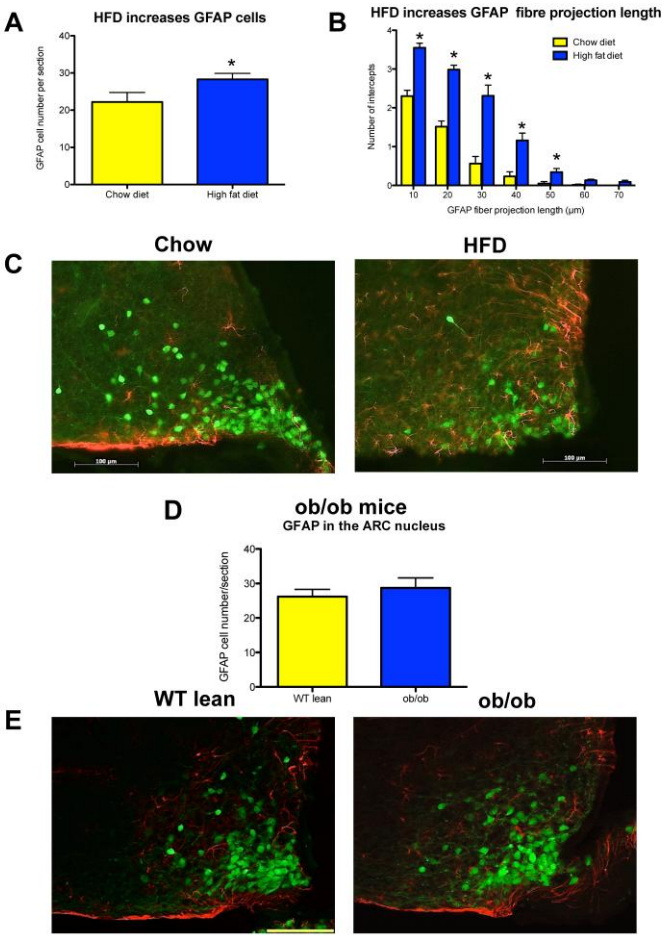

Figure 5 - Briggs et al

6. Zusammenfassung der Arbeit

6.1 Deutsch

Adipositas ist eines der größten Gesundheitsprobleme der modernen Wohlstandsgesellschaft und einer der Hauptrisikofaktoren für die Entstehung von Diabetes mellitus Typ II. Beiden metabolischen Störungen liegen Veränderungen des neuroendokrinen Systems zu Grunde. Hierbei ist vor allem der Verlust der Leptinsensitivität zu nennen, die für die Verknüpfung von Adipositas und Diabetes Typ II verantwortlich sein könnte. Mittlerweile ist das zentrale Nervensystem, insbesondere der mediobasale Hypothalamus (MBH), als Hauptregulationszentrum der zentralen Energie- und Glukosehomöostase anzusehen. Daher ist der Zusammenhang von Adipositas und Diabetes mellitus Typ II auf eine Modulation der beteiligten Signalwege im zentralen Nervensystem zurückzuführen.

In dieser Arbeit konnte gezeigt werden, dass der Verlust der zentralen Leptinsignalweiterleitung adipöser Individuen maßgeblich an dem Zusammenhang von Adipositas und Diabetes mellitus Typ II beteiligt ist. Darüber hinaus interagierte Leptin mit dem zentralen WNT/β Catenin- (WNT) Signalweg und inhibierte dabei das Schlüsselenzym, die Glykogen- Synthase- Kinase- 3β (GSK-3β), in Neuronen des MBH. Des Weiteren waren die positiven Effekte von Leptin auf den Glukosemetabolismus von einem intakten WNT- Signalweg abhängig. Im Einklang mit diesen Ergebnissen ging eine zentrale Inhibition der GSK-3β mit einer verstärkten Aktivierung des hypothalamischen Insulin- Signalweges einher, verbesserte die Glukosetoleranz und verringerte die Nahrungsaufnahme von leptindefizienten Mäusen. Eine erhöhte Aktivität im MBH hingegen war mit Adipositas assoziiert, steigerte die Nahrungsaufnahme, führte zu Regulationsstörungen der Energie- und Glukosehomöostase und war mit einer verminderten Leptinsensitivität assoziiert. Diese Daten legen nahe, dass Leptin seine katabolen Eigenschaften über die hypothalamische GSK-3β vermittelt und, dass dieses Enzym als zentraler Regulator des Energie- und Glukosemetabolismus angesehen werden kann.

Neben dem zentralen Verlust der Leptinsignalweiterleitung spielen auch noch andere, mit dem Körperfett assoziierte, Faktoren eine entscheidende Rolle bei der zentralen Regulation des Glukosemetabolismus. Neuere Forschungsergebnisse weisen darauf hin, dass die Veränderungen der zentralen Signalwege auf eine hypothalamische Inflammation zurückzuführen sein könnten. Die Zunahme des Fettgewebes geht mit einer erhöhten Sekretion von Zytokinen einher, die pro-inflammatorische Signalwege im Hypothalamus induzieren können. Es konnte gezeigt werden, dass eine erhöhte Aktivität der pro-inflammatorischen c-Jun N-terminale Kinase (JNK) in verschiedenen Nuclei des MBH mit Adipositas assoziiert ist. Die akute Inhibition dieser zentralen Kinase führte zu einer erhöhten Aktivierung des zentralen Insulin- Signalweges und verbesserte die Glukosetoleranz.

Die Daten deuten darauf hin, dass die beobachteten Effekte auf eine Inhibition der zentralen GSK-3β zurückzuführen waren, wodurch die Rolle dieser Kinase in der zentralen Regulation der Glukosehomöostase weiter bekräftigt wurde.
Neben der JNK ist auch der zentrale pro-inflammatorische NF-κB- Signalweg mit Adipositas verknüpft und eine Aktivierung wird mit einer aktiven GSK-3β in Verbindung gebracht. Eine akute Inhibition dieses Signalweges, mit dem Flavonoid Butein, brachte eine Verbesserung der Glukosetoleranz von diabetischen und adipösen Mäusen mit sich. Des Weiteren verminderte die chronische Inhibition des NF-κB- Signalweges (mittels Gentherapie) im MBH die Zunahme des Körpergewichtes und der Körperfettmasse von Mäusen auf einer hochkalorischen Diät. Dabei verbesserte diese Behandlung die Glukosetoleranz der Tiere, erhöhte die Sauerstoffaufnahme, den Energieverbrauch sowie die basale metabolische Rate und war mit einer erhöhten Leptinsensitivität verbunden.

Mit dieser Arbeit konnten neue Aspekte der zentralen Regulation der Energie- und Glukosehomöostase entschlüsselt werden. Unsere Daten deuten darauf hin, dass die zentrale GSK-3β ein Schlüsselenzym ist, welches die metabolischen Eigenschaften von Leptin und Insulin vermittelt. Die Aktivierung dieser hypothalamischen Kinase durch pro-inflammatorische Signalwege scheint die Entstehung einer zentralen Leptinresistenz zu vermitteln, was eine Dysregulation der Glukosehomöostase nach sich zieht. Die zentrale Inhibition dieses Enzyms oder der zugrundeliegenden Inflammation liefert somit neue therapeutische Interventionsmöglichkeiten bei der Entstehung von Adipositas und Diabetes mellitus Typ II.

6.2 Englisch

Obesity is one of the most common medical problems of the 21st century and represents a critical risk factor for the development of type II diabetes. Both metabolic derangements are associated with profound alterations of the neuroendocrine system, such as leptin resistance, which might present a possible link between these two diseases. In the last decade, the hypothalamus has been identified as a main insulin target tissue for the regulation of energy- and glucose- metabolism. Therefore, modifications of signalling pathways in the central nervous system are thought to be responsible for these metabolic disorders.

In this thesis, we have shown that functional leptin- signalling of obese individuals is crucial for the maintenance of whole body glucose homeostasis. In neurons of the mediobasal hypothalamus (MBH), leptin inhibited the key enzyme of the WNT/β catenin- (WNT) pathway, glycogen-synthase-kinase 3β (GSK-3β), thereby activating this pathway. Furthermore, the glucose lowering capacity of leptin largely depends on neuronal WNT signalling. Moreover, acute inhibition of the central GSK-3β improved glucose tolerance and deceased food intake in leptin deficient mice. These results involved beneficial effect on central insulin- signalling and thereby decreasing hepatic glucose output. In contrast, increased hypothalamic GSK-3β activity was associated with obesity, increased food intake, disrupted whole body energy and glucose homeostasis and might be a result of reduced hypothalamic leptin sensitivity. Conclusively, these data suggest that the catabolic actions of central leptin-signalling are mediated via the WNT- pathway and that hypothalamic GSK-3β might be a key enzyme in the regulation of whole body glucose homeostasis.

Besides the essential role of central leptin- signalling, we also detected other important aspects in the regulation of whole body glucose homeostasis, involving body fat mass. Recently, it was suggested that an enhanced release of cytokines by white adipose tissue might also activate hypothalamic pro-inflammatory pathways, thereby disrupting central insulin-signalling. Here, we observed increased activity of c-Jun N-terminale Kinase (JNK) in different nuclei of the MBH during obesity. Acute inhibition of this central kinase improved hypothalamic insulin- signalling and glucose tolerance in mice. Moreover, our data suggest that the observed effects were mediated via inhibition of central GSK-3β, further emphasizing a major role of this central kinase in the regulation of glucose metabolism.
In addition to central JNK- signalling, pro-inflammatory signalling via central NF-κB is also associated with obesity and activation correlates with increased GSK-3β activity. Acute inhibition of central NF-κB- signalling, using the flavonoid Butein, strikingly improved glucose tolerance of obese and diabetic mice. Furthermore, long-term inhibition of NF-κB- signalling in the MBH, using a viral construct, decelerated diet induced obesity and improved whole-body glucose metabolism in mice fed

a high fat diet. Moreover, this treatment increased oxygen consumption, energy expenditure and resting metabolic rate, which was associated with restored leptin sensitivity.

Taken together, this thesis provides novel insights into the central regulation of whole body energy- and glucose metabolism. Our data indicate that the hypothalamic GSK-3β represents a key enzyme that mediates the metabolic actions of central leptin- and insulin- signalling. Pro-inflammatory pathways activate this central kinase, thereby inducing hypothalamic leptin resistance and subsequently disrupt the central regulation of whole body glucose homeostasis. Thus, this thesis reveals new potential therapeutic intervention in obesity and the development of type II diabetes.

7. Erklärung

Hiermit versichere ich, dass ich meine Dissertation

Neuroendokrine Regulation der Energie und Glukosehomöostase

-Vom zentralen WNT- Signalweg über hypothalamische Inflammation und Leptinsensitivität-

selbstständig, ohne unerlaubte Hilfe angefertigt und mich keiner anderen als der von mir ausdrücklich bezeichneten Quellen und Hilfen bedient habe.

Die Dissertation wurde in der jetzigen oder in einer ähnlichen Form noch bei keiner anderen Hochschule eingereicht und hat noch keinen sonstigen Prüfungszwecken gedient.

Marburg, August 2013 _____

(Jonas Benzler)